MULTI-PATH AUTOMATIC GROUND COLLISION AVOIDANCE SYSTEM FOR PERFORMANCE LIMITED AIRCRAFT WITH FLIGHT TESTS: PROJECT HAVE MEDUSA

THESIS

Kenneth C. Gahan, Capt, USAF

AFIT-ENY-MS-19-M-213

DEPARTMENT OF THE AIR FORCE
AIR UNIVERSITY

AIR FORCE INSTITUTE OF TECHNOLOGY

Wright-Patterson Air Force Base, Ohio

AFIT-ENY-MS-19-M-213

MULTI-PATH AUTOMATIC GROUND COLLISION AVOIDANCE SYSTEM FOR PERFORMANCE LIMITED AIRCRAFT WITH FLIGHT TESTS: PROJECT HAVE MEDUSA

THESIS

Presented to the Faculty

Department of Aeronautics and Astronautics

Graduate School of Engineering and Management

Air Force Institute of Technology

Air University

Air Education and Training Command

in Partial Fulfillment of the Requirements for the

Degree of Master of Science in Aeronautical Engineering

Kenneth C. Gahan, B.S.M.E., M.S.E., M.S.F.T.E

Capt, USAF

March 21, 2019

AFIT-ENY-MS-19-M-213

MULTI-PATH AUTOMATIC GROUND COLLISION AVOIDANCE SYSTEM FOR PERFORMANCE LIMITED AIRCRAFT WITH FLIGHT TESTS: PROJECT HAVE MEDUSA

THESIS

Kenneth C. Gahan, B.S.M.E., M.S.E., M.S.F.T.E
Capt, USAF

Committee Membership:

Dr. Richard G. Cobb
Chair

Col Angela W. Suplisson, PhD
Member

Dr. Bradley S. Liebst
Member

Dr. Donald L. Kunz
Member

Abstract

A multi-path automatic ground collision avoidance system (Auto-GCAS) for performance limited aircraft was further developed and improved to prevent controlled flight into terrain. This research includes flight test results from the United States Test Pilot School's Test Management Project (TMP) titled Have Multi-Path Escape Decisions Using Sophisticated Algorithms (MEDUSA). Currently, the bomber and mobility aircraft communities lack an Auto-GCAS. The F-16 Auto-GCAS was proven successful for fighter-type aircraft with seven aircraft and eight lives saved from 2014 to 2018. The newly developed and tested Rapidly Selectable Escape Trajectory (RSET) system included a 5-path implementation which continuously updated at a rate of up to 12.5 Hz. The research employed Level 1 Digital Terrain Elevation Data (DTED) to identify the offending terrain and an augmented 6 Degree-of-Freedom (DoF) Stitched aerodynamic model to create terrain avoidance paths based on the aircraft's current state and location. The system then triggered when all paths predicted collision with the DTED and automatically activated the path which had the longest time until impact. A terrain safety buffer (TSB) of 200 ft added to the DTED to allowed for the time needed to process and execute the maneuver. The RSET system was flight tested against DTED using the Calspan Learjet 25D Variable Stability System (VSS). Path prediction error (PPE) did not meet the specified criteria and was larger than expected for the 30-second path predictions; however, at the maximum refresh rate of 12.5 Hz, the RSET system ensured terrain clearance in all cases tested. The RSET system was able to achieve and maintain target load factor and flight path angle with momentary overshoots. The system showed no tendency for nuisance. The RSET hand-back was favorable and can be used as a baseline for future Auto-GCASs.

This work is dedicated to the men and women who, in the line of service to our great country, lost their lives to CFIT. Let their sacrifice not be in vain when we now have the tools and the knowledge to prevent these tragedies in the future.

Acknowledgements

I would first like to thank Dr. Richard Cobb, my advisor. Thank you for giving me the knowledge needed to undertake this task and for providing the right balance of autonomy and guidance. I am proud to be part of a legacy of Auto-GCAS contributors that you have mentored.

I would also like to thank Colonel Angela Suplisson (PhD) for entrusting me to continue this important research. Your incredible energy and ability to see the big picture have been an inspiration. Thank you for sharing your wealth of experience and insight over these last few years.

I can't say enough about my TPS class 18A teammates. This was a challenging TMP and it wouldn't have happened without all of the hard work you put into this project. I would personally like to thank: Maj Carl "Solo" Gotwald, Capt Mike "Smoked" Bakun, Capt Mark "COBE" Hammond, Capt Shannon "Caddy" Mak Jian Ming, and Capt Ryan "Hex" Kolesar. Thanks for putting up with me and making a demanding year one of the most memorable of my life.

Finally I would thank my wife Rachel. For the last 10 years you have been by my side through all the ups and downs of this Air Force life. The last couple years have been some of the most difficult, but you've always supported me. Thank you for all the hours you've smiled at me and understood that although I was there physically, I was miles away mentally in the work in front of me. I wouldn't be who I am today without you. I love you.

Kenneth C. Gahan

Table of Contents

Page

Page

Page

Page

List of Figures

List of Tables

Table Page

List of Acronyms

3-D 3-Dimensional 17

ACB Aircraft Clearance Buffer 23, 24, 26

AFIT Air Force Institute of Technology 1

AGL Above Ground Level 94

AIB Accident Investigation Board 4

AoB angle of bank 125

ART Available Reaction Time 43

ATC air traffic control 2

ATON aid to navigation 2

Auto-ACAS Automatic Air Collision Avoidance System 14, 15

Auto-GCAS Automatic Ground Collision Avoidance System 1, 4, 6, 10, 14–20, 36, 38, 42, 51, 66, 147

BCA business case analysis 2, 3

CDR Conflict Detection and Resolution 14, 17

CFIT Controlled Flight into Terrain 1, 2, 4, 14, 27

CG Center of Gravity 45

CNC Computer Numerical Control 41

COTS commercial off-the-shelf 36

CPA Closest Point of Approach 17, 39

CRM crew resource management 2

DAS Data Acquisition System 97

DEM Digital Elevation Model 15, 20–22, 24, 27

DoF degree of freedom 9, 19, 31, 144

DROID Dryden Remotely Operated Integrated Drone 33

DSOC Defense Safety Oversight Council 2, 33

DTED Digital Terrain Elevation Data 11, 20–22, 27, 34

EGPWS Enhanced Ground Proximity Warning System 18, 27

EP evaluation pilot 11, 80, 81, 88, 137

ESCAPE Emergency Safe Calculated Autonomous Predetermined Exit 22

FAA Federal Aviation Administration 2

FBW Fly-by-Wire 51, 52

FL flight level (hundreds of feet above MSL) 5

FPA flight path angle 125

FSS Flight Sciences Simulator 51, 52

g-LOC g-induced Loss of Consciousness 19

GCAS Ground Collision Avoidance System 22, 39, 42

GCB Ground Clearance Buffer 23, 24, 26, 39, 74

GPWS Ground Proximity Warning System 17, 18

HaT Height Above Terrain 17

HUD Heads-Up Display 28, 30, 33

IATA International Air Transport Association 7

IFS In-Flight Simulator 51, 52

KIAS knots indicated airspeed 4

LOC-I Loss of Control In-flight 1

LPV Linear Parameter Varying 43

LTI Linear Time Invariant 44

MCP Maximum Continuous Power 69

MEDUSA Multi-Path Escape Decisions Using Sophisticated Algorithms 87

MSL mean sea level 4, 45

NACP Nervous-Aggressive Copilot 67

NAF Norwegian Air Force 5

NASA National Aeronautics and Space Administration 20

NED National Elevation Dataset 34

NGA National Geospatial-Intelligence Agency 20

NM nautical miles 5

ORT Oblique Recovery Trajectory 28

PA pressure altitude 89

PPE Path Prediction Error 89

qLPV quasi-Linear Parameter Varying 43

R&D Research and Development 14

RMS Root Mean Squared 31

RSET Rapidly Selectable Escape Trajectory 1, 9, 68, 87, 145

SecDef Secretary of Defense 2

SLUF straight, level, unaccelerated flight 89, 102

SOP standard operating procedure 2

SP Safety Pilot 81, 88

SRTM Shuttle Radar Topography Mission 20

SUT System Under Test 87

TAD Terrain Awareness Display 30

TAWS Terrain Awareness Warning System 6, 28

TBB Time-based Buffer 23, 24, 26, 31, 34, 38

TC test conductor 62, 88

TIC Theil's Inequality Coefficient 47

TMP test management project 11, 36, 51, 52, 64, 87

TPA Trajectory Prediction Algorithm 31, 66–69, 71

TPS Test Pilot School 1, 11, 12, 36, 64, 85, 87

TSB Terrain Safety Buffer 75

UAV unmanned aerial vehicle 1, 2, 16, 39

USAF United States Air Force 4, 11, 12

VISTA Variable Stability In-Flight Simulator and Test Aircraft 51, 52

VRT Vertical Recovery Trajectory 28

VSS Variable Stability System 11, 12, 37, 51, 52, 87

MULTI-PATH AUTOMATIC GROUND COLLISION AVOIDANCE SYSTEM
FOR PERFORMANCE LIMITED AIRCRAFT
WITH FLIGHT TESTS:
PROJECT HAVE MEDUSA

I. Introduction

Despite advances in technology and training, as of this writing Controlled Flight into Terrain (CFIT) remains a significant cause of fatal aircraft accidents [1]. Substantial progress has been made in developing and fielding Automatic Ground Collision Avoidance Systems (Auto-GCASs) for fighter aircraft and unmanned aerial vehicles (UAVs), but there has been limited work done for performance limited (Class III) aircraft. Class III aircraft, as defined in MIL-STD-1797B, are generally less maneuverable and have low power-to-weight ratios, and thus, recovery trajectories must be developed which take into account these performance limitations [2]. This work presents the research, design, and testing efforts to develop an Auto-GCAS for performance limited aircraft. The Auto-GCAS discussed herein, known as the Rapidly Selectable Escape Trajectory (RSET) system, leveraged previous Air Force Institute of Technology (AFIT) and Test Pilot School (TPS) research efforts and sought to significantly advance Auto-GCAS technology.

1.1 Background

As of 2019, CFIT was a primary reason for aircraft total losses and fatalities [3]. In fact it was only in 2014 that Loss of Control In-flight (LOC-I) overtook CFIT as the leading cause of fatal accidents in air transportation [4]. Figure 1.1 presents a

ten-year look at CFIT accident rates in commercial aviation [4]. According to the Federal Aviation Administration (FAA), "CFIT occurs when an airworthy aircraft is flown, under the control of a qualified pilot, into terrain, water, or obstacles with inadequate awareness on the part of the pilot of the impeding collision" [5]. The issues that arise which lead to CFIT then are directly related to the pilot and crew. These issues are both external (weather/visibility, air traffic control (ATC) error, aid to navigation (ATON) malfunction, etc.)and internal (poor crew resource management (CRM), failure to adhere to standard operating procedures (SOPs), poor cross-check, etc.) [6]. Over the years, manual warning systems have been put into service to notify crew of impending terrain impact, yet CFIT still occurs.

To date, the majority of Auto-GCAS research has focused on fighter type aircraft and UAVs. The successful F-16 Fighting Falcon Auto-GCAS program can be traced back to the 1980s [7]. What ultimately catalyzed the program was a 2003 memorandum by then Secretary of Defense (SecDef) Donald Rumsfeld challenging military leaders to reduce preventable accidents by 50% [8]. This prompted a Defense Safety Oversight Council (DSOC) business case analysis (BCA) which identified that CFIT was in fact the #1 cause of fighter pilot fatalities [9]. In 2007 SecDef Robert Gates pushed for a reduction in preventable accidents of 75% [10]. The F-16 Auto-GCAS system was fielded in 2014 and has since saved eight pilots and seven aircraft [11–13].

UAVs provide a cost-effective and ideal platform for researchers to develop and test Auto-GCAS technologies. Many effective approaches and solutions to prevent UAV ground collisions have been developed, but those solutions are not necessarily applicable to transport aircraft. This research continued the foundational works by Suplisson and Trombetta that have been the primary direct efforts towards making multi-path Auto-GCAS a reality [14, 15].

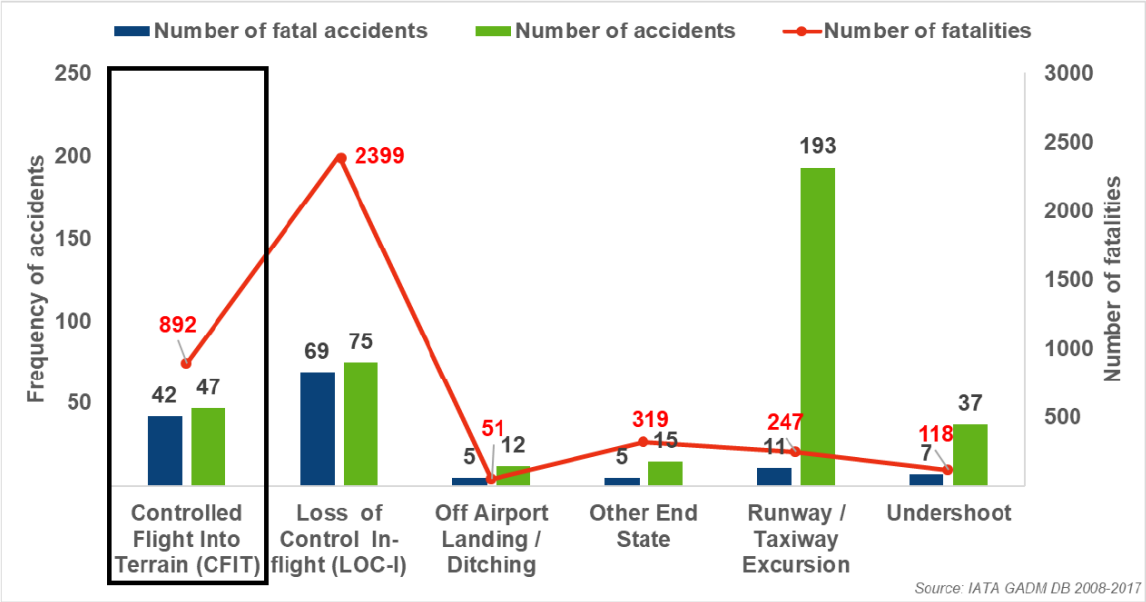

Figure 1.1. Top Commercial Aviation Fatal Accident Categories 2008-2017 [4]

1.2 Research Problem Motivation and Description

Although a thorough BCA had not been performed as of 2018, data existing supports the need for Auto-GCAS on performance limited aircraft. Col Peter Mapes, author of the 2006 Fighter/Attack BCA, stated "the reaction timing of the human beings in the cockpits sometimes fell below the reaction timing required to avoid collision with the ground..." [16]. Clearly reaction time and human error is not a problem just for fighter aircraft, but all aircraft. 2011 data from C-130 Hercules builder Lockheed Martin identified 30 CFIT accidents for that aircraft over its life resulting in 433 deaths not including the HAZE 01 mishap described next in Section 1.2.1 which brings the total to 31 CFITs and 438 deaths for C-130s alone [17]. Furthermore in 2017 a group of students from the U.S. Air Force Academy, under the supervision of Col Angela Suplisson, performed an initial business study and found that at least five USAF C-130 CFITs could have been prevented by Auto-GCAS. Those five CFITs alone account for 34 lives lost and $385M worth of aircraft destroyed [18].

To highlight the need for Auto-GCAS on performance aircraft, two tragic but preventable mishaps are presented below.

1.2.1 Case Studies: HAVOC 58 and HAZE 01.

This section discusses two CFIT incidents where an Auto-GCAS system would have likely prevented impact with terrain.

HAVOC 58.

The information for the following case study was provided in an article by the Flight Safety Foundation [19].

HAVOC 58, a United States Air Force (USAF) Lockheed C-130H Hercules, took off from Jackson Hole Airport in Jackson, Wyoming at 2247L on 17 August 1996. Three minutes and 20 seconds later the aircraft impacted Sheep Mountain east of Jackson at an altitude of 10,392 feet mean sea level (MSL). The USAF Accident Investigation Board (AIB) determined that the crew

> "failed to avoid the mountainous terrain ahead. They were complacent and not situationally aware of their proximity to that terrain. Visual cues were limited by a dark, moonless night. Radar information, which would have been showing on the navigators radar scope, was not correctly interpreted. Arrival/departure charts were not studied by the pilot/copilot and were incorrectly interpreted by the navigator"[20].

The combination of errors led to the deaths of the eight crew members and one passenger. At the time of impact the estimated aircraft states were a magnetic heading (ψ) of 77 degrees, 173 knots indicated airspeed (KIAS), and climbing flight with a pitch angle (θ) of seven to eight degrees. HAVOC 58 struck the mountain 500 ft below the ridge. Beginning 30 seconds from the time of impact, had the pilot increased their pitch angle by just 3.3^o they would have avoided the ridge-line. The presence of a functioning Auto-GCAS system on HAVOC 58 could have alerted the crew of a

Figure 1.2. HAVOC 58 Flight Path

potentially dangerous aircraft state and, if needed, executed an escape maneuver to avoid terrain.

HAZE 01.

The information for the following case study was provided by a report produced by the Swedish Accident Investigation Authority [21].

HAZE 01, a Norwegian Air Force (NAF) Lockheed-Martin C-130J Super Hercules, took off from Harstad/Narvik Airport in Norway at 1340Z with a flight planned route to Kiruna Airport in Sweden. Following takeoff the crew climbed to flight level (hundreds of feet above MSL) (FL) 130 and established a holding pattern 45 nautical miles (NM) south of the departure airport. The crew established a holding pattern for one hour, then headed east towards the destination airport. At 1454Z HAZE 01 was cleared from FL 130 to FL 100. One minute later upon contacting Kiruna Airport HAZE 01 was cleared to descend to FL 70, which it reached at 1457Z. 29 seconds later, the aircraft impacted Kebnekaise mountain 150 ft below the ridge-line, as shown in Figure 1.4. Similar to HAVOC 58, had the pilot adjusted the aircraft

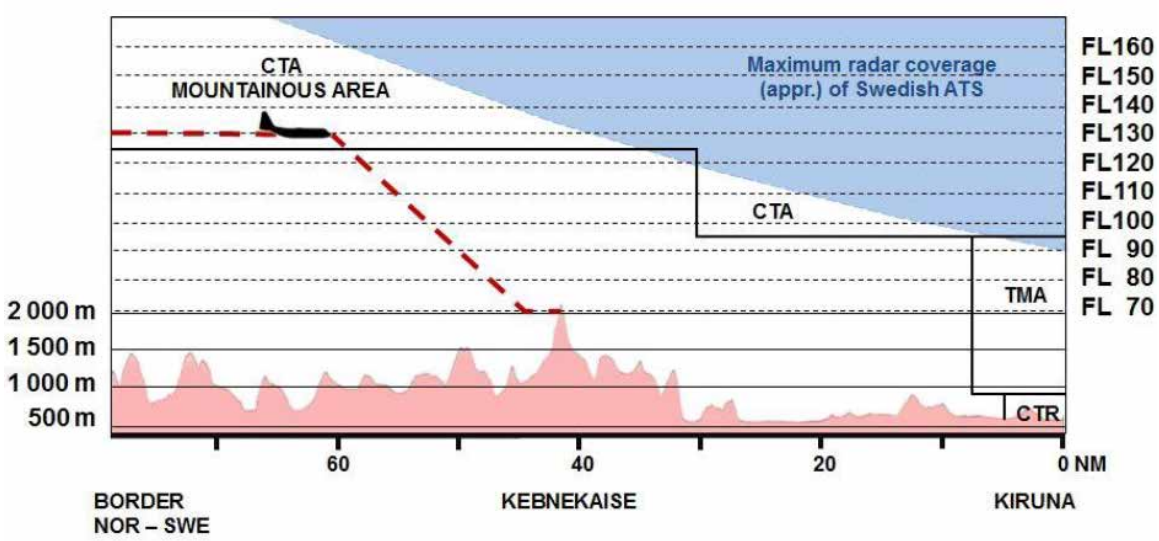

Figure 1.3. HAZE 01 Flight Path [21]: (CTA = "control area", TMA = "terminal control area")

flight path by 1^o 30 seconds earlier, the aircraft would have avoided the mountain. A functioning Auto-GCAS could have easily avoided the terrain and saved the 4 crew members and 1 passenger on board.

It is worth noting that although the crew members of HAZE 01 were not U.S. military they were all seasoned aircrew who were trained and certified in the United States. This accident could have just as likely happened to a proficient U.S. crew.

1.2.2 Mishap Causal Factors.

In the two cases just presented, as well as all CFIT incidents, a number of contributing factors are involved. For HAVOC 58 it was mostly crew error that led to the CFIT occuring. For HAZE 01 it was a combination of misunderstanding, miscommunication, and technological shortfalls. First, the crew of HAZE 01 believed they were under the control of Kiruna Approach and within Kiruna's radar coverage, which they were not. Second the Terrain Awareness Warning System (TAWS) installed on the C-130J lacked terrain data above 60^o N latitude where the crew was transiting,

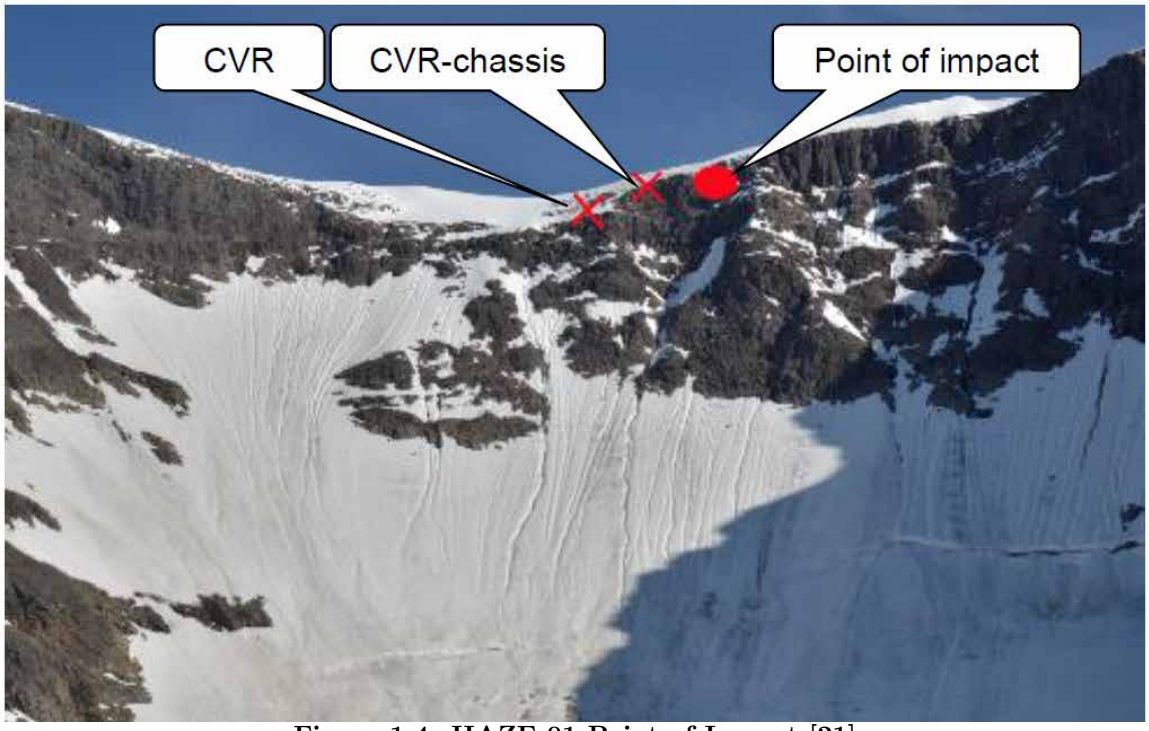

Figure 1.4. HAZE 01 Point of Impact [21]
(CVR = "cockpit voice recorder")

as shown in Figure 1.5.

Figure 1.6 shows a summary of all CFIT contributing factors for commercial aircraft according to the International Air Transport Association (IATA). An asterisk, " * ", is used to indicate causal factors that this research identified could either be prevented by or would not negatively affect a well-designed and functioning Auto-GCAS. With sufficient motivation given, the following sections describe the goals and limitations of this research.

1.3 Objectives and Scope

The purpose of this research was to further develop, improve, and flight test an Auto-GCAS system for performance limited aircraft. As with all USAF ground collision avoidance systems, this system was designed based on the principal requirements

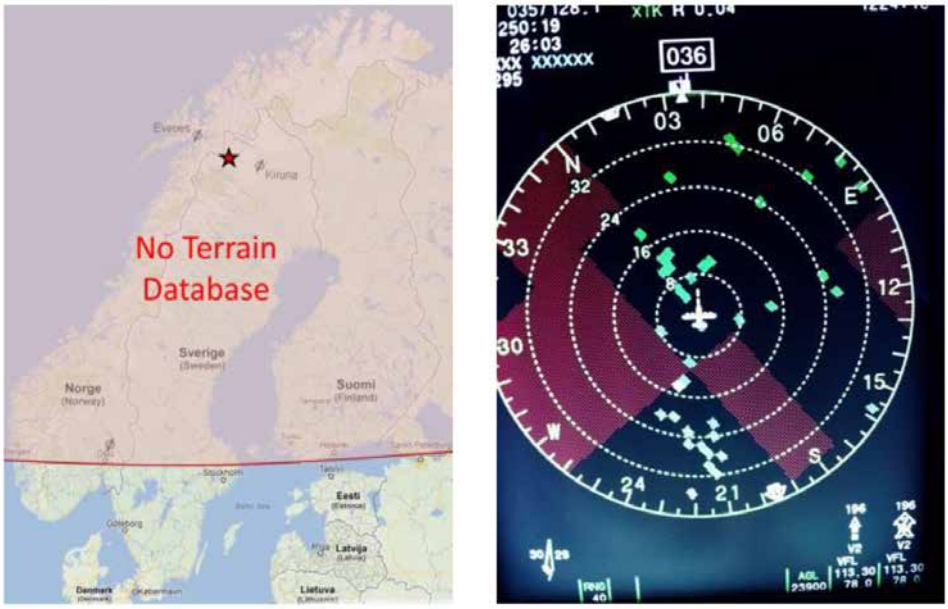

(a) TAWS Void Above 60^o N ($\star$ indicates HAZE 01 crash site)

(b) TAWS display. Voids appear in magenta.

Figure 1.5. TAWS Terrain Void [21]

Latent Conditions (deficiencies in...)	
Regulatory Oversight	56%
Technology & Equipment	47%
Safety Management	32%
Flight Operations	21%
Flight Ops: Training Systems	15%
Environmental Threats	
Meteorology	44%*
Ground-based nav aid malfunction or not available	41%*
Nav Aids	41%*
Poor visibility / IMC	38%*
Terrain / Obstacles	18%
Airline Threats	
Aircraft Malfunction	3%
Autopilot / FMS	3%
Avionics / Flight Instruments	3%
Maintenance Events	3%
Operational Pressure	3%

Flight Crew Errors (related to...)	
SOP Adherence / SOP Cross-verification	38%*
Intentional	26%
Unintentional	12%*
Callouts	15%
Manual Handling / Flight Controls	15%*
Undesired Aircraft States	
Controlled Flight Towards Terrain	41%*
Vertical / Lateral / Speed Deviation	41%
Unnecessary Weather Penetration	12%
Unstable Approach	6%
Long/floated/bounced/firm/ off-center/crabbed land	3%
Countermeasures	
Monitor / Cross-check	38%
Overall Crew Performance	35%
Communication Environment	12%
Leadership	12%
Plans Stated	12%

Figure 1.6. Worldwide CFIT Contributing Factors (* denotes Auto-GCAS unaffected by) [4]

of [22]:

1. Do No Harm
2. Do Not Impede Mission Performance
3. Avoid Ground Collision

These requirements, which are listed in priority order, were key to creating a system which would be acceptable to the operational aviation community.

1.3.1 Research Objectives.

This research continued the works of Suplisson, Trombetta, and Sorokowski et al. Suplisson's research addressed how to determine the optimal ground collision avoidance path. Trombetta conducted the first USAF flight test of a heavy aircraft ground collision avoidance algorithm. Sorokowski et al. leveraged the success of the F-16 Auto-GCAS program to develop and flight test Auto-GCAS on a small UAV. As such, this research adopted several of their recommendations as objectives. These objectives are listed briefly below and are described in detail in later chapters. Each objective, where applicable, includes the reference from which it was motivated.

1. Apply 6-degree of freedom (DoF) equations of motion for aircraft path prediction [14]
2. Allow for a variable aircraft initial state [15]
3. Determine necessary number of RSETs [15, 23]
4. Integrate auto-throttle for maneuver execution [14]
5. Perform continuous path analysis, even during maneuver [15]
6. Achieve $\geq$ 6 Hz operation with MATLAB implementation [14]

7. Include wind and density altitude effects [15, 23]

Additionally the author, through careful review of existing literature, has identified other important objectives that have yet to be explored.

8. Use of identical control laws for both path prediction and maneuver execution
9. Identify multi-path Auto-GCAS nuisance criteria
10. Determine maneuver termination criteria

Ultimately this research aimed to not only demonstrate the feasibility of Auto-GCAS for performance limited aircraft but to also provide an RSET flight-tested solution that could be adapted to multiple platforms.

1.3.2 Flight Test Objectives.

The overall test objective was to demonstrate the utility of the RSET system as a multi-path automatic ground collision avoidance system for performance limited aircraft. The specific test objectives were to:

1. Demonstrate the path prediction accuracy of the RSET system.
2. Demonstrate the impact of changing the refresh rate on the RSET system's ability to calculate an achievable escape path
3. Observe the RSET system tendency to nuisance activation
4. Observe the control hand-back of the RSET system after maneuver termination

The rationale behind the choice of flight test objectives is covered in Section 3.7.

1.4 Constraints

Due to available resources, the Calspan Learjet 25D (LJ-25D) Variable Stability System (VSS) was used as a surrogate for performance limited aircraft. As is discussed throughout this document the maneuver performance of the LJ-25D was restricted to simulate the capabilities of the objective military aircraft. Additionally all testing was conducted as part of a USAF TPS test management project (TMP). TMPs are limited to a fixed number of test flights within a two week testing window and have several safety limitations. Operational testing of an Auto-GCAS would ultimately requires more test flights and higher risk test points than those presented here.

The auto-throttle in the LJ-25D VSS was not capable of setting consistent throttle settings and, as such, was not used. Because of this, when an escape maneuver was commanded, the evaluation pilot (EP) had to manually advance the throttles to the required setting. This added some variability to the model path prediction and actual path performance. This was accepted since it was already understood that the engine model was low fidelity and would induce error even with an auto-throttle. The engine model is discussed further in Section 3.2.2.

Many of the design choices made with respect to algorithm structure, propagation length, and integration step size were made due to computational performance limitations. With increased computing power more robust or sophisticated solutions may become viable.

Navigation errors and Digital Terrain Elevation Data (DTED) accuracy were not evaluated in this project. As such, any reference to the distance between the aircraft and terrain refers to the distance between the aircraft's navigation solution and the DTED loaded in the research laptop. This was different than the actual distance between the aircraft and real terrain features since DTED elevations and navigation solutions are known to have error.

1.5 Limitations

The primary limitation identified is that this research relied upon existing models available and it was beyond the scope of this work to develop a custom model. Recommendations regarding application specific model tailoring are presented later.

1.6 Assumptions

This research sought to be as rigorous and portable to multiple aircraft as possible. Nevertheless, assumptions were necessary given the time and resources available. First, it is assumed that the Calspan Learjet 25D VSS can serve as a surrogate for an actual performance limited aircraft as defined in Section 2.9. Second it is understood that the algorithm presented herein, though designed for use on a performance limited aircraft, may not necessarily be applicable to all such aircraft. Each aircraft has its own unique flight characteristics and careful consideration and testing is needed to tailor an Auto-GCAS solution to aircraft performance. Lastly, it is assumed that the design choices and navigation/DTED accuracy discussed in Section 1.4 do not invalidate the results presented herein.

1.7 Expected Contributions

The results of this research will ultimately increase the growing body of knowledge for ground collision avoidance systems. It is the author's hope that the efforts described herein will be a significant leap forward towards developing and fielding an effective and life-saving Auto-GCAS for performance limited aircraft. Through extensive simulator testing and flight testing at USAF TPS the system presented here should prove to be both a valid and feasible solution for CFIT prevention in bomber/transport aircraft.

1.8 Chapter Summary and Document Outline

This chapter serves as a starting point for presenting the research efforts and results of developing a multi-path Auto-GCAS. From the tragic CFIT accidents described and the data presented herein, the case for Auto-GCAS was made. Chapter II presents a review of literature from academia and industry regarding GCASs and is the body of knowledge upon which this research effort expands. Chapter III outlines the methodology used and Chapter IV presents the results of real-world manned flight test. Lastly, Chapter V presents the conclusions, recommendations, and lessons learned which will be beneficial for subsequent work supporting this important research. Additionally there are a number of appendices which provide amplifying information and are referenced throughout this document: Appendix A: Supporting Figures, Appendix B: Daily Flight Reports (from flight test), Appendix C: Data Analysis Procedures, Appendix D: Test Points, Appendix E: Path Prediction Error (explained in Chapter III), Appendix F: Virtual Terrain Activation Results (explained in Chapter III), Appendix G: Software Configuration Tracker, Appendix H: 412th Test Wing Objective Rating Criteria, Appendix I: Digital Appendix, Appendix J: Control Hand-back in-flight survey, and Appendix K: Aircrew Comments.

II. Literature Review

2.1 Overview

Chapter II provides the background for this research. First a common vernacular when discussing and categorizing Ground Collision Avoidance Systems is established. Next, several existing GCASs both operational and still in Research and Development (R&D) are presented. Then the computer model on which this research is built, the Learjet 25D Stitched Model, is introduced. Lastly, various classification criteria as well as the test framework planned for this research are presented to set the stage for the methodology described in Chapter III.

2.2 Conflict Detection and Resolution

With the increasing ubiquity of autonomous and semi-autonomous systems, extensive research has been done on Conflict Detection and Resolution (CDR) systems for applications on land, sea, and air. While significant work has been accomplished in recent years with regard to aircraft CFIT avoidance, the majority of CDR methods focus on air-to-air collision avoidance solutions [14]. Following the structure of Suplisson and Trombetta, this chapter will discuss CDR as it relates to Auto-GCAS in five of the six key design factors identified by Kuchar and Yang [14, 15, 24]. The sixth design factor that Kuchar and Yang discuss is "Multiple Conflicts", but that is only applicable to Automatic Air Collision Avoidance Systems (Auto-ACASs). The Kuchar and Yang design factors presented here are:

- State Propagation
- State Dimensions
- Conflict Detection Threshold

- Conflict Resolution
- Resolution Maneuvers.

This research has also identified other key implementation areas that distinguish Auto-GCAS approaches, which are:

- Model Fidelity
- Trajectory Limitation
- Digital Elevation Model (DEM) Post Capture
- Safety Buffer.

2.2.1 State Propagation.

Kuchar and Yang discussed three approaches to propagating the state of an aircraft to predict its location at some time in the future [24]. These three methods, which are depicted in Figure 2.1, are identified as (a) nominal, (b) worst-case, and (c) probabilistic. Before diving into these scenarios, it is worth noting that Kuchar and Yang were addressing Auto-ACAS which involves an avoiding "ownship" aircraft and an avoided "intruder" aircraft, such as instances described by Richardson et al. [25]. In the case of Auto-GCAS the avoiding aircraft is maneuvering to avoid the ground, which is of course stationary. This is an important distinction to keep in mind when considering the applicability of each method.

In the nominal case, the path of the aircraft is forecast along one trajectory, such as using current location, velocity, and heading to predict a future location assuming no change in velocity or heading. The Auto-GCAS system on the F-16, which is discussed later in detail in Section 2.3.2.1 relies on a nominal path prediction based on a roll to wings-level and a 5-g pull-up maneuver [26]. A clear limitation of this

method is the inability to account for trajectory uncertainty, introduced by such things as navigational error or atmospherics such as wind.

The worst-case approach assumes "that an aircraft will perform any of a range of maneuvers. If any one of these maneuvers could cause a conflict, then a conflict is predicted" [24]. It will be shown that this approach is the most relevant for developing a minimum nuisance Auto-GCAS system for heavy aircraft. In the case of Auto-GCAS, however, the "worst-case" corollary is "maximum performance" [14, 15]. In other words, the Auto-GCAS implementation of the "worst-case" approach is at the point where the aircraft is required to use the maximum of some performance parameter, be it load factor, bank angle, etc., else the aware aircrew would consider the maneuver a nuisance.

Lastly the probabilistic method is implemented either by applying uncertainty analysis to a nominal model or a set of possible trajectories are given weights based on their likelihood of occurring. Sorokowski et al. use a probabilistic approach to account for trajectory uncertainty in their development of a small UAV Auto-GCAS system. Their system is discussed in Section 2.3.3.1.

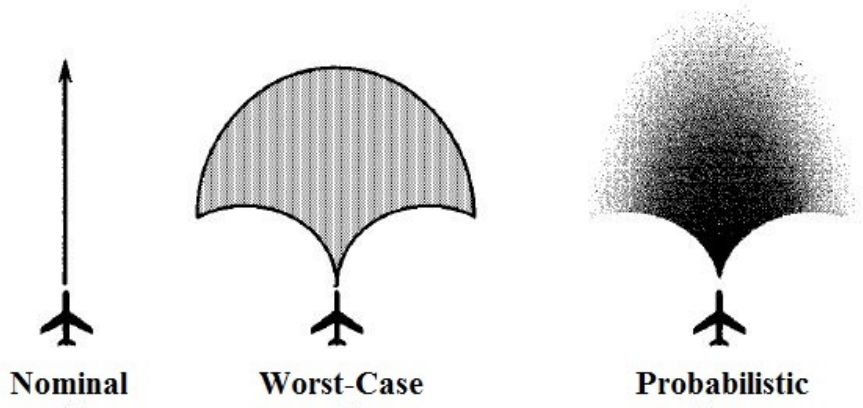

Figure 2.1. Kuchar and Yang State Propagation Methods [24]

2.2.2 State Dimensions.

Kuchar and Yang described state dimensions as the planes in which the CDR model operates [24]. This means the horizontal plane, the vertical plane, or both. Through their exhaustive research, Kuchar and Yang identified that the majority of CDR models operated in either the horizontal plane or both the horizontal and vertical plane, with only one, Ground Proximity Warning System (GPWS), operating in the vertical plane. Suplisson identified the necessity of 3-Dimensional (3-D) state information for Auto-GCAS so that terrain in all directions can be avoided [14]. Consequently, among Auto-GCAS, 3-D state information is the most common as is shown in the survey of ground avoidance systems in Section 2.3.

2.2.3 Conflict Detection.

There are a number of ways in which CDR algorithms can determine if a potential conflict is present. These methods include, but are not limited to, time until Closest Point of Approach (CPA), horizontal range to a terrain feature, Height Above Terrain (HaT), or a combination of these. For instance, Suplisson examined a left-center-right look-down method wherein the terrain to the left and right as well as beneath the optimal path is evaluated for collision detection [14]. Typically GCAS algorithms analyze the terrain directly beneath the predicted path to determine if a conflict exists and rely on safety buffers, discussed in Section 2.2.9, to account for maneuver delays or lateral terrain features.

2.2.4 Conflict Resolution.

Of the five conflict resolution methods identified by Kuchar and Yang and discussed in depth by Suplisson, the prescribed and optimal resolution methods are the

most relevant to Auto-GCAS applications [14, 24, 27]. Force field[1] provides neither the predictability of a prescribed maneuver nor the nuisance minimization of the optimal maneuver. By definition, manual and no resolution approaches are irrelevant for Auto-GCAS. As such, the force field, manual, and no resolution methods will be ignored for the discussion herein.

Prescribed solutions can take on a variety of forms. They can be fixed or flexible and have one or multiple evasion options. GPWS and Enhanced Ground Proximity Warning System (EGPWS) both provide a simple "PULL UP" command when the conflict is in the warning area [28, 29]. NASA's Small UAV, by contrast, used an on-board autopilot to calculate its three recovery trajectories. Though these paths were still prescribed, the autopilot adapted to changes in the UAV's flight profile [23].

The optimal conflict resolution sought to find the best possible solution to a given set of rules and objective. In the case of Auto-GCAS, an objective could be to use maximum control, or performance, while avoiding ground collision subject to the limits of the aircraft. A problem of this form was addressed by Suplisson, and will be discussed in Section 2.3.3.3 [14]. The optimal resolution is by nature adaptive and unique for each situation.

2.2.5 Resolution Maneuvers.

Resolution maneuvers refer to the myriad of possible escape trajectory options the model calculates and allows. The escape maneuvers can involve the vertical plane, horizontal plane, a change in speed, or a combination. Note that this is different from state dimension, such as how the F-16 Auto-GCAS accounted for terrain in three dimensions, but only determines a climbing (vertical) escape and not a lateral escape or speed change.

[1]The force field method, which is generally used in AACAS scenarios, treats each aircraft as a charged particle and relies on electrostatic physics equations to determine avoidance and ensure separation. [24]

2.2.6 Model Fidelity.

Model fidelity is important as it encompasses the degree to which a model can accurately predict the future location of the aircraft. A highly accurate model can be used to make reliable estimates of possible future locations, including during an avoidance maneuver. Increasing fidelity, be it by moving from 3 to 6 DoFs or including wind and other perturbations, comes at the expense of increased computation requirements. There is a balance that must be struck between the fidelity of the model and the need to operate in real-time. Indeed the majority of systems discussed here rely upon 3-DoF point mass models for path propagation. As described in Chapter III, this research utilized a high fidelity 6-DoF model to accurately estimate the aircraft states continuously throughout the aircraft's flight and during escape maneuvers, and in a timely manner.

2.2.7 Trajectory Limitations.

Trajectory limitations describe the driving factor in why one escape profile would be preferred over another. In all cases, the Auto-GCAS is operating in a manner so as to avoid nuisances, but not all systems are inherently capable of the same maneuvers. For instance the F-16 was capable of more than a 5-g pull, yet it was designed to use less than maximum load factor to account for the fact that the pilot may have become incapacitated due to g-induced Loss of Consciousness (g-LOC). Other systems are limited by the structural or performance limit of the aircraft itself. An Auto-GCAS operates so that these limitations are not exceeded, but take full advantage of the maximum flight envelope of the aircraft.

2.2.8 DEM Post Capture.

Common among Auto-GCASs proposed and is use is the use of a Digital Elevation Model (DEM) to serve as the terrain which is to be avoided. A DEM is "a representation of a surface in terms of elevation values that change with position" [30]. This elevation data is usually presented in matrix form with uniformly spaced elevation values, or "posts". Among DEMs, Digital Terrain Elevation Data (DTED), which refered to terrain data gathered from either the National Geospatial-Intelligence Agency (NGA) or National Aeronautics and Space Administration (NASA) Shuttle Radar Topography Mission (SRTM) DTED, is the most common. The manner in which the projected aircraft position is compared to this terrain to determine if a conflict exists, however, varies. Table 2.1 shows the various levels of DTED and the corresponding resolution of the terrain and how far apart the individual height measurements, or "posts", were spaced. In all cases the DEM is not continuous, and therefore some method must be used to resolve the aircraft's propagated path compared to a set of discrete DTED posts. The methods found in current research included scanning, interpolating, or placing a buffer, or "bubble", around the aircraft. These methods are depicted in Figure 2.2, and are described next.

Table 2.1. Digital Terrain Elevation Data (DTED) Types [14, 31]

DTED Level	Post Spacing (arc-sec)	Post Spacing (horiz. distance)	Cells per Degree
DTED-0	30	$\approx$ 900 m	120
DTED-1	3	$\approx$ 90 m	1,200
DTED-2	1	$\approx$ 30 m	3,600
DTED-3	$\frac{1}{3}$	$\approx$ 10 m	10,800

2.2.8.1 Scan Method.

There are a variety of scan methods but each work essentially by widening the projected future path so as to ensure one or more DTED posts are captured. Various scan methods are employed by the F-16, NASA SUAV, and UAV P-GCAS [23, 32]. An advantage of the scan method is that, assuming a wide enough scan pattern is used, the highest DTED post within a given range bin is used to determine terrain height for the entire bin, thus being conservative. The inherent disadvantage to this method is that although within that range bin there may exist a trough through which it is both safe and desirable to fly, the trough is not identified and would be considered a nuisance by the aircrew. The scan method also allows for track uncertainty to be included in the scan pattern, but as will be shown with the NASA SUAV research, this does not guarantee that the actual flight path will fall within the scan [23].

2.2.8.2 Interpolation Method.

The interpolation approach solves the problem of discontinuous elevation data by using the projected location of the aircraft and interpolating between the discrete DEM posts. There are numerous numerical methods to accomplish this interpolation. Suplisson examined methods that use the nearest DTED post, linear interpolation

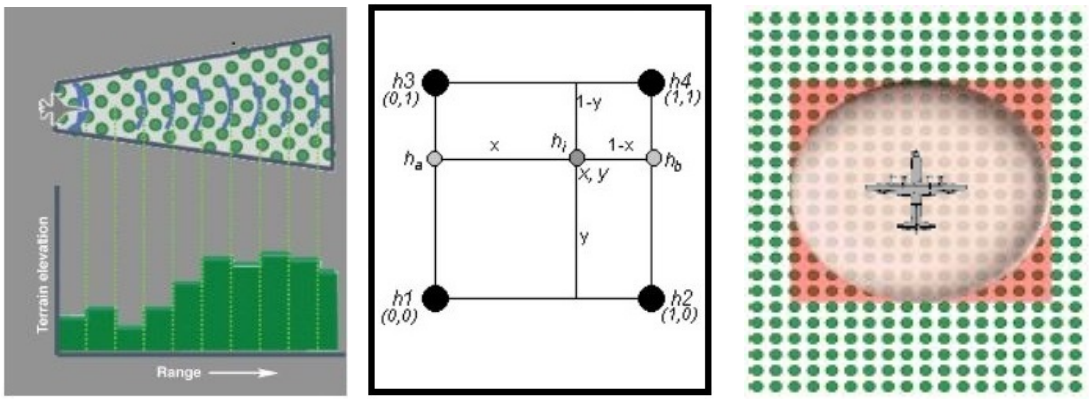

(a) Scan [23] **(b) Interpolation [33]** **(c) Bubble [15]**

Figure 2.2. DEM Post Capture Methods

between neighboring posts, as well as cubic and spline interpolations [14]. An advantage of interpolating is that the projected path of the aircraft need not be artificially widened to ensure post capture. This allows for the projected path and any error or uncertainty to be analyzed independently. Consequently the DTED posts do not guarantee that a higher terrain feature doesn't exist between discrete posts, so interpolating could place the aircraft below the actual terrain. This problem also exists with the scan and bubble methods but to a lesser extent since interpolating does not inherently add in any safety buffer (discuss in Section 2.2.9).

2.2.8.3 Bubble Method.

The bubble method works by enclosing the aircraft in an ellipsoidal "buffer" that is sized appropriately to capture the terrain posts. The bubble method was used by Trombetta for his Have Emergency Safe Calculated Autonomous Predetermined Exit (ESCAPE) algorithm, discussed further in Section 2.3.3.2 with the modification of using the sphere to define the dimensions of a quadrilateral rather than using the sphere directly [15]. The bubble approach has the benefit of allowing track uncertainty to be evaluated directly while still providing some inherent terrain clearance margin. The disadvantage is that, as with the scan method, the necessary size of the bubble could trigger nuisance activations when flying laterally near terrain or attempting to fly through a saddle.

2.2.9 Safety Buffer.

The design of and inclusion of a safety buffer in a Ground Collision Avoidance System (GCAS) is prudent and necessary to account for errors in both the path prediction of the aircraft as well as the terrain uncertainty in the DEM. This research has identified multiple approaches to implementing an intentional safety buffer: adding

an aircraft clearance buffer (ACB) around the aircraft, adding a Ground Clearance Buffer (GCB) to the terrain itself at each DEM post, adding a Time-based Buffer (TBB) to the projected path, or a combination of these three.

2.2.9.1 Aircraft Clearance Buffer (ACB).

As discussed in Section 2.2.8, the bubble method is a potential solution to ensuring the aircraft path cannot simply fly between terrain posts. In a similar fashion the ACB can be used to provide an offset from the terrain. Figure 2.3 depicts three 300 ft (92 m) radius bubbles against DTED-1 terrain with 90 m spacing. If it fact DTED-2 terrain was used, the bubble radius could be made much smaller and still capture the same number of DTED posts. It might still be desirable, however, to keep the radius at 300 ft to allow protection for any of the aforementioned sources of error. There are two downsides to the bubble buffer method; it provides an inconsistent safety buffer and is not consistent computationally. Referring again to Figure 2.3 from left to right, the equal red, green, and blue spheres show instances where, versus the same level terrain, they provide differing terrain clearances. The red sphere which is positioned directly above a single DTED post provides the maximum buffer of one radius. The buffer provided by the green sphere which is positioned between two DTED posts is governed by Equation 2.2. In the scenario given, the green sphere only provides a buffer of 79.6 m, a reduction of 13%. The blue sphere "rests" on four DTED posts, and the buffer it provides is given by Equation 2.3. In this scenario with assumed symmetric post spacing, the buffer provided is 65.7 m, a reduction of 28%. It is clear that these deviations could lead to a dangerous situation if not accounted for properly. It is worth noting that the ACB need not be a sphere. Using superquadrics, the ACB could mimic the shape of the aircraft itself [34].

$$B_1 = r \tag{2.1}$$

$$B_2 = r * \sqrt{1 - \frac{0.5d_1}{r}} \tag{2.2}$$

$$B_4 = B_2 * \sqrt{1 - \frac{0.5d_2}{B_2}} \tag{2.3}$$

where:

r = radius of sphere

d_1 = distance between posts in x (or y) direction

d_2 = distance between posts in y (or x) direction

2.2.9.2 Ground Clearance Buffer (GCB).

The implementation of a GCB can be a simple as adding a fixed height value to each terrain post, as in Figure 2.4b. This method is favored by several researchers as shown in Table 2.4. Benefits of using a GCB are its ease of application and consistency. As already mentioned, applying a GCB only requires adding a constant value to the matrix of DEM height values. There are of course numerous ways to adjust these values such as for various terrain classifications, but a constant value is the most basic and common usage. The GCB also overcomes the problem with varying safety buffer provided by the Aircraft Clearance Buffer (ACB). A disadvantage to this approach is that it does not directly apply an additional lateral safety buffer. This is most problematic with steeply rising terrain. This shortcoming can be mitigated by the addition of a TBB.

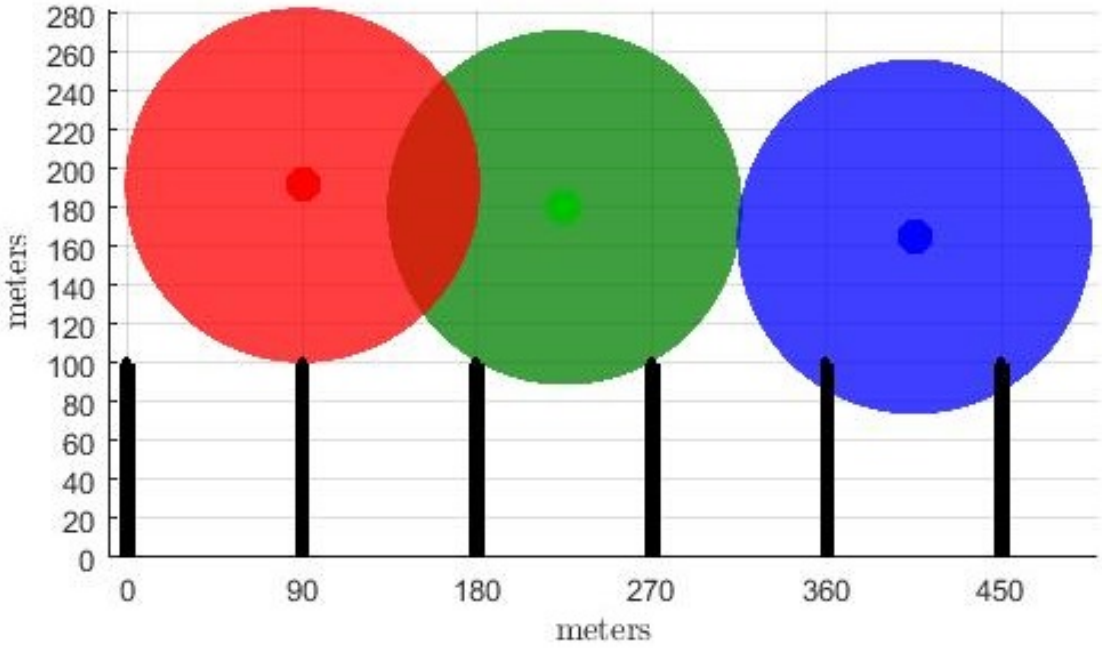

(a) Lateral View

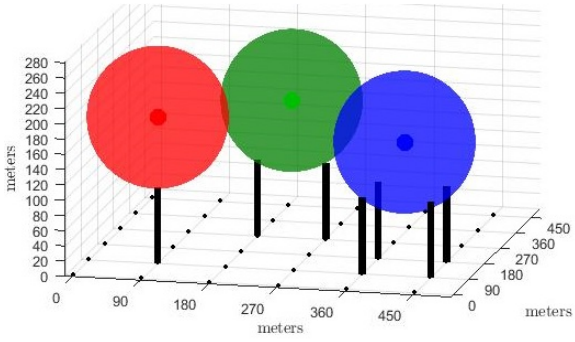

(b) 3-D View

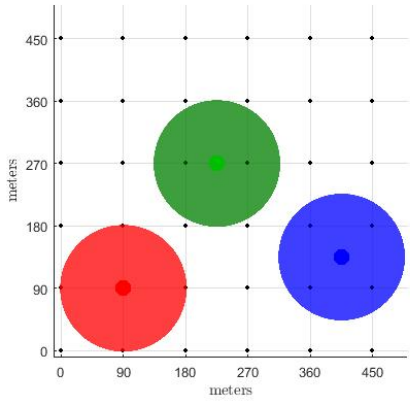

(c) Overhead View

Figure 2.3. Variation in terrain clearance from ACB due to relation to DEM post

2.2.9.3 Time-based Buffer (TBB).

The TBB is applied by using a fixed or variable amount of time, δt_B, to project the current aircraft location forward before calculating the escape trajectories. This is beneficial because it provides lateral terrain separation and accounts for any delays in algorithm response or aircraft dynamic response, such as pitch rate. The TBB can be calculated by the current or recent average aircraft velocity and heading and δt_B to estimate a future position. The TBB is highly dependent on the aircraft states used to predict the future position so care must be taken when applying a TBB to a highly maneuvering aircraft. The TBB is often used in conjunction with the ACB, as with Have ESCAPE, or GCB, as with F-16 Auto-GCAS [15, 35]. Trombetta's use of an ACB and TBB is shown in Figure 2.4b.

Ultimately, all buffer methods are useful for accounting for the uncertainties in the propagated aircraft trajectory and DEM posts. For each Auto-GCAS application the designer will need to identify which method produces the quickest and most accurate results while providing the desired level of safety.

With the defining characteristics of Auto-GCASs identified, next a brief survery of existing systems is presented.

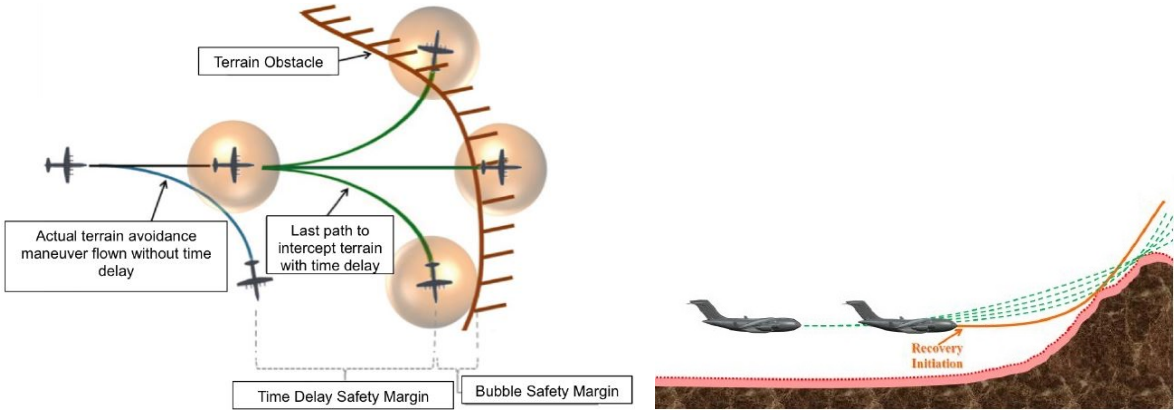

(a) ACB and TBB [15] **(b) GCB [14]**

Figure 2.4. Safety Buffer methods used by Trombetta (a) and Suplisson (b)

2.3 Survey of Ground Collision Avoidance Systems

Over the years a number of systems, mostly manual, have been developed to assist in preventing CFIT. Kuchar and Yang, as well as Suplisson, provide an in-depth survey of many of these systems. For the purposes of this research only systems whose primary source of terrain information is DTED or another DEM are discussed. To provide background, a few manual systems will be presented before moving on to automatic systems.

2.3.1 Fielded Manual Systems.

Herein fielded systems are defined as those that are currently in use in either military or commercial applications. Manual systems are those that provide a prediction of collision but do not automatically control the aircraft to avoid collision.

2.3.1.1 Enhanced Ground Proximity Warning System (EGPWS).

The Enhanced Ground Proximity Warning System built by Honeywell International Inc. "uses aircraft inputs including geographic position, attitude, altitude, airspeed, and glideslope deviation. These are used with respect to internal terrain, obstacle, and airport databases to predict a potential conflict between the aircraft flight path and terrain or an obstacle. A conflict will result in the EGPWS providing a visual and audio caution or warning alert" [28, 29]. While EGPWS does predict terrain collisions and even provides a visual display of surrounding terrain, the extent of the resolution maneuver is to advise the pilot "OBSTACLE AHEAD, PULL UP". An interesting feature of EGPWS is what Honeywell calls "Envelope Modulation" where, at certain airports, higher resolution terrain data and modified alerting margins are used to reduce nuisance and missed alerts [28, 29]. Envelope Modulation is automatic and does not require the flight crew to select this mode. EGPWS is

currently in use on both the C-17 Globemaster III and C-130J Super Hercules. As the case study of HAZE 01 in Section 1.2 showed, EGPWS is not adequate by itself for preventing CFIT.

2.3.1.2 U.S. Navy Terrain Awareness Warning System.

The Navy's Terrain Awareness Warning System (TAWS) is currently in use on the F/A-18 Hornet and Super Hornet, EA-18G Growler, AV-8B Harrier, T-45C, Goshawk, and MH-60 Helicopter [36]. According to Anderson, the U.S. Navy TAWS "is a safety backup system developed to provide protection against Controlled Flight Into Terrain. The algorithm predicts 3-dimensional recovery flight paths and compares with DTED to identify terrain intersections. If intersections exist along the predicted trajectories, an audio and visual directive warning is issued to the aircrew to affect a recovery away from the imminent CFIT condition" [36]. The Navy TAWS calculates two trajectories. The first trajectory is a referred to as the Vertical Recovery Trajectory (VRT), which is a roll to wings-level followed by a 5-g pull. The second trajectory, the Oblique Recovery Trajectory (ORT), is used when the aircraft is turning and is a 5-g pull at the current bank angle. Though the VRT is similar to the "roll-pull" performed by the F-16 Auto GCAS, it and the ORT are not flown automatically but are rather directed maneuvers to the pilot. The pilot receives both an aural direction as well as visual cues on their Heads-Up Display (HUD) with multiple phases to aid in executing the maneuver [14]. According to the F/A-18 Navy Flight Manual [37], the computed trajectories assume:

- Pilot Response Time is the time from issuance of a TAWS warning to the time that the pilot actually initiates recovery. Pilot Response Time is set at 1.3 seconds.

- Roll Recovery Phase is the time necessary to roll the aircraft to near wings-level.

This assumes at least lateral stick will be used for bank angles less than 70 and at least $\frac{3}{4}$ lateral stick will be used for bank angles ≥ 70.

- G-Onset Phase is the time required to pull to the target recovery g. The target recovery g is 80% of the instantaneous g available, or 5g, whichever is less. The g-onset phase assumes that rapid aft stick motion will be used (full deflection within $\frac{3}{4}$ second). In addition, TAWS assumes that the pilot will move the throttles to MAX if below corner speed and to IDLE if above corner speed.

- Dive Recovery Phase is the remainder of the trajectory until terrain clearance is achieved. TAWS assumes a terrain clearance of 50 ft.

2.3.1.3 A400M Tactical GCAS.

The Airbus A400M is a multi-role advanced airlifter used by several European and Middle Eastern militaries. As can be seen in Figure 2.5, the A400M falls between the C-17 and C-130J in terms of size. It also has similar performance to a C-17. The A400M has a version of TAWS produced by Cassidian that has been optimized for low-level flight. "The high update rate Threat Detection and Alert Generator uses position, hybridized geometric altitude, aircraft attitude, radar altimeter and air data to determine the caution and warning alerts. The threat detection algorithms include allowance for military operational specific pilot reaction time based on a pilot in the loop operation close to ground. Additionally, the lead time is fine tuned to cover different tactical flight phases and aircraft attitudes. The highly efficient threat calculation allows a provision of CFIT protection down to 150 ft above ground level in cruise condition and down to 5 ft above ground level in landing or very low level extraction. The Forward Looking Terrain Avoidance (FLTA) functionality terrain clearance margin can be adjusted manually by the flight crew during flight if needed"[38, 39].

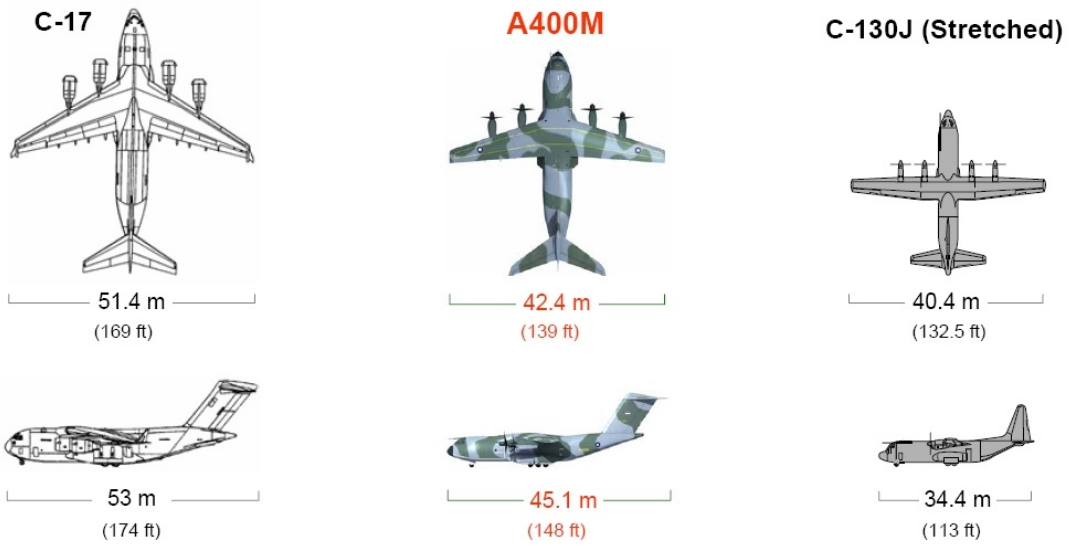

Figure 2.5. Comparison of A400M to the C-17 and C-130J [40]

The A400M's Tactical GCAS uses a combination of aircraft performance lookup tables, including flap setting, cargo door position, anti-icing, etc., and real-time calculations to allows such close ground clearance. This system provides an aural warning to the crew as well as visual display on the HUD and a separate Terrain Awareness Display (TAD). The exact design of Cassidian's Tactical GCAS algorithm is proprietary, but the use of an adaptable and highly detailed aircraft model as well as accurate performance modeling and small incremental step size is in the same vein as this research [39].

2.3.2 Fielded Automatic Systems.

Automatic systems are defined as those that upon determination of the need to maneuver to avoid terrain do so without input from the pilot. These maneuvers are flown until a termination criteria is met, be it time based or simply clear of the offending terrain. This section will discuss automatic systems that are currently in operational use.

2.3.2.1 USAF F-16 Auto-GCAS.

The F-16 Auto-GCAS program has been a resounding success and has paved the way for Auto-GCAS on other aircraft. The decades long development process is well documented and this text will only provide a broad overview of the operation of the system. The F-16 Auto-GCAS works by projecting a single recovery trajectory and comparing that trajectory to DTED [22]. The recovery trajectory is an automatic roll to wings-level followed by a 5-g pull. The 5-g pull is held until a termination angle is reached that ensures the aircraft is clear of the terrain. The operating concept of the F-16 Auto-GCAS is presented in Figure 2.6.

The F-16 Trajectory Prediction Algorithm (TPA) models the predicted behavior of the aircraft once the recovery is initiated. The details of the TPA itself are proprietary. The developers of the TPA sought to strike a balance between protection, nuisance, and reducing model complexity [22]. The TPA was developed by using an optimization routine along with an augmented 6-DoF simulation. The optimization routine was used to reduce the Root Mean Squared (RMS) error between the 6-DoF model and the TPA at various design conditions. Since the TPA uses a reduced fidelity model of the F-16, a 0.5 sec delay (TBB) was added to allow for uncertainty in calculation and maneuver time. Figure 2.7 shows a typical ground avoidance scenario. The inset of Figure 2.7 also shows the various DTED scan patterns that are used during level, turning, and diving flight.

The F-16 Auto-GCAS development team performed extensive research and flight testing to evaluate the nuisance potential of the automatic recovery maneuver. Flight testing revealed that, at least in the case of fighter aircraft, recovery activation with less than 1.5 sec remaining until ground impact resulted in a low perception of nuisance. The flight tests also revealed that the F-16 Auto-GCAS should be effective in preventing 98% of future CFIT incidents. As evinced by the recorded saves discussed

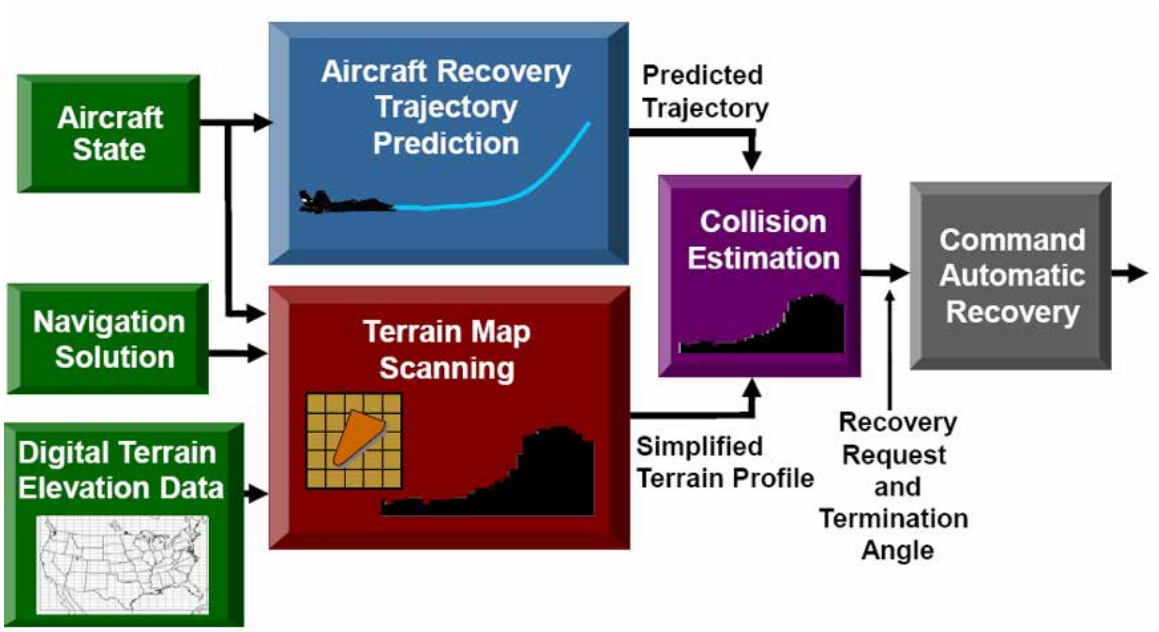

Figure 2.6. F-16 Auto-GCAS Block Diagram [26]

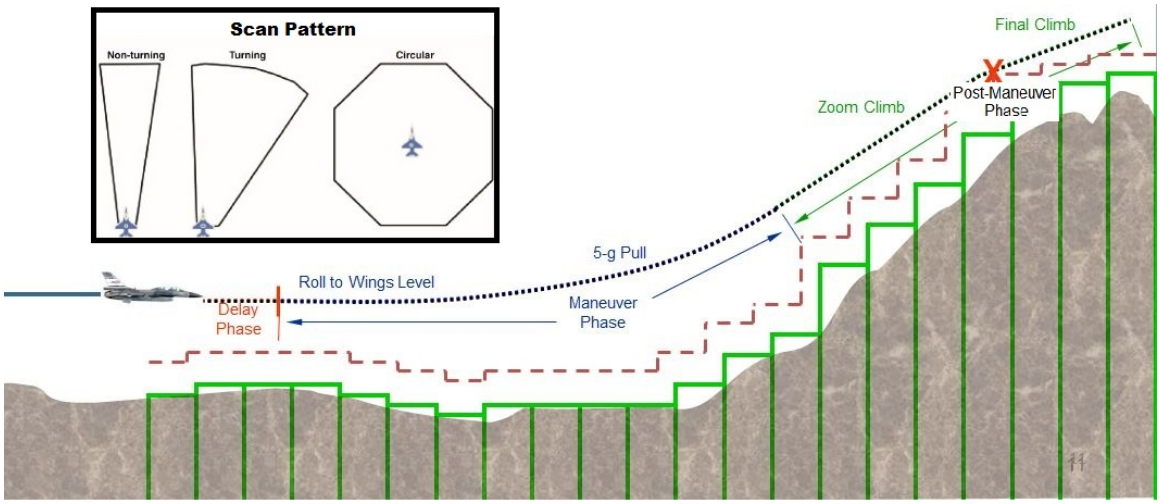

Figure 2.7. F-16 Auto-GCAS Phases [35]

in Section 1.1, so far the system is working exceptionally well.

2.3.2.2 Swedish Gripen Auto GCAS.

The Auto GCAS installed on the Swedish Air Force Saab JAS-39 C/D Gripen was developed concurrently with the F-16 Auto GCAS [41]. The two systems operate similarly by using a single roll and pull escape trajectory. Unlike the F-16, the Gripen provides visual and aural direction to the pilot to initiate the recovery maneuver 1.5-2.5 seconds prior to automatic recovery [14]. The F-16, on the other hand, gives two chevrons which appears on the left and right sides of the HUD 5 seconds prior to automatic activation and meet to form an "X" upon activation. Because the Swedish Air Force frequently operates the Gripen in a low-level environment, the Swedish Air Force is continuing to make efforts to reduce the amount of terrain safety buffer needed for safe and nuisance free operation [41, 42].

2.3.3 Research Level Automatic Systems.

Research level systems are those that have shown promise to the extent they were tested but are not ready to be implemented on fleet aircraft. In the cases of the NASA Small UAV Auto GCAS and Have ESCAPE, successful flight tests were accomplished as part of the research effort [15, 23, 35].

2.3.3.1 NASA Small UAV Auto-GCAS.

The NASA Small UAV (SUAV) was developed in response to a Defense Safety Oversight Council (DSOC) funded request to design and flight-test Auto GCAS technologies on different aircraft types while leveraging the work already done on the F-16 [23]. The SUAV, also known as the Dryden Remotely Operated Integrated Drone (DROID), is shown in Figure 2.8a in front of an F-16. The DROID was chosen

for this research because it is significantly different to the F-16 and its flying qualities mimic that of an MQ-9 Reaper [35]. The comparative performance of the DROID and MQ-9 is summarized in Table 2.2.

The NASA SUAV trajectory algorithm was developed by flight testing the proposed escape trajectories and using an adjustable TBB and onset rate parameters to allow for variation in flight condition [23]. The SUAV team determined that a high fidelity model was not needed due to the simplistic nature of the autopilots employed. These trajectories are a roll to wings-level followed by a 1000 fpm climb capturing 60 KIAS or a left or right 40 degree bank to capture a 60 KIAS/ 800 fpm climbing turn. Once again these maneuvers were chosen to represent what could be performed by a medium-to-large UAV [23]. During flight each trajectory is compared to the surrounding terrain to determine if a conflict exists. When the last path available predicts a collision, an on-board Piccolo II autopilot commands the maneuver. The "last man standing" trajectory selection method used by the SUAV as well as this research is shown in Figure 2.8b.

The SUAV terrain scan uses a both DTED and National Elevation Dataset (NED)[2].

[2] "The National Elevation Dataset (NED) is a seamless raster product produced by the U.S. Geological Survey (USGS). The NED provides elevation data coverage of the continental United States, Alaska, Hawaii, and the island territories in a seamless format with a consistent projection,

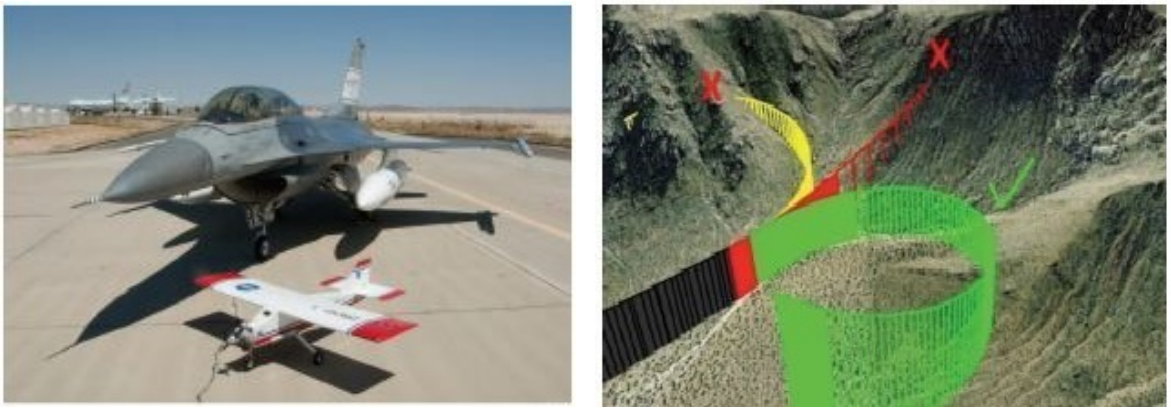

(a) DROID and F-16 [23] **(b) SUAV "Last Man Standing" [23]**

Figure 2.8. NASA SUAV Aircraft and Avoidance Maneuvers

Table 2.2. DROID vs. MQ-9 Specifications [23]

Aircraft	Wing Span	Weight	Power	$\frac{\text{Power}}{\text{Weight}}(\frac{hp}{lb})$	Speed	Rate of Climb
DROID	9 ft 8 in	58 lb	11 HP	0.19	80 KIAS	1000 $\frac{ft}{min}$
MQ-9	65 ft 7 in	7000 lb	900 HP	0.13	190 KIAS	1000 $\frac{ft}{min}$

Using NASA's advanced compression algorithm, the SUAV is able to carry large amounts of terrain data while taking up minimal storage. The predicted trajectories are compared to the terrain using a scan method as described in Section 2.2.8.1. The SUAV researchers used Equation 2.4 to calculate the appropriate safety buffer to ensure safe ground clearance. The *TPA* term can be used to reduce the need for a high fidelity model.

$$Buffer = NAV + (DEM^2 + TPA^2)^{\frac{1}{2}} \tag{2.4}$$

where:

$NAV =$ buffer due to navigation uncertainty
$DEM =$ buffer due to DEM uncertainty
$TPA =$ buffer due to trajectory uncertainty

and the total represents the required buffer.

The SUAV researchers state in their recommendations that;

> "A full six-degrees-of-freedom simulation is not required to model the trajectory predictions for this module. High-fidelity aerodynamic, thrust, and flight control models are not required, although a simulation using those models can provide a very helpful starting point if available. If a high-fidelity simulation is not available, the necessary parameters can be determined directly from a few simple flight tests" [23].

While it may not always be necessary to have an extremely detailed aircraft model,

resolution, elevation units, and horizontal and vertical datums" [43]

it can be seen from Figure 2.9 that a simplified 3-DoF model does not guarantee sufficient path prediction accuracy. It is for this reason that this research seeks to retain a high fidelity model while still achieving the needed algorithm speed. Additionally, it was determined that the use of a commercial off-the-shelf (COTS) autopilot to execute the escape maneuvers which were triggered by path predictions that did not have the same control laws as the COTS autopilot was a potentially large source of error. This is different from the approach used by this research, wherein internal control laws are continuously calculating the escape trajectories before cueing an autopilot which is of identical design to the control laws to fly the maneuver.

The NASA SUAV was the primary inspiration for Trombetta's Have ESCAPE research and continues to provide a great deal of direction and lessons learned for the research presented here.

2.3.3.2 Have ESCAPE.

Have ESCAPE was the predecessor to this research effort. Have ESCAPE was undertaken by Major John "Cowboy" Trombetta as his thesis/TMP for the AFIT/TPS Master's program. This foundational work, titled "Multi-trajectory Automatic Ground Collision Avoidance System with Flight Tests (Project Have ESCAPE)", was the first effort to flight test an Auto-GCAS for heavy aircraft and identified several of the research objectives listed in Section 1.3.2. The ESCAPE in Have ESCAPE stands for Emergency Safe Calculated Autonomous Preplanned Exit. The philosophy behind his approach is captured in this clever acronym. The following sections discuss Trombetta's methods and findings.

The Have ESCAPE algorithm used a 3-DoF point mass model to predict five escape trajectories. The 3-DoF model was also favored and used by Rahunathan and Suplisson [14, 44]. Equations 2.5-2.9 were used by Trombetta to predict the aircraft

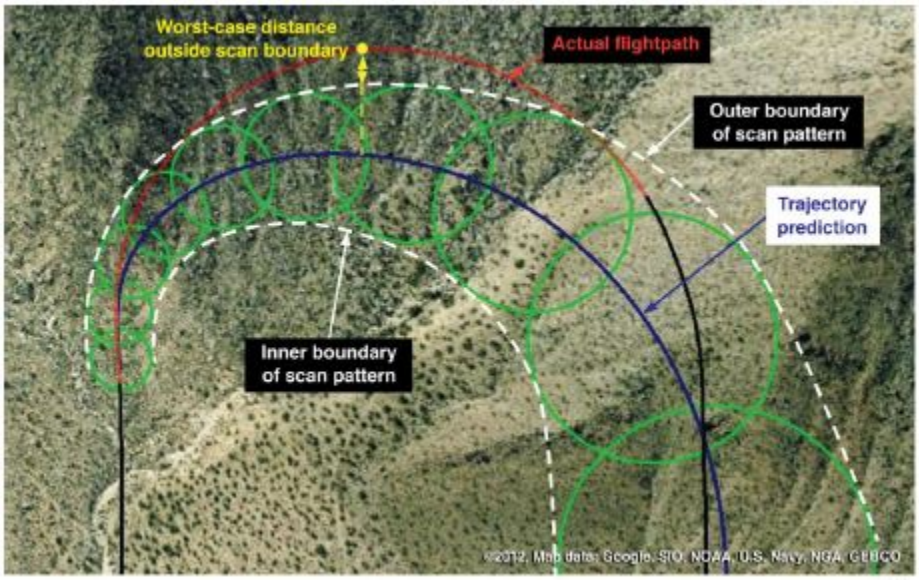

Figure 2.9. SUAV Path Inaccuracy [23]

trajectories. These trajectories included a straight-ahead 2-g pull to a 15^o flight path angle limit, a left and right 15^o roll followed by a 2-g pull, and a left and right level 60^o/2-g turn [15]. Using the "last man standing" concept, when the last path is predicted to intersect terrain, the escape maneuver is commanded. Have ESCAPE used fixed Nz and bank angle (ϕ) commands which were sent to external autopilots that ultimately commanded the Learjet 25D VSS.

$$\dot{x} = V\cos\gamma\cos\chi \tag{2.5}$$

$$\dot{y} = V\cos\gamma\sin\chi \tag{2.6}$$

$$\dot{z} = V\sin\gamma \tag{2.7}$$

$$\dot{\gamma} = \frac{N_z\cos\phi - g\cos\gamma}{V} \tag{2.8}$$

$$\dot{\chi} = \frac{N_z\sin\phi}{V\cos\gamma} \tag{2.9}$$

Trombetta's algorithm relied on a 300 ft "bubble" around the aircraft to capture

the Level 1 DTED posts as well as provide terrain buffer. Have ESCAPE also used a 0.5 sec TBB to account for g and roll/pitch onset rates that were not captured in the 3-DoF model. Based upon the terrain analysis described in Section 2.8. Trombetta determined that the appropriate forward projection time was 31 sec. Based on this, RSET adopted a 30 sec time horizon. Before full implementation, further research is needed to determine necessary look-ahead for all scenarios (and airframes).

Due to the preplanned nature of Have ESCAPE, the Learjet test aircraft was restricted to straight-and-level flight at 310 KtGS. Any deviation from these conditions would cause the predicted path to be significantly different from the executed escape maneuver.

2.3.3.3 Optimal Auto GCAS.

Suplisson's research, titled *Optimal Recovery Trajectories for Automatic Ground Collision Avoidance Systems (Auto GCAS)*, is vital for establishing a basis on which to benchmark Auto-GCAS technologies. In the same manner as Have ESCAPE, Optimal Auto GCAS modeled the aircraft as a 3-DoF point mass model. Where Optimal Auto GCAS differed was that for each test case a unique solution was generated that satisfied the optimal control cost function.

The optimal control problem is predicated on the idea of *Aggressive* and *Timely* avoidance maneuvers. These concepts are key to minimizing nuisances and avoiding interference with mission execution [14]. Suplisson defines *Aggressive* as requiring at least one control be at maximum deflection to execute the maneuver. In reality an aircraft often reaches some other dynamic limit, be it Nz, flight path angle, stall, before the actual deflection limit of the control surface. Nevertheless the *Aggressive* formulation serves to motivate the approach used herein where escape maneuvers are flown at either the limit of the control, the dynamic limit, or both. The *Timely*

requirement specifies that the escape maneuver be flown at the last possible moment to prevent intersecting terrain or the terrain buffer, if used. Suplisson concluded that for Auto-GCAS on military aircraft, "a last-second aggressive recovery is essential in order to be nuisance-free and still accomplish the operational mission" [14]. Suplisson applied a 350 ft GCB as described above to allow for errors in terrain data and path prediction.

With the *Aggressive* and *Timely* criteria defined, Suplisson determined two primary optimal control formulations that were relevant to Heavy Auto GCAS; Max Distance with a Timely Trigger or Min Control with an Aggressive Trigger. The Max Distance formulation seeks to maximize the distance from terrain with the caveat that the escape maneuver is not performed until the CPA is equal to the GCB of 350 ft. The Min Control formulation, in contrast, seeks to find the least amount of control required to avoid the offending terrain and the avoidance path is not followed until a control is at its maximum. These formulations are shown in Figure 2.10. Suplisson concluded that climb performance limited aircraft are best associated with the Min Control with an Aggressive Trigger, which inspired the development of the RSET system.

2.3.3.4 Predictive GCAS for UAVs.

The research on Predictive GCAS for UAV applications performed by Lee et al. provides some useful insight into handling variation in terrain and reducing nuisance [32, 45]. The Predictive GCAS algorithm uses the familiar wings-level 5-g pull as its only escape maneuver, and it is applied to a notional UAV application. The simulations are run using MATLAB and the X-Plane10 simulator. Lee et al. present a method of "binning and hulling" the terrain in the scan pattern of the aircraft. The bins are determine by the maximum terrain height at a given time-distance away

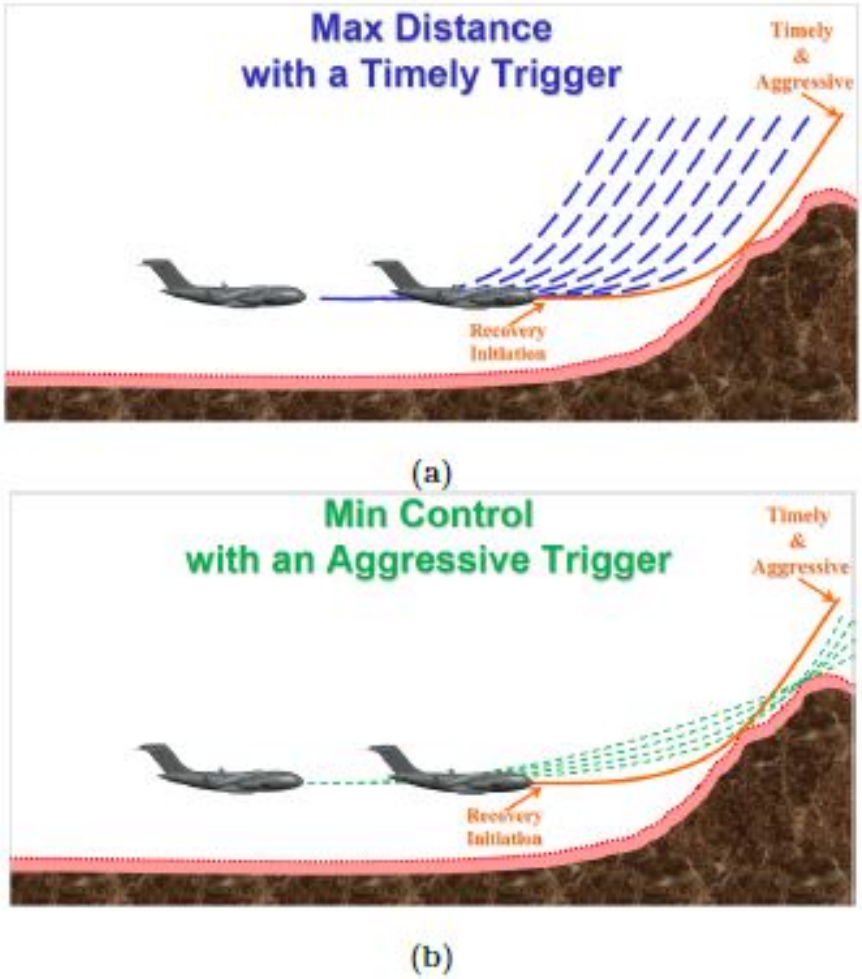

Figure 2.10. Optimal Auto GCAS Approaches: (a) Max Distance and (b) Min Control [14]

from the aircraft. Predictive GCAS differs from the F-16 GCAS binning process by applying a decreasing weighting factor to terrain that is farthest from the predicted path. Once the data is binned, those bins are covered by a continous curve, or "hull" [32]. The hulling process is analogous to the tip of a Computer Numerical Control (CNC) machine probe, where the probe radius is analogous to the aircraft maximum decent angle, pull-up radius, and climb angle. The binning and hulling process is shown in Figure 2.11.

2.3.4 GCAS Survey Summary.

Tables 2.3 and 2.4 summarize the various GCAS methods discussed thus far. As can clearly be seen, there are numerous approaches to solving the problem of preventing CFIT. This research takes inspiration from each research effort described here and seeks to advance the state of the art.

2.4 Nuisance Criteria

Of concern to every Auto-GCAS researcher, including the author, is the concept of "nuisance". Swihart and Barfield identified early in Auto-GCAS research that "a ground collision avoidance system is a tradeoff between system safety and nuissance

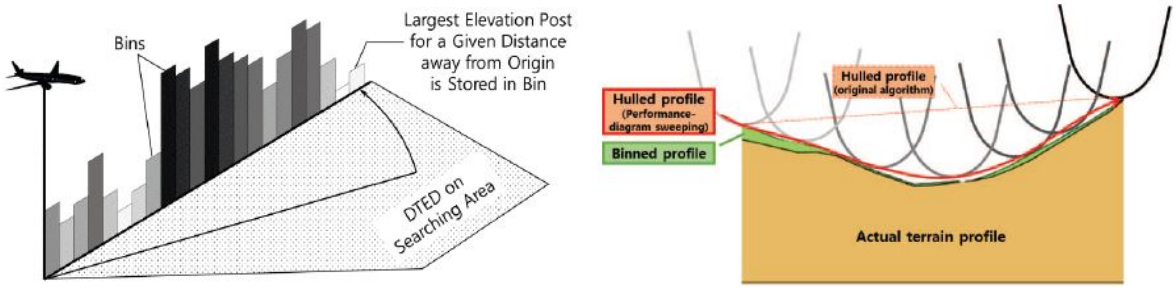

(a) Data binning **(b) Data hulling**

Figure 2.11. PGCAS Terrain Data Handling Methods [32, 45]

Table 2.3. Kuchar and Yang CDR Design Factors Applied to Existing and Proposed Systems

Model	State* Prop.	State Dim.	Detection Threshold	Conflict Resolution	Resolution** Maneuvers
EGPWS#	Nominal	3-D	time, range	Prescribed[a]	V
F-16	Worst-Case	3-D	distance	Prescribed[b]	C(T/V)
NASA SUAV	Worst-Case	3-D	xxx	Prescribed[c]	C(T/V)
Have ESCAPE	Worst-Case	3-D	xxx	Prescribed[d]	C(T/V)
Optimal	Worst-Case	3-D	xxx	Optimal	C(T/V/S)
UAV P-GCAS [32]	Probabilistic	3-D	distance	Prescribed[b]	V
RSET^{TT}	Worst-Case	3-D	xxx	Adaptive[e]	C(T/V/S)

* In the context of Auto-GCAS "worst-case" implies a max-performance maneuver to minimize nuisance. See Table 2.4 Trajectory Limitations for the determining factor.

** V = Vertical Maneuver, T = Turn, S = Speed Change, C() = Simultaneous

EGPWS is not an automatic system

TT Proposed herein

[a] Aural warning and "Pull Up" command.

[b] Single autopilot based climb trajectory.

[c] Three autopilot based trajectories (climb, left and right climbing turn).

[d] Five pre-determined bank angle and g-force commands (climb, left and right climbing turns, left and right level turns) sent to internal Learjet autopilots.

[e] Adaptive: Five autopilot based trajectories (climb, left and right climbing turns, left and right level turns).

Table 2.4. Expanded CDR Design Factors

Model	Model Fidelity	Trajectory Limitations	DEM Post Capture	Safety Buffer
F-16	Proprietary	Pilot	scan	TBB, GCB
NASA SUAV [23]	3-DoF	Structure	scan	TBB, GCB
Have ESCAPE [15]	3-DoF	Structure	bubble	TBB, ACB
Optimal [14]	3-DoF	Structure	interpolate	TBB, GCB
P-GCAS for UAV [32]	6-DoF	Performance	scan	GCB
RSET^{TT}	Augmented 6-DoF	Structure	interpolate	TBB, GCB

TT Proposed herein

warnings to the pilot which may force the pilot to turn the system off" [41]. In short, nuisance is any intervention or warning given by the collision avoidance system when it is not needed or warranted. This could happen in the case of an overly sensitive system on an aircraft performing a low-level mission. Although nuisance is easy to identify on a case-by-case basis, it is difficult to generalize for the purpose of algorithm design. In the words of Swihart et al., "it can also be reasoned that the dividing line between a valid warning and a nuisance warning is this point where an aware pilot feels an aggressive recovery must be initiated to avoid collision" [46]. Extensive flight testing was done during the development of the F-16 Auto GCAS system to determine that 1.5 sec of Available Reaction Time (ART) was the appropriate nuisance threshold. This means that there is 1.5 sec to initiate the maneuver before it would no longer avoid collision. As recommended by Suplisson, this research aims to quantify this threshold for heavy aircraft [14]. The SUAV researchers also identified the difficulty in evaluating nuisance potential [23]. Sorokowski et al. also recommend that platform-specific flight testing of operationally relevant mission tasks is necessary to determine nuisance ART threshold.

2.5 Learjet 25D Stitched Model

Beginning with a series of flight tests in May 2015, the U.S. Army Aviation Development Directorate, Textron Aviation, and the USAF Test Pilot School undertook a collaborative effort to develop a full flight-envelope model of the Learjet 25D [47]. The model developed was referred to as a "stitched model" since it involved nonlinear equations of motion combined with trim data at specific flight conditions [48]. Throughout this document this model will be referred to as the "Stitched Model".

The core of the Stitched Model is the quasi-Linear Parameter Varying (qLPV) model. A Linear Parameter Varying (LPV) model is a linearization of a nonlinear

system, shown in Equations 2.10 and 2.11, where, as opposed to a Linear Time Invariant (LTI) system, the entries of the state-space matrices are allowed to vary with time [49]. "If the scheduling parameter vector $\boldsymbol{\rho}(t)$ contains any states of the system, then the system is quasi-LPV, and is said to be "stitched" in those states"[47].

$$\dot{\boldsymbol{X}}(t) = f\big(\boldsymbol{X}(t), \boldsymbol{U}(t)\big) \tag{2.10}$$

$$\boldsymbol{Y}(t) = h\big(\boldsymbol{X}(t), \boldsymbol{U}(t)\big) \tag{2.11}$$

where:

$\boldsymbol{X}, \boldsymbol{U},$ and $\boldsymbol{Y}$ are the total states, inputs, and output, respectively, of the system, and f and h are nonlinear functions.

For a qLPV system, Equations 2.10 and 2.11 become (note that the (t) is dropped for the sake of brevity) [47]:

$$\boldsymbol{X} = \begin{bmatrix} \boldsymbol{Z} \\ \boldsymbol{W} \end{bmatrix} \tag{2.12}$$

$$\begin{bmatrix} \dot{\boldsymbol{Z}} \\ \dot{\boldsymbol{W}} \end{bmatrix} = \begin{bmatrix} \boldsymbol{A_{11}}(\boldsymbol{\rho}) & \boldsymbol{A_{12}}(\boldsymbol{\rho}) \\ \boldsymbol{A_{21}}(\boldsymbol{\rho}) & \boldsymbol{A_{22}}(\boldsymbol{\rho}) \end{bmatrix} \begin{bmatrix} \boldsymbol{Z} - \boldsymbol{Z}_0(\boldsymbol{\rho}) \\ \boldsymbol{W} - \boldsymbol{W}_0(\boldsymbol{\rho}) \end{bmatrix} + \begin{bmatrix} \boldsymbol{B}_1(\boldsymbol{\rho}) \\ \boldsymbol{B}_2(\boldsymbol{\rho}) \end{bmatrix} \Big[\boldsymbol{U} - \boldsymbol{U}_0(\boldsymbol{\rho}) \Big] \tag{2.13}$$

$$\boldsymbol{Y} = \boldsymbol{C}(\boldsymbol{\rho})\big(\boldsymbol{X} - \boldsymbol{X}_0(\boldsymbol{\rho})\big) + \boldsymbol{D}(\boldsymbol{\rho})\big(\boldsymbol{U} - \boldsymbol{U}_0(\boldsymbol{\rho})\big) + \boldsymbol{Y}_0(\boldsymbol{\rho}) \tag{2.14}$$

where:

$\boldsymbol{Z}$ are states that are stitching parameters, $\boldsymbol{W}$ are states that are not stitching parameters,

$\boldsymbol{A}, \boldsymbol{B}, \boldsymbol{C},$ and $\boldsymbol{D}$ are linearized state-space matrices, and

$\boldsymbol{\rho}$ is the vector of scheduling parameters.

The derivation of the qLPV model is complex and is only discussed briefly here. For a more detailed explanation of the rationale behind this formulation see the works of Berger et al., Tischler, and Tobias [47, 48, 50]. The Learjet 25D Stitched Model is stitched in the x-body axis velocity state U. What this means is that the aircraft true airspeed is both a state and a scheduling parameter. Flap deflection, δ_f, is also a scheduling parameter but it is not a state, so the model is not stitched in δ_f. Therefore the lookup tables of state space matrices and trim values gathered from flight test are with respect to U and δ_f [47]. Figure 2.12 along with Table 2.5 graphically depict the operation of the Stitched Model.

There are three additional features of the Stitched Model which lend to its robust nature. The first is that flight test data need not be available at all altitudes. Rather, scaling based on the ratio of actual aircraft density altitude to the flight test density altitude, in this case 15,000 ft MSL, can be applied to determine trim values throughout the flight envelope. Second is that only aerodynamic forces and moments are applied using lookup tables while all other forces and moments are retained in their full nonlinear form [47]. Lastly is the ability to scale these forces and moments based upon variation in aircraft mass and Center of Gravity (CG). With the Learjet 25D, which has large wingtip fuel tanks, these variations can be significant.

Given the significance of the Stitched Model to this research, future discussion on the validation and characteristics of the model are presented throughout Chapter III.

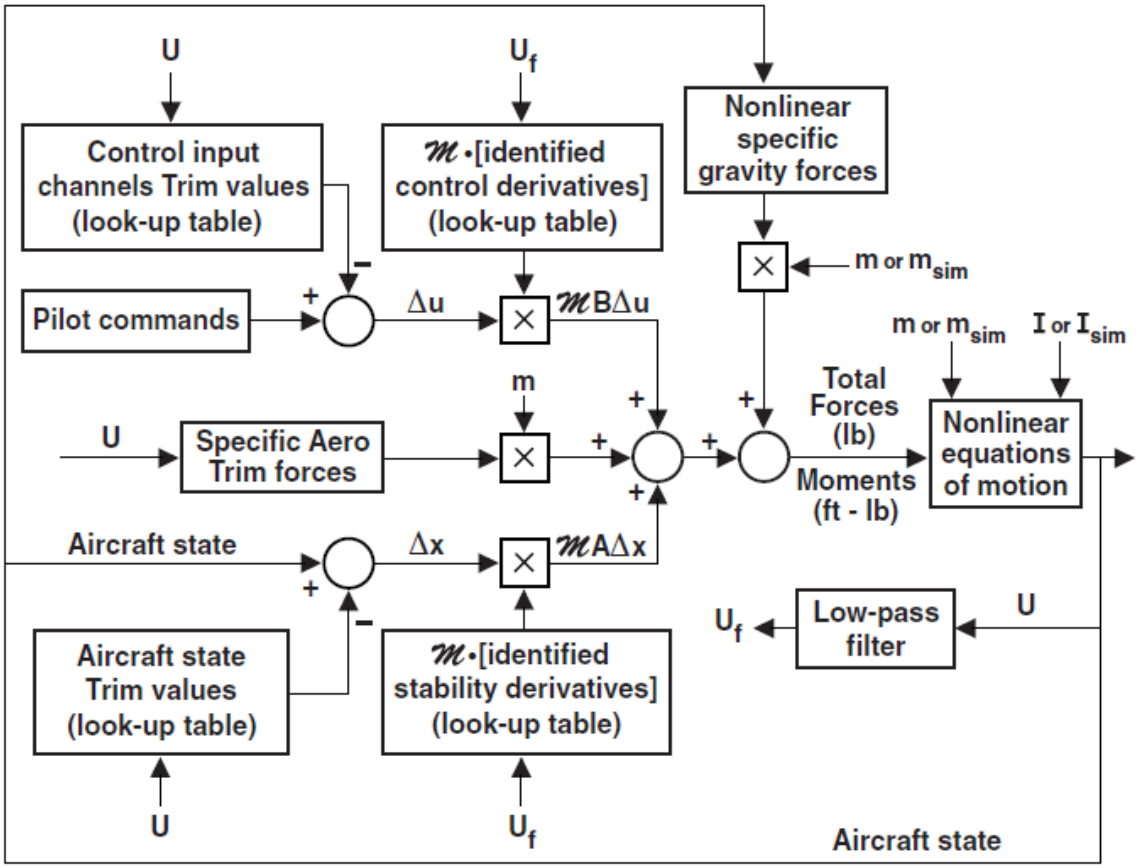

Figure 2.12. Model Stitching Block Diagram [47] (see Table 2.5 for variable descriptions)

Table 2.5. Model Stitching Block Diagram Variables [47]

Variable	Description
U	Total longitudinal body axis velocity
U_f	Filtered Velocity
Δu	Control Perturbations (e.g. $delta_e$)
Δx	State Perturbations [e.g., $w = (W - W_0)$]
M	Mass and Inertia Matrix
A	Dimensional stability derivatives
B	Dimensional control derivatives
m	Aircraft mass
I	Aircraft inertia matrix

2.6 Theil's Inequality Coefficient

One of the major efforts of this research is to convert the Stitched Model into a form which can be used for path prediction with an Auto-GCAS. As such, a metric is needed to determine the consistency between the converted and original models.

Murray-Smith highlights Theil's Inequality Coefficient (TIC) as a useful quantitative measure of model performance [51]. Equation 2.15 shows one form of TIC. One of the benefits of TIC is that all values lie between 0 and 1, with 0 being a perfect fit and 1 meaning the two data sets are very significantly different. Jategaonkar et al. used TIC for aerodynamic modeling and system identification, and later Dorobantu et al. used TIC to successfully validate uncertain aircraft simulation models. Given the proven utility of Theil's Inequality Coefficient, the author adopted this metric for the research herein. Furthermore, Tischler and Remple as well as Jategaonkar et al. agree that values TIC $<$ 0.25-0.30 correspond to accurate models when comparing trusted and un-trusted data [50, 52].

$$TIC = \frac{\sqrt{\frac{1}{N}\sum_{i=1}^{N}[x(i) - \hat{x}(i)]^2}}{\sqrt{\frac{1}{N}\sum_{i=1}^{N}[x(i)]^2} + \sqrt{\frac{1}{N}\sum_{i=1}^{N}[\hat{x}(i)]^2}} \tag{2.15}$$

where:

$$x = \text{trusted model state (original Stitched Model)}$$

$$\hat{x} = \text{un-trusted model state (Converted Model)}$$

$$N = \text{number of data points (in time horizon)}$$

2.7 Refresh Rate

Computing power is a valuable commodity on most aircraft. As such, Auto-GCAS algorithms must strike a balance between complexity, accuracy, and "refresh rate". Refresh rate dictates the speed at which the predicted paths can be compared to

the terrain. This becomes increasingly important for fast-moving aircraft and widely spaced DEM posts. A fast-moving aircraft with a slow Auto-GCAS algorithm could easily miss a mountain peak if the time step between iterations is too great. Table 2.6 summarizes the refresh rates of existing algorithms.

Table 2.6. GCAS Algorithm Refresh Rates

Model	Model Fidelity	Number of Trajectories	Refresh Rate (Hz)
F-16 [22]	Proprietary	1	12
Navy TAWS [36, 37]	Simplified 6-DoF	2	10
NASA SUAV [23]	3-DoF	3	5
Have ESCAPE [15]	3-DoF	5	12.5
Optimal [14]	3-DoF	Infinite	2
RSET	Augmented 6-DoF	5	12.5

2.8 Terrain Classification

Trombetta provides a detailed analysis of terrain classification and the implication of terrain on path propagation times. Referencing USAF AFI11-202V3 and borrowing terminology from Dragut, Trombetta provides a common vernacular GCAS terrain categorization as shown in Table 2.7 [53, 54].

Table 2.7. Terrain Classification Based on Terrain Height Data [15]

Terrain Class	Terrain Rise vs Horiz. Distance
Upland	$\geq$ 500 ft per 1/2 nm
Midland	$\geq$ 250 ft & $<$ 500 ft per 1/2 nm
Lowland	$<$ 250 ft per 1/2 nm

Trombetta further used the terrain classifications to determine the required propagation time for aircraft operating at different speeds. These times assume the aircraft

is climbing at a 15^o fight path angle and are summarized in Table 2.8.

2.9 Aircraft Classification

MIL-STD-1797B *Flying Qualities of Piloted Aircraft* groups aircraft based on weight and maneuverability. A depiction of these groupings can be seen in Figure 2.13. As noted by Trombetta, just because two aircraft are in the same class does not mean they have similar performance with respect to ground avoidance maneuvers [15].

The aircraft shown in Table 2.9 are all Class III but clearly have dramatically different performance with respect to low-level operating speed, turn rate, and turn radius. The common ground among these aircraft is that, unlike Class IV and some Class I aircraft, they are unable to perform high-g maneuvers to avoid ground collision. It is worth noting that although a "one-size-fits-all" solution is not possible among Class III aircraft the basic architecture and design philosophy for one is applicable to all. In essence, once the appropriate maneuver criteria is established the aircraft model need only be changed.

2.10 Aircraft with Auto-throttle

One of the major advances this research attempted was the use of auto-throttle in trajectory prediction and maneuver execution. Even in the case of the highly

Table 2.8. Avoidance Path Propagation Times [15]

Aircraft Velocity (KtGS)	Lowland	Midland	Upland
210	17.25 s	29.19 s	44.54 s
310	17.20 s	21.14 s	30.72 s
540	28.25 s	28.25 s	28.25 s

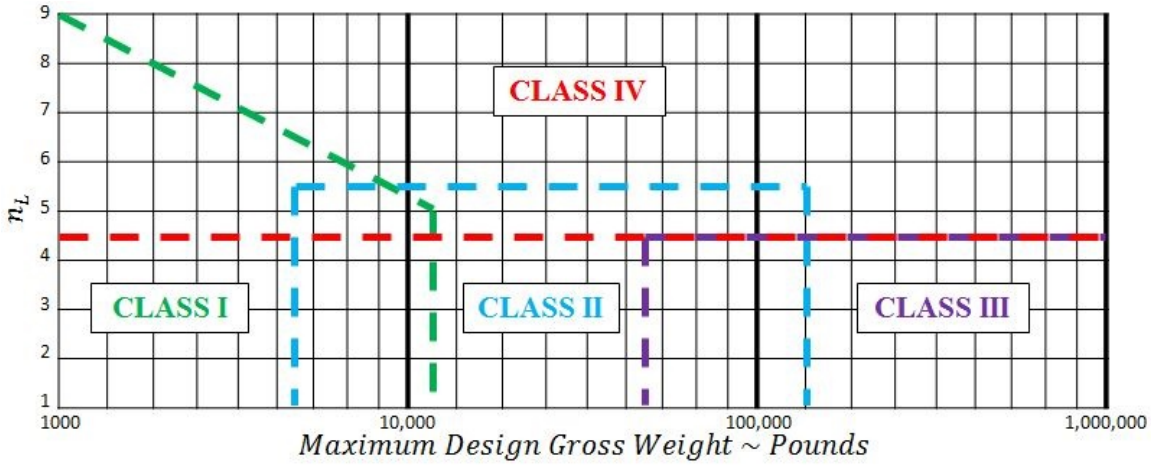

Figure 2.13. MIL-STD-1797B Classification of Aircraft [2]

Table 2.9. Military Aircraft Low Level Flight Performance [14, 15]

Aircraft	Airspeed (KtGS)	Altitude AGL	Nz (g)	Bank Angle	Turn Radius	Turn Rate ($\frac{deg}{sec}$)
C-130J	210	300-500 ft	2	60 deg	2,254 ft	9.01
C-17	310	300-500 ft	2	60 deg	4,913 ft	6.10
B-52	350	500 ft	2	60 deg	6,262 ft	5.41
B-1	540	500 ft	2	60 deg	14,906 ft	3.50

successful F-16 Auto-GCAS the throttle is not changed. For aggressive recoveries, however, it is often necessary to advance or even retard the throttles to achieve the best climb or turning performance. This is achievable on the research testbed, the Calspan Learjet 25 In-Flight Simulator (IFS), which has full-authority Fly-by-Wire (FBW) capability for the ailerons, elevator, rudder, and throttles. It is also possible on many operational aircraft, such as the B-1, C-17, F-35, and C-130J, all which have auto-throttle capability. In light of this, the author identified that not only was auto-throttle a novel approach to Auto-GCAS implementation, but also germane to the future fielding of a system for heavy aircraft.

2.11 USAF TPS Flight Test

USAF Test Pilot School along with Calspan Corporation has a rich history of flight test. Futhermore, "Calspan Corporation has been the primary innovator, developer, and operator of in-flight simulators in the United States as well as the rest of the world since 1947" [55]. Calspan's first VSS, the F4U-5 Corsair, had its first flight in March 1949. Now, almost 70 years later, Calspan operates the Learjet 25 IFS and F-16/Variable Stability In-Flight Simulator and Test Aircraft (VISTA) IFS. As is shown throughout this text, the Learjet IFS is an ideal test bed for Auto-GCAS research. The following sections discuss to key components of the flight test program at TPS used for this research, the Flying and Handling Qualities simulator and the Learjet 25D VSS.

2.11.1 Flight Sciences Simulator.

TPS's Flight Sciences Simulator (FSS), shown in Figure 2.14, was a two-simulator bay facility which is used for student curriculum and TMPs [56]. The two identical simulators are capable of mimicking the T-38A Talon, the F-15 Eagle, multiple F-16

variants including the VISTA, the Blanik Glider, and the Learjet 25D. Furthermore the F-16 VISTA and Learjet 25D VSS aircraft are able to be remotely piloted from the FSS if needed or desired for the project. An important feature of the FSS is the "Hot Bench Lite". According to Kemper and Cotting, "the Hot Bench Lite is a software emulation of the VSS system on Calspan's inflight simulators" [56]. The Hot Bench Lite accepts the same software and loading configuration as the aircraft and allows for software checkout prior to actual flight testing. This is extremely valuable because software can be tested and familiarity with operation can be built without needing the actual aircraft.

2.11.2 Calspan Learjet 25D VSS.

Calspan's Learjet 25D VSS IFS, shown in Figure 2.15, is a highly modified twin-engine business jet. The Learjet VSS is equipped with a FBW control system that allows the aircraft to be modified to behave like a more or less responsive aircraft [57]. The ability of the flight behavior and controls to be modified, tested in the simulator, and then used during actual flight test is invaluable to this research.

Recently, as part of 2016 AFIT/TPS TMP titled Have VAPOR, Major Mark "Zog" Vahle successfully used the Learjet 25 VSS to perform off-nominal aircraft performance modeling [59]. His research compared 6 DoF nonlinear simulations of the Learjet 25 with various failures of the ailerons, rudder, elevators, and engines to flight test data with simulation of the same failures. Access to this level of analysis is both rare and expensive in research and testing and is a key advantage of this research. Additional details on the physical description of the LJ-25D and dynamic models are contained in Vahle's research.

Figure 2.14. USAF Test Pilot School Flight Sciences Simulator

Figure 2.15. Calspan Learjet 25D VSS [58]

2.12 Chapter Summary

This chapter provided an overview of traditional and expanded CDR design factors for GCAS, a review of GCASs at different stages of development for various aircraft, and the Learjet Stitched Model which served as the foundation of the RSET system. Additional consideration was given to Auto-GCAS nuisance, aircraft and terrain classification, and the TPS Flight Test capabilities. Next, Chapter III presents the methodology used to develop and test the RSET system.

III. Methodology

3.1 Introduction

This chapter describes the methodology used to develop the RSET system and execute the flight test of the Have MEDUSA TMP. Presented are the equations of motion, the steps taken to convert the Learjet 25D aerodynamic model, and the rationale and architecture of the RSET system. Lastly, the flight test resources and methodology are presented in detail. This chapter sets the foundation for understanding the results presented in Chapter IV.

3.2 Learjet Model Conversion

As discussed in Section 2.5 the Stitched Learjet Model was a highly sophisticated and accurate model which was flight test validated. In its original Simulink based form, however, it was not able to be used in the manner needed for this research. The main reasons that the original model was not suitable were the original model's slow operating speed and the fact that the model would need to be operated in both real-time and faster-than-real-time simulations simultaneously. In other words, as the Auto-GCAS read in current state data from the Learjet VSS (in real-time) the escape paths were calculated and projected into the future (faster-than-real-time). Calspan utilized a Simulink interface to connect to the Learjet VSS flight controls. Unfortunately, the Simulink environment did not easily allow for dissimilar time environments (i.e. operating at both real-time and faster-than-real-time).

Correspondence with the developers of the Stitched Model as well as engineers familiar with programming flight simulators revealed two paths forward for converting the Simulink model into a usable form [60–62]. The options were to either "auto-code" the Simulink model into C++ and modify as needed, or to rewrite the Stitched

Model as one or a series of MATLAB functions which could be called by Simulink. It was agreed that while "auto-coding" to C++ would ensure no loss of accuracy from the flight-tested model it would require significant engineering support to execute and may be premature while other aspects are still be answered. The MATLAB function option was identified as the more straight-forward route with the caution that resulting model accuracy was not guaranteed. As can been seen in Table 4.2 and in Appendix A, the converted MATLAB function produced excellent results. For the remainder of this thesis the original Simulink based Stitched Learjet Model will be referred to as the "Stitched Model" and the converted MATLAB function based model will be called the "Converted Model". It is important to note that the Converted Model is still a stitched model in that it uses a combination of flight-test data and equations of motion. These names were simply adopted for ease of discussion.

The first step in converting the Stitched Model to a MATLAB function was identifying which components of the Stitched Model needed to be kept and which could be omitted. Figures A.1 and 3.1 show the Stitched Model with an "X" placed over the subsystems that were omitted during the conversion. Then, starting from the lowest level and working up by subsystem, each subsystem was individually hand-coded over to a MATLAB function and tested individually along with the remainder of the Stitched Model. As each individual subsystem was converted from Simulink blocks to MATLAB functions the partially converted system was compared to the original system to ensure accuracy. This systematic process, though tedious, reduced sources of error and assisted greatly in troubleshooting. Once each individual subsystem was written and validated they were consolidated into a single MATLAB function. This MATLAB function contains all of the equations of motion, engine models, actuators, etc. which comprise the Stitched Model. The complete Converted Model is included in the Digital Appendix (Appendix I).

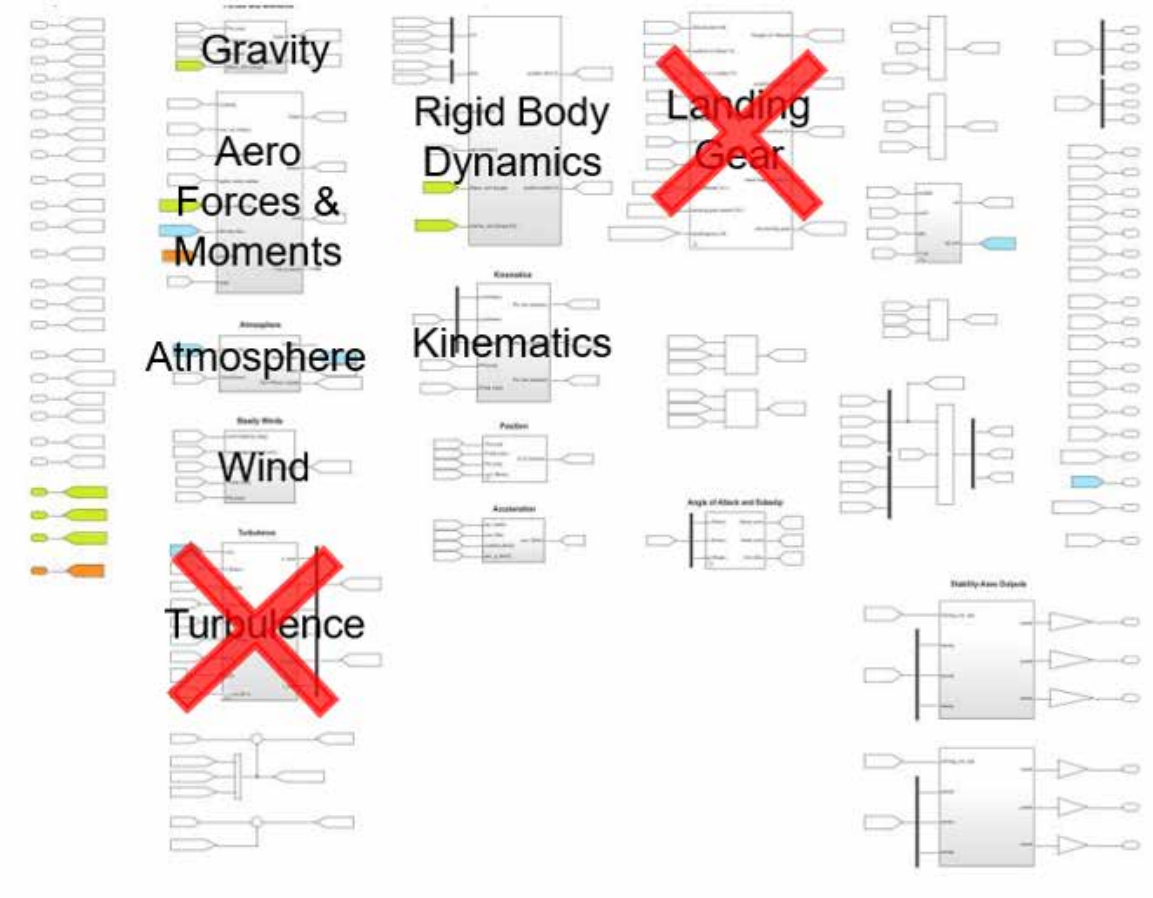

Figure 3.1. Stitched Model Simulink Overview ("X" indicates removed section)[47]

3.2.1 Equations of Motion.

The final model which included the bare airframe, actuator dynamic, control surfaces, and control laws contained 6 degrees-of-freedom (6-DoF). This augmented 6-DoF model included the traditional aircraft 6 DoF aircraft states (body velocities (U, V, W) and body rotational rates (P, Q, R)) as well as additional integrators and dynamics which were associated with the control surface (elevator, ailerons, rudder, and horizontal stabilizer) actuators and rate limiters. Equations 3.1 thru 3.4 present the state-space equations of motion. Figures 3.2 and 3.3 present the stability derivative values which were scheduled with x-body axis velocity U as described in Section 2.5.

$$\begin{bmatrix} \dot{u} \\ \dot{w} \\ \dot{q} \\ \dot{\theta} \end{bmatrix} = \begin{bmatrix} X_u & X_w & X_q - W_0 & -g\cos(\Theta_0) \\ Z_u & Z_{\dot{w}} & Z_q + U_0 & -g\cos(\Theta_0) \\ M_u & M_w & M_q & 0 \\ 0 & 0 & 1 & 0 \end{bmatrix} \begin{bmatrix} u \\ w \\ q \\ \theta \end{bmatrix} + \begin{bmatrix} X_{\delta_e} & X_{\delta_T} \\ Z_{\delta_e} & Z_{\delta_T} \\ M_{\delta_e} & M_{\delta_T} \\ 0 & 0 \end{bmatrix} \begin{bmatrix} \delta_e \\ \delta_T \end{bmatrix} \quad (3.1)$$

$$\begin{bmatrix} q \\ \alpha \\ a_x \\ a_z \\ \dot{u} \\ \dot{w} \end{bmatrix} = \begin{bmatrix} 0 & 0 & 1 & 0 \\ 0 & 1/U_0 & 0 & 0 \\ X_u & X_w & X_q & 0 \\ Z_u & Z_w & Z_q & 0 \\ X_u & X_w & X_q - W_0 & -g\cos(\Theta_0) \\ Z_u & Z_w & Z_q + U_0 & -g\cos(\Theta_0) \end{bmatrix} \begin{bmatrix} u \\ w \\ q \\ \theta \end{bmatrix} + \begin{bmatrix} 0 & 0 \\ 0 & 0 \\ X_{\delta_e} & X_{\delta_T} \\ Z_{\delta_e} & Z_{\delta_T} \\ X_{\delta_e} & X_{\delta_T} \\ Z_{\delta_e} & Z_{\delta_T} \end{bmatrix} \begin{bmatrix} \delta_e \\ \delta_T \end{bmatrix} \quad (3.2)$$

$$\begin{bmatrix} \dot{v} \\ \dot{p} \\ \dot{r} \\ \dot{\phi} \end{bmatrix} = \begin{bmatrix} Y_v & Y_p + W_0 & Y_r - U_0 & g\cos(\Theta_0) \\ L_v & L_p & L_r & 0 \\ N_v & N_p & N_r & 0 \\ 0 & 1 & \tan(\Theta_0) & 0 \end{bmatrix} \begin{bmatrix} v \\ p \\ r \\ \phi \end{bmatrix} + \begin{bmatrix} Y_{\delta_a} & Y_{\delta_r} \\ L_{\delta_a} & L_{\delta_r} \\ N_{\delta_a} & N_{\delta_r} \\ 0 & 0 \end{bmatrix} \begin{bmatrix} \delta_a \\ \delta_r \end{bmatrix} \tag{3.3}$$

$$\begin{bmatrix} p \\ r \\ a_y \\ \beta \\ \dot{v} \end{bmatrix} = \begin{bmatrix} 0 & 1 & 0 & 0 \\ 0 & 0 & 1 & 0 \\ Y_v & Y_p & Y_r & 0 \\ 1/V_{tot} & 0 & 0 & 0 \\ Y_v & Y_p + W_0 & Y_r - U_0 & g\cos(\Theta_0) \end{bmatrix} \begin{bmatrix} v \\ p \\ r \\ \phi \end{bmatrix} + \begin{bmatrix} 0 & 0 \\ 0 & 0 \\ Y_{\delta_a} & Y_{\delta_r} \\ 0 & 0 \\ Y_{\delta_a} & Y_{\delta_r} \end{bmatrix} \begin{bmatrix} \delta_a \\ \delta_r \end{bmatrix} \tag{3.4}$$

3.2.2 Engine Model.

A known weakness of the overall Learjet aerodynamics model was the engine model. Since the model was developed using primarily flying qualities flight test techniques with limited engine performance data the engine model consisted of lookup tables. The lookup tables provided maximum and idle thrust values at 0 and 40,000 ft., both at 0, 0.25, and 0.8 Mach. For intermediate airspeeds and altitudes, the thrust values were simply interpolated and scaled linearly based on the percent of throttle commanded. The impact is that as the aircraft throttle is changed, the response of the engine and thrust changes are not accurately reflected in the path prediction, leading to deviation from the actual aircraft response.

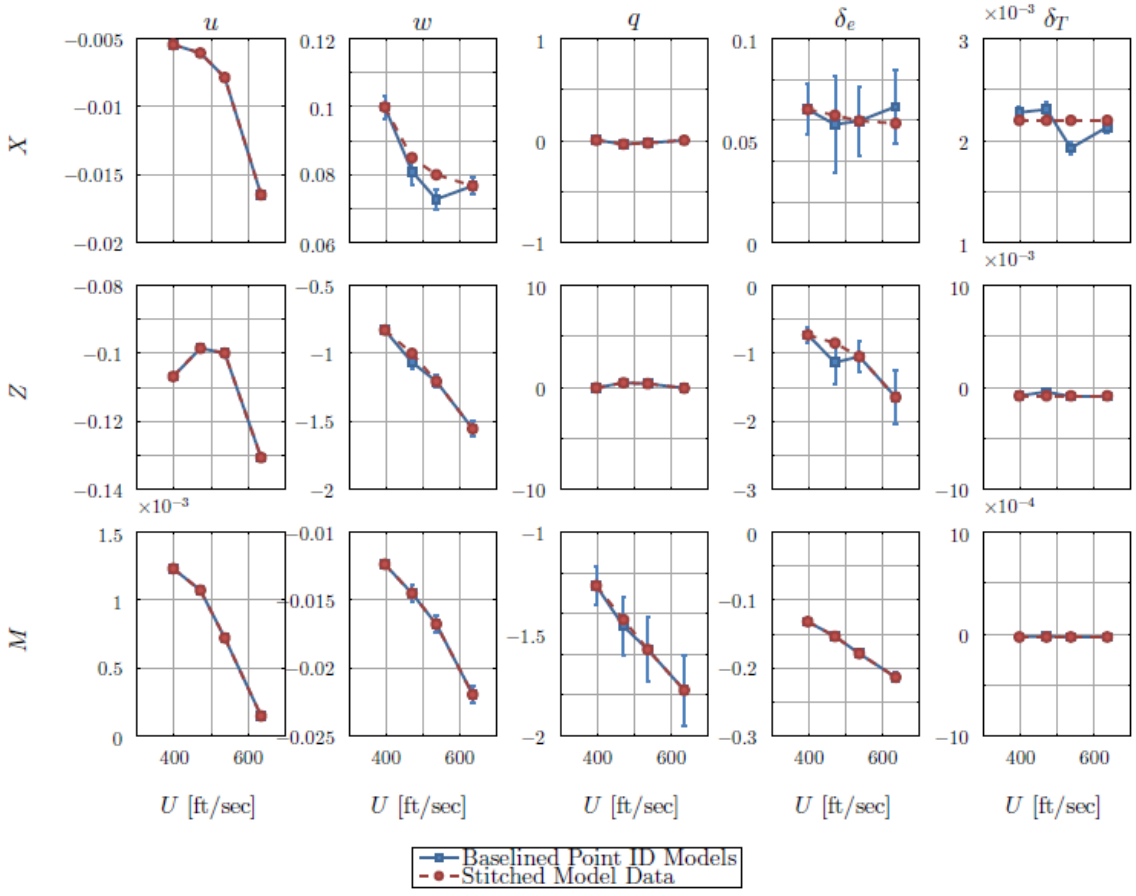

Figure 3.2. Longitudinal Axis Stability and Control Derivatives as a Function of Airspeed (15,000 ft MSL) [47]

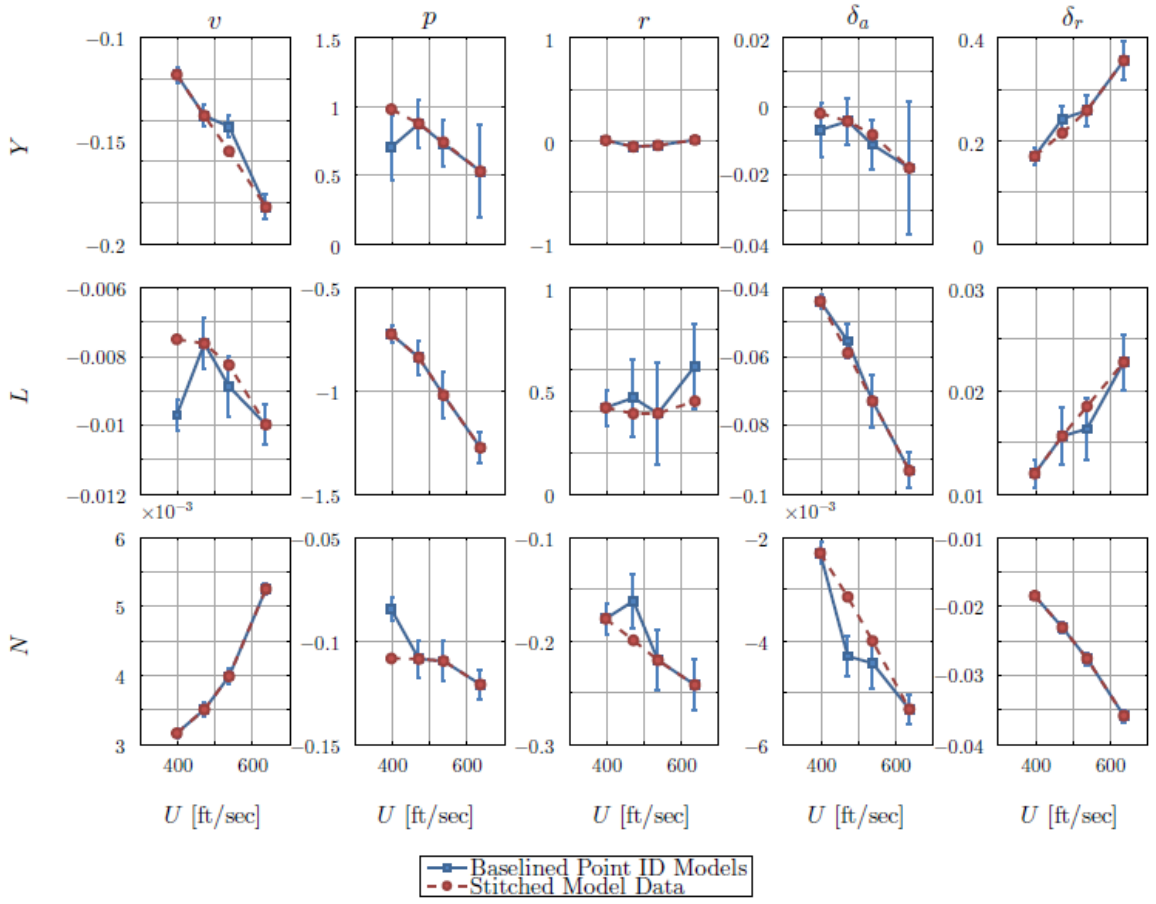

Figure 3.3. Lateral/Directional Axis Stability and Control Derivatives as a Function of Airspeed (15,000 ft MSL) [47]

3.2.3 Terrain Slewing Tool.

The Terrain Slewing Tool was a Simulink based interface designed by Calspan which could translate, rotate, and elevate or lower current aircraft position to place it on a collision course with the objective virtual DTED terrain feature. This tool was used and proven during Trombetta's Have ESCAPE test flights [15]. The Terrain Slewing Tool was instrumental in allowing quick progression through test points and for safely executing the tests against realistic terrain features while safely away from the actual terrain. At the test conductor (TC) station the TC was able to selection the terrain feature and, upon initiation of the RSET system, virtually relocate the aircraft.

3.3 Converted Model Performance

Once the Converted Model was complete it was then necessary to determine if the desired computational speed had been achieved and how much, if any, accuracy was lost during the conversion. The following sections present an analysis of the findings.

3.3.1 Research Laptop Computer.

The laptop used for the development of the RSET system was a Hewlett-Packard EliteBook 8570w. Specifications for this laptop are listed in Table 3.1. The reader should note that the development laptop was less powerful than the one used during flight test, as discussed in Section 3.9, and assumed that in the research laptop was sufficient, the flight test would be sufficient.

3.3.2 Converted Model Computational Speed.

To determine the speed gained by converting the Stitched Model several simulations were run on both the Stitched Model and the Converted Model. Every effort was

Table 3.1. Research Laptop Specifications

Model	Hewlett-Packard EliteBook 8570w
Operating System	64-Bit Windows 7 Pro
MATLAB Version	R2015B
RAM	16 GB
Processor	Intel Core I7-3720QM, 2.6 GHZ
Graphics	NVIDIA Quadro K1000M
Microarchitecture	Ivy Bridge
Data width	64 bit
Number of cores	4
Number of threads	8
Level 1 cache size	256 KB
Level 2 cache size	1 MB
Level 3 cache size	6 MB

made to remove bias from the comparison including Simulink configuration, similar output variables, and similar subsystems retained. The results of those simulations are shown in Table 4.1 in Section 4.2. Per discussion with the Stitched Model developers, the recommended integration method was MATLAB's ode4 (Runge-Kutta) with an integration time-step (dt) of 0.005 sec which serves as the baseline for comparison [60, 62]. Other integration methods are shown with the Stitched Model to show the effect of integration order on operating speed. During the conversion process the Euler-Forward integration method was adopted for simplicity, as shown in Equation 3.5 [63]. Ultimately, the Euler-Forward method provided the required operating speed and accuracy.

$$y_{n+1} = y_n + hf'(x_n, y_n) \tag{3.5}$$

3.3.3 Converted Model Accuracy.

To validate the Stitched Model, Berger et al. compared the response of the simulation to actual Learjet 25 flight test data for a pitch doublet and a roll doublet as shown in Figures A.2 and A.3 [47]. To validate the Converted Model, the Stitched model was treated as the baseline and the two were compared using the same pitch and roll doublets. The resulting plots for that comparison are presented in Appendix A.2. Figure 3.4 is a sample of the Appendix A figures and shows the strong agreement between the Stitched Model and Converted Model. There are a number of techniques available to quantify the accuracy of two data sets, in this case the time history of Stitched Model and Converted Model doublet responses. Following the example of Vahle for his recent TPS TMP, this research used Theil's Inequality Coefficient [59].

3.3.3.1 Theil's Inequality Coefficient Analysis.

Using TIC as described in Section 2.6, Table 4.2 in Section 4.2 shows TIC values for the Converted Model using various dt values. Pitch and roll doublets were used to generate the time histories. In all cases the Stitched Model with a dt of 0.005 sec was used as the "trusted model". It can be seen that at dt $\leq$ 0.010 sec the Converted Model has very strong agreement to the Stitched Model (TIC $\leq$ 0.3). With increasing dt the TIC value increases and at dt = 0.015 sec the model fit is unacceptable. Based on this information dt = 0.010 sec was used for the propagated trajectories discussed in Section 3.5.1.

3.4 Identical Path Prediction and Execution Control Laws

Section 2.3 presented a number of different approaches to path prediction and execution in both operational and research level systems. Some systems rely purely on equations of motion for trajectory propagation while others, such as the NASA SUAV,

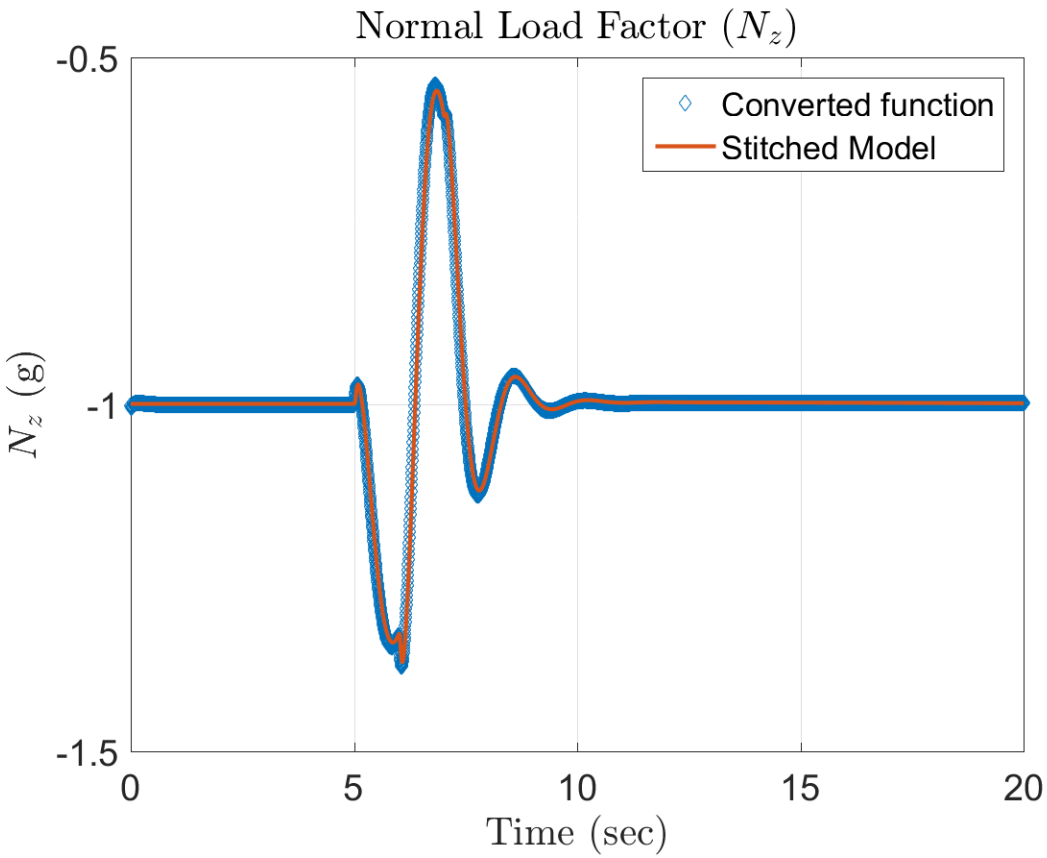

Figure 3.4. Normal Load Factor Response to Pitch Doublet

use flight test data [23]. In all cases, as of this writing, Auto-GCASs used dissimilar control laws for prediction and execution. This research sought to apply a novel approach by using the same control law to both predict and execute the trajectories. The challenged was that for multi-path systems there are many predictions to perform but only one to execute. The reasoning behind this approach was that by using the same control law for prediction and execution, the accuracy of the maneuver would be retained, reducing error and ultimately nuisance. A model which uses pre-planned trajectories calculated from straight-and-level flight, on the other hand, may lose significant accuracy if the aircraft is maneuvering. Such was the case with the F-16 Auto-GCAS. Swihart et al. state "determining how closely the TPA should match the true recovery maneuver requires a balance between providing protection, eliminating nuisance, and minimizing model complexity" [22]. The identical control law approach sought to negate the need for a trade-off by using the same high fidelity model for the prediction and control of the escape maneuvers.

Since the Euler-Forward integration method produced the desirable operating speed and accuracy, as shown in Section 3.3.3, it was kept. The Converted Model using, a dt of 0.005 sec, showed a reduction in simulation time of 93%. Clearly this is a significant improvement in operating speed and met the needs of this research.

3.5 RSET System Description

The test item was the RSET system, which was designed to predict terrain collision potential and to automatically command an appropriate ground avoidance maneuver. As with F-16 Auto-GCAS and Have ESCAPE, the RSET system was designed with three overarching design requirements in mind: Do No Harm, Do Not Impede Mission Operations, and Avoid Ground Collisions. These algorithms, written in MATLAB and Simulink, were adapted to be integrated with the Learjet VSS flight control

system, which was able to be controlled externally via a laptop which sent commands through a Simulink interface. The RSET system is a significant step forward in Auto-GCAS development for performance limited aircraft and meets most of the recommendations, outlined in Chapter I, from the works of Suplisson, Trombetta, and Sorokowski. The improvements of RSET over the previously tested Have ESCAPE system are summarized in Table 3.4.

The RSET system consisted of three major components: the trajectory prediction algorithms (TPAs), the collision detector, and the maneuver autopilots. The RSET system logic flow diagram is depicted in Figure 3.5 and the system block diagram is shown in Figure 3.10.

3.5.1 Trajectory Prediction Algorithms.

The RSET system received time, space, position information (TSPI) and the aircraft states from the VSS and, using this information as a starting point, used trajectory prediction algorithms (TPAs) to predict the paths of the terrain avoidance maneuvers. At the core of the path predictions was the Converted Model.

A design philosophy used in the development of these TPAs was the idea of a "nervous yet aggressive copilot" (NACP). The Nervous-Aggressive Copilot (NACP) was envisioned as a competent vigilant copilot who is constantly concerned with safely avoiding terrain (nervous), but would not take control of the aircraft to do so until the last possible moment (aggressive). In this manner, the NACP embodies the design

Table 3.2. Auto-GCAS Requirements in Order of Importance [22]

Priority	Auto-GCAS Requirement
1	Do No Harm
2	Do Not Impede Mission Performance
3	Avoid Ground Collisions

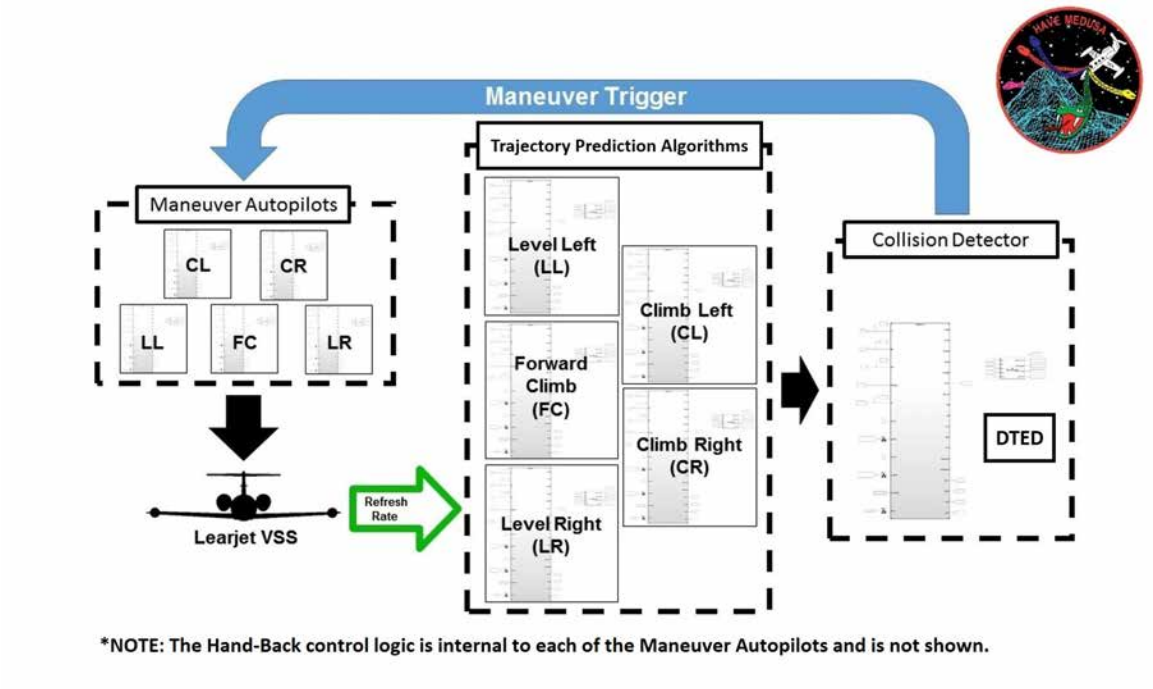

Figure 3.5. RSET System Logic Flow Diagram

criteria for RSET including continuous path analysis and minimizing nuisance via maximizing performance. As discussed in Section 2.3.3.3, Suplisson uncovered the importance of Min Control with and Aggressive Trigger as the appropriate optimal control formulation for heavy aircraft. The Aggressive Trigger is necessary for the Min Control formulation to be nuisance-free whereby the avoidance maneuver is not performed until a control is at a maximum. This research applies this concept with the modification that it be maximum *performance* instead of *control*, since the aircraft need not be at the limit of a particular control to be at its maximum performance.

Using the NACP design concept, five TPAs were developed and are described as follows:

- Forward Climb (Path 3)
  - Roll to wings-level
  - 2-g pull to 12^o flight path angle (γ)

- Advance throttle to Maximum Continuous Power (MCP)

- 60^o Left (Path 1) and 60^o Right (Path 5) Turns
  - Roll to 60^o right or left bank
  - Pull 2 g
  - Advance throttle to MCP
- 30^o Climbing Left (Path 2) and 30^o Climbing Right (Path 4) Turns
  - Roll to 30^o right or left bank
  - Pull 2 g
  - Advance throttle to MCP

All five TPAs used a speed-scaled flight path angle (gamma, γ) with an Nz limiter control law as well as a coordinated turn control law. The control laws were developed using control design techniques described by Stevens and Lewis, Nelson, and Ogata [64–66] as well as with guidance provided by the Learjet 25D VSS operator Calspan [62]. Basic block diagrams for the two control feedback loops used by the five TPAs are shown in Figures 3.6 and 3.7.

Figure 3.6 depicts the control law used to execute the pull portions of the maneuvers, which was a speed-scale flight path angle (gamma, γ) command with a load factor (Nz) limiter. The control law was designed to primarily achieve the maximum aircraft flight path angle at maximum continuous power (MCP). From simulator testing and early checkout flights this was found to be 12^o at 270 KCAS. For safety purposes the lower airspeed limit was set at 200 KCAS, so the speed scaler was used to adjust the target γ down as speed decreased during a climb. Due to the simple nature of this design, at high speed from level flight the initial pull command was aggressive enough to overshoot the target of approximately 2 g. For this reason, the Nz limiter was added. Additionally there were instances during a maneuver where the aircraft would unload to a low g condition, so a lower Nz limiter of 0.6g was added.

The coordinated turn control law loop is shown in Figure 3.7. This simple control law design was effective at producing the desired bank angle with minimal sideslip.

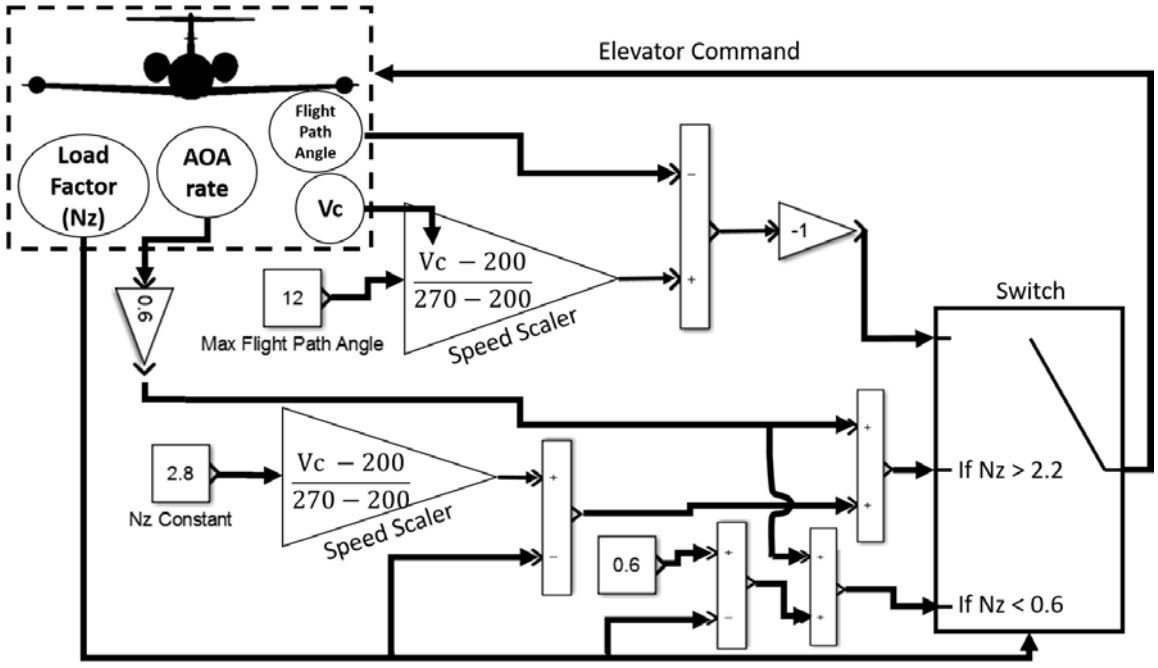

Figure 3.6. RSET Speed Scaled Gamma (γ) Command with Load Factor (Nz) Limiter Control Diagram

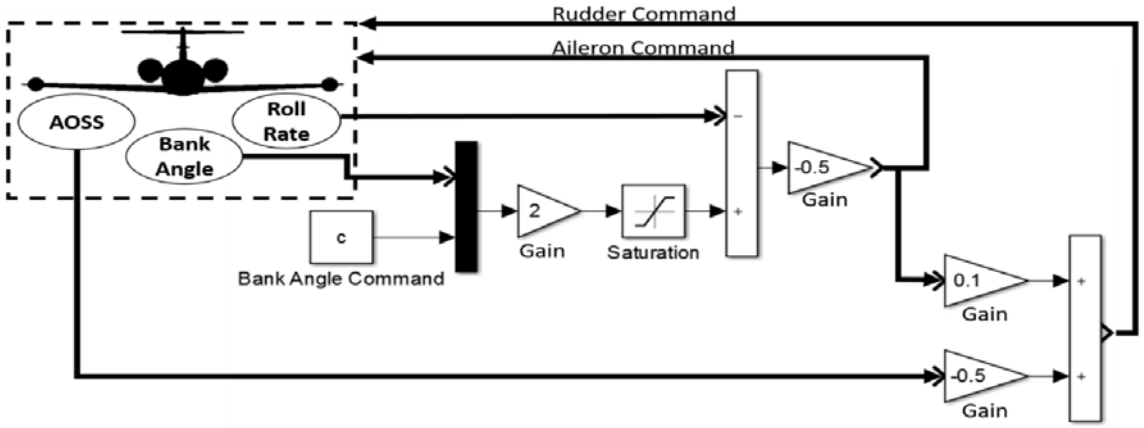

Figure 3.7. RSET Coordinated Turn Control Diagram

As discussed above, the bank angle command was changed depending on the path to be performed.

The control law gains were tuned by running simulations at various initial conditions and observing the behavior of the aircraft. Wherever possible the feedback loop itself was tuned to ensure the aircraft operated at or near maximum performance (i.e. aggressive) throughout the maneuver. Otherwise limits were put in place that prevent the autopilot from over-controlling the aircraft beyond the Learjet 25D safety limits given in Table 3.5. Since the Converted Model was of such a high fidelity the majority of the autopilot design was accomplished via simulation. The simulation derived gains were then adjusted during flight test.

To prevent altitude loss and asymmetric loading during the maneuver, additional restrictions were place on the control laws as described in Table 3.3. The restrictions were used to allow for safe and effective path execution regardless of aircraft maneuvering (e.g. calculating a 60^o left turn when in a right turn).

3.5.1.1 Trajectory Propagation Length and Update Rate.

Based upon the analysis performed by Trombetta, and presented in Table 2.8, the paths were each propogated for 30 seconds into the future. All five 30-second look-aheads, known as the path prediction time, were computed at a planned rate of 12.5 Hz, 6.25 Hz, or 1.5625 Hz, known as the refresh rate. The TPAs were calculated based on the throttle being advanced to maximum continuous power, which for testing was manually activated by the test pilots as discussed in Section 1.4. Figure 3.8 shows a visual representation of the five paths generated by the RSET system TPA logic in simulation.

The TPAs used a fundamental time-step, dt, of 0.010 seconds which Tables 4.1 and 4.2 show provided an excellent balance of speed and accuracy. Once each TPA

Table 3.3. RSET Bank Angles and Maneuver Restrictions

Path	Bank Angle Command	Maneuver Restrictions
1	-60^o	If flight path angle (γ) drops below 0, the bank angle command goes to 0.
2	-30^o	If flight path angle (γ) drops below 0, the bank angle command goes to 0. Delay gamma command loop until bank angle is less than +5^o
3	0^o	Delay gamma command loop until bank angle is between -10^o and +10^o.
4	+30^o	If flight path angle (γ) drops below 0, the bank angle command goes to 0. Delay gamma command loop until bank angle is less than -5^o
5	+60^o	If flight path angle (γ) drops below 0, the bank angle command goes to 0.

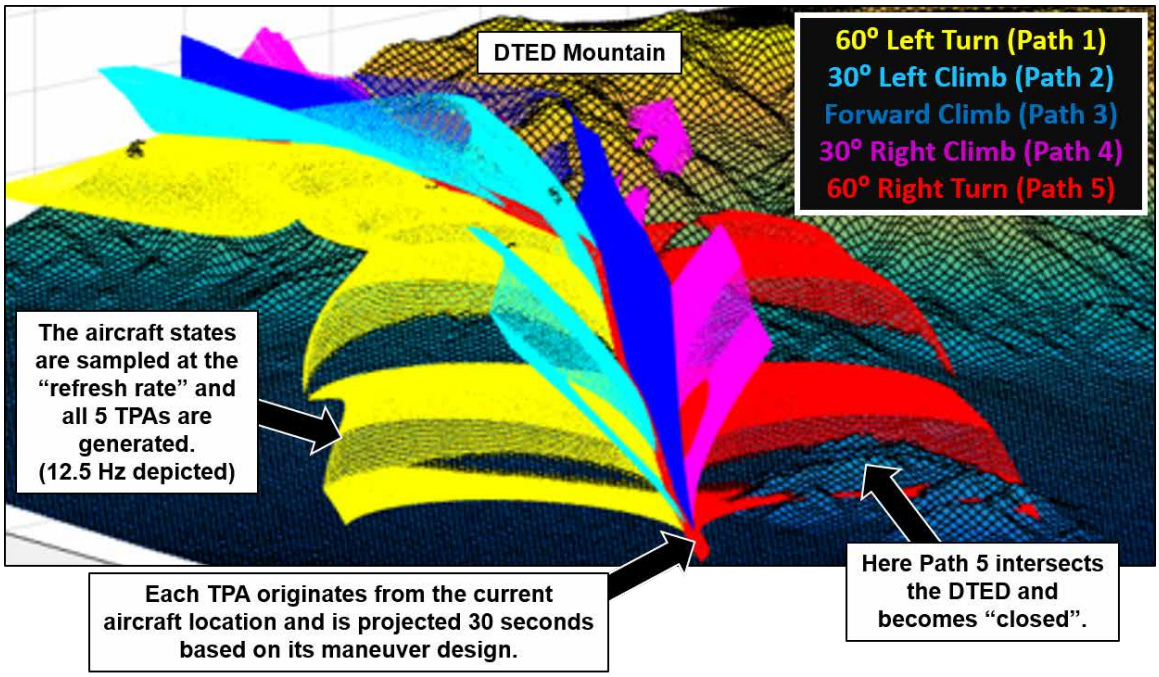

Figure 3.8. RSET Path Prediction Example with 12.5 Hz Refresh Rate (from simulation)

calculated its respective predicted path, the vectors of aircraft position were passed to the collision detector as shwon in Figure 3.5 and is discussed next.

3.5.2 Collision Detection.

As presented in Sections 2.2.3 and 2.2.8 there were a number of ways to compare the predicted aircraft trajectory to the terrain elevation model and determine if a conflict exists. To preserve speed this research opted to use interpolation to compare the projected path to the terrain directly beneath each point.

At each sample time all five paths were evaluated for terrain collision. As long as one of the five paths was available, the RSET system did not intervene with the operation of the aircraft. Once all five paths predicted a collision along their respective 30 second path, the path which was the last to predict a collision is chosen as the escape route. This "Last Man Standing" approach to multi-path selection is

the same as that used by Sorokowski et al. and Trombetta [15, 23]. Once the "Last Man Standing" was identified, be it the Forward Climb or one of the turning paths, the collision detector sent a flag[1] to the controlling autopilots to execute the escape maneuver.

The generated paths were compared to Level 1 DTED, available from the National Geospatial Intelligence Agency website, to find the distance between the flight path and the terrain for each possible maneuver. The aircraft path was compared against the interpolated DTED posts to determine the distance between the aircraft altitude and the height of the terrain. Since Level 1 DTED had a spacing of approximately 295 ft between posts, interpolation was used to ensure that the aircraft did not simply fly between posts and fail to identity a collision. The MATLAB interpolation method used was called *nearest*, and referenced the closest DTED post to the TPA. This interpolation method was chosen since it significantly reduced computational time versus other interpolation methods, such as *cubic* or *spline*. Refer to Section 5.3 for further discussion on this. If one or more maneuvers was predicted to maintain safe separation from the terrain, the system did not take any action because it assumed an aware pilot would be able to avoid the collision in a timely manner. This was an important feature to avoid nuisance activations. When the system predicted that every path intersected the GCB (evaluated at 200 feet), the system immediately took control of the aircraft and commanded the maneuver which was last predicted to violate the GCB. In this way, the algorithm waited for the last path to intersect terrain allowing for pilot intervention up to the point where a collision would become imminent. Safety buffers added to the terrain elevation accounted for TSPI and path prediction errors as well as the time needed for the last available path to be selected and executed. The GCB was simply a fixed height value added to each DTED post.

[1]Here a flag refers to a number between 1 and 5 which identified the autopilot to be engaged.

Level 1 DTED was required to have a vertical error of less than 30 meters (98.4 ft) from Performance Specification: Digital Terrain Elevation Data (DTED) [MIL-PRF-89020B] [67]. Level 1 DTED error was accounted for in the Terrain Safety Buffer (TSB).

3.5.3 Maneuver Autopilots.

One of the elegant features of the newly developed RSET system was that the same control logic used to determine the five escape paths was used to execute the actual escape maneuver. Another feature of the RSET system was that at each sample time all five paths are evaluated to see if a conflict exists and if there is a more aggressive, i.e. less nuisance, path. In other words, once an avoidance path had been selected it need not be flown for any predetermined amount of time. Depending on the terrain being traversed the RSET system could switch between several trajectories to form an overall more aggressive route than if just one path had been followed. This design was motivated by Bellman's Principle of Optimality as presented by Kirk [68]. The optimal policy, as presented by R.E. Bellman and S.E. Dreyfus,

> "...has the property that whatever the initial state and initial decision are, the remaining decisions must constitute an optimal policy with regard to the state resulting from the first decision" [69].

While this research does not assert that any of the generated paths were optimal, it is accepted that they were optimal in a sense by nature of their aggressiveness.

When the collision detector identified the need to perform an avoidance maneuver, a flag was sent to autopilot control laws which were capable of commanding the Learjet VSS. The maneuver autopilots were identical in architecture and control law design to the TPAs. This was important for ensuring the path flown by the aircraft matched the path calculated by the RSET system as closely as possible. Once the system

identified that the aircraft was no longer on a collision course with terrain based on one or more paths opening, control was relinquished back to the pilot. Identical to the TPAs, the maneuver autopilots included left and right 60^o-bank turns, left and right 30^o-bank angle climbing turns limited to 2 g, and a wings-level climb. All five maneuver autopilots also used a speed-scaled flight path angle control law with a load factor (Nz) limiter. Simulator results indicated that forward climbing escape maneuvers resulted in a steady-state flight path angle of approximately 8^o. The evaluation pilot (EP) had the ability to paddle off, or manually disconnect, the maneuver autopilots and regain control of the Learjet VSS for safety or test efficiency. Once the collision detector determined that one path was again available, a hand-back autopilot was engaged. The hand-back autopilot rolled the aircraft to wings-level and targeted zero flight path angle in preparation of handing the controls back to the EP. Any time after the hand-back autopilot was engaged, the collision detector could reengage if another collision event was detected. Figure 3.9 shows the results of a simulation with the path color-coded to depict which autopilot was controlling the aircraft (green means the pilot was in control).

3.5.4 Maneuver Termination and Control Hand-Back.

As discussed in the Collision Detector section, the RSET system took control of the aircraft when all paths became unavailable, or closed, and executed the last available path to avoid the terrain. During an RSET activation, if another path became available, or open, then the system would hand back control to the pilot. The hand-back sequence consisted of a roll to wings-level and targeting zero flight path angle. The hand-back algorithm was fairly simple and immature, as is discussed later in the test results. At the same time that the RSET system tests were being conducted at TPS, at AFIT Carpenter was investigating various aspects of Auto-

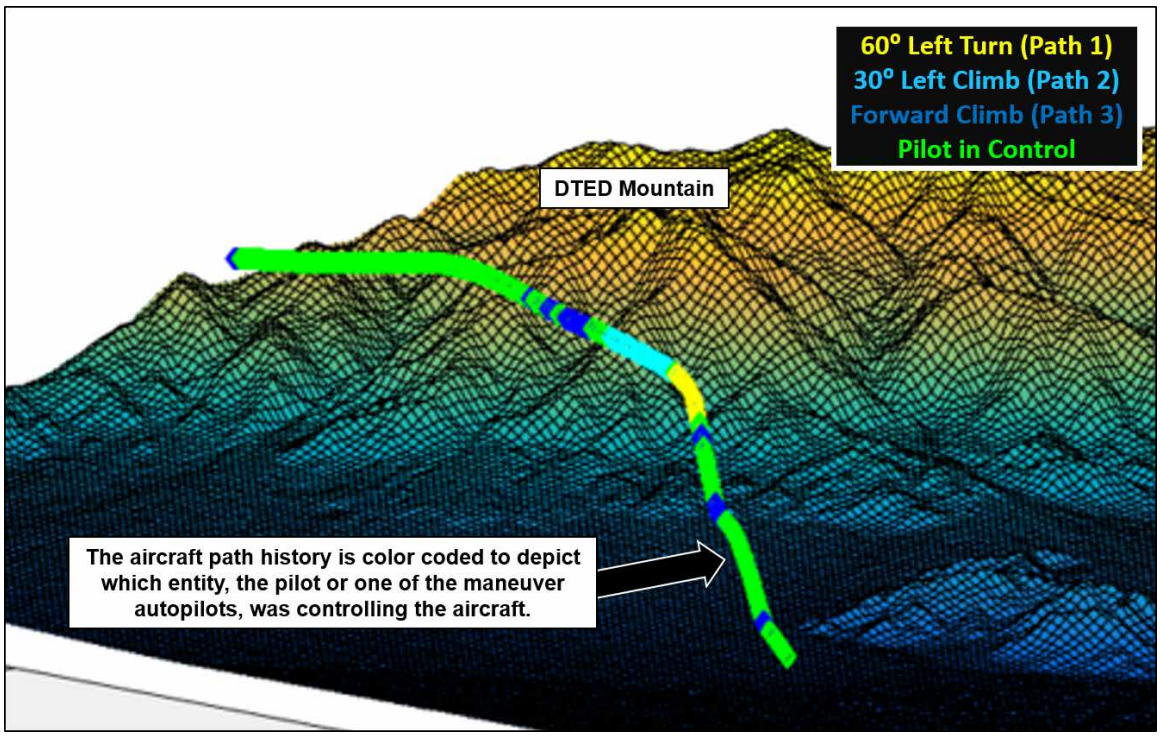

Figure 3.9. RSET Active Path History (from simulation)

GCAS improvement, including maneuver termination and hand-back. His thesis, title "Automatic Ground Collision Avoidance System for Performance Limited Aircraft", provides additional information on this topic [70].

3.6 RSET versus Have ESCAPE Differences Summary

Since Have ESCAPE served as a foundational work and motivation for the RSET system, it is germane to provide a comparison between the two Auto-GCASs. Table 3.4 summarizes the primary differences between the RSET system and the Have ESCAPE algorithm from the Have ESCAPE test report, and shows the contributions of the RSET research [71].

Table 3.4. Differences Between Have ESCAPE and RSET

	Have ESCAPE	RSET
Model fidelity	3-DoF	Augmented 6-DoF
Path prediction	5 pre-calculated 3-DoF paths	5 autopilot calculated 6-DoF paths
Full Flight Envelope Compatible?	No - only compatible with 1 airspeed and altitude and in straight-and-level flight	Yes - able to adapt to changing airspeed, altitude, and attitude.
DTED used	Level 1	Level 1
Collision detection method	"bubble" around aircraft touched DTED post	Aircraft position interpolated against DTED
Maneuver execution	Time series of g and bank angle commands	Used same autopilots as path prediction
Continuous Path Analysis?	No - Once triggered the system flies out the full duration of the maneuver	Yes - Continuously analyzes all 5 paths and hands back control if conflict is resolved

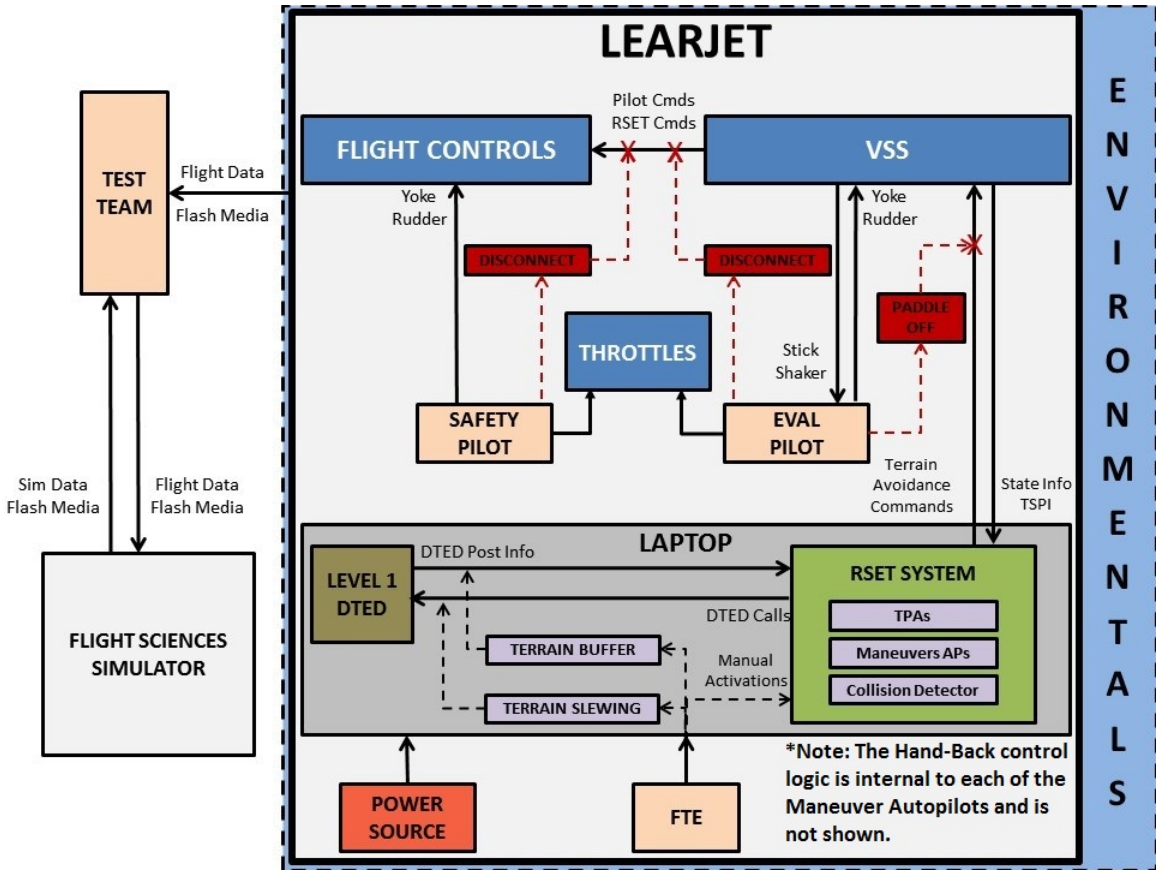

Figure 3.10. RSET System Block Diagram

3.7 Flight Test Objective Selection

There was extensive discussion among the Have MEDUSA test team and supporting personnel regarding flight test objective selection. Presented here is a brief explanation for the reasoning behind the objectives chosen.

1. Demonstrate the path prediction accuracy of the RSET system.

   Since the RSET system utilized a more complex aerodynamic model and used identical control laws for TPA calculation and maneuver execution, it was important to determine how well a predicted path matched that actual flown path.

2. Demonstrate the impact of changing the refresh rate on the RSET system's

ability to calculate an achievable escape path.

As has already been discussed, computational power and model fidelity are design trade-offs. This objective was chosen to identify the threshold for minimum path analysis speed (refresh rate).

3. Observe the RSET system tendency to nuisance activation.

   The second overarching requirement for Auto-GCAS design is "Do Not Impede Mission Performance". As such, a successful design needs to be as free of nuisance as possible. This objective was chosen to evaluate the RSET system in several terrain environments for unwarranted activation.

4. Observe the control hand-back of the RSET system after maneuver termination.

   As Auto-GCAS technology moves closer toward being a reality for performance limited aircraft, the question of when and how the Auto-GCAS should relinquish control back to the pilot will be a design challenge. The test team realized that the Have MEDUSA test flights were a valuable opportunity to gather data and aircrew comments on hand-back conditions.

3.8 Test Equipment

3.8.1 Flight Sciences Simulator.

The USAF TPS FSS, described in Section 2.11.1, was used to check communication between the Test Laptop Computer and the Learjet VSS interface. The FSS was also used to adjust the control law gains and prepare the EPs for the RSET system taking control of the aircraft in flight. Due to manning and time constraints the FSS was not used to gather any flight test objective data.

3.8.2 Calspan Learjet 25D VSS.

The Calspan VSS-equipped Learjet LJ-25D (LJ-25D), displayed in Figure 3.11, was employed as a platform to test the RSET system. The VSS was capable of inflight simulation of different aircraft control laws and aircraft responses in four degrees of freedom (pitch, roll, yaw, and thrust) using control surface and feel system[2] actuators. Since the aircraft model at the core of the RSET system was developed using the baseline LJ-25D, the VSS was used in the baseline configuration for this test. The cockpit accommodated a pilot and copilot crew. There was seating in the cabin for a Test Conductor (TC) and one more occupant to include technical representatives or incentive flyers. Minimum test aircrew included the two pilots and a TC. A TPS student EP flew from the right seat control stick with VSS components. A Calspan instructor pilot served as the pilot-in-command as well as the Safety Pilot (SP) from the left seat. The left seat pilot controls were mechanically linked to the flight control surfaces, and provide un-augmented flight control when the VSS was disengaged. Under normal operation, the right seat EP controlled the VSS via an interface that sent electrical signals from his controls to the hydraulic actuators connected to the control surfaces.

In the VSS mode, engagement and safety trip logic existed which detected failure conditions including aircraft states and loads, feel system, control surface parameters, and hydraulic fluid level. If a failure condition or safety trip logic was satisfied, as shown in Table 3.5, hydraulic pressure was removed from the control surface and feel actuators, failures were annunciated in the cockpit, and the VSS was disengaged as discussed in Learjet Flight Syllabus and Background Material for the US Air Force/US Naval Test Pilot School Variable Stability Programs, TM-FRG-LJ1-0061-R05 [72]. The VSS could also be manually disengaged by either pilot. Any VSS

[2]The feel system is part of the normal LJ-25D VSS an is meant to provide the sensation of a reversible flight control system despite the VSS being "fly-by-wire"

Figure 3.11. Calspan Variable Stability System Learjet LJ-25D with the Have MEDUSA Test Team

disengagement automatically returned aircraft control to the SP. The Learjet-25D was instrumented to collect aircraft performance and state data required to evaluate test objectives at a rate of 200 Hz.

The RSET system interfaced with the VSS, which directly implemented the escape maneuvers. During flight tests, the VSS operated using autopilots of the same design as those used to generate the RSETs. The LJ-25D had a radar altimeter but did not incorporate TAWS, GPWS, or any other altitude-dependent systems that would interfere with the RSET system. When the RSET system commanded a maneuver to the aircraft, it sent a flag to the maneuver autopilots to perform the ground avoidance maneuver. These maneuvers were commanded until a clear of terrain flag was sent at which time the system activate the hand-back autopilots and rolled the aircraft to wings-level and targeted zero flight path angle in preparation of handing the controls back to the EP. Then, the RSET system disengaged and control of the aircraft was returned to the EP. The EP also had the option to manually terminate the automatic

Table 3.5. LJ-25D VSS Safety Parameters [57]

Parameter[a]	Limits[b]	Automatic VSS Trip?
Airspeed (At or below 14K Ft)	306 KCAS	No[c]
Airspeed (Above 14K Ft)	325 KCAS / 0.79 M	No[c]
Normal Load Factor (n_z)	+0.25g to +2.8g	Yes
Lateral Load Factor (n_y)	±0.3g	Yes
Angle of Attack (α)	-5^o to $+12^o$	Yes
Angle of Sideslip (β)	10^o	Yes

[a] This table presents just a small sample of the VSS safety trips. Several additional sensors (such as load factor onset rate, control surface actuator pressure, etc.) are not discussed here.
[b] The safety trip logic for the above parameters was within the normal LJ-25D flight envelope.
[c] Airspeed was not monitored by VSS Trip Logic. The aircrew ensured limits were not exceeded.

maneuver by pressing a paddle-off button on the yoke. The TC had the ability to monitor the activation and termination of the RSETs on the test laptop. Additionally, the center console displayed the status of the five RSET paths during flight. Figure 3.12 shows the status of the Center Console System (CCS) during an RSET activation with all five paths unavailable (highlighted white). The CCS did not give an indication of which path, if any, was currently being flown. Rather, other than the motion of the aircraft, the only way from the CCS to know which path was active was to see which path was the last to remain open. The test laptop at the TC station, however, gave a visual depiction of path closures as well as the current active path, as shown in Figure 3.13. Note that the two circles shown were intended to be used as an anticipatory and an execution notification for a path, but the anticipatory function was not implemented. Instead both indicators were used to show whether a path was open or closed. When the RSET system was controlling the aircraft, a stick shaker on the right yoke (EP) activated to notify the pilots. The left seat yoke stick shaker still only activated to indicate a stall.

One key aspect of this research was the use of the Learjet VSS as a stand-in for

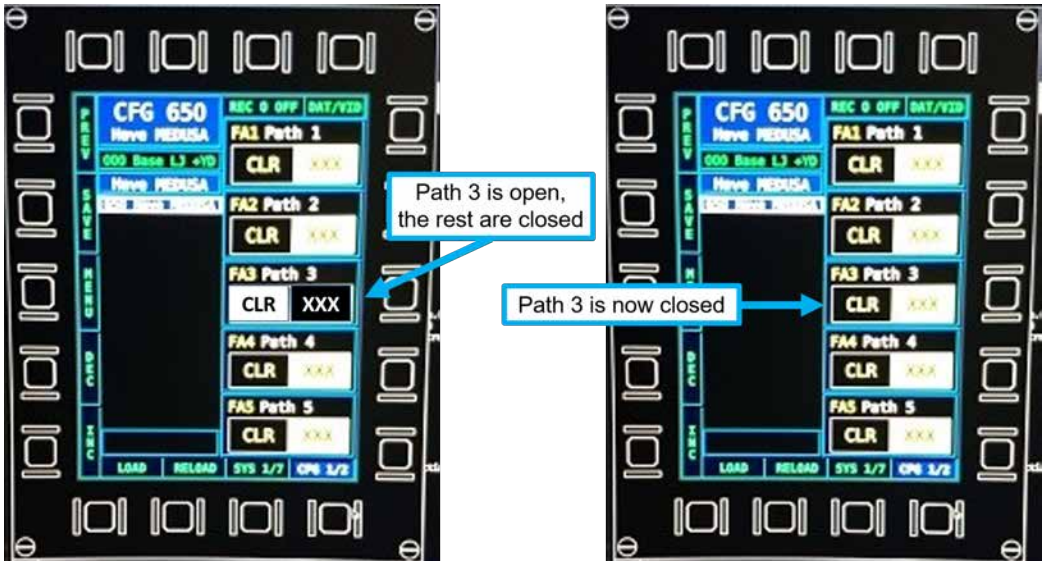

Figure 3.12. Learjet Center Console System RSET Path Status Page

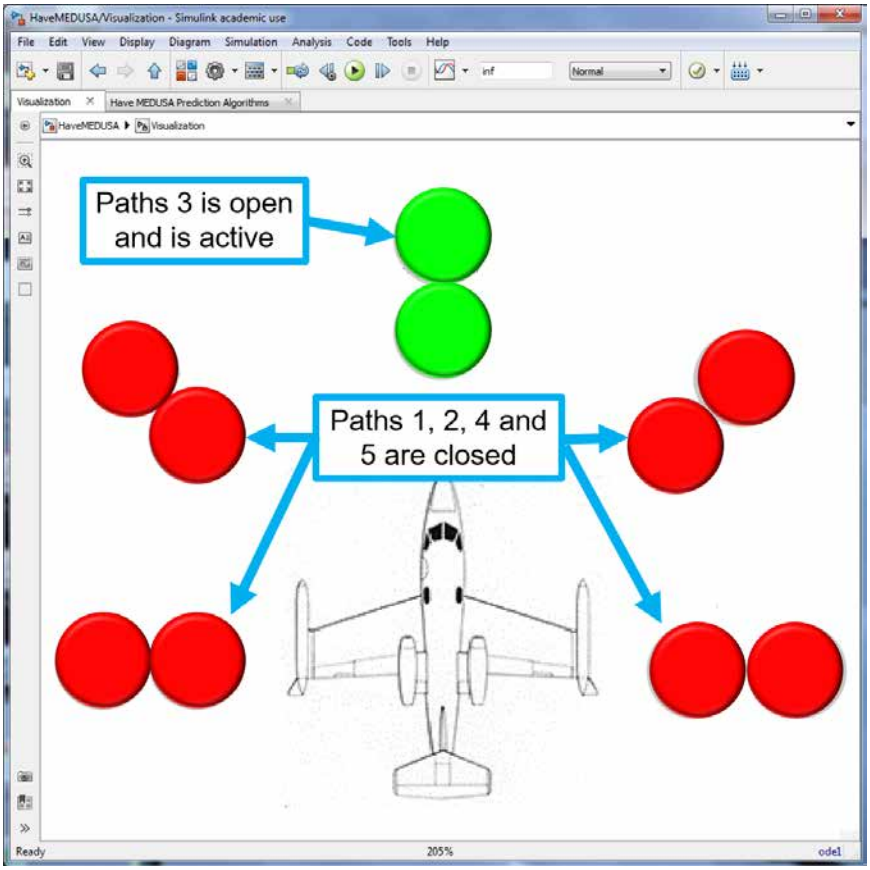

Figure 3.13. Test Conductor Station Path Status Indication

a performance-limited aircraft, such as a C-130 or C-17. The Learjet VSS was exceptional in this regard because it could be modified to behave as a heavy aircraft. Due to time constraints (the Learjet VSS also serves regularly as a curriculum aircraft at TPS), a "performance-limited" configuration was not developed. Rather, the Learjet VSS maneuvers were restricted to the limits given in Table 3.5 which were representative of larger mobility type aircraft. Roll rates were also limited to behave accordingly.

3.8.3 Test Laptop Computer.

The RSET system was run via MATLAB and Simulink on a laptop computer which interfaced with the VSS on the Learjet, referred to herein as the test laptop computer. It was the physical hardware which both received the aircraft state information as input to the RSET system and communicated the maneuver commands to maneuver the aircraft. The test laptop computer specifications can be found in Table 3.6.

The laptop was equipped with a solid-state hard drive to minimize the probability of malfunctions caused by aircraft motion. During flight, the test laptop was securely fastened to the TC workstation in the aircraft cabin. The view from the TCs workstation is shown in Figure 3.14.

It is important to note that the results related to operating speed and refresh rate are directly related to the performance of the host computer. As such, the pre-flight test results should be compared to the research laptop computer and the flight test results should be compared to the test laptop computer. The test laptop computer was a more powerful and newer laptop than the research laptop computer and was capable of running the RSET system faster.

Table 3.6. Test Laptop Specifications

Model	ASUS ROG G701VI
Operating System	64-Bit Windows 10 Pro
MATLAB Version	R2015B
RAM	32 GB
Processor	Intel Core I7-7820HK, 2.9 GHZ
Graphics	NVIDIA GTX 1080
Microarchitecture	Kaby Lake
Data width	64 bit
Number of cores	4
Number of threads	8
Level 1 cache size	256 KB
Level 2 cache size	1 MB
Level 3 cache size	8 MB

Figure 3.14. View from Test Conductor's Workstation

3.9 Test Methodology

The following sections discuss the flight test methodology as performed for the USAF TPS Have Multi-Path Escape Decisions Using Sophisticated Algorithms (MEDUSA) TMP.

3.9.1 Aircraft Ground Checkout.

The Learjet was equipped with a ground simulation mode that was used to verify that the RSET system sent the proper commands to the VSS. This simulation was used as a functionality check only, but it allowed a real-time determination that the System Under Test (SUT), VSS, and flight controls were communicating and operating correctly prior to flight. The goals of ground checkout were as follows:

- Verify integration of the RSET system by ensuring information exchange between the algorithm and the VSS computer.
- With the VSS in Simulator Mode, trigger every terrain avoidance maneuver and verify proper control surface deflection.
- Verify the operation of the DTED coordinate and elevation slewing function.
- Verify that the VSS handed back control to the pilot after escape path maneuver was complete.

The ground checkout found no major discrepancies.

3.9.2 Briefings.

Briefings were conducted prior to and immediately after each test sortie in accordance with TPS standards. All crew members for the day's test mission were required

to attend the briefing. These briefings were similar to those used by the Have ESCAPE TMP [15]. The minimum crew consisted of a TPS student EP, a Calspan SP, and a TC. The crew member annotated in parentheses was responsible for briefing the associated items. The pre-flight brief consisted of:

- Flight Safety (EP)
  - Weather and NOTAMs
  - Crew duties, responsibilities and Crew Resource Management (CRM)
  - Exchange of aircraft control and engaging VSS
  - Joker and bingo fuel
  - Emergency procedures
- Departure and Recovery (EP)
  - Radio Frequencies
  - Airspace Management
  - Departure and recovery routing
- Specific Mission Brief (TC)
  - Test Objectives
  - Software version
  - Test hazards and general minimizing procedures
  - Go/No-Go Criteria
  - Communication plan
  - Test card review

The post-flight brief consisted of:

- Safety of Flight Concerns (EP)
  - Crew members bring up any issues encountered
- Mission Recap (EP)
  - Brief review of test mission

Test Card Review (TC)

Test Points Completed

Data Quality

Lessons Learned for next test mission

3.9.3 Execution.

3.9.3.1 RSET System Prediction Accuracy.

The prediction accuracy of the RSET system was demonstrated by comparing the difference of the predicted flight path of the aircraft for a given collision avoidance maneuver and the actual path of the aircraft while executing that maneuver. Path Prediction Error (PPE) was defined as the distance between the two flights paths, and was computed at each sampled time from maneuver activation until hand-back of the aircraft. Refer to Appendix C for the details on how PPE was calculated. The evaluation criteria for RSET prediction accuracy was expressed in terms of the maximum value of PPE encountered during a 30-second maneuver. A maximum PPE of less than 100 ft was classified as satisfactory, between 100 ft to 300 ft as acceptable and above 300 ft as marginal.

The RSET system was flight tested at 15,000 ft pressure altitude (PA), 8,000 ft PA, and 500 ft AGL, each at 220 and 270 KIAS. Entry conditions consisted of straight, level, unaccelerated flight (SLUF)[3], 45^o left and right banked turns, 5^o wings-level climbs, and 5^o wings-level dives. All 500 ft AGL SLUF entry test points were repeated on separate flights. No diving entries were performed at 500 ft AGL. All five RSET system escape paths were tested at each of the stipulated pressure altitude, airspeed and entry conditions.

Prior to flight, the TC entered the number of passengers into the RSET system

[3]SLUF refers to a flight condition in which the aircraft is stable (i.e. trimmed) at a constant altitude, heading, and airspeed.

via a laptop at the engineers station. This increased the accuracy of the weight and balance measurement. At the established test point conditions, the TC entered the current wind speed and direction derived from the onboard embedded GPS/INS (EGI) and air data systems, and manually activated the RSET system escape path via the laptop. Immediately upon indications of an RSET path activation, the pilot set the throttle for maximum continuous power (MCP) (95 $\pm$ 2% RPM) in approximately 3 seconds to simulate auto throttle. The maneuver was completed after 30 seconds had passed since the autopilot commanded the aircraft to fly the chosen RSET system escape path, which allowed for comparison to the 30-sec path prediction.

Flights 1-3 were used to debug the RSET system, and only data from Flight 4-11 were used for data analysis. For the 30 test points collected during Flight 4 (SLUF at 15,000 ft PA, 8,000 ft PA, and 500 ft AGL (only for the first set of data) at 220 and 270 KIAS), the RSET system did not consider any inputs on the number of passengers, wind conditions, and had an allowable maximum flight path angle of up to 20 degrees instead of 12 degrees for the chosen RSET system escape path. Flights 5-11 accounted for wind through TC entered parameters. Wind drift was identified as a potential source of error as discussed later.

3.9.3.2 Refresh Rate Impact on Escape Path Calculation.

The second test objective was to gather terrain miss distance and forward look-ahead time data to characterize a baseline performance model for the RSET solution.

The baseline performance of the RSET system was tested using one terrain feature which included large mountain peaks located within the R-2508 complex as shown in Figure 3.15. The terrain feature was located at 35^o 31' 42.0" N, 116^o 18' 31.2" W. The base of the mountain was approximately at 0 ft MSL, and the peak was approximately 6,200 ft MSL. The test included three altitudes (15k ft PA, 8k ft PA,

and 500 ft AGL), two airspeeds (220 and 270 KIAS), and three initial conditions (ICs). The three initial conditions were selected to present different headings which provided varying terrain features to ensure all five paths were exercised. While the real aircraft was flown at varying altitudes, the virtual altitude induced by the terrain slewing tool, described in Section 3.2.3, was always set to 2,000 ft MSL. Three refresh rates were tested at each of these conditions (12.5 Hz, 6.25 Hz, and 1.5625 Hz).

The terrain miss distance data were analyzed by calculating the difference of the aircraft altitude to the height of the interpolated DTED surface directly below the aircraft. The sign of this value was used to determine whether the aircraft was above or below the virtual terrain. The actual distance to the virtual terrain was calculated as the smallest distance from the aircraft's location to a plane defined by the three closest DTED posts. This calculation was repeated at every time step throughout the path activation. The details of this calculation can be seen in Appendix C. The minimum value for each test run was then recorded as the terrain miss distance, with a negative value indicating terrain impact. Those miss distances were plotted against refresh rate with markers identifying either the initial condition (starting point and heading), test altitude, or test airspeed. This method was not the originally planned analysis method. An alternate method for calculating terrain miss distance using a root sum squared distance from the aircraft location to the nearest DTED posts of the surrounding terrain was planned. However, this presented scenarios that displayed a terrain impact when the aircraft was clear of the interpolated DTED terrain, since only the DTED posts were used in this method.

The forward look-ahead time was analyzed by determining the first point along the prediction path that impacted terrain, at the moment the last remaining path was determined to be closed by the collision detector. This point was reported as a time along the path, with the point closest to the aircraft at zero seconds, and the end of

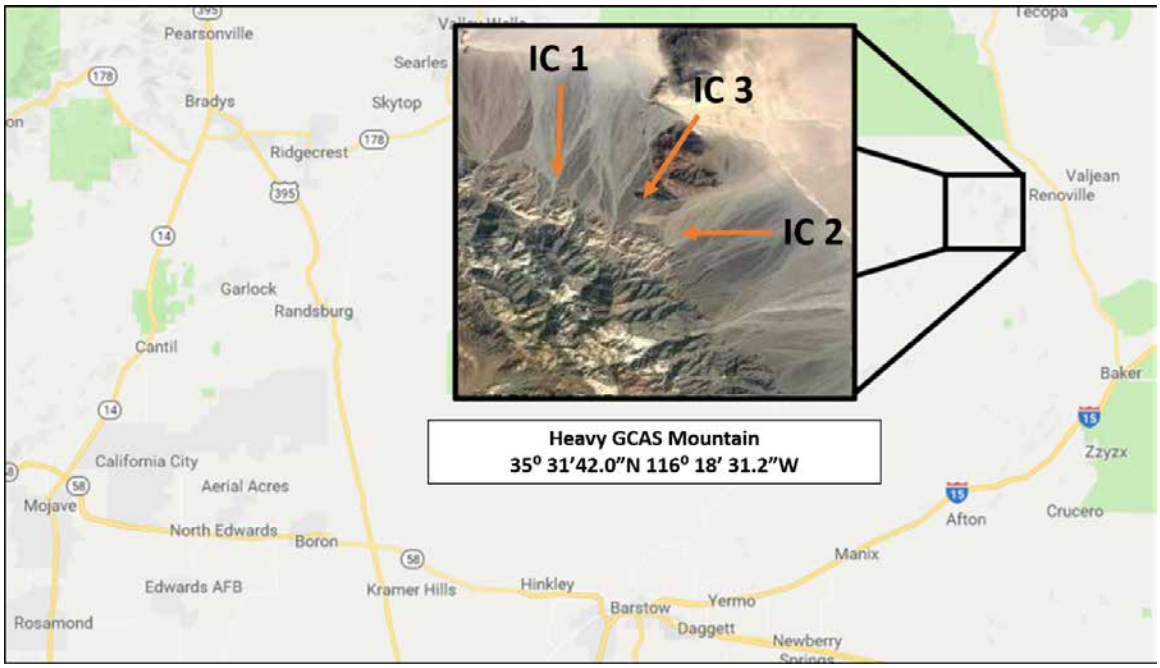

Figure 3.15. Location of "Heavy GCAS Mountain"

the path being 30 seconds (30 seconds was the length of each path prediction, known as the path prediction time). All five paths were analyzed, and the highest of the five times was used as the required forward look-ahead time. Figure 3.16 shows a graphical representation of this analysis. These look-ahead times were plotted to compare the impact of refresh rate on forward look-ahead time. The plots also included indications of whether each activation impacted terrain or not. A terrain impact implied that the current path prediction time was not adequate.

3.9.3.3 Nuisance Activation Tendency.

The third test objective was to observe the system's tendency for nuisance activations. The European Aviation Safety Agency (EASA) defined nuisance alerts as inappropriate alerts, occurring during normal safe procedures, which are the result of design performance limitations. The FAA defined nuisance alerts as alerts generated by a system that is functioning as designed but which are inappropriate or

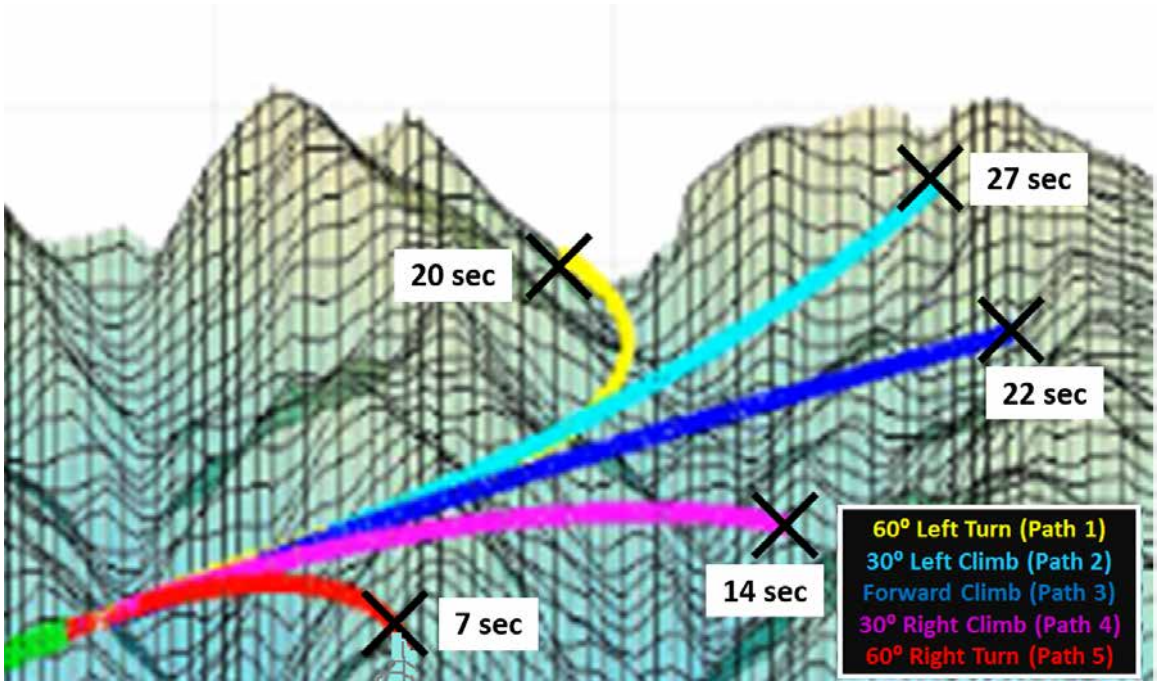

Figure 3.16. Forward Look-Ahead Time

unnecessary for the particular condition. For this evaluation, nuisance activations were defined as RSET path closures that were perceived as unnecessary for terrain avoidance.

To evaluate path performance, data were collected during manually activated escape paths to compare predicted escape paths and actual aircraft flight paths. The TC manually activated escape paths via a laptop at the engineer's station. The laptop communicated a value from 1-5 to the VSS, which then activated the corresponding RSET path autopilot (1: 60^o Left Turn, 2: 30^o Climbing Left Turn, 3: Forward Climb, 4: 30^o Climbing Right Turn, 5; 60^o Right Turn). That autopilot then commanded the aircraft to fly the chosen maneuver and data were collected to compare the predicted and actual aircraft paths. The pilot set MCP for each maneuver within three seconds of path activation. Maneuvers were considered complete once the RSET system returned control of the aircraft to the pilot following the escape maneuver. The

RSET system was designed to command escape maneuvers near the Learjet VSS safety trip limits, specifically +2.2 g and 12^o flight path angle when at the maximum test speed of 270 KCAS. Flight test data were gathered to identify how well the RSET system commanded maneuvers at or near its performance design targets.

To evaluate nuisance activations, each safety pilot performed multiple lateral passes on the North portion of terrain identified in Figure 3.17. A 60^o level banked turn was first conducted at 2,000 ft Above Ground Level (AGL) to estimate turning radius and verify RSET system disconnect. The EP then descended to 500 ft AGL and made three passes abeam the terrain while the RSET ran in the background evaluating the terrain. During each pass, the EP moved closer to the terrain until subjectively inside his comfort level needed to execute a 60^o escape maneuver. Figure 3.18 shows the view from the right side of the aircraft during these test points.

Lastly, for the operational nuisance evaluation, the EP flew multiple 60^o level banked turns at 2,000 ft AGL and clear of terrain to gain familiarity with the aircraft's turn radius at both 220 and 270 KIAS. The EP then descended to 500 ft AGL and flew a low-level profile at what the EP determined to be an operationally representative lateral offset from terrain to gather nuisance activation data at each respective airspeed. The RSET's ability to control the aircraft was severed to protect against inadvertent activations, but it still accepted state parameters from the VSS to determine if an escape maneuver was necessary. The TC informed the pilots anytime a path closed and collected comments on whether the pilots thought the path closure was necessary or not. Aircraft state parameters were recorded for all RSET activations.

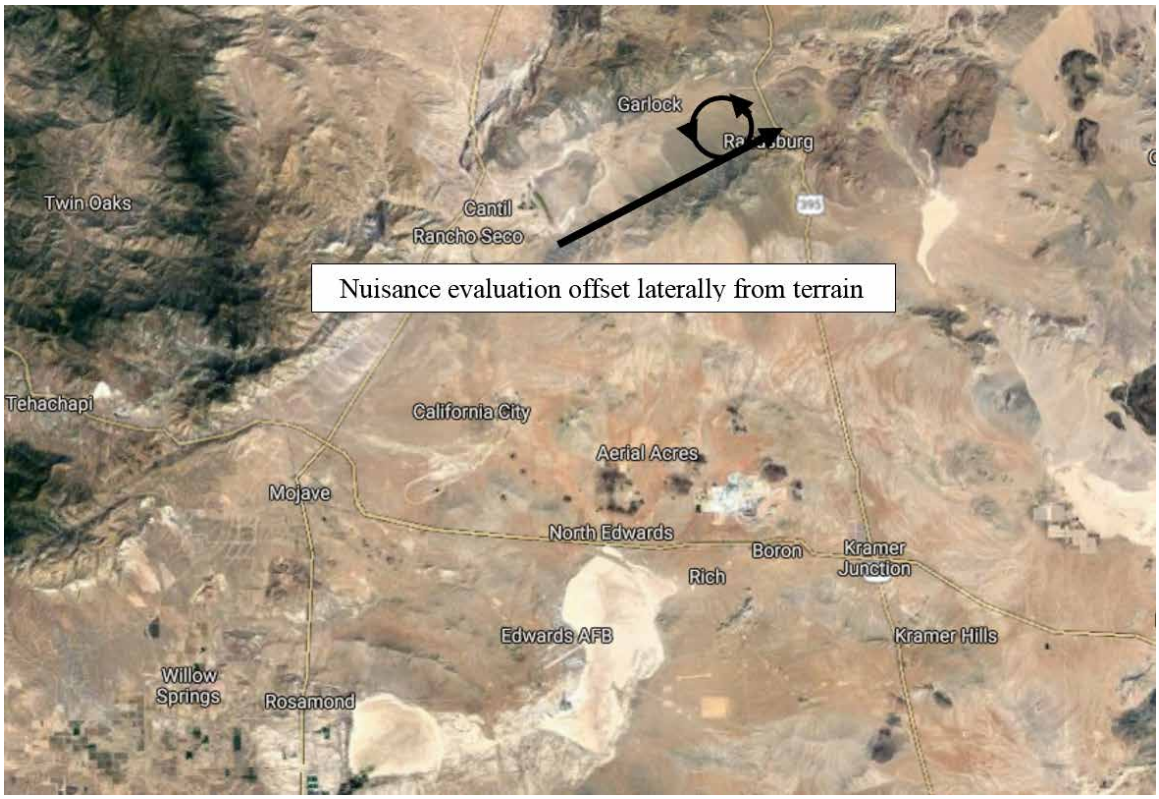

Figure 3.17. Nuisance Terrain Route

Figure 3.18. Lateral Offset from Terrain (view from TC station)

3.9.3.4 Maneuver Termination Control Hand-Back.

Following any maneuver where the RSET system was activated, the EP qualitatively evaluated the control hand-back immediately following maneuver termination. The test team produced an aircrew survey to guide EP commentary following control hand-back. Before flight, the team familiarized themselves with the survey flow and comments were given in accordance with survey criteria. A copy of the hand-back survey can be found in Appendix J.

3.10 Data Analysis

The data analysis procedures used are described in Appendix C. The sources of data were the Learjet VSS Data Acquisition System (DAS) and the test laptop computer. The Learjet DAS sampled parameters at 200 Hz and saved those parameters to a Microsoft Excel compatible file, which could be imported into MATLAB. The tables and graphs depicted in Appendix C were used as a guide during data collection and analysis to ensure the appropriate information was being presented. A review of the data analysis methods is recommended to understand the results presented in Chapter IV.

3.11 Chapter Summary

This chapter discussed the development and architecture of the RSET system. The preliminary results of converting the Stitched Model into a usable form was presented. Then the resources, test methodology, and analysis method for flight test were outlined. The next chapter presents the results and analysis of the RSET system flight test executed under USAF TPS TMP Have MEDUSA.

IV. Results and Analysis

4.1 Overview

This chapter outlines the data, results, and analysis of the model development and test flights for the Have MEDUSA TMP. The flights were conducted from 5 to 18 September 2018. The Daily Flight Test Reports for each flight can be found in Appendix B which outlines the crew, conditions of the flight, the test points flown, and amplifying information related to the collection and quality of the data or the performance of the system. As discussed in Section 3.7, the flight test objectives were:

1. Demonstrate the path prediction accuracy of the RSET system
2. Demonstrate the impact of changing the refresh rate on the RSET system's ability to calculate an achievable escape path
3. Observe the RSET system tendency to nuisance activation
4. Observe the control hand-back of the RSET system after maneuver termination.

The specific test points are detailed in Appendix D. A brief summary of the test parameters is presented in Table 4.3. The "Manual Path Activation" test points were used to gather data for the PPE and System Hand-back related objectives. The "Virtual Terrain Activation" test points supported the Terrain Miss Distance, Forward Look-Ahead Time, and System Hand-Back objectives. The "Low-Level Maneuvering" test points were used to evaluate nuisance.

4.2 Model Development Results

The following sections present the results for the computational speed and model accuracy of the Converted Model. These results were used to evaluate the utility of the Converted Model for use in the RSET system.

4.2.1 Converted Model Computational Speed.

Table 4.1 presents the results of the Converted Model operating speed analysis as described in Section 3.3.2. As can be seen for the Converted Model with an integration time-step (dt) of 0.01 sec, the value used for the RSET system, the computation time needed was reduced by 97%, which provided the performance needed to progress to flight test.

Table 4.1. Stitched and Converted Model Speed Comparison

Stitched Model Operating Speed			
Integration Method	**Integration Time-step (dt)**	**Real second / Simulated min**	**Improvement vs Baseline**
ode4 (Runge-Kutta)	0.005 sec	18.6 $\frac{sec}{min}$	Baseline
ode3 (Bagacki-Shampine)	0.005 sec	16.0 $\frac{sec}{min}$	-14%
ode2 (Heun)	0.005 sec	13.0 $\frac{sec}{min}$	-30%
ode1 (Euler)	0.005 sec	10.6 $\frac{sec}{min}$	-43%

Converted Model Operating Speed			
Integration Method	**Integration Time-step (dt)**	**Real second / Simulated min**	**Improvement vs Baseline**
ode1 (Euler)	0.005 sec	1.3 $\frac{sec}{min}$	-93%
ode1 (Euler)	0.010 sec	0.5 $\frac{sec}{min}$	-97%
ode1 (Euler)	0.015 sec	0.4 $\frac{sec}{min}$	-98%

4.2.2 Converted Model Accuracy.

Table 4.2 presents the results of the TIC analysis as described in Section 3.3.3. The Converted Model, which uses Euler-Forward integration, with a dt of 0.01 sec achieved good model agreement with the Stitched Model while providing greatly reduced computation times, as discussed in Section 4.2.1.

Table 4.2. TIC for Converted Model vs. Stitched Model (Stitched Model dt: 0.005s)

Pitch Doublet			
State	**TIC Value**		
	dt:0.005s	dt:0.010s	dt:0.015s
Pitch Rate (Q)	0.269	0.284	0.948
Pitch Attitude (θ)	0.008	0.0084	0.345
Normal Load Factor (n_z)	4.27e-04	4.37e-04	0.024
Angle of Attack (α)	8.84e-04	8.64e-04	0.037
Average	0.070	0.073	0.338

Roll Doublet			
State	**TIC Value**		
	dt:0.005s	dt:0.010s	dt:0.015s
Roll Rate (P)	0.025	0.053	0.052
Yaw Rate (R)	0.002	0.004	0.004
Lateral Load Factor (n_y)	0.009	0.020	0.043
Angle of Side Slip (β)	0.005	0.015	0.037
Average	0.010	0.023	0.034

4.3 Flight Test Results

Overall, the RSET system performance successfully implemented in flight test a methodology to use a multi-path collision avoidance system for performance limited aircraft. Path prediction error (PPE) did not meet the specified criteria and was larger than expected for the 30-second path predictions; however, at the maximum

refresh rate of 12.5 Hz, the RSET system ensured terrain clearance in all cases tested. Incorrect accounting for wind drift effects, the Learjet VSS auto-trim feature, and the low-fidelity engine model were possible sources of PPE. The test team recommended the main sources of PPE be determined prior to further testing. Despite the simple design of the control logic, the RSET system was able to achieve and maintain target load factor and flight path angle with momentary overshoots. The system showed no tendency for nuisance activations for all cases tested. The RSET hand-back implementation utilized was immature and the Learjet VSS safety trips were repeatedly triggered. Despite the unrefined hand-back, the response was deemed favorable in most cases and could be utilized as a baseline for future Auto-GCAS implementations and research. Overall, the RSET system was assessed to be MARGINAL. System assessments were made according to the 412th Test Wing Rating Criteria shown in Appendix H.

4.3.1 RSET System Prediction Accuracy.

The prediction accuracy of the RSET system was demonstrated by comparing the difference of the predicted flight path of the aircraft for a given collision avoidance maneuver and the actual path of the aircraft while executing that maneuver. Path Prediction Error (PPE) was defined as the distance between the two flights paths, and was computed at each sampled time from maneuver activation until handback of the aircraft. Refer to Appendix C for the details on how PPE was calculated. The evaluation criteria for RSET prediction accuracy was expressed in terms of the maximum value of PPE encountered during a 30-second maneuver. A maximum PPE of less than 100 ft was classified as satisfactory, between 100 ft to 300 ft as acceptable and above 300 ft as marginal. The test objective was met and the prediction accuracy of the RSET system was MARGINAL.

Table 4.3. Test Parameters

Test Point Type	Altitude	Airspeed	Entry Attitude	Refresh Rate	Initial Condition
Manual Path Activation	15,000 ft PA 8,000 ft PA 500 ft AGL	220 KIAS 270KIAS	SLUF climb dive turn	N/A	N/A
Virtual Terrain Activation	15,000 ft PA 8,000 ft PA 500 ft AGL	220 KIAS 270KIAS	SLUF	12.5 Hz 6.25 Hz 1.5625 Hz	IC 1 IC 2 IC 3
Low-Level Maneuvering	500 ft AGL	220 KIAS 270KIAS	Dynamic Flying	12.5 Hz	N/A

Overall, the prediction accuracy of the RSET system was BORDERLINE. None of the conditions tested had a maximum PPE of less than 100 ft, which was the threshold for the satisfactory region. Only three of the conditions tested had a maximum PPE of less than 300 ft, which was the threshold for the acceptable region. The remaining 117 test points had a maximum PPE above 300 ft, which was the threshold for the marginal region. The summarized maximum PPE results across all altitudes are presented in Figure 4.1 through Figure 4.4, and in Table 4.4 for the four different entry condition: SLUF, level turn, climbing, and diving. The reader should again note that the predecessor to RSET, Have ESCAPE, was only valid for SLUF entry. The results for each test point are detailed in Appendix E.

Additionally, figures for every manual activation can be found in Appendix I. The smallest maximum PPE of 172 ft was encountered during the following test condition: 500 ft AGL, 220 KIAS, SLUF entry, Path 3 activation. The largest maximum PPE of 6568 ft was encountered during the following test condition: 15,000 ft PA, 270 KIAS, diving entry, Path 1 activation.

Since the majority of test points represent a unique test condition that was only tested once, there was no statistical significance in the error data. However, a few

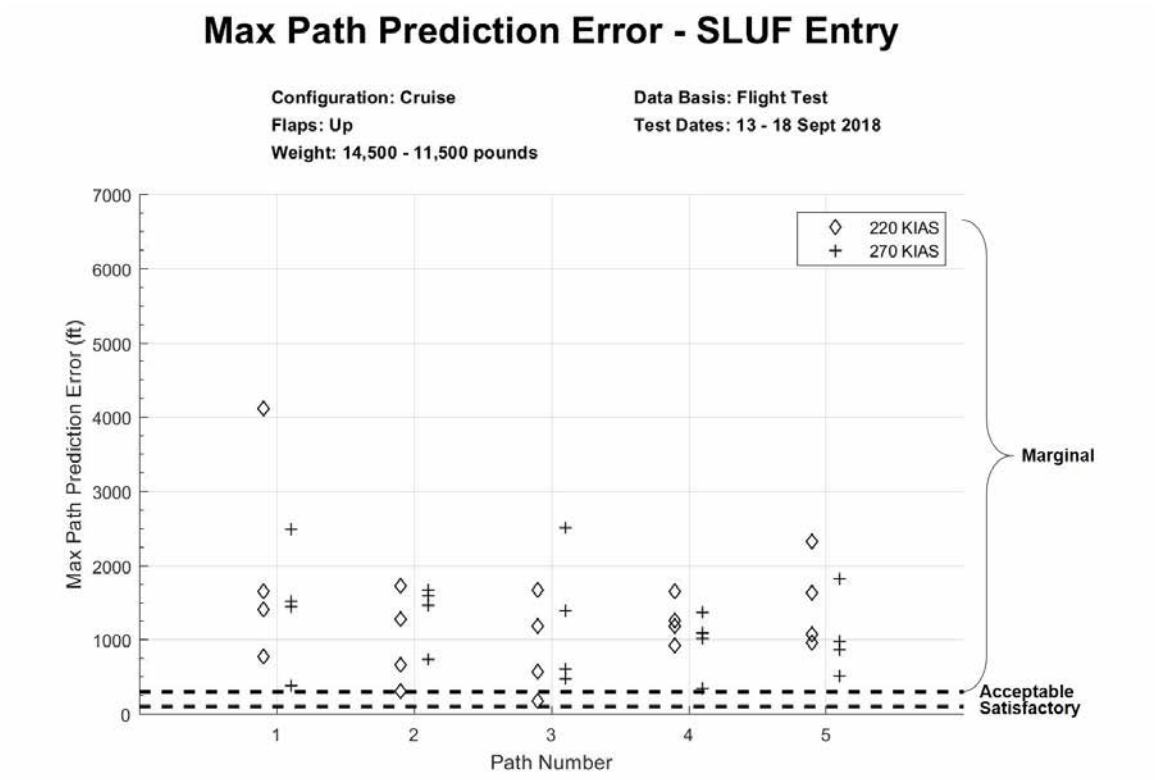

Figure 4.1. Maximum Path Prediction Error - SLUF Entry

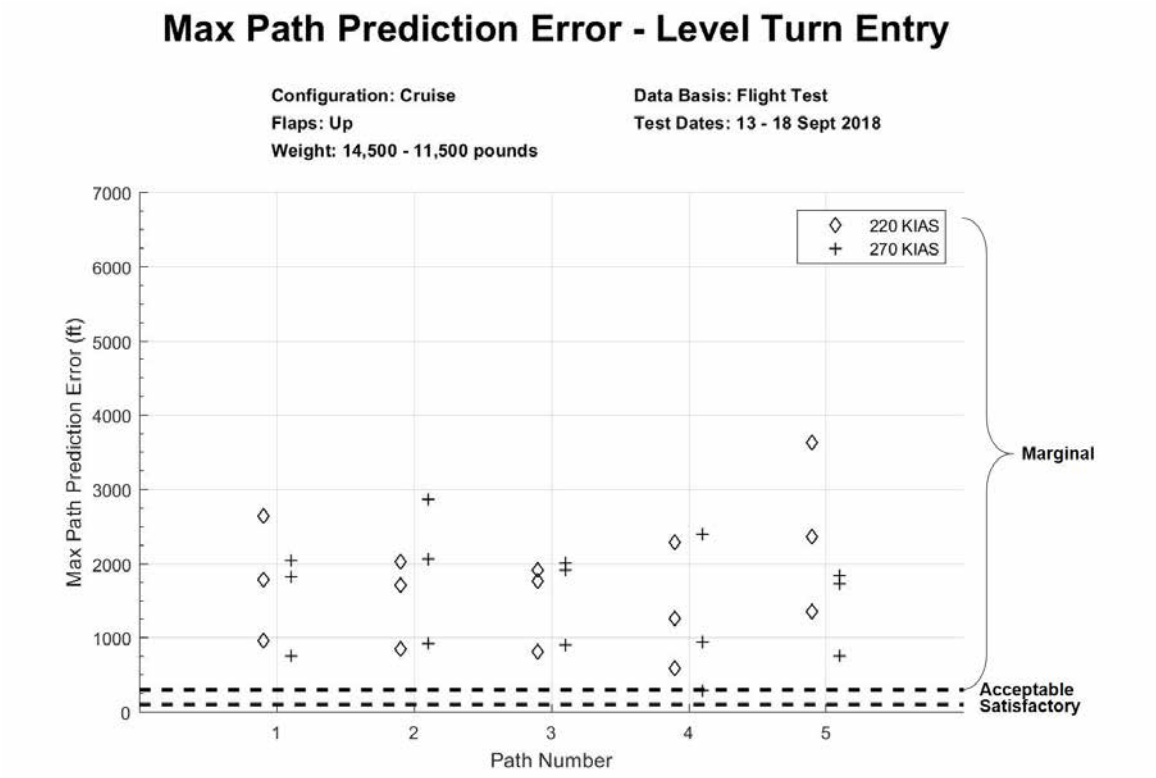

Figure 4.2. Maximum Path Prediction Error - Level Turn Entry

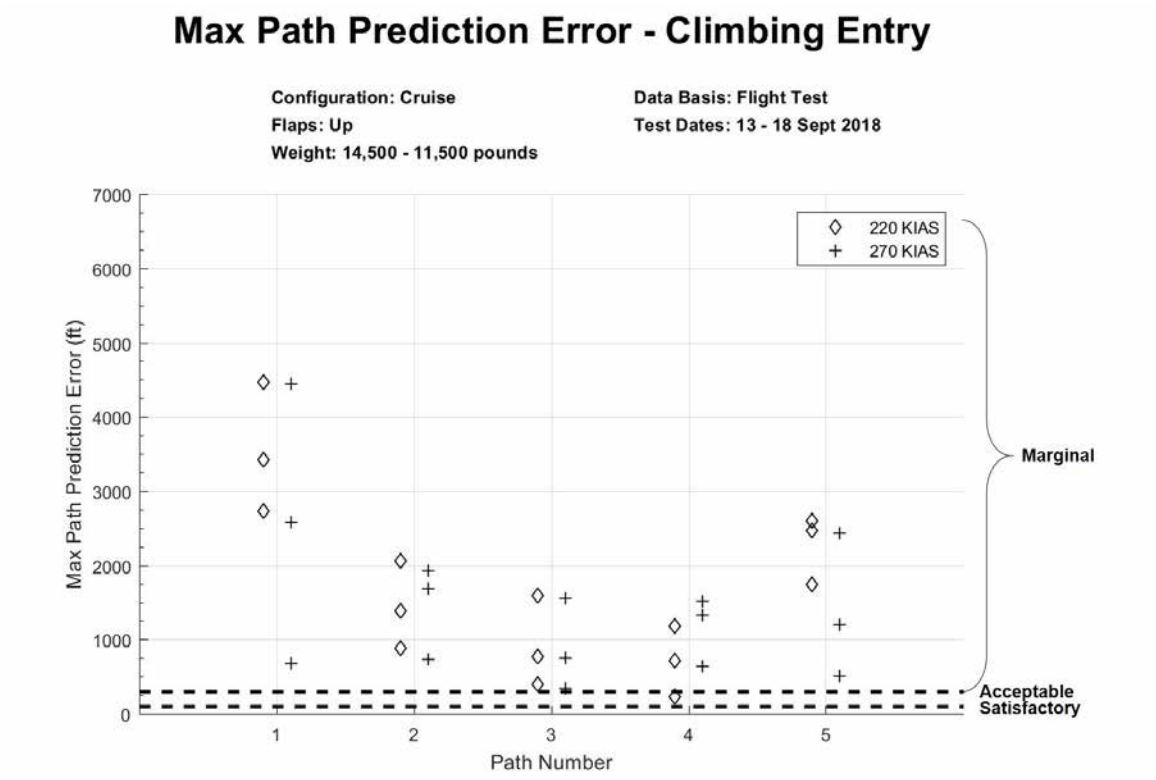

Figure 4.3. Maximum Path Prediction Error - Climbing Entry

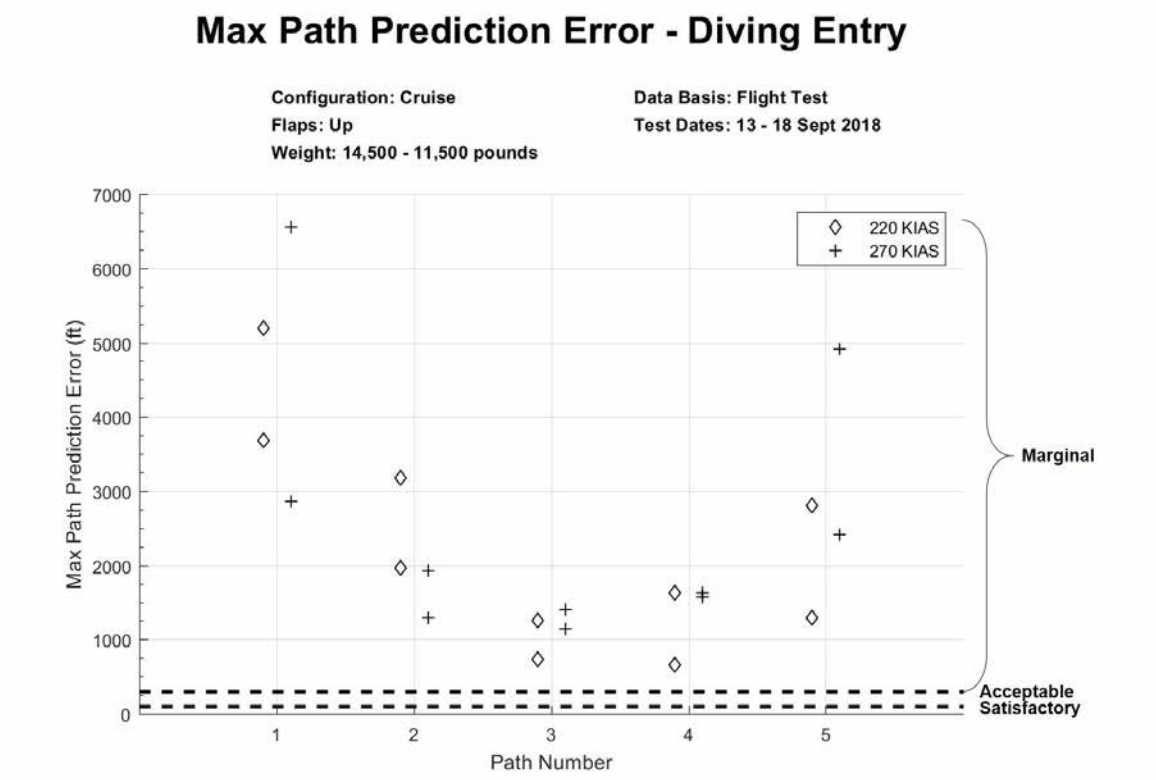

Figure 4.4. Maximum Path Prediction Error - Diving Entry

trends were observed. In general, error tended to be higher for Path 1 and 5 activations, followed by Path 2 and 4 activations and lowest for Path 3 activations. In addition, error tended to be higher for the diving entries, followed by level turn and climbing entries, then SLUF entries.

Table 4.4. Average Maximum Path Prediction Error Based On Varied Entry Condition

		Average of Maximum PPE (ft) by Path Type					Average of Maximum PPE (ft) regardless of Path Type
		Path 1	Path 2	Path 3	Path 4	Path 5	
Entry Conditions	SLUF	1723	1178	1073	1106	1270	1270
	45° Level Left Turn	1665	1735	1555	1294	1948	1640
	5° Climb	3056	1447	906	940	1831	1636
	5° Dive	4577	2093	1133	1376	2856	2407
Average of Maximum PPE (ft) regardless of Entry Conditions		2517	1537	1162	1157	1844	--

Notice that these figures and tables mask dynamic pressure effects, as the effect of altitude and airspeed on error is not apparent. Table 4.5 shows a summary table of PPE results categorized by airspeed and altitude. In general, there was no observed effect of airspeed on error, and error tended to increase with increasing altitude.

Table 4.5. Average Maximum Path Prediction Error Based On Varied Starting Airspeed

		Average of Maximum PPE (ft) by Altitude			Average of Maximum PPE (ft) regardless of Altitude
		500 ft AGL	8k ft MSL	15k ft MSL	
Entry Airspeed	220 KIAS	1365	1781	1930	1692
	270 KIAS	864	1810	2109	1594
Average of Maximum PPE (ft) regardless of Entry Airspeed		1115	1796	2020	--

The RSET system did not meet the evaluation criteria for the magnitude of the PPE over a 30-second path activation, indicating that the TPAs are not adequately

modeling the aircraft's motion during the collision avoidance maneuvers. However, one must look at the directionality of the error in addition to the magnitude in order to fully assess whether RSET had utility as a ground collision avoidance system. For instance, if the aircraft position was 1000 ft off from the predicted position, but it resulted in the aircraft being farther away from terrain than predicted, then the system was still successful in preventing a collision. It may have caused the aircraft to command a collision avoidance maneuver sooner than necessary, which may be considered a nuisance by the pilots, but that is a more desirable outcome than CFIT.

In order to characterize the directionality of the PPE for a given manual activation, the actual path of the aircraft was compared with the predicted path in two aspects: climb performance and turn performance. To compare the climb performance, the actual and predicted paths were plotted and viewed from the side to determine if the aircraft out-climbed the prediction. Figure 4.5 shows an example of a side view of a Path 3 manual activation. The actual aircraft path, shown in blue, stayed below the predicted path for the entire maneuver, which indicates that the aircraft had worse climb performance than was predicted by the TPA and that the path error was towards the terrain.

To compare the turn performance of the actual aircraft to the TPA, the paths were plotted and viewed from above to determine if the aircraft had a smaller or larger turn radius than what was predicted by the algorithm. Figure 4.6 shows an example top-down view of a Path 5 manual activation. The actual aircraft path had a larger turn radius than the predicted path, which indicates that the aircraft had worse turn performance than was predicted and that the path error was towards the terrain.

If both the climb and turn performance of the actual aircraft exceeded (i.e. out-performed) the prediction, then it was concluded that the error was in a direction

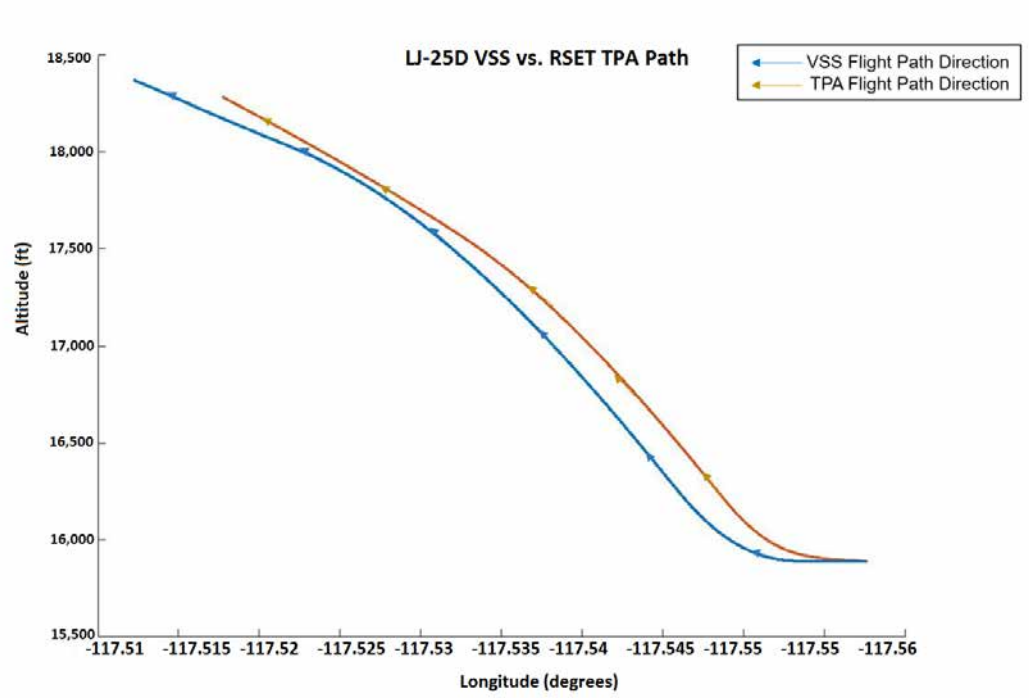

Figure 4.5. Side View of Forward Climb

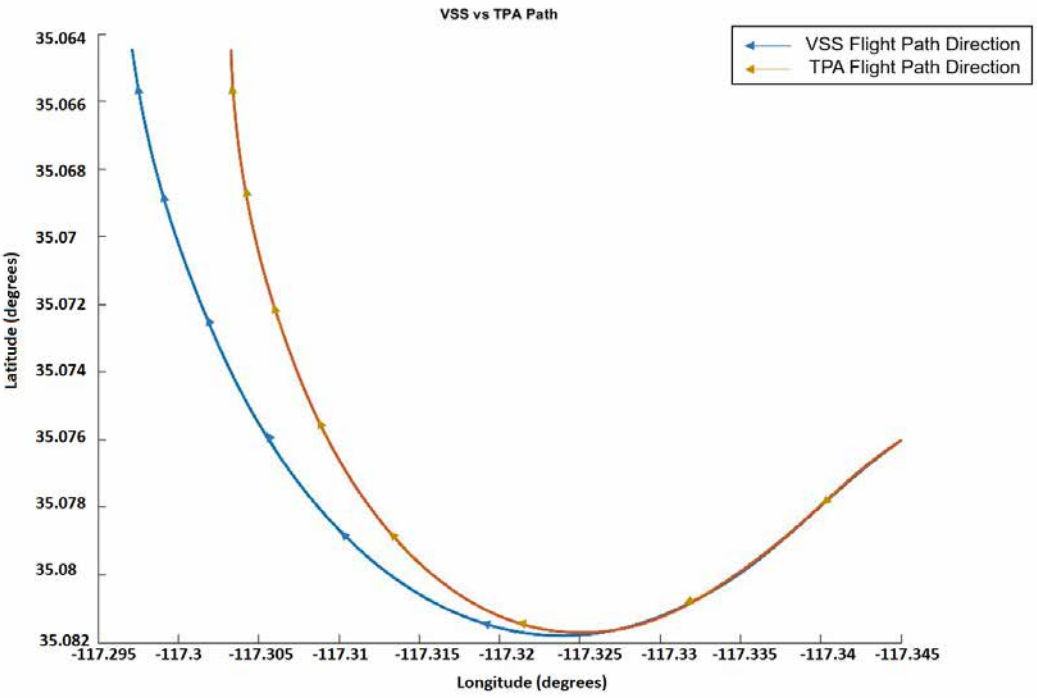

Figure 4.6. Bird's Eye View of 60^o Right Turn

"away from terrain". Alternatively, if both the climb rate and turn radius of the actual aircraft under-performed the prediction, then it was concluded that the error was in a direction "toward terrain", indicating a more dangerous situation. If the actual aircraft out-performed the prediction in one aspect but under-performed in the other aspect, then the direction of the error was deemed to be "inconclusive", because the safety of the maneuver would be dependent on the terrain feature. A summary of the results for the directionality of the PPE is presented in Table 4.6. Results for each test point are provided in Appendix E.

Table 4.6. Summary of PPE Directionality

	# Test Points	Total Test Points	Percentage
Actual Climb Performance Exceeded Prediction (Applicable for all Paths)	61	120	50.8%
Actual Turn Performance Exceeded Prediction (N/A for Path 3 activations)	41	96	42.7%
Error Away from Terrain	**44**	**120**	**36.7%**
Error Towards Terrain	**54**	**120**	**45.0%**
Inconclusive	**22**	**120**	**18.3%**

Two general trends were observed in the PPE direction data. First, the direction of the PPE was correlated to the airspeed flown. At the slower airspeed, 220 KIAS, the actual path generally had a smaller turn radius than predicted, but worse climb performance than predicted. This resulted in Paths 1 and 5 generally erring away from terrain and Path 3 erring toward terrain. At the higher airspeed, 270 KIAS, the actual path generally had a larger turn radius than predicted, but better climb performance than predicted. This resulted in Paths 1 and 5 generally erring toward terrain and Path 3 erring away from terrain. The second trend observed from the PPE direction data was a correlation with the entry condition. For SLUF and climbing entries, the aircraft generally out-performed the prediction and erred away from terrain. For level turn and descending entries, the aircraft generally under-performed

the prediction and erred toward terrain. This suggests that the current implementation of RSET performs best when the aircraft starts from straight-and-level flight or from a slight climb. Thus far, the discussion has focused on trends in the PPE magnitude and direction data with respect to the control variables (airspeed, altitude, entry condition, and RSET path). However, there are several confounding variables that could have had a significant effect on the PPE results. Possible sources of error include (1) the auto-trim feature of the VSS, (2) incorrect accounting of wind speed and direction in the TPAs, and (3) the low fidelity of the Learjet engine model used in the TPAs. The first two error sources were investigated in post-flight analysis, but the error due to engine model inaccuracies was not investigated. The engine model used by the TPAs was a simplistic model, but its impact on overall model performance are not fully understood. A separate study would need to be performed to understand the accuracy of the model for various flight conditions.

One potential source of error was the auto-trim feature of the VSS. This function was in place to reduce hinge loads on the horizontal stabilizer, and was a normal part of the LJ-25D flight control system. Therefore, this feature could not be disabled for flight safety, and was not accounted for due to the discovery of this feature only after flight test began. The RSET system used the initial value for the horizontal stabilizer deflection at activation, and did not account for auto-trim changes during the maneuver. This error can be seen in Figure 4.7 and Figure 4.8. At the time the auto-trim functions activates, the RSS error begins to grow at a faster pace. While this was not the only source of error, it did appear to be a contributing factor.

Another confounding variable that was investigated as a source of error was wind. The wind data entered by the TC was derived from the onboard EGI and air data systems. The TPAs compensated for the wind in its path predictions. The wind speed and direction were assumed to be constant throughout the RSET maneuver.

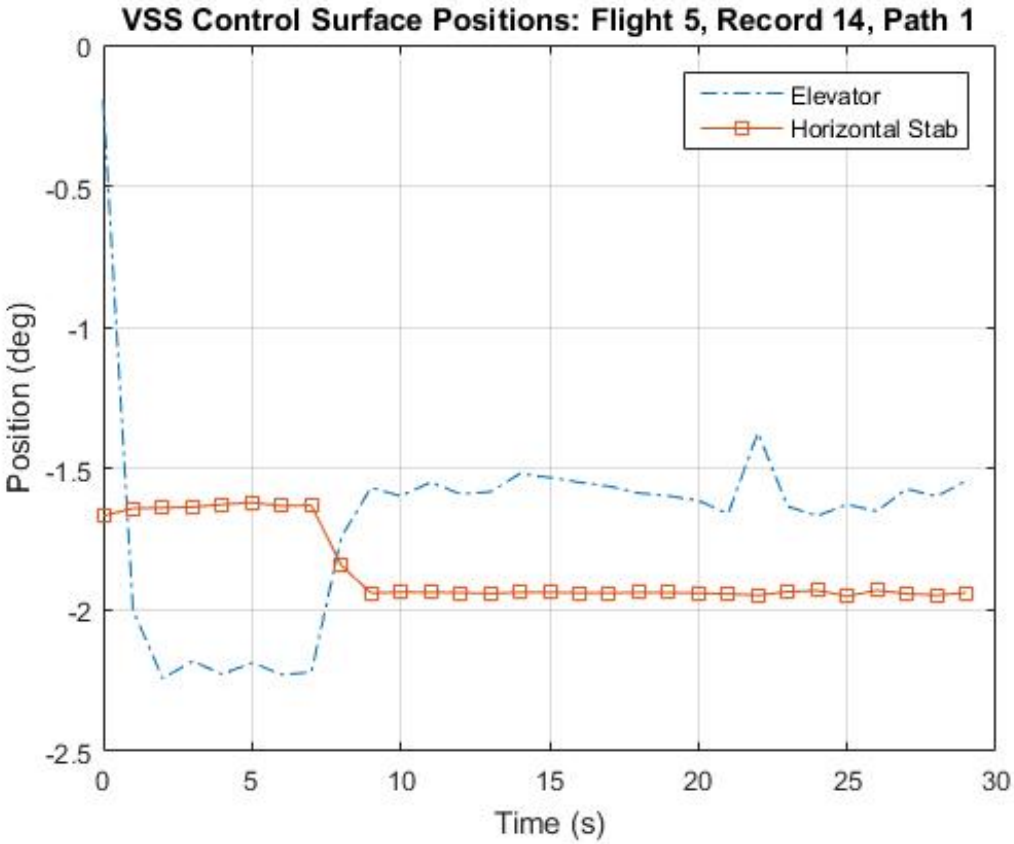

Figure 4.7. VSS Control Surface Positions (Auto-Trim at 7 Seconds)

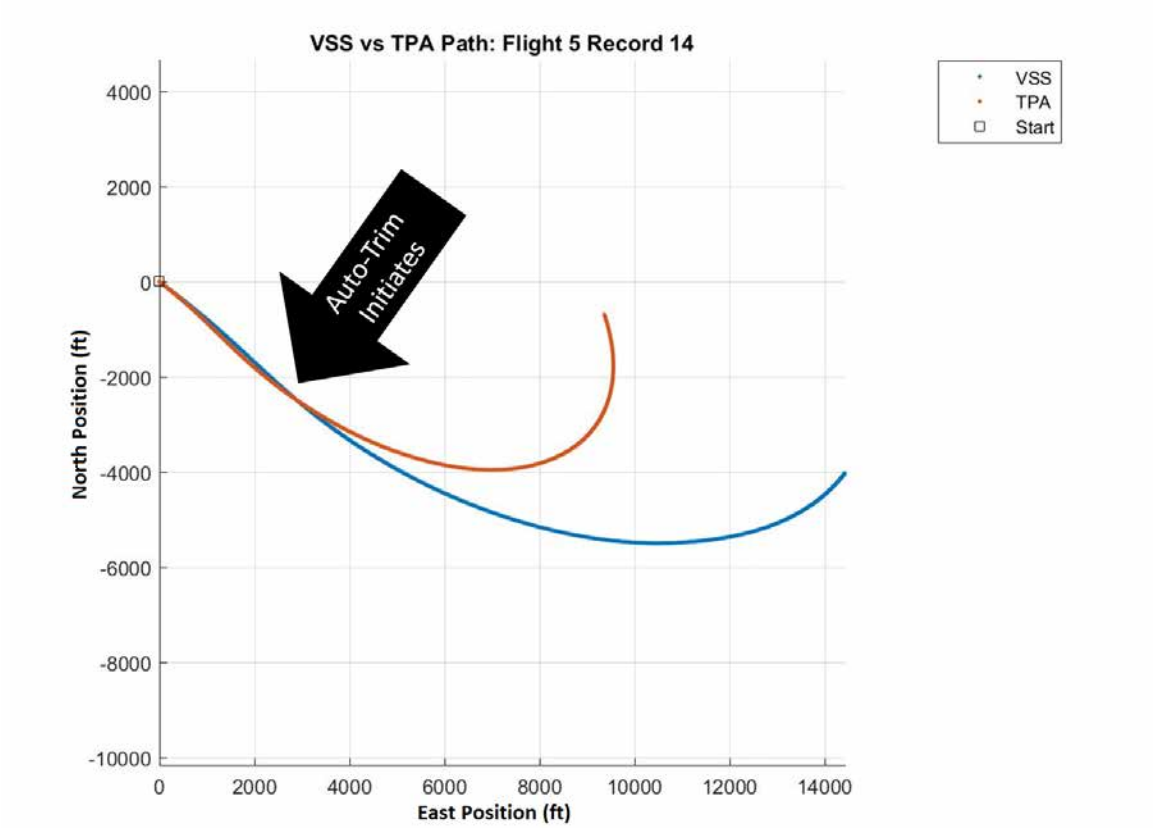

Figure 4.8. Bird's Eye View of VSS vs TPA Paths: Flight 5 Record 14 (Auto-Trim at 7 Seconds)

However, post-flight data analysis showed that the aircraft was consistently drifting away from the predicted path in the direction of the wind during manually activated RSET maneuvers. Figure 4.9 shows a bird's eye view of the actual aircraft path and the predicted path with the wind vectors overlaid for the following test point: 500 ft AGL, 270 KIAS, level turn entry, Path 1 activation. The actual aircraft path appears to be drifting away from the predicted path in roughly the same direction that the wind is blowing. The same plot was generated for all 120 manual activation test points, and Appendix E presents the wind speed for each point and whether or not the wind direction appears to be contributing to the PPE. For 88% of the test points, the actual aircraft path appears to be drifting away from the predicted path in the same direction as the wind. These results suggest that the TPAs are not accurately accounting for winds in their path predictions. Furthermore, this error due to wind could explain some of the previous trends. For instance, since wind speed generally increased with increasing altitude, the inability to fully account for winds could explain why PPE increased with increasing altitude.

While the maximum PPE calculated during each 30-second maneuver was found to be, on average, much higher than the amount deemed to be acceptable (300 ft), it is believed that this metric is not a fair indicator of the overall utility of the RSET system. Since the actual aircraft position drifted from the predicted path as time progresses during an RSET maneuver, the calculated PPE is usually at a maximum at the very end of the 30-second maneuver. As will be seen in the results for forward look-ahead time, it typically takes significantly less than 30 seconds to clear a terrain feature when a refresh rate of 12.5 Hz is used. Hypothetically, if it takes the aircraft 10 seconds to clear a terrain feature from the start of a commanded RSET maneuver, then there is a chance that the PPE at the 10-second point is within the acceptable amount; whereas the PPE at the 30-second point would have grown enough to be

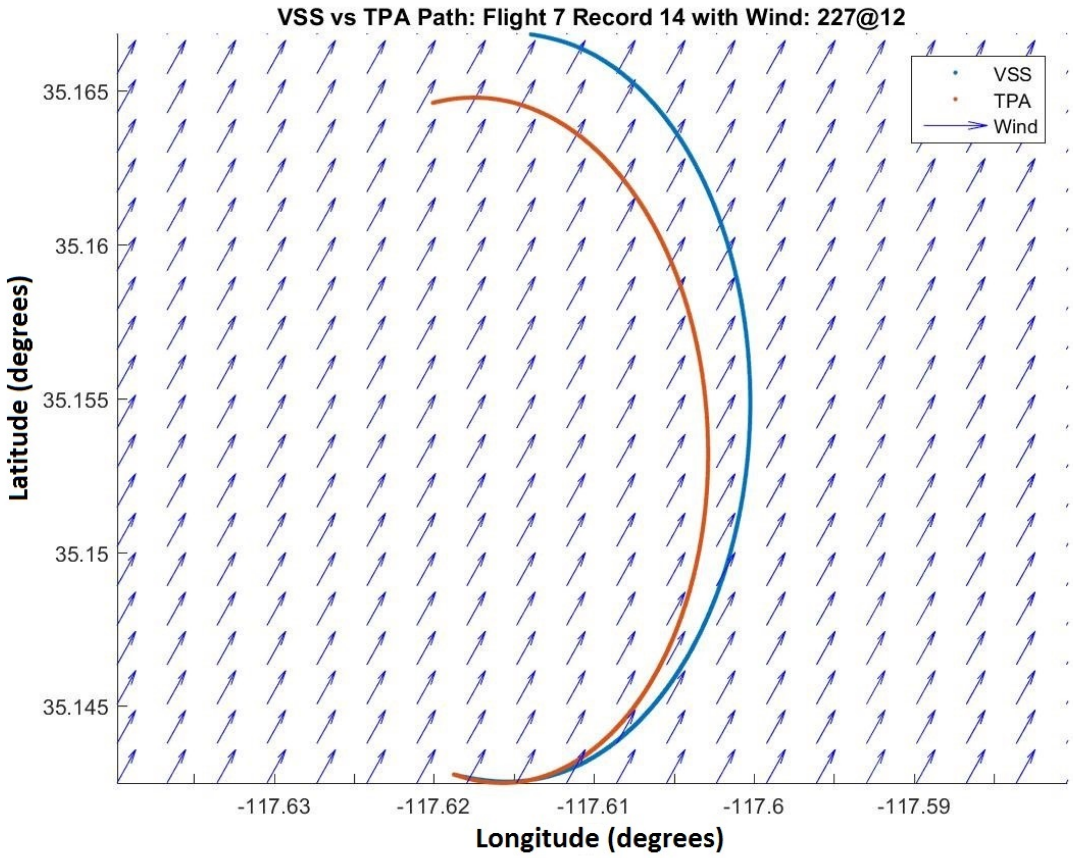

Figure 4.9. VSS vs TPA Paths: Flight 7 Record 14 with Wind: 227^o at 12 knots

outside the acceptable amount. Since the evaluation criteria for RSET prediction accuracy did not take into account intermediate time steps within a manual activation and the direction of the error (toward vs. away from terrain), little can be concluded on the utility of RSET as a ground collision avoidance system with this metric alone. Figure 4.10 shows a time history of the PPE during a manual maneuver of RSET Path 3 at the following conditions: 15,000 ft PA, 270 KIAS, climbing entry. It can be seen that while the maximum PPE, which occurs at 30 seconds after activation, is 754 ft, the PPE stays under the acceptable value of 300 ft for the first 13 seconds during the maneuver. If the terrain had been cleared within 13 seconds, then the unacceptable PPE error for the remainder of the maneuver is irrelevant to the utility of the RSET system.

Overall, the RSET system received a MARGINAL rating. Three test points were acceptable with a maximum PPE between 100 ft to 300 ft, and the remaining 117 test points were marginal with maximum PPE above 300 ft. The smallest maximum PPE was 172 ft and the largest maximum PPE was 6568 ft. It was observed that maximum PPE tended to be higher for Path 1 and 5 activations, followed by Path 2 and 4 activations and lowest for Path 3 activations. Next, maximum PPE was higher for diving entries compared to the other three entries. Lastly, it was concluded that out of the 120 test points analyzed, 44 had PPE erring away from terrain, 54 had PPE erring towards terrain and the remaining 22 test points were inconclusive. The possible sources of error that could account for the marginal rating of the prediction accuracy of the RSET system could be the auto-trim feature of the VSS, incorrect accounting of wind speed and direction in the TPAs, and the low fidelity of the Learjet engine model used in the TPAs. In particular, post-flight analysis suggested that the TPAs were not properly accounting for winds. **Recommendation 1 (R1): Conduct further data analysis to determine the sources of error and their**

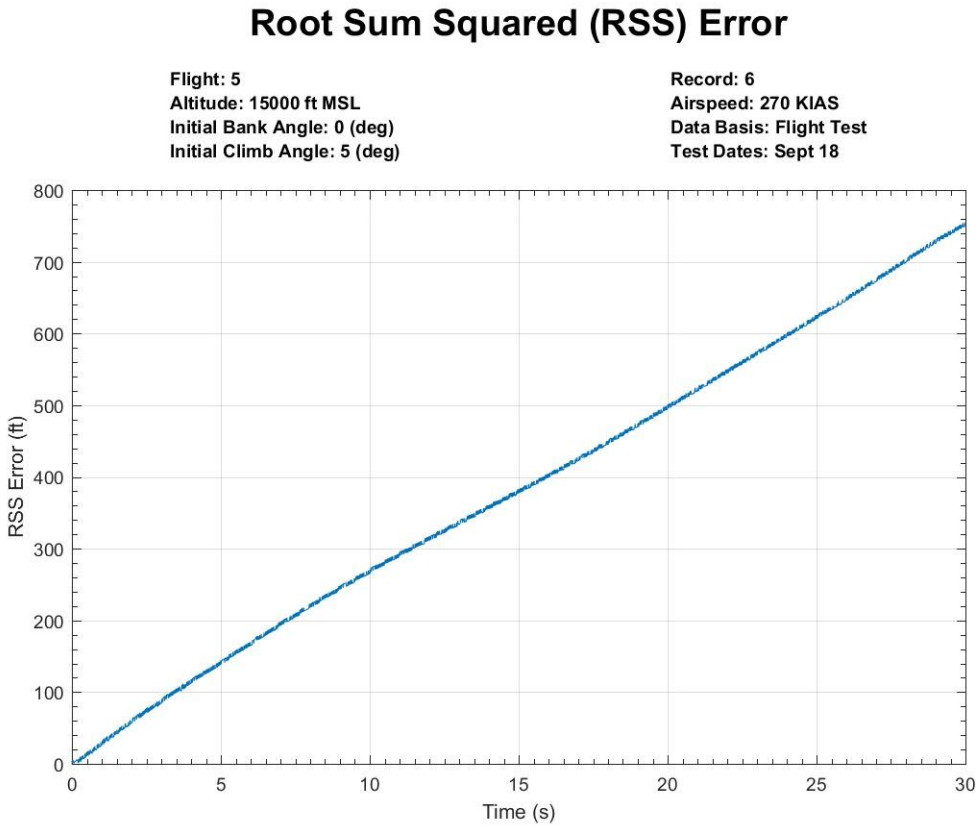

Figure 4.10. Time History of RSS Error (PPE) during a manual activation

impact to PPE. Furthermore, the majority of test points were only tested once and had no statistical significance in PPE. **R2: Conduct repeat runs of specific test conditions to increase statistical significance of PPE results.**

4.3.2 Refresh Rate Impact on Escape Path Calculation.

An initial baseline was demonstrated for the RSET system. Slower refresh rates appeared to have a negative impact on the ability of the system to safely avoid virtual terrain. No significant correlation between, airspeed, altitude or initial condition and terrain miss distance was found. Additionally, the necessary forward look-ahead time increased as refresh rate decreased. At the lowest refresh rates, the 30 sec path prediction time used did not appear to be adequate to ensure sufficient terrain miss distance. The test objective was met.

4.3.2.1 Terrain Miss Distance.

The results showed that the highest refresh rate was required to ensure a successful terrain avoidance maneuver. A 12.5 Hz refresh rate showed no virtual terrain impacts, while at lower refresh rates terrain impacts did occur for the same test conditions. Figure 4.11 shows the effect of the starting location and heading on miss distance. Although it was beyond the scope of this test to exercise the RSET system against numerous terrain types, the obstacle chosen, "Heavy GCAS Mountain", presented different terrain profiles from each of three starting points. These profiles included slowly rising terrain, steeply rising terrain, and valleys.

The initial conditions did not appear to have a significant impact on terrain miss distance at the highest refresh rate. At the lower refresh rates there appeared to be slightly more variation in initial condition 3 which flew directly towards the mountain. Initial conditions 1 and 2 placed the aircraft on more of a "glancing" angle with the

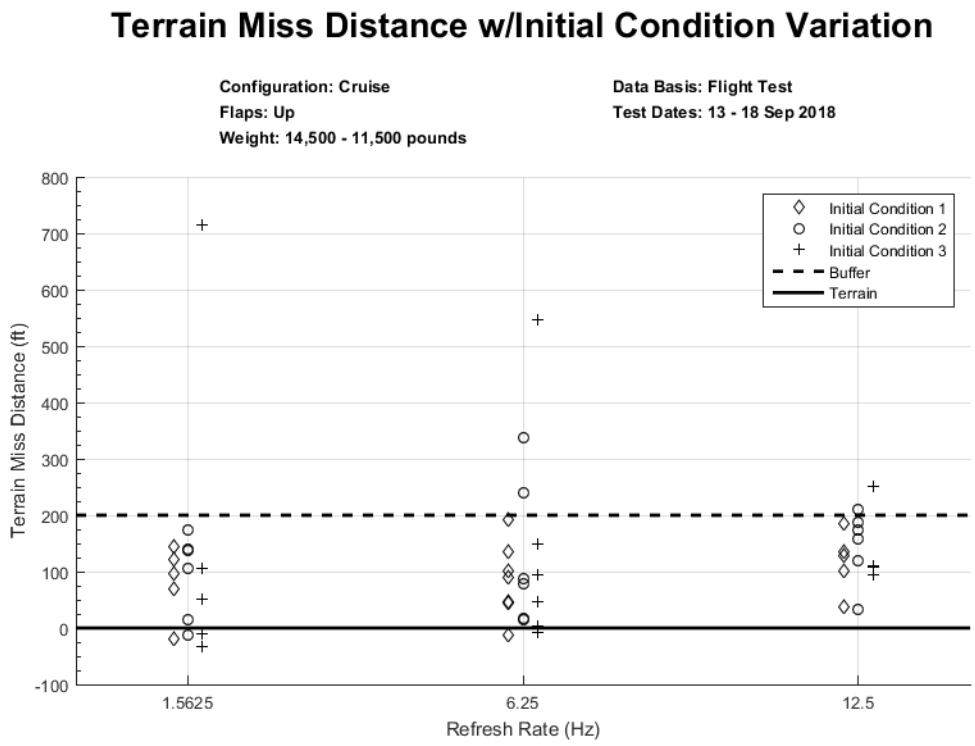

Figure 4.11. Terrain Miss Distance with Initial Condition Variation

terrain, which meant that, in general, once the avoidance maneuver away from the terrain was executed then the aircraft was clear of any other local co-altitude terrain.

Figures 4.12 and 4.13 show a typical terrain miss distance profile. The low speed, and therefore energy, was the primary cause of the flight path closely following the terrain. However, at no time did the aircraft's flight path intersect the digital terrain. This was also the case for all the other runs at a 12.5 Hz refresh rate. The rest of the data results can be found in Appendix I.

As can been seen from Figure 4.14, at the highest refresh rate there appeared to be no significant change in performance with altitude variation. At the 6.25 Hz refresh rate there was slightly more variation with higher altitude, but this was not significantly observed at the other refresh rates.

As seen in Figure 4.15, airspeed also had no well-defined trend. The terrain miss

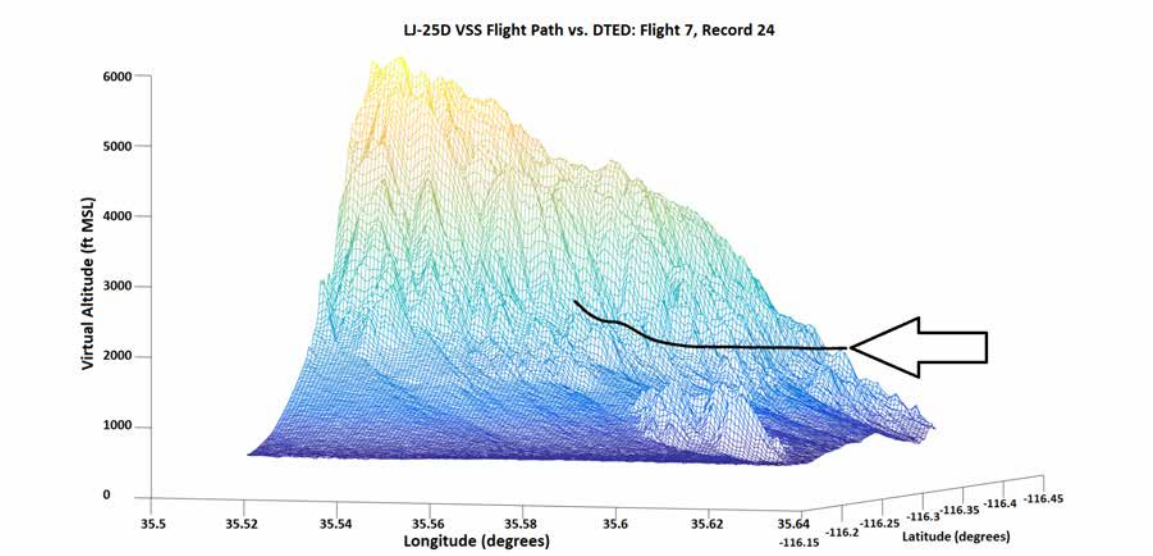

Figure 4.12. Learjet VSS Flight Path versus DTED: Flight 7, Record 24, 220 KIAS, 500 ft AGL, IC 1

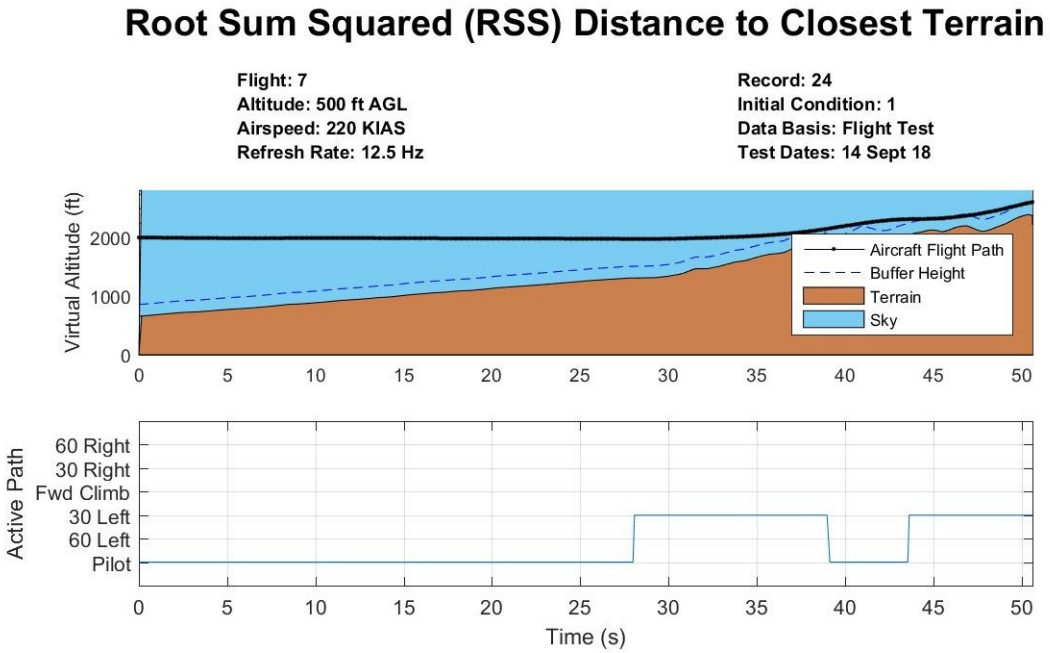

Figure 4.13. Distance to Terrain: Flight 7, Record 24, 220 KIAS, 500 ft AGL, IC 1

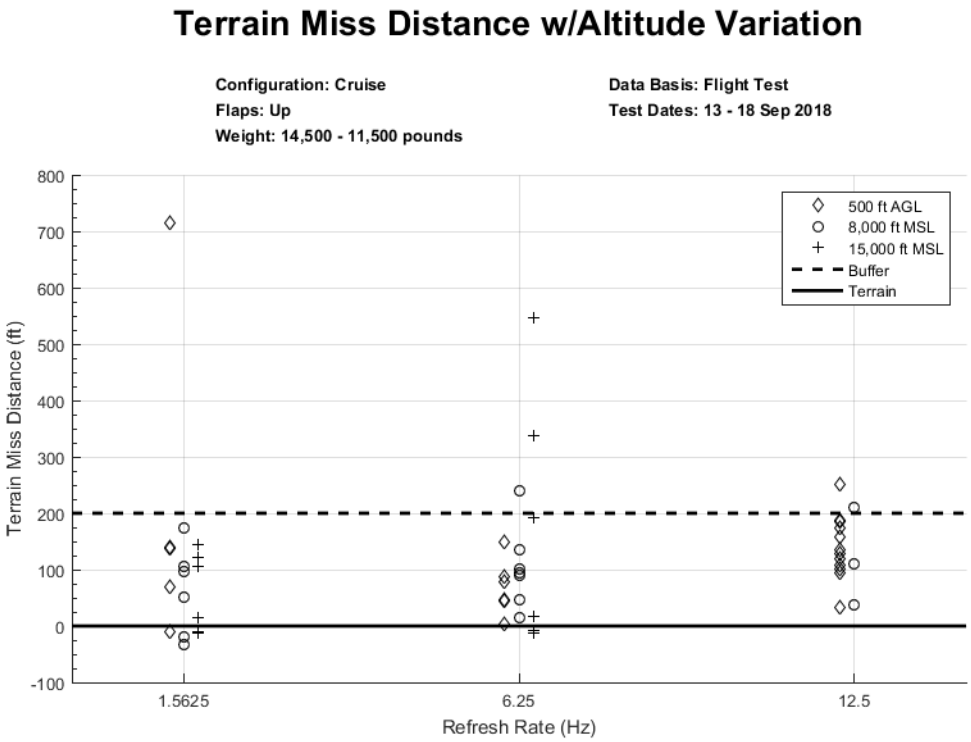

Figure 4.14. Terrain Miss Distance with Altitude Variation

distance appeared to vary randomly across both airspeeds.

Based on these results, it appeared that a higher refresh rate near 12.5 Hz was required to ensure terrain clearance with this implementation of the RSET system. The other factors appeared to have no significant impact on terrain clearance. The selection of an appropriate terrain buffer was also a critical parameter for system performance. The 200 ft terrain buffer used in this implementation provided an initial reference for the size of terrain buffers for future system implementations. Future systems must also evaluate the mission set and aircraft performance ability when determining a terrain buffer. Overall, these findings should provide a reference for future multi-path systems on required system performance. **R3: Using a refresh rate of 12.5 Hz or faster, investigate the effect of varied operationally representative terrain types and terrain buffers on miss distance.**

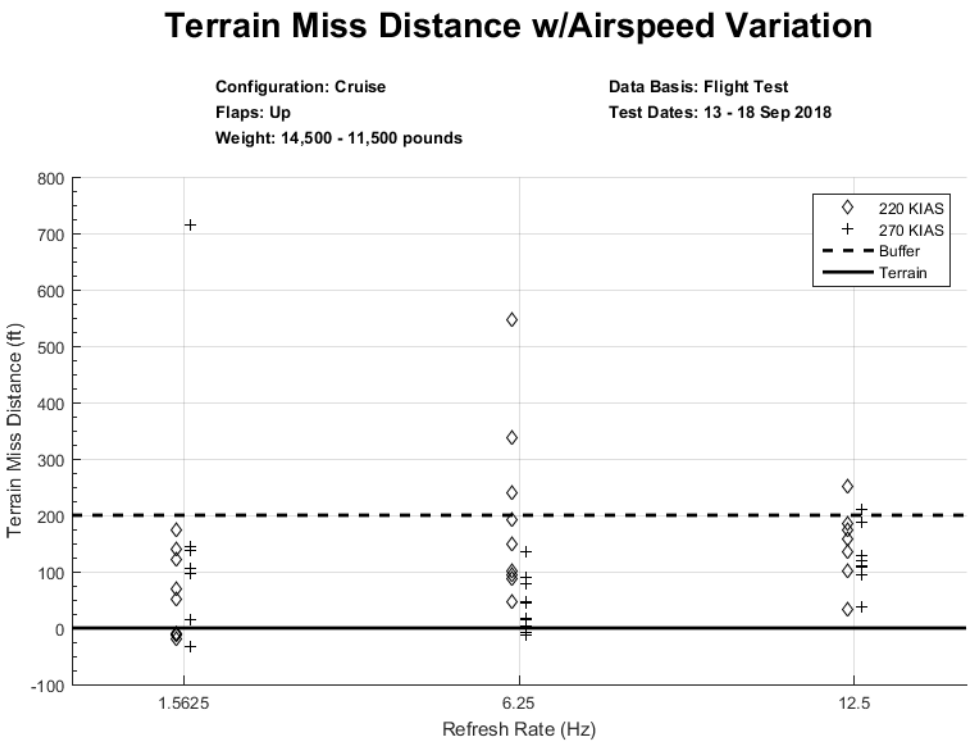

Figure 4.15. Terrain Miss Distance with Airspeed Variation

4.3.2.2 Forward Look-Ahead Time.

Figure 4.16 shows a trend of decreasing forward look-ahead time required with increasing refresh rate. At the lowest refresh rate all 30 seconds or more were required indicated by the number of virtual impacts seen, but at the highest refresh rate 16 seconds was the highest required forward look-ahead time with no virtual impacts observed. No significant trend was seen based on initial condition, although it was predicted that more look-ahead time would be required for more aggressive terrain. This trend may not have been clearly seen during this test since all initial conditions contained fairly aggressive terrain features.

As seen in Figure 4.17, no clear trend was seen across refresh rates for the effect of altitude on forward look-ahead time. Model accuracy was expected to decrease with deviation from 15,000 ft, the model's validation altitude. However, this trend

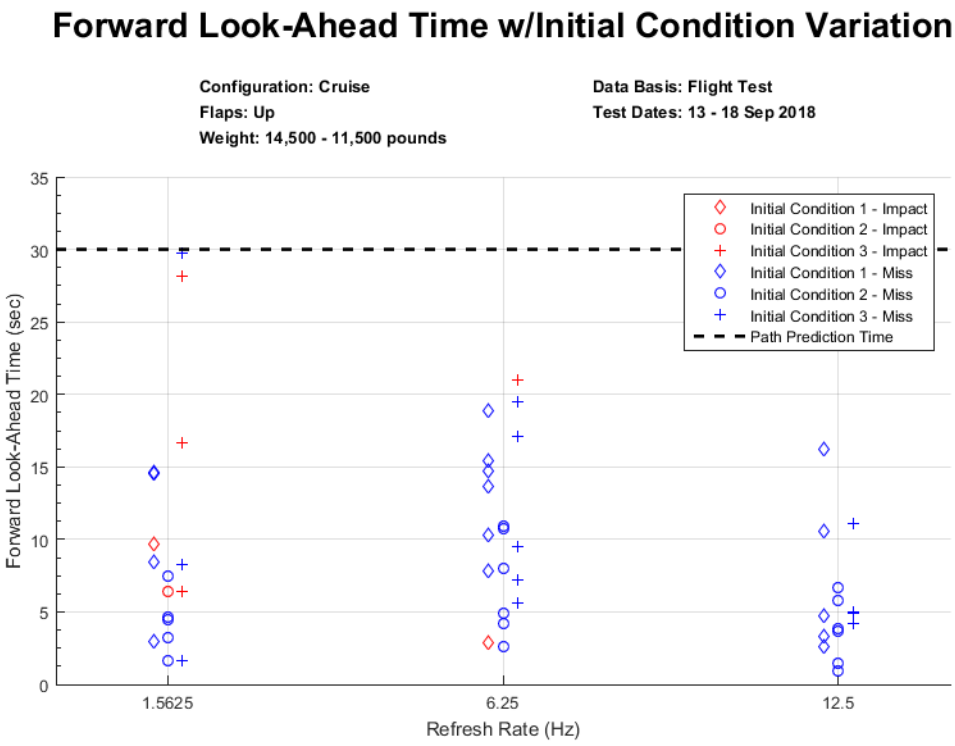

Figure 4.16. Forward Look-Ahead Time with Initial Condition Variation

was not seen consistently across refresh rates.

Figure 4.18 shows the variation of airspeed across each refresh rate. No significant trend was observed from flight test. This behavior was expected since the paths were a fixed time, e.g. a 30 sec prediction path at 270 KIAS was a longer distance than a 220 KIAS prediction path.

The data showed that an increased refresh rate yielded a shorter required forward look-ahead time. Forward look-ahead time did not appear to be significantly affected by other factors such as initial condition, airspeed, or altitude. The system refresh rate will drive the forward look-ahead time, and the presented data should provide a rough starting point for future multi-path collision avoidance systems. **R4: Evaluate the need for forward look-ahead times beyond 30 seconds.**

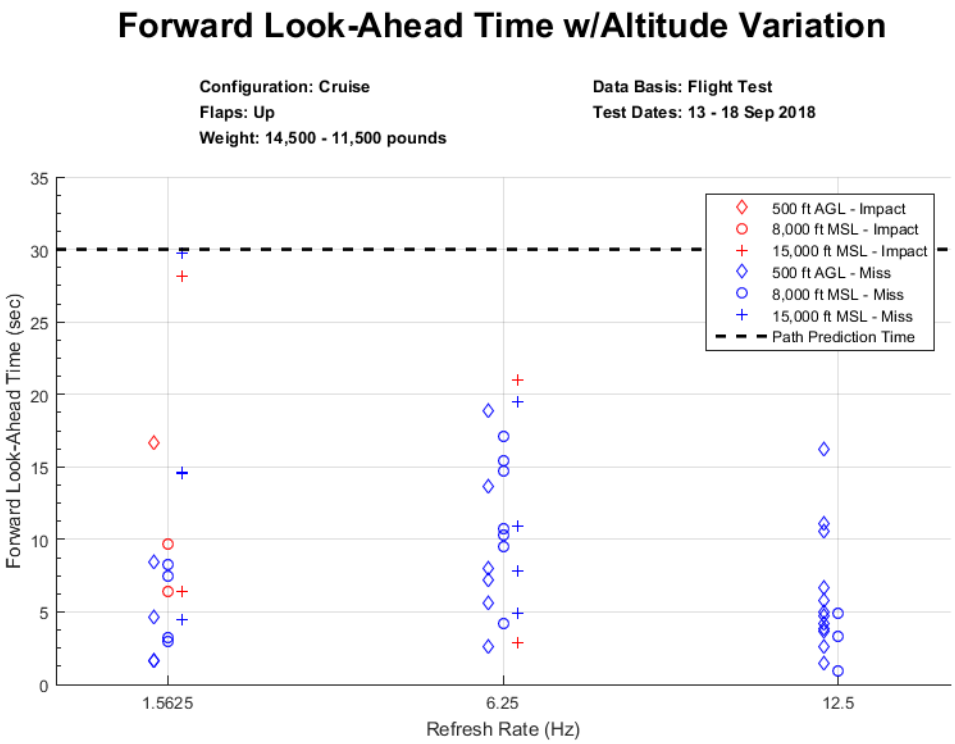

Figure 4.17. Forward Look-Ahead Time with Altitude Variation

4.3.3 Nuisance Activation Tendency.

The pilots' perception of nuisance relies heavily on the system's ability to operate both timely and aggressively. Since the system already demonstrated its timeliness, the test team looked to characterize its aggressiveness. That is, ability of the RSET to command escape maneuvers at or near the VSS limits, as well as the aircraft's ability to perform at or near the RSET-commanded conditions, which was demonstrated in Chapter III in simulation. The system's aggressiveness was important to characterize since the pilots would have considered a system that maneuvered less aggressively than they would have as nuisance prone. The test objective was met.

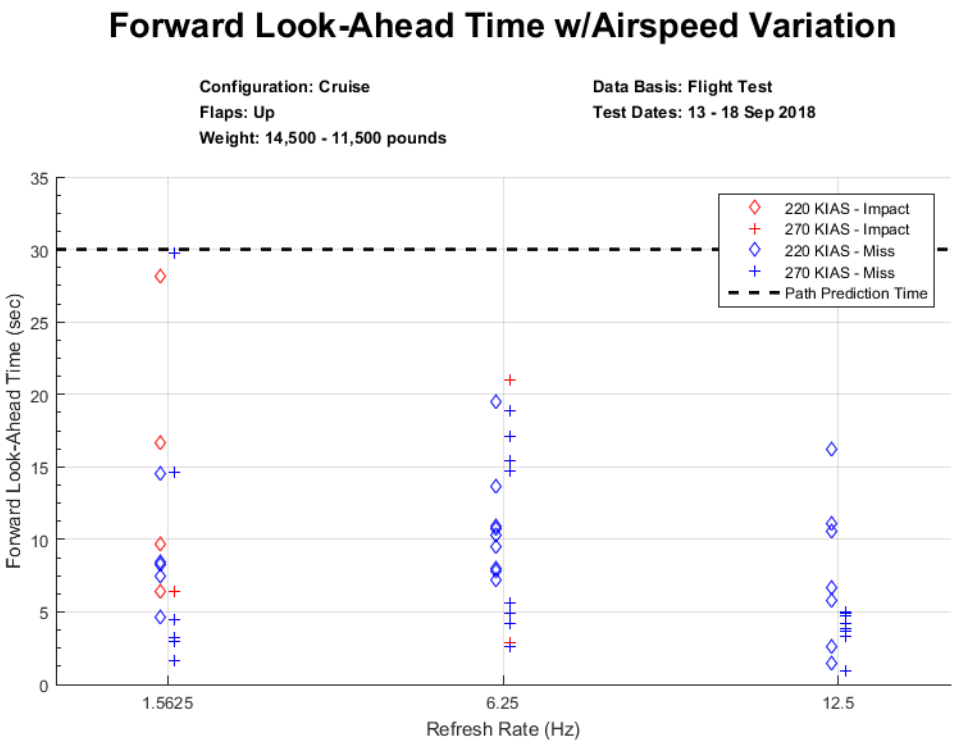

Figure 4.18. Forward Look-Ahead Time with Airspeed Variation

4.3.3.1 Path Performance.

The RSET system commanded maneuvers commensurate with available aircraft performance. For all activations, MCP was set within three seconds of the escape maneuver beginning. By design, the VSS commanded more aggressive escape maneuvers during the 270 KIAS test points than it did during the 220 KIAS test points. That is, the RSET commanded higher load factors and flight path angles (FPAs) when more aircraft performance was available. As a result, airspeed and RSET commanded load factor and FPA gradually decreased throughout the escape maneuver until reaching a steady energy state. The aircraft generally achieved steady state, RSET-commanded angle of bank (AoB) within five seconds of escape maneuver activation. With less performance available during the 220 KIAS escape maneuvers, the aircraft initially performed at reduced load factors and FPAs but gained energy as the throttles were

advanced. As a result, airspeed and RSET commanded load factor and FPA gradually increased throughout the escape maneuvers until reaching a steady energy state. These behaviors can be seen in Figure 4.19 through Figure 4.24. Path performance of Paths 4 and 5 (right turning escape maneuvers) was representative of Paths 1 and 2 (left turning escape maneuvers).

Figure 4.19 shows a Path 3 escape maneuver initiated from straight and level flight, at 220 KIAS and 500 ft AGL. Initially, performance available was low so the RSET commanded a gradual increase in load factor and FPA. The available performance increased as power reached MCP and the aircraft stabilized on the RSET-commanded limit of approximately 8^o FPA. Once on the RSET limit of FPA, the system no longer commanded an increase in load factor.

Figure 4.20 shows a Path 3 escape maneuver initiated from a left 45 bank, at 270 KIAS and 500 ft AGL. Initially, performance available was high so the RSET commanded the aircraft to simultaneously roll wings-level and increase load factor to keep the FPA greater than or equal to zero. The aircraft reached the RSET-commanded load factor limit when wings-level was achieved and the FPA began to rapidly increase to the RSET limit. The RSET commanded the aircraft to maintain the load factor limit until reaching the FPA limit. As a result of this binary-style logic, the aircraft overshot the FPA limit by approximately 5^o (42%). The FPA gradually decreased until the RSET-commanded limit and the aircraft's actual FPA were in agreement. The airspeed never decreased below the test limit of 200 KIAS during the FPA overshoot; however, the system should account for potential FPA overshoots to preclude unsafe airspeeds during escape maneuvers. **R5: Account for FPA overshoots in the escape maneuver control laws for high aircraft performance conditions.**

Figure 4.21 shows a Path 4 escape maneuver initiated from a left 45^o bank, at

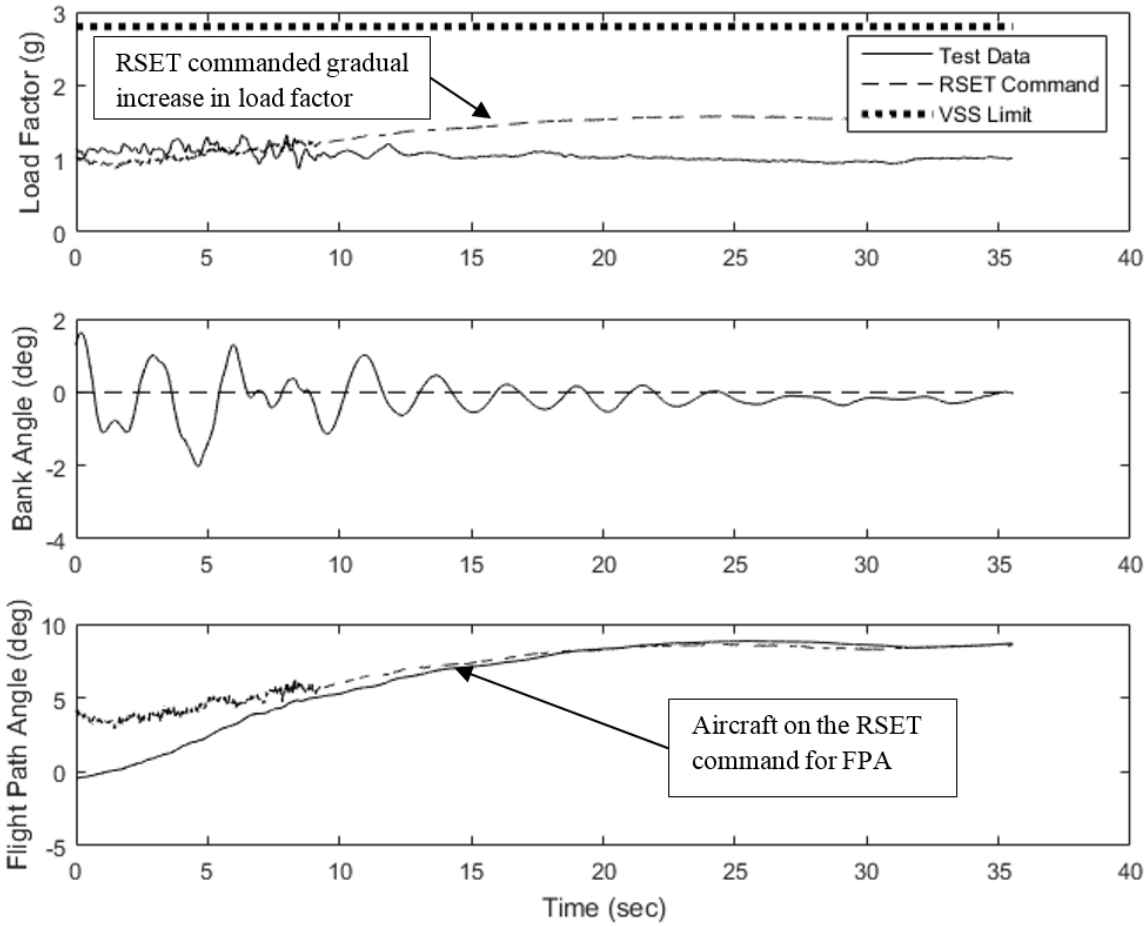

Figure 4.19. Path 3 Performance, 220 KIAS, 500 ft AGL, SLUF Entry

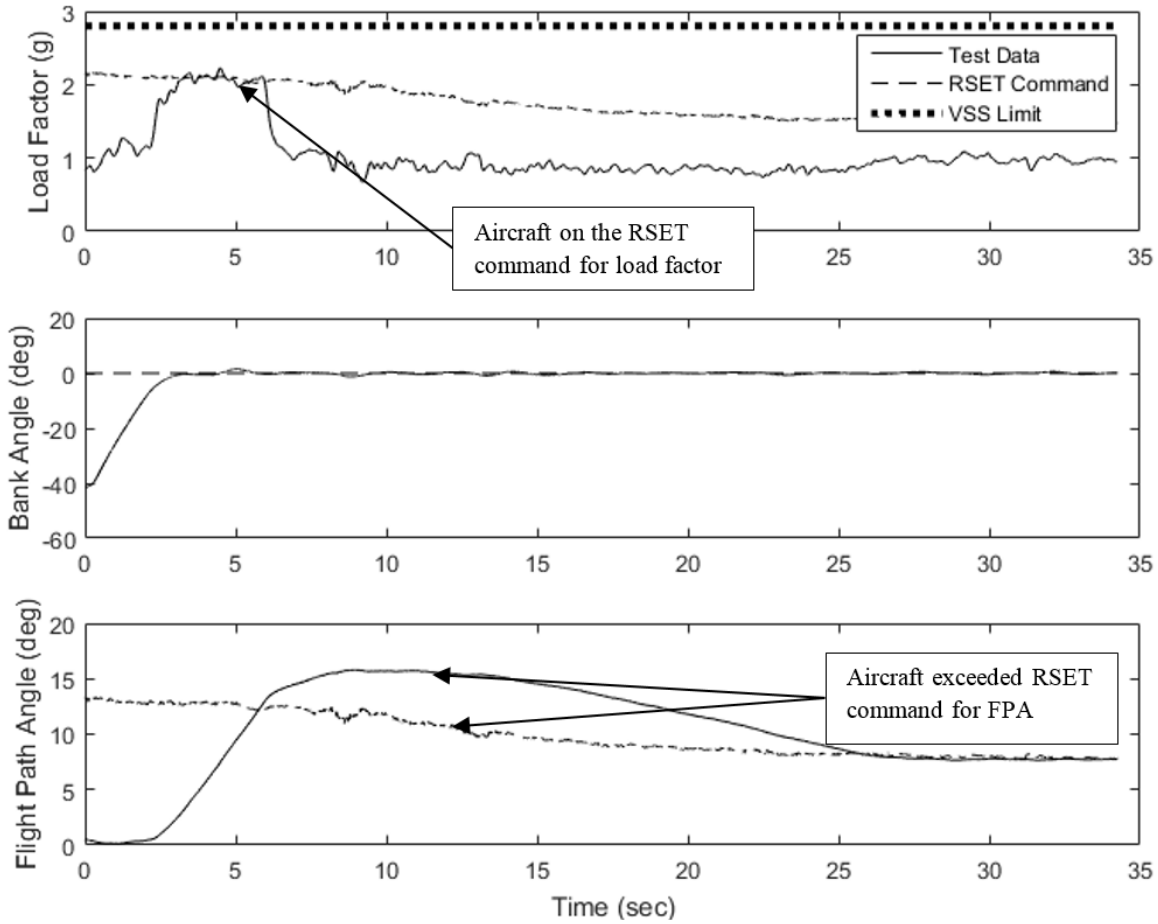

Figure 4.20. Path 3 Performance, 270 KIAS, 500 ft AGL, 45^o Left Turning Entry

220 KIAS and 500 ft AGL. Initially, performance available was low so the RSET commanded a gradual increase in load factor and FPA. The available performance increased as power reached MCP and the aircraft stabilized on the RSET-commanded limit of approximately 8^o FPA. Once on the RSET limit of FPA, the system no longer commanded an increase in load factor.

Figure 4.22 shows a Path 4 escape maneuver initiated from a left 45^o bank, at 270 KIAS and 500 ft AGL. Initially, performance available was high so the RSET commanded the aircraft to roll wings-level and, passing through 0^o of bank, increase load factor to keep FPA greater than or equal to zero. The aircraft reached the RSET-commanded load factor limit and the FPA began to rapidly increase to the RSET limit. The RSET commanded the aircraft to maintain the load factor limit until reaching the FPA limit. As a result of the excess performance available, the aircraft overshot the FPA limit by approximately 2^o (17%). The FPA gradually decreased until the RSET-commanded limit and the aircraft's actual FPA were in agreement.

Figure 4.23 shows a Path 5 escape maneuver initiated from straight and level flight, at 220 KIAS and 500 ft AGL. Initially, performance available was too low to maintain the RSET-commanded 60^o AOB without descending. The RSET control logic prioritized maintaining greater than or equal to zero FPA over the escape maneuver's 60^o AOB. As a result, the aircraft decreased AOB, raised the nose until greater than or equal to zero FPA could be reestablished, and then continued its 60^o AOB. This "ratcheting" was undesirable, and could lead to confusion and incorrect pilot actions. This behavior was not common during the 270 KIAS test points as enough aircraft performance was available to keep greater than or equal to zero FPA throughout the entire escape maneuver. Additional consideration of low aircraft performance conditions in the control laws could alleviate this behavior. **R6: Tailor escape maneuver control laws for low aircraft performance conditions.**

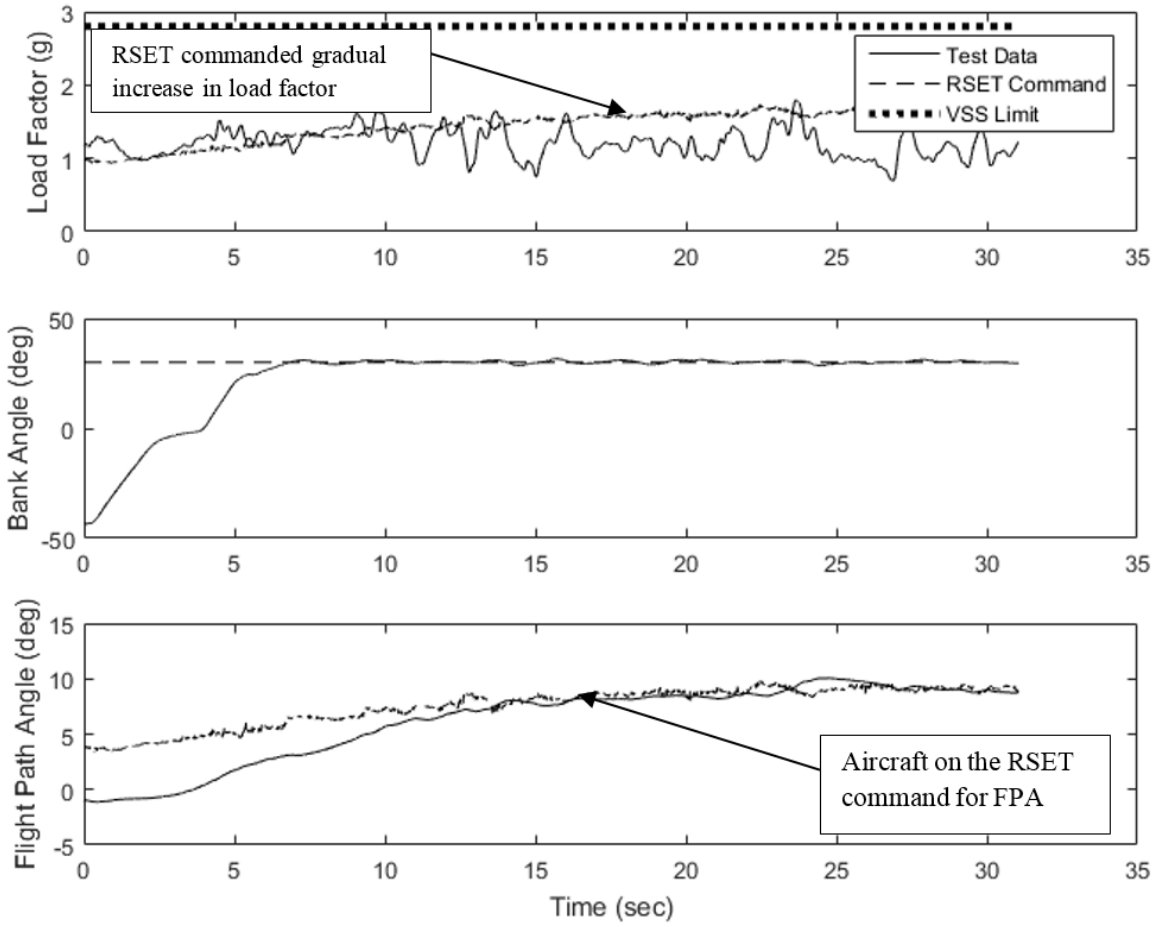

Figure 4.21. Path 4 Performance, 220 KIAS, 500 ft AGL, 45^o Left Turning Entry

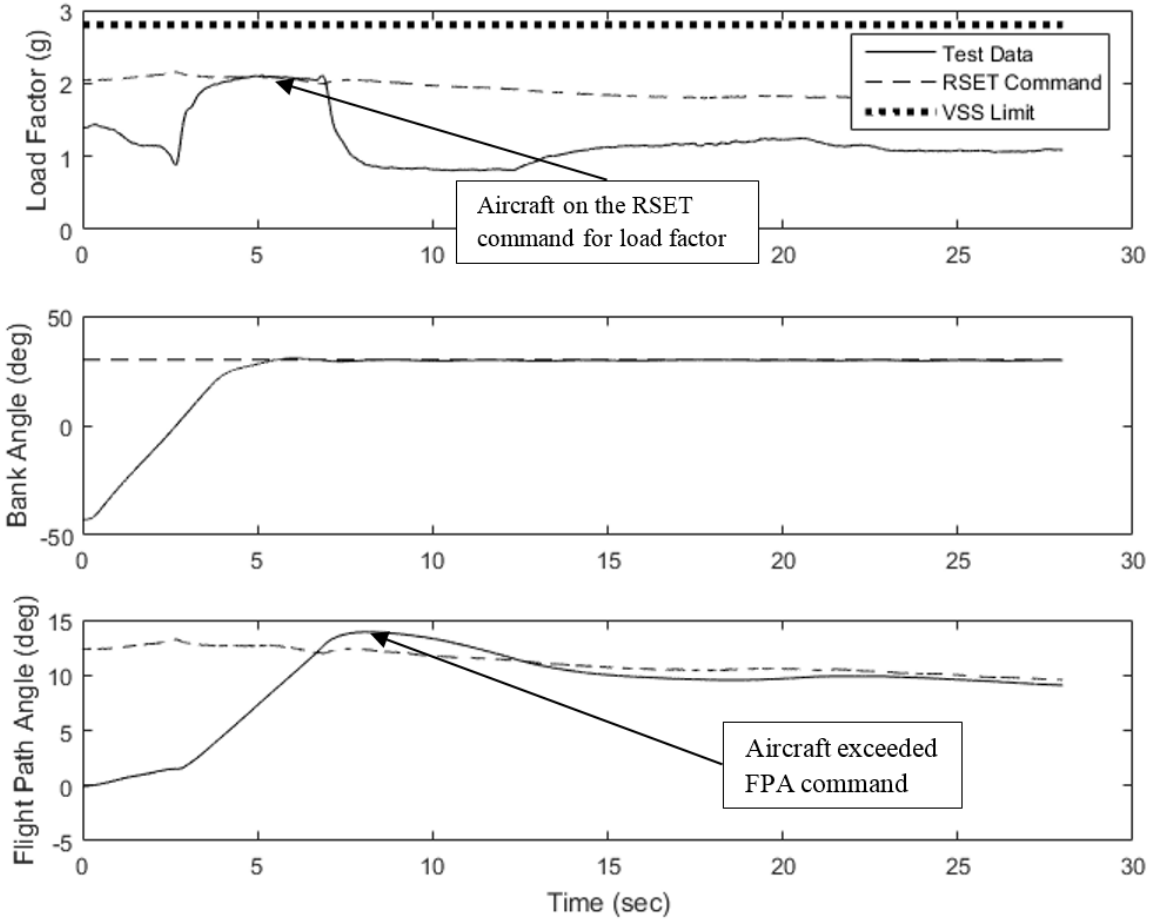

Figure 4.22. Path 4 Performance, 270 KIAS, 500 ft AGL, 45^o Left Turning Entry

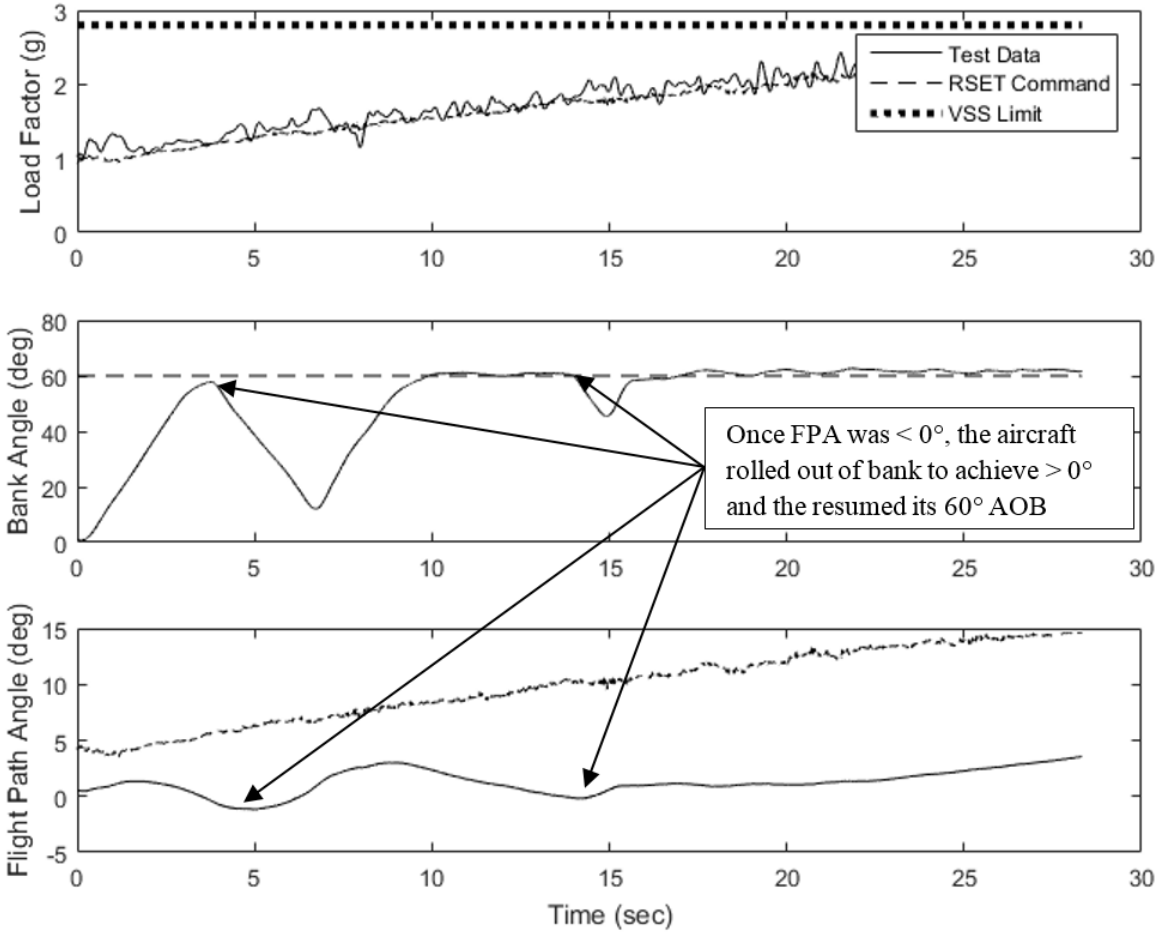

Figure 4.23. Path 5 Performance, 220 KIAS, 500 ft AGL

Figure 4.24 shows a Path 5 escape maneuver initiated from a left 45^o bank, at 270 KIAS and 500 ft AGL. Initially, performance available was high so the RSET commanded the aircraft to simultaneously roll into a right 60^o bank and increase load factor to increase FPA. The aircraft reached the RSET-commanded load factor limit and the FPA began to rapidly increase to the RSET limit. The RSET commanded the aircraft to maintain the load factor limit until reaching the FPA limit. As a result of the excess performance available, the aircraft overshot the FPA limit by approximately 2^o (17%). After the FPA overshoot was rectified, the aircraft remained on the RSET limit for load factor.

4.3.3.2 Nuisance Activations.

The aircraft did not exhibit nuisance activations during testing against lateral terrain. For each pass flown, the RSET showed the level escape maneuver was available and would avoid terrain, but the EP commented that he would not consider turning in the direction of terrain if he were to manually fly a 60^o level turn escape maneuver. Figure 4.25 and Figure 4.26 depict the path of the aircraft in green and the RSET 60^o right turn predictions of Path 5 in red. At no point did the RSET path nuisance activate near lateral terrain.

4.3.3.3 Operational Nuisance Activations.

The RSET system did not exhibit nuisance activations during operationally representative profiles against lateral terrain. Typically, the RSET showed the 60^o bank escape maneuver was available and would avoid terrain, but the EP commented that they would not consider turning in the direction of terrain if they were to manually fly a level turn escape maneuver. On each flight against operational terrain, the team observed at least one to two instances when the turning escape path towards

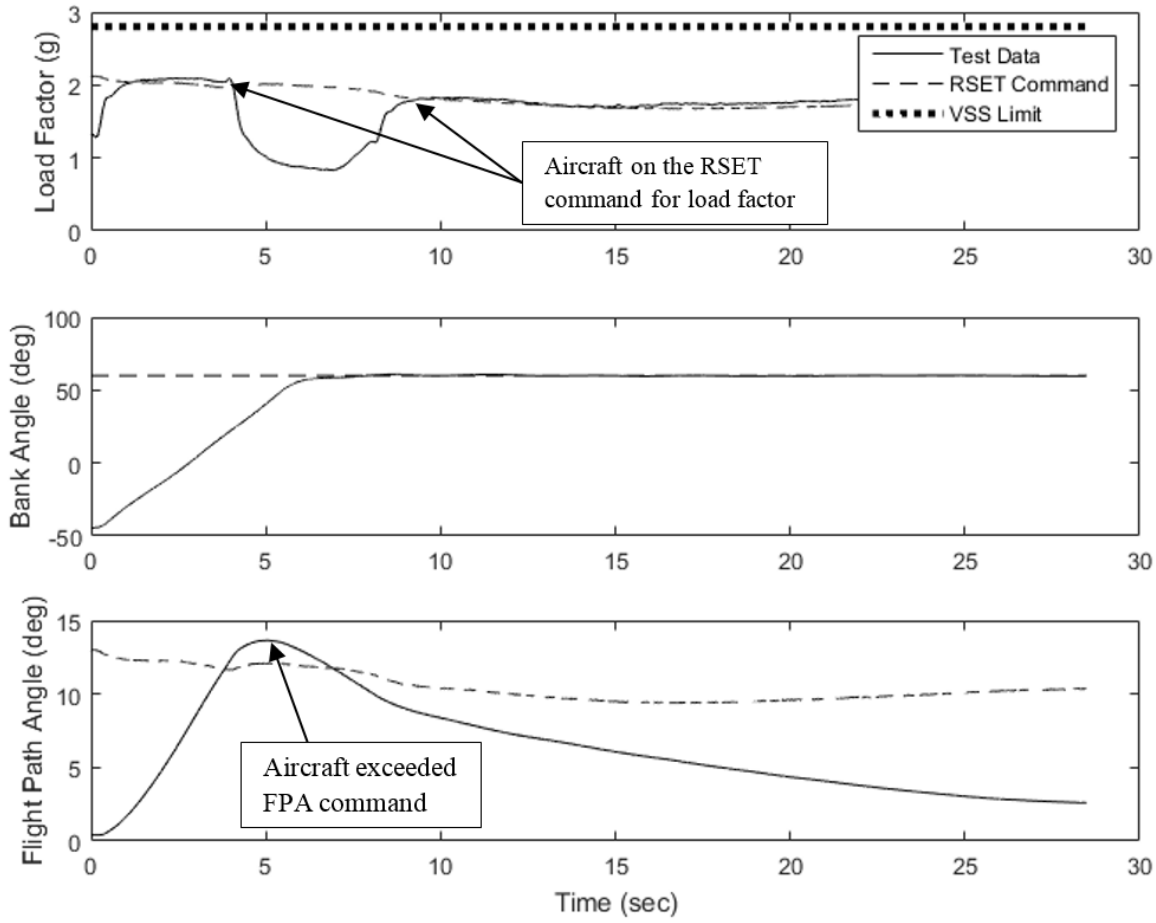

Figure 4.24. Path 5 Performance, 270 KIAS, 500 ft AGL

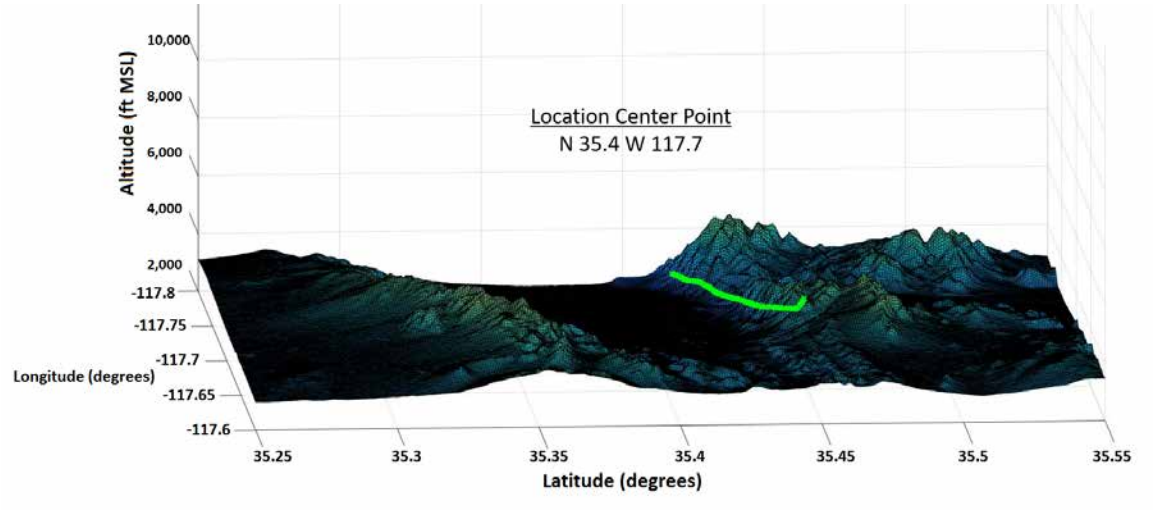

Figure 4.25. Path of Aircraft During Lateral Offset Test Points

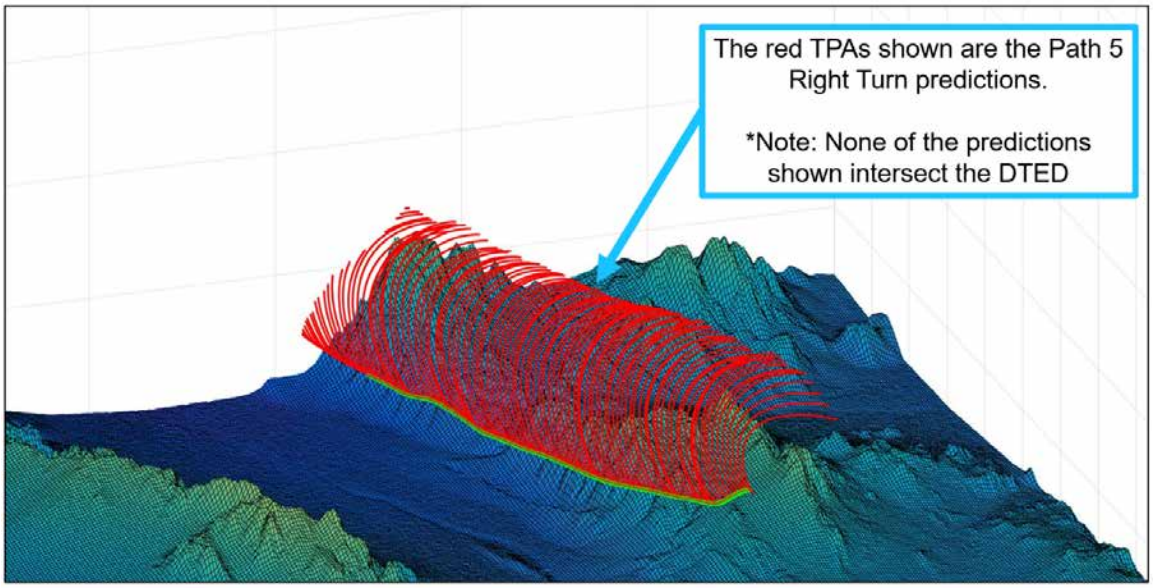

Figure 4.26. Path of Aircraft with 60^o Right RSET Predictions during Lateral Offset Test Points

terrain would momentarily close. In all cases, the crew agreed that the closure was appropriate. This data was also objectively confirmed via numerous team comments during the operational terrain evaluation which stated surprise that the path towards terrain was not closed off. In spite of the large path prediction error, the system still demonstrated no tendency to nuisance for the operational profile flown.

4.3.4 Maneuver Termination Control Hand-Back.

Upon completion of any RSET path maneuvering, the aircraft autopilots commanded a roll to wings-level and pitch reduction to zero gamma as described in Section 3.5.4. The test objective was met.

For low-speed test points, aircrew comments indicated a smooth, logical, and safe hand-back. However, the test team found that at higher airspeeds, the hand-back would trip the Learjet VSS safety logic, as was seen in Table 3.5, due to an under-g condition (less than 0.25 g). Because of this, the team was unable to fully characterize and evaluate every single hand-back scenario. During these maneuvers where the VSS tripped, the aggressive unload from 2 g to 0.25 g repeatedly caused aircrew motion sickness. This maneuver would likely have caused an aircraft limit exceedance without the VSS safety logic. This behavior would need to be addressed prior to any hand-back implementation in order to avoid airframe limit exceedance and aircrew discomfort. Additionally, based on aircrew comments, airframe mission also needs to be considered in future versions of the hand-back. This consideration would need to account for tactics such as terrain masking where unnecessary maneuvering would be detrimental to platform survivability.

The addition of the stick shaker during escape maneuver activation was well received by the pilots. It provided tactile feedback that the RSET was handing back control of the aircraft after the initial escape maneuver was complete. The stick

shaker ceased concurrent with the completion of RSET hand-back. The stick shaker was the only usable indication to the aircrew that the RSET was still in control of the aircraft as the location of the CSS made it unusable to the pilots during "heads up" flying. Aircrew comments were in favor of a display that could be incorporated into a normal crosscheck for the low-level phase of flight. **R7: System hand-back should be less aggressive for aircrew comfort and PVI should be placed in pilot's line-of-sight.**

Aircrew were in favor of the ability to "paddle off" the system and take control any time the RSET was controlling the aircraft. Paddling off the system during the hand-back was common when the pilots felt like the aircraft was in a safe condition and they did not want to wait for the RSET to complete the entire hand-back process. The aircrew strongly agreed the ability to paddle off the system was a requirement rather than a desired feature. **R8: Future implementation of the RSET should require a means for aircrew to override the system and take control of the aircraft.**

Throughout the test period, all EPs provided their qualitative opinion of the hand-back following RSET maneuver completion. An extensive listing of EP comments can be found in Appendix K. A sampling of EP comments are displayed below:

> "Felt smooth and safe. Adequate for system maturity."
>
> "Hand-back took a little too long in order to stay smooth. I would probably pickle off and take command earlier to recover faster."
>
> "Higher airspeed hand-back was more aggressive vs lower energy state hand-backs."
>
> "During low speed points, it's hard to tell if the aircraft is in a hand-back state or attempting a different path. Visual indication of system state would

be useful."

"In a non-combat environment this would be totally fine. It gets the aircraft back to a place I feel comfortable taking control."

4.4 Chapter Summary

This chapter presented the results of the Have MEDUSA flight tests. Overall, the results were positive and represented a significant advance from the Have ESCAPE tests, although there is still research to be done. Throughout this chapter recommendations based on data analysis were presented for the flight test objectives. The complete list of conclusions and recommendations, including those related to the overall research objectives, are given in Chapter IV.

V. Conclusions, Recommendations, and Lessons Learned

5.1 Overview

As presented in Chapter I, the goal of this research was to research, design, and test an Auto-GCAS for performance limited aircraft. The motivation for this research was to reduce the number of CFIT accidents across the Air Force inventory. This research primarily used the works of Trombetta and Suplisson as a starting point for system development [14, 15]. Their work demonstrated the advantage of a multi-path system for performance limited aircraft, and identified the need for RSET. The RSET system was developed through the adaptation of a flight tested Learjet 25D aerodynamic model combined with 5 TPAs to project the aircraft's position forward in time. These forward projections were then compared to the surrounding DTED posts to determine whether a collision risk was present and maneuver the aircraft in an aggressive and timely manner when necessary. Once developed, this system was flight tested under USAF TPS TMP Have MEDUSA. The following chapter presents the conclusions and recommendations gleaned from the results presented in Chapter IV. Additionally, lessons learned from this effort and guidance are given to aid future research.

5.2 Conclusions and Recommendations

This section is divided into conclusions and associated recommendations based on the flight test objectives and overall research objectives. Although several of the research objectives were not explicit flight test objectives, they were evaluated or observed during the development and execution of the flight test and are thus recorded herein.

5.2.1 Flight Test Objective Conclusions.

The flight test objectives from Section 1.3.2 are repeated below with their associated conclusions and specific recommendations for both future research and inclusion in the requirements for a fielded system. The flight test objectives are presented first since many of the research objectives where realized through pursuit of the flight test objectives.

1. Demonstrate the prediction accuracy of the RSET system.

   For path prediction accuracy, the RSET system was evaluated as MARGINAL with 117 out of 120 test points having a maximum path prediction error (PPE) above 300 ft. It was observed that maximum PPE tended to be highest for Path 1 activation and lowest for Path 3 activation. Maximum PPE was higher for diving entries compared to the other three entries. Out of 120 test points analyzed, 44 had PPE erring away from terrain, 54 had PPE erring towards terrain, and the remaining 22 test points were inconclusive. Possible sources of error could be the auto-trim feature of the VSS, incorrect accounting of wind speed and direction in the TPAs, and the low fidelity of the Learjet engine model used in the TPAs.

   R1: Conduct further data analysis to determine the sources of error and their impact to PPE.

   Furthermore, the majority of test points were only tested once and had no statistical significance in PPE.

   R2: Conduct repeat runs of specific test conditions to increase statistical significance of PPE results. Additionally, since TIC showed that the Stitched and Converted models matched very closely the Stitched

model should be investigated throughout the aircraft flight envelope to verifying its applicability and accuracy.

2. Demonstrate the impact of changing the refresh rate on the RSET system's ability to calculate an achievable escape path

   With respect to terrain miss distance, it appeared that a refresh rate near 12.5 Hz was required to ensure terrain clearance with this implementation of the RSET system. The selection of an appropriate terrain buffer was a critical parameter. Future systems should evaluate the mission and aircraft performance ability when determining a terrain buffer.

   R3: Using a refresh rate of 12 Hz or faster, investigate the effect of varied operationally representative terrain types and terrain buffers on miss distance.

   Data showed that increasing refresh rate also required a shorter forward look-ahead time. Forward look ahead time was evaluated at 30 seconds only and did not appear to be significantly affected by other factors. System refresh rate drove forward look-ahead time, and the presented data would provide a rough starting point for future multi-path collision avoidance systems. Please see Carpenter's research for supporting information on varying forward look-ahead time [70].

   R4: Evaluate the need for forward look-ahead times beyond 30 seconds.

   For path performance, the aircraft generally achieved steady state, RSET-commanded AOB within five seconds of escape maneuver activation. With less performance available during the 220 KIAS escape maneuvers, the

aircraft initially performed at reduced load factors and FPAs but gained energy as the throttles were advanced. With more performance available during the 270 KIAS escape maneuvers, the aircraft exhibited the tendency to overshoot the RSET-commanded FPA by up to 5^o (42%). The FPA gradually decreased until the RSET-commanded limit and the aircraft's actual FPA agreed. The airspeed never decreased below the test limit of 200 KIAS during FPA overshoots; however, the system should account for FPA overshoots to preclude unsafe airspeeds during escape maneuvers.

R5: The RSET system specification should include a requirement to account for FPA overshoots in the escape maneuver control laws for high aircraft performance conditions.

During 60^o-AOB escape maneuvers at low performance states, the aircraft was unable to maintain the RSET-commanded 60^o-AOB without descending. The RSET control logic prioritized maintaining greater than or equal to zero FPA over the escape maneuvers 60^o-AOB. As a result, the aircraft decreased AOB, raised the nose until greater than or equal to zero FPA, and then continued its 60^o AOB. This "ratcheting" was undesirable and could lead to confusion or incorrect pilot actions. This behavior was not common during the 270 KIAS test points as enough aircraft performance was available to keep greater than or equal to zero FPA throughout the entire escape maneuver. Additional consideration of low aircraft performance conditions in the control laws could alleviate this behavior.

R6: The RSET system specification should tailor escape maneuver control laws for low aircraft performance conditions.

3. Observe the RSET system tendency to nuisance activation.

   The aircraft did not exhibit nuisance activations during testing against lateral terrain as well as for operationally representative profiles against lateral terrain. Typically, the RSET showed the 60^o AOB escape maneuver was available, but the aircrew commented they would not consider turning in the direction of terrain if they were to manually fly a 60^o AOB escape maneuver. As a result of these findings and the aggressive path performance results, this RSET implementation was not nuisance prone.

   R7: Continue to incorporate aggressive maneuvers to limit nuisance potential.

4. Observe the control hand-back of the RSET system after maneuver termination.

   For low-speed test points, aircrew comments indicated a smooth, logical, and safe hand-back. However, the test team found that at higher airspeeds, the hand-back would trip the Learjet VSS safety logic due to an under-g condition ($\leq$ 0.25 g). During maneuvers where the VSS tripped, the aggressive unload from 2 g to 0.25 g caused aircrew motion sickness. Based on aircrew comments, airframe mission also needs to be considered in future versions of the hand-back. Consideration should be given to tactics such as terrain masking where unnecessary maneuvering would be detrimental to platform survivability.

   The addition of the stick shaker during escape maneuver activation was well received by the pilots. It provided tactile feedback that the RSET was handing back control of the aircraft after the initial escape maneuver was complete. The stick shaker ceased with the completion of RSET hand-

back. The stick shaker was the only usable indication to the aircrew that the RSET was still in control of the aircraft as the location of the CSS made it unusable to the pilots during "heads up" flying. Aircrew comments were in favor of a display that could be incorporated into a normal crosscheck for the low-level phase of flight.

R8: The RSET system specification should require system hand back to be less aggressive for aircrew comfort and relocate PVI to pilots line-of-sight and include a positive indication (such as a stick shaker) when active.

Aircrew were in favor of the ability to "paddle off" the system and take control any time the RSET was controlling the aircraft. Paddling off the system during the hand-back was common when the pilots felt like the aircraft was in a safe condition and they did not want to wait for the RSET to complete the entire hand-back process. The aircrew strongly agreed the ability to paddle off the system was a requirement rather than a desired feature.

R9: The RSET system specification should also include a means for aircrew to override the system and take control of the aircraft.

5.2.2 Research Objective Conclusions.

The overall research objectives from Section 1.3.2 are repeated below with their associated conclusions and recommendations.

1. Apply 6-DoF equations of motion for aircraft path prediction [14].

   An augmented 6-DOF model was implemented for the RSET system. Although the higher fidelity model did not provide the desired small PPE,

it was nevertheless able to provide enough prediction accuracy to avoid terrain. Furthermore it was an important step forward for multi-path Auto-GCAS research to show that a more complicated flight dynamics model could operate at a fast enough refresh rate.

R10: Continue to investigate the tradeoffs between model fidelity and prediction accuracy. Based on this research, TIC and PPE appear to be effective ways of calculating the quality of fidelty and accuracy respectively.

2. Allow for a variable aircraft initial state [15].

   A variable initial state was implemented for the RSET system. Since adaptive control laws, described in Sections 3.5.1 and 3.5.3, were used for both path prediction and execution, the aircraft was not constrained to one starting condition. This was another step forward towards developing an operationally relevant Auto-GCAS and shows that this RSET approach is feasible.

   R11: An RSET system specification should require the system to be capable of operating within as much of the host aircraft flight envelope as possible.

3. Determine necessary number of RSETs [15, 23].

   While the research presented here cannot say conclusively how many RSETs are necessary for a multi-path Auto-GCAS, flight testing did show that all five paths were used based on terrain and aircraft energy state. Indeed path selection and utility is entirely dependent on the design of the paths themselves as well as aircraft performance and mission. The finding that a five path solution may be necessary is contrary to the conclusion of Trom-

betta [15].

R12: Continue to investigate other multi-path implementations, to include more than five path options.

4. Integrate auto-throttle for maneuver execution [14].

   Due to system constraints discussed in Section 1.4, the auto-throttle feature of the Learjet VSS was not used. Instead the EP served as the "human auto-throttle". The three EPs were adept at consistently setting MCP and were not identified as a major source of error in the test results. Still, the nature of performance limited aircraft will necessitate the use of a pilot-free auto-throttle system for a fielded Auto-GCAS.

   R13: An RSET system specification should incorporate auto-throttle.

5. Perform continuous path analysis, even during maneuver [15].

   As discussed, the adaptive control laws provided increased flexibility of the RSET system compare to Have ESCAPE. The RSET system was able to continually calculate TPAs and, if clear of offending terrain, automatically hand control back to the EP.

   R14: Continuous path analysis should be an RSET system requirement.

6. Achieve $\geq$ 6 Hz operation with MATLAB implementation [14].

   Using a laptop with the specifications provided in Section 3.8.3, the RSET system was able to operate at 12.5 Hz, which was in agreement with fielded systems such as F-16 Auto-GCAS (which operates at 12 Hz).

R15: An RSET system should use 12 Hz as a baseline refresh rate.

7. Include wind and density altitude effects [15, 23].

   The Stitched Model which was at the core of the RSET system included wind and density effects. As discussed in Section 4.3.1 it was determined that wind effects were not properly accounted for in the flight tested system. Indeed wind was identified to play an important role in error propogation.

   R16: Future research efforts should ensure that wind effects are appropriately accounted for in the RSET system and existing autopilots.

8. Use of identical control laws for both path prediction and maneuver execution.

   As has been discussed several times already, the approach of using identical control laws for TPA calculation and maneuver execution was desirable.

   R17: Recommend the use of similarly designed control laws for path prediction and maneuver execution for future RSET systems.

9. Identify multi-path Auto-GCAS nuisance criteria.

   This research used a simple and limited approach to evaluating nuisance which was constrained by the safety requirements of the USAF TPS student TMP process. Clearly, quantifying nuisance is important but it is also challenging. It is especially challenging when evaluating against terrain that is laterally offset from the aircraft and therefore does not have a "time until impact" associated with it.

R18: Continue to investigate appropriate metrics to quantify multi-path nuisance.

10. Determine maneuver termination timeliness criteria.

    There are an infinite number of maneuver termination criteria and hand-back methods. This research simply identified when the projected paths no longer predicted collision with terrain and then began a simple hand-back to the pilot. As can be seen from the results in Chapter IV, this implementation was generally favored.

    R19: Investigate maneuver termination criteria and hand-back state as appropriate for the aircraft customer and operational environment.

5.3 Lessons Learned

While there were many technical and programmatic challenges, the overall perception of how the program went was excellent. At the 12.5 Hz refresh rate, the RSET system met the three key design requirements: **Do No Harm, Do Not Impede Mission Performance, Avoid Ground Collision**. Still, there were many lessons learned that should be incorporated, or at least addressed, in follow-on and similar programs.

Configuration Management Essential for Test Effectiveness and Efficiency

There were instances throughout the test program where the improper RSET build was loaded onto the Learjet following code changes. This either resulted in early termination of the sortie (when realized in flight) or data gathered in the incorrect configuration. A list of configuration details and changes is shown in Appendix G.

The opportunities to load the incorrect build were greater earlier in the test window when new RSET builds were commonplace. As the test window progressed, the configuration was finalized and locked down, which resulted in fewer opportunities to load the incorrect build. Follow-on programs should ensure tight configuration management.

Test Conductor Communication Increased Pilot Situational Awareness

The pilots had minimal indications in the cockpit regarding the current state of the RSET. The one display that did show RSET status was located on the center console (between the pilots) and was not viewable during heads-up flying. As such, the pilots relied heavily on the TCs to paint them a picture of what the RSET was currently doing and what was going to be doing in the near future. This awareness allowed pilots to anticipate what was next and keep an efficient airspace plan for subsequent test points. This was primarily achieved with effective TC communication over the aircraft intercom system. Follow-on programs should emphasize additional means (that are readily available while flying, such as line-of-sight displays or haptic feedback) to provide pilots awareness of RSET behavior.

Effect of Interpolation on DTED Terrain Interpretation

The interpolation method chosen has a direct impact on the Auto-GCAS terrain miss distance. Using a nearest method, such as the one used for the RSET system, is computationally efficient, but does not smoothly transition from one DTED post to another as *linear* or *cubic* methods would. Conversely, the nearest method is the only method that always uses truth data, whereas the other methods attempt to calculate intermediate terrain heights between posts. Auto-GCAS developers should further research into the pros and cons of the interpolation approach chosen. Note:

the ability to use Level 2 DTED would reduce interpolation errors, but would require more computational power to evaluate.

Terrain Safety Buffer Considerations

The terrain safety buffer method used during this test was a simple vertical offset added to the DTED. As can be seen in Figure 5.1, this method provides a consistent vertical buffer, but does not provide a consistent orthogonal or shortest distance, offset from sloped terrain. In fact, in the case of sheer terrain such as a canyon wall, a vertical offset terrain safety buffer provides no protection laterally. Consideration should be given to other methods of adding a terrain safety buffer to prevent these variations.

Integration Issues

As a follow-on program to Have ESCAPE, there were no show-stopping integration issues throughout the program. There were a myriad of instances, though, where the test team expected data to flow from the VSS to the RSET in a certain manner only to find out otherwise later on. Appendix G contains many of these instances. This occurred well into the test window and resulted in lots of time sunk investigating the issues. This also occurred with specific data parameters. For example, the test team expected to receive certain parameters from the VSS only to find out during integration they were not available or they were in a different format. Having the equivalent of an Interface Control Document (ICD) would have been instrumental in ensuring seamless integration and more effective flight testing. Follow-on programs should ensure sufficient understanding of the system(s) their system under test will interface with.

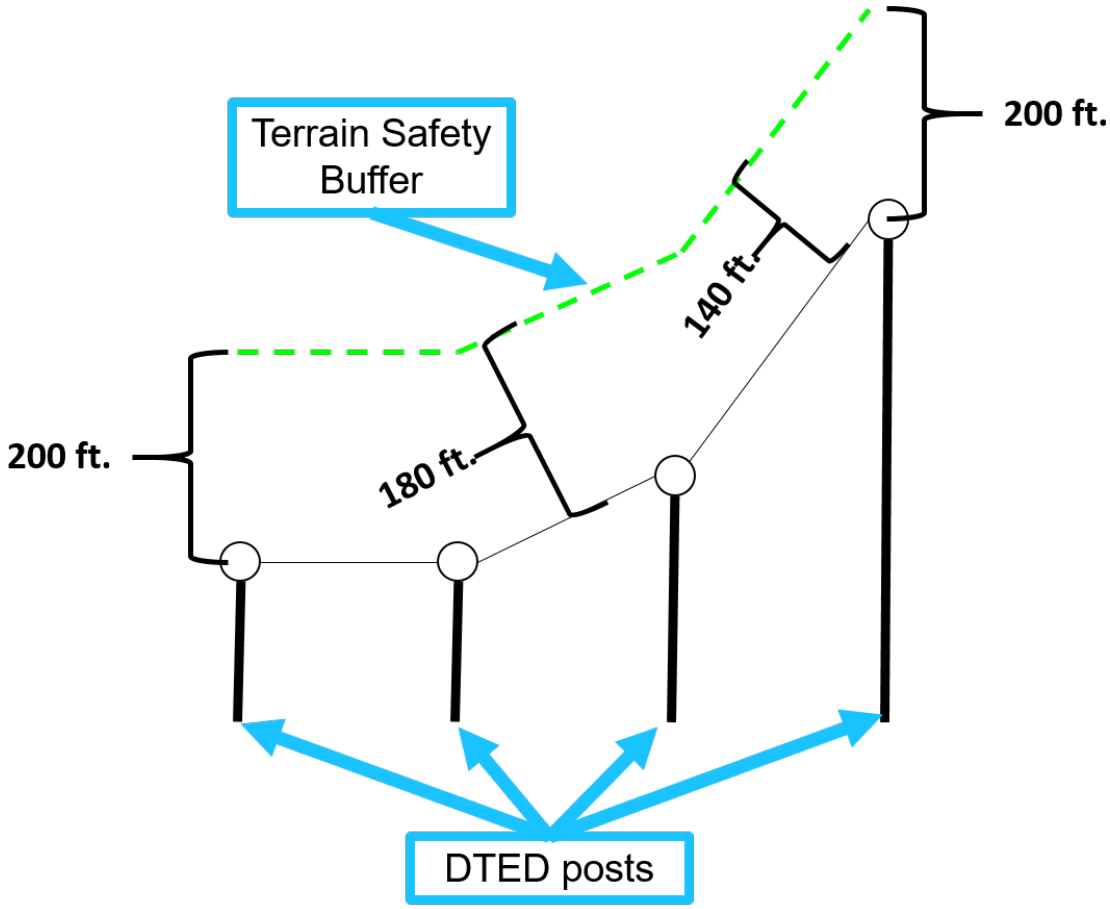

Figure 5.1. Effect of Terrain Slope on Vertical Offset Terrain Safety Buffer

5.4 Guidance for Future Research

This section provides guidance that the author felt was important for future Auto-GCAS researchers and developers. This guidance is in addition to, and not in lieu of, the recommendations and lessons learned already presented.

Standardized Terminology

As more and more individuals, institutions, and corporations add to the body of knowledge for Auto-GCAS, the need for a common vernacular grows. Standardized terminology is key to effectively share ideas, to compare performance, and to educate the operational community on Auto-GCAS. Terms such as Path Prediction Error (PPE) used in this document establish a clear understanding of the performance metric in question.

Adaptive Paths

Though outside the scope of this research, the author feels that adaptive path analysis is a potential solution to the nuisance/operating performance trade-off. Ideally if an Auto-GCAS has a large number of paths to chose from then it can delay intervening longer, decreasing nuisance. A large number of paths comes at a steep computational cost. Instead, for example, a five-path system could be used where once a path becomes closed, that TPA could be reallocated to calculate an escape along a different route. In this way, the computer is still only calculating five paths at any given time, but is not wasting resources on a path that is not a viable option. This thought process could also be applied to adapting the length of the look-ahead, as has been researched by Carpenter [70].

Maneuver Data to Improve Aerodynamic Model

In addition to the data gathered to support the flight test objectives for the

RSET system, a wealth of additional data was gathered during each ground avoidance maneuver. This additional data could be highly useful in improving the prediction aerodynamic model (Stitched Model) and, thus, greatly decreasing PPE. The author advises consideration be given to using flight test to its fullest potential to not just evaluate the Auto-GCAS under test, but to also improve it.

5.5 Contributions

As has been described throughout this chapter, the RSET system was successful in achieving that majority of the objectives that were based on previous research. The RSET system was demonstrated, in simulation and in flight test, that a complex aerodynamic model can be computed quickly enough and used to generate a multi-path Auto-GCAS solution that consistently avoids terrain. Clearly, technology and the state of the art are ready for Auto-GCAS for performance limited aircraft.

5.6 Summary

Over the last five years Auto-GCAS, largely thanks to the success of the F-16 Auto-GCAS, has gained not only acceptance but respect within the aviation community. It is the author's humble desire that the research presented here, and the successes listed abovea will help bring this much needed technology to all aviators.

Appendix A. Supporting Figures

A.1 Learjet Model Conversion

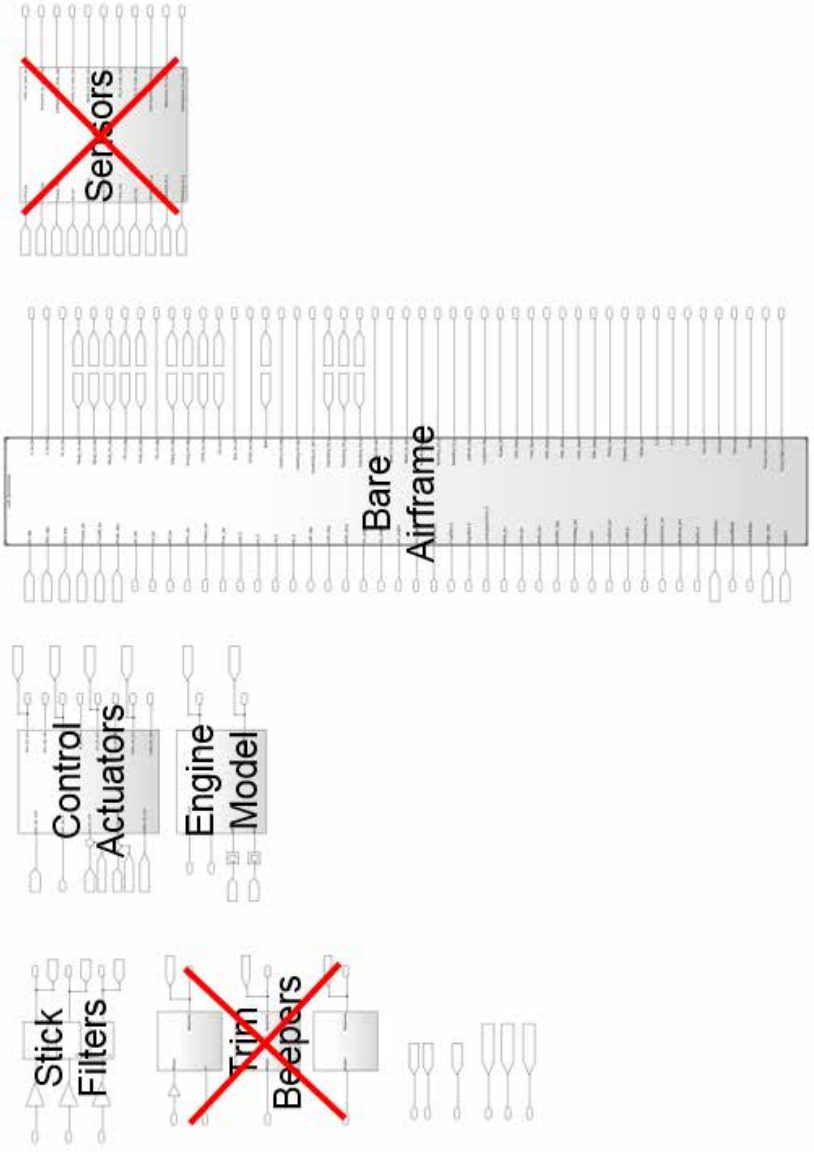

Figure A.1. Stitched Model Simulink Top Level [47]

A.2 Stitched and Converted Model Comparison

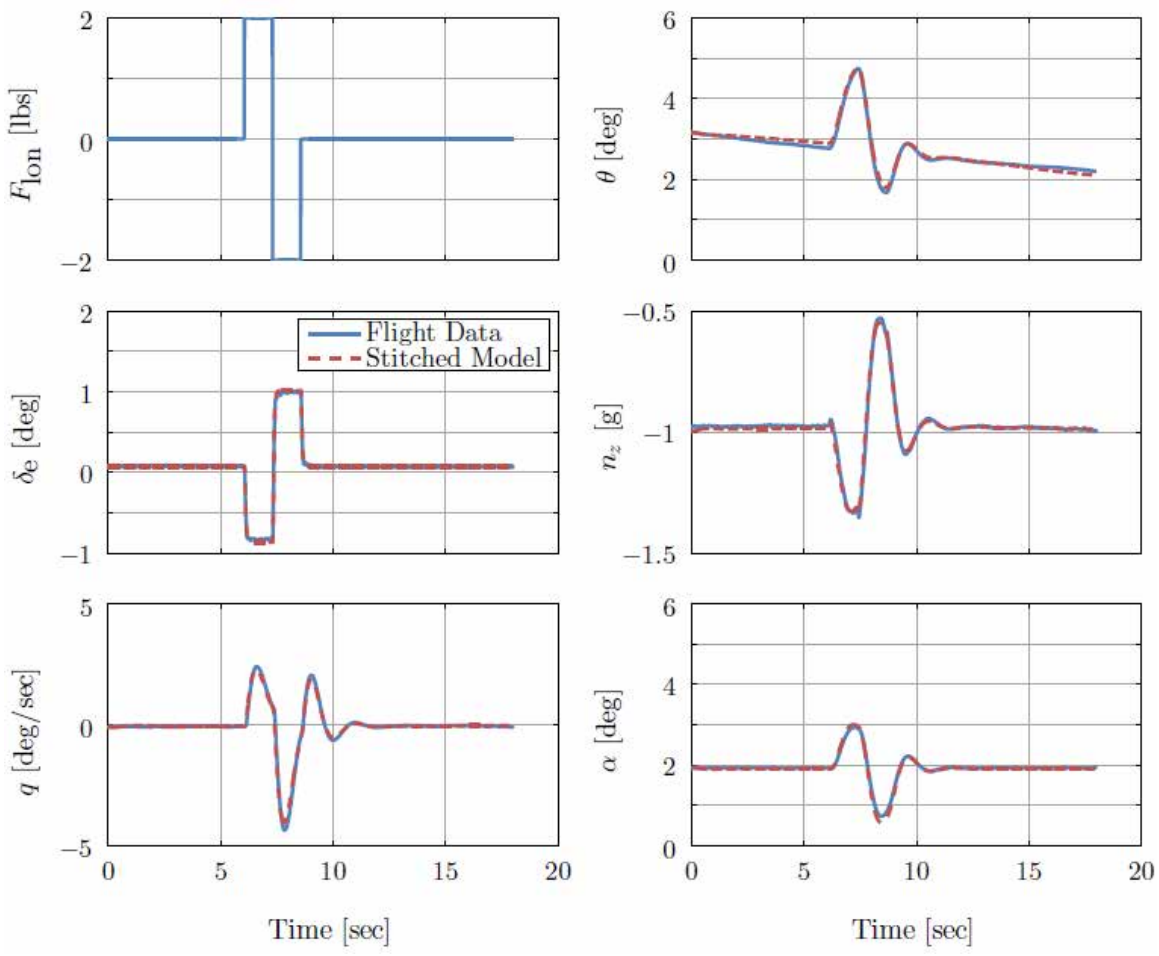

Figure A.2. Stitched Model versus Flight Data Pitch Doublet Response (250 kts, 15,000 ft) [47]

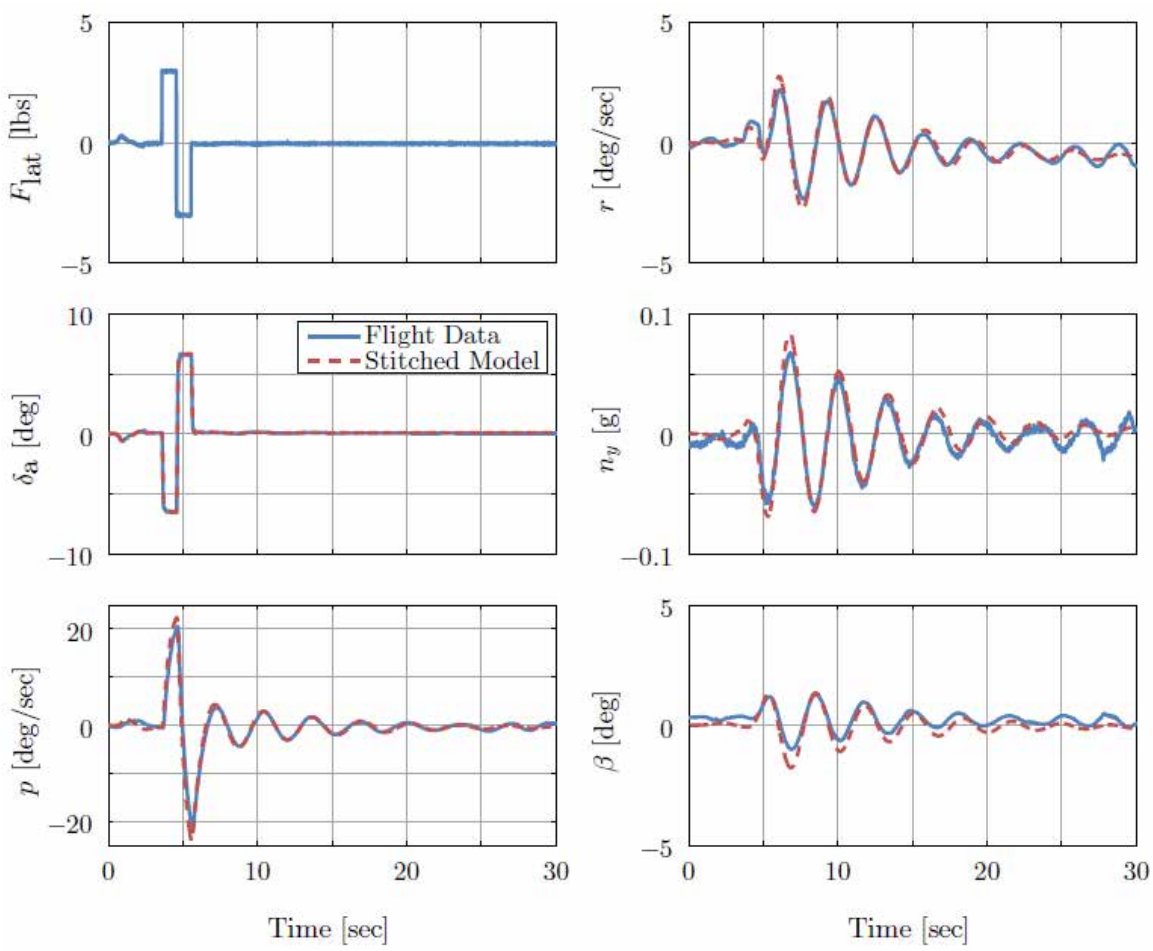

Figure A.3. Stitched Model versus Flight Data Roll Doublet Response (250 kts, 15,000 ft) [47]

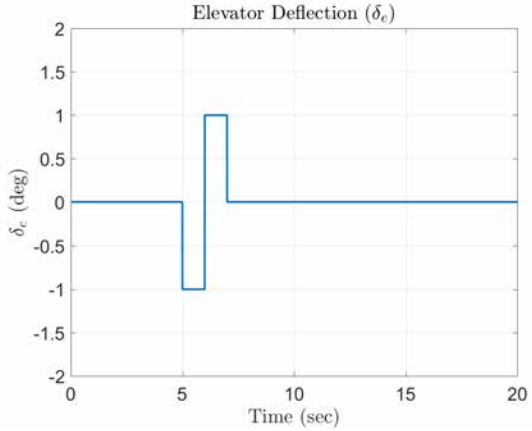

Figure A.4. Pitch Doublet applied to Converted Model

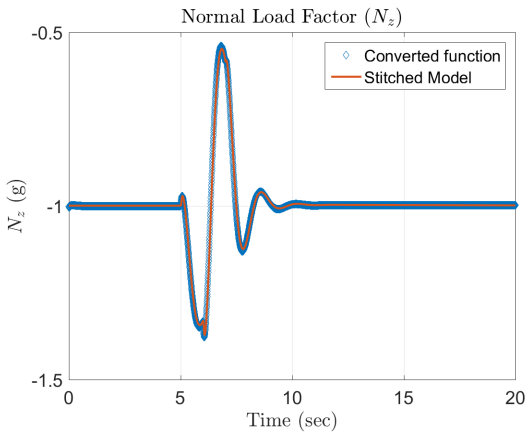

(a) Normal Load Factor

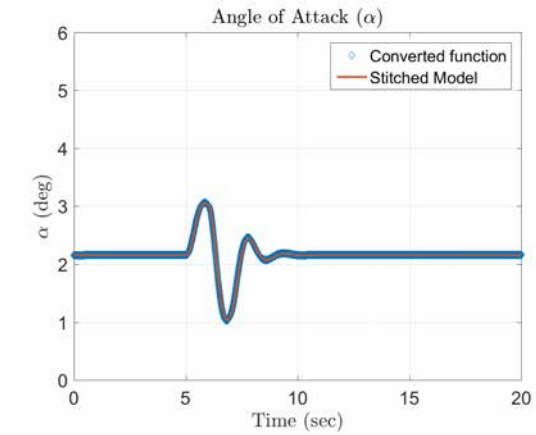

(b) Angle of attack

Figure A.5. Converted Model Pitch Doublet Response for dt = 0.005 s

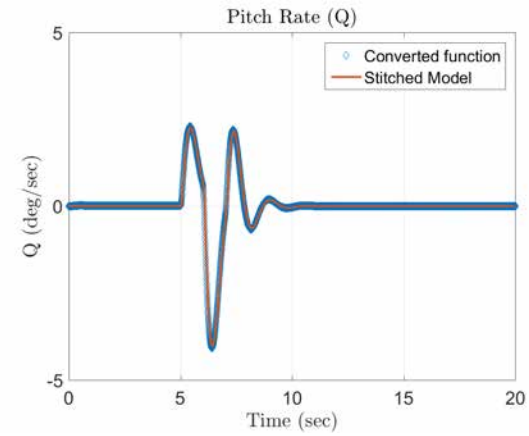

(a) Pitch rate

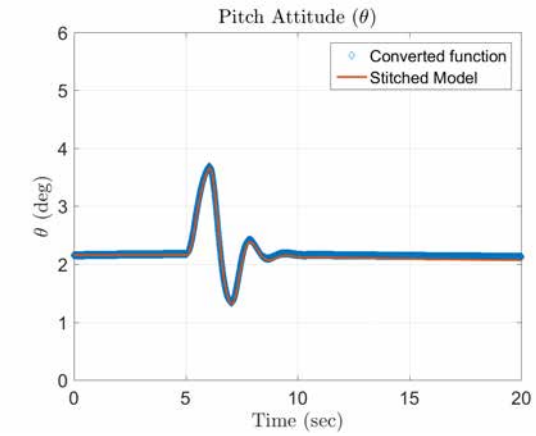

(b) Pitch attitude

Figure A.6. Converted Model Pitch Doublet Response for dt = 0.005 s

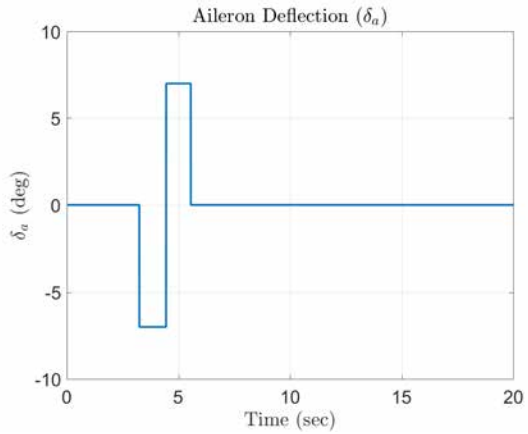

Figure A.7. Roll Doublet Applied to Converted Model

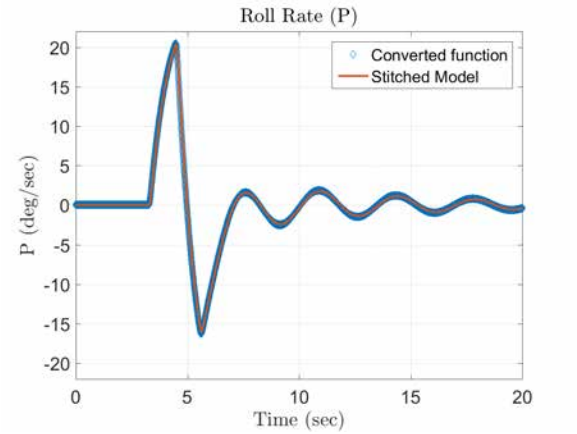

(a) Roll rate

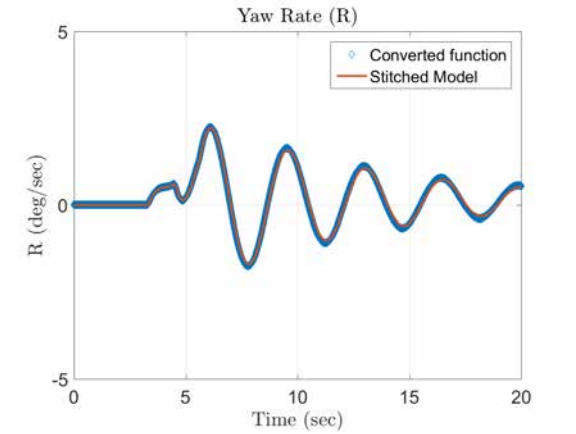

(b) Yaw rate

Figure A.8. Converted Model Roll Doublet Response for dt = 0.005 s

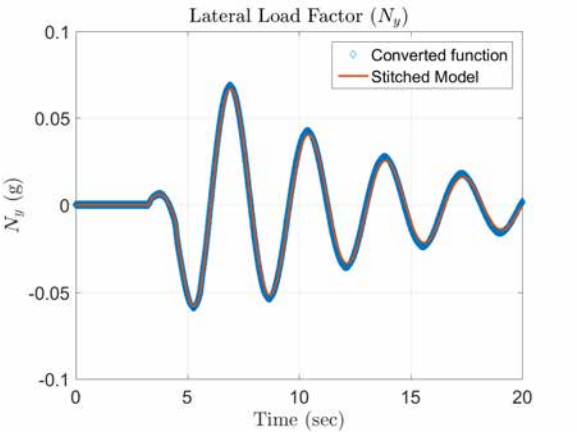

(a) Lateral load factor

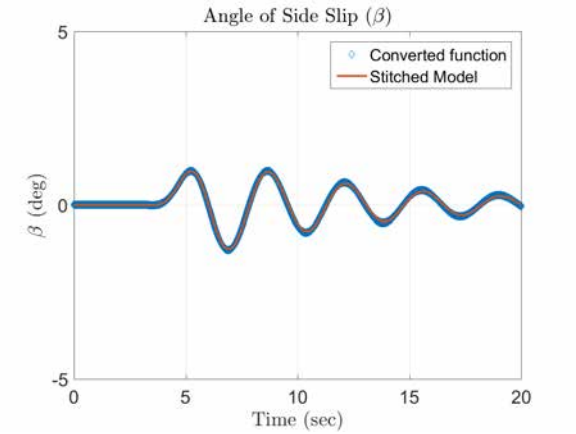

(b) Angle of side slip

Figure A.9. Converted Model Roll Doublet Response for dt = 0.005 s

Appendix B. USAF TPS Daily Flight Test Reports

The following pages present the daily flight test reports (TPS Form 5314) for the 11 Have MEDUSA test flights conducted from 05 September 2018 to 18 September 2018. These reports were used to document data quality, anomalies encountered, and aircrew comments for each test sortie.

The remainder of this page is intentionally blank

DAILY/INITIAL FLIGHT TEST REPORT

1. AIRCRAFT TYPE	2. SERIAL NUMBER
LJ-25	N203VS

3. CONDITIONS RELATIVE TO TEST

A. PROJECT / MISSION NO	B. FLIGHT NO / DATA POINT	C. DATE
HAVE MEDUSA	1	5 Sep 18
D. FRONT COCKPIT	**E. FUEL LOAD**	**F. JON**
Crunch/Solo	5,600	
G. REAR COCKPIT	**H. No Fuel Weight**	**I. WEATHER**
Caddy/Hula	9916	SKC clm 24 deg
J. TO TIME / SORTIE TIME	**K. CONFIGURATION / LOADING**	**L. SURFACE CONDITIONS**
1225/1.1	001	2237' PA Alt: 30.00
M. CHASE ACFT / SERIAL NO	**N. CHASE CREW**	**O. CHASE TO TIME / SORTIE TIME**
N/A	N/A	N/A

4. PURPOSE OF FLIGHT / TEST POINTS

RSET Check out

5. RESULTS OF TESTS *(Continue on reverse if needed)*

Able to check RADAR altimeter on ground, showed approximately 5 ft. Should work up to 2500 ft. Recommend adding systems check to ground block card.
Rest of taxi/takeoff was uneventful

Crunch recommended having more rigid checklist steps…

Worked Kohn to Cuddeback which was not bad, did require some extra turning. Should be fine working cords/ black mtn.

Some issues getting the FTE console and laptop set up, but after discussion with control (Jay/George) we were able to execute as planned.

Conducted manual activations of each path at 15k, with no issues.
Conducted flight against virtual terrain also with no major issues.

Then went to 8k and was able to fly all manual activation points with no issue.

Started experiancing aileron pressure differential VSS trips during handback. Adjusting ailerons gains which helped some, but then led to elevator pressure differential trips. Those trips occurred at path activation. Gains seemed to work everywhere else, troublehooting required to understand what these trips are. Records 21-25
All trips were seen at 8k, IC#1, also the airplance was experiencing moderate turbulence.

GUI had no major issues once laptop IP issue was fixed.

6. RECOMMENDATIONS

Lockdown RSET rate limting and press to data collection. Also recommend to complete low level fam on next sortie.

COMPLETED BY	SIGNATURE	DATE
Capt Carl Gotwald	e-signed //cag//	5 Sep 18

DAILY/INITIAL FLIGHT TEST REPORT

1. AIRCRAFT TYPE	2. SERIAL NUMBER
LJ-25	N203VS

3. CONDITIONS RELATIVE TO TEST

A. PROJECT / MISSION NO	B. FLIGHT NO / DATA POINT	C. DATE
HAVE MEDUSA	2	7 Sep 18
D. FRONT COCKPIT	**E. FUEL LOAD**	**F. JON**
Crunch/COBE	5,600	998TMP0004
G. REAR COCKPIT	**H. No Fuel Weight**	**I. WEATHER**
HEX/Hula	9916	SKC clm 18°C
J. TO TIME / SORTIE TIME	**K. CONFIGURATION / LOADING**	**L. SURFACE CONDITIONS**
0733/1.9	002	2200' PA Alt: 30.04
M. CHASE ACFT / SERIAL NO	**N. CHASE CREW**	**O. CHASE TO TIME / SORTIE TIME**
N/A	N/A	N/A

4. PURPOSE OF FLIGHT / TEST POINTS

RSET Validation flight and low level fam to satisfy safety package for 500' AGL data points.

5. RESULTS OF TESTS *(Continue on reverse if needed)*

Implemented new RSET ground checkout using mode 802 on CSS (ground sim w/o hydro). Initially failed the test until surface servos were turned off. Recommend adding this step (and reactivation of switches) to next ground block checklist.

NSTR through climbout/system checks. Left seat instruments showed 3kts slower and 100ft higher than right seat instruments.

Worked Cords road which was satisfactory. This area did require some planning regarding which maneuver to fly next especially for virtual terrain activations. Planned mission frequency did not work for Sport which required some radio dancing when we needed to call back to CALSPAN DE.

Conducted manual activations of each path at 15k, with no issues.
Conducted virtual activations at 15k. IC 1&2 performed as expected. Following IC #2, MATLAB froze which required calling back to control for reset instructions. Following this reset, RSET would not activate against virtual terrain. It was determined that initial parameters in MATLAB (latitude, longitude, altitude) were populating incorrectly. Following these corrections, virtual activations occurred as expected, but RSET would not "handback" control following the handback maneuver for the remainder of the flight.

Manual activations at 8k' were then performed. Initial path 3 at 270kts had VSS trip due to elevator pressure differential. Rate limit adjusted from 50 to 35 with no further issues. Paths ¾ at 8k' and 270kts showed approximately 5-10° of gamma hunting in the climb. Due to time constraints, paths 1/5 were not tested and we dropped down to perform low level fam near Harpers lake area to include 60° banked turns.

6. RECOMMENDATIONS

Lockdown RSET to learjet wind model and press to data collection. Also recommend to complete low level manual activations on next sortie.

COMPLETED BY	SIGNATURE	DATE
Capt Mark Hammond	e-signed //mah//	10 Sep 18

TPS Form 5314 NOV 86 NOT REALLY AN OFFICIAL FORM, BUT THIS IS WHAT WILL BE USED AT TPS.

DAILY/INITIAL FLIGHT TEST REPORT

1. AIRCRAFT TYPE	2. SERIAL NUMBER
LJ-25	N203VS

3. CONDITIONS RELATIVE TO TEST

A. PROJECT / MISSION NO	B. FLIGHT NO / DATA POINT	C. DATE
HAVE MEDUSA	3	10 Sep 18
D. FRONT COCKPIT	**E. FUEL LOAD**	**F. JON**
Crunch/Smoked	5,600	998TMP0004
G. REAR COCKPIT	**H. No Fuel Weight**	**I. WEATHER**
Caddy/Hula	9916	Winds 220/11, SKC, >5500ft
J. TO TIME / SORTIE TIME	**K. CONFIGURATION / LOADING**	**L. SURFACE CONDITIONS**
1104L/1.0	002	2339' PA Alt: 29.89
M. CHASE ACFT / SERIAL NO	**N. CHASE CREW**	**O. CHASE TO TIME / SORTIE TIME**
N/A	N/A	N/A

4. PURPOSE OF FLIGHT / TEST POINTS

Highest priority points were the manual activations with varied entry conditions starting at 15k ft and working down to 500 ft AGL. Lowest priority points were the different refresh rates for virtual terrain activations.

5. RESULTS OF TESTS *(Continue on reverse if needed)*

NSTR through climbout/system checks. Left seat instruments showed 6kts faster and 40ft higher than right seat instruments. Worked Cords road in the block 7-20k ft.

Manual activations of all five paths were accomplished from the starting conditions of 270 KIAS, level flight, and 45° left bank. Power was routinely set between 94-96% rpm within 3 seconds of manual activations. The majority of the escape maneuvers appeared to be flown as the team expected. The first time we activated path 4, the aircraft rolled right and buried the nose below the horizon. EP and SP intervention was required to disconnect the system and recover to level flight. This appeared to be an anomaly as subsequent activations of path 4 performed in the correct sense (climbing right turns). One VSS trip (aileron pressure differential) occurred during these activations.

In general, the nose of the aircraft "hunted" longitudinally between ~13-15° flight path angle (FPA) during the escape maneuvers. The RSET would not "handback" control following the handback maneuver for the majority of the flight and the EP had to paddle the system off to take control.

Manual activation of path 3 was accomplished from the starting condition of 270 KIAS, wings level, 5° FPA and resulted in a VSS trip (aileron pressure differential). The TC paused testing and investigated the output parameter list to troubleshoot the recurring issue. The TC discovered that the elevator (h_stab) deflection was being fed in to the ailerons within the OFP. We called back to control and discussed with the Calspan DE a way forward. It was determined the OFP was incorrect and the mix-up was due to a copy/paste error in the code. The TC stopped test and the pilots proceeded to spiral down to 500 ft AGL over Harper's Lake to accomplish low-level fam for the EP. The EP built his site picture and cross check down at 500 ft AGL and then accomplished left and right 60 ° AOB turns for familiarity.

RTB was routine.

6. RECOMMENDATIONS

Analyze flight data for the path 4 activation that descended. Troubleshoot gamma hunting during activations. Fix OFP issues, perform ground check-out, and lock down the code for the remainder of the flight test window.

COMPLETED BY	SIGNATURE	DATE
Capt Mike Bakun	e-signed //mab//	11 Sep 18

DAILY/INITIAL FLIGHT TEST REPORT

1. AIRCRAFT TYPE	2. SERIAL NUMBER
LJ-25	N203VS

3. CONDITIONS RELATIVE TO TEST

A. PROJECT / MISSION NO	B. FLIGHT NO / DATA POINT	C. DATE
HAVE MEDUSA	4	12 Sep 18
D. FRONT COCKPIT	**E. FUEL LOAD**	**F. JON**
Hineline/Hammond	5,600	998TMP0004
G. REAR COCKPIT	**H. No Fuel Weight**	**I. WEATHER**
Gahan	9916	SKC 210/8 17°C
J. TO TIME / SORTIE TIME	**K. CONFIGURATION / LOADING**	**L. SURFACE CONDITIONS**
0749/2.0	003	2200' PA Alt: 30.04
M. CHASE ACFT / SERIAL NO	**N. CHASE CREW**	**O. CHASE TO TIME / SORTIE TIME**
N/A	N/A	N/A

4. PURPOSE OF FLIGHT / TEST POINTS

RSET Validation flight with updated configuration.
MANUAL ACTIVATIONS – 15K' PA
VIRTUAL TERRAIN ACTIVATIONS – 15K' PA
MANUAL ACTIVATIONS – 8K' PA
VIRTUAL TERRAIN ACTIVATIONS – 8K' PA (priority 2)
MANUAL ACTIVATIONS 500 AGL

5. RESULTS OF TESTS *(Continue on reverse if needed)*

NSTR for ground Ops through climbout. Left seat instruments showed 3kts slower and 100ft higher than right seat instruments.

Manual Activations (15k' PA)-Initial climbing activations had a Gamma command for 20° nose high. This resulted in airspeed dropping below 200kts (point termination) before wings level. Gamma command was reduced to 15° resulting in min speed of 203kts. Final command was set at 12° with new min airspeed of 210kts. Test proceeded with new Gamma command set.

Virtual Activations (15k' PA)-Aircraft maneuvered as predicted in the sim with no Gamma hunting as experienced in prior RSET config. Did experience VSS trips due to under G on handback theorized to be a result of multiple paths rapidly changing to handback conditions. These trips shouldn't affect testing as it stands. Also noted that winds displayed by the aircraft during dynamic maneuvering were higher than when flying straight and level.

Manual Activations (8k' PA)-All paths were flown with NSTR.

Virtual Activations (8k' PA)-Accomplished 220 kts all 3 IC's at max refresh rate. NSTR.

Manual Activations (500' AGL)-Points were flown towards top of databand to increase safety margin. All paths showed at least a 2000' climb with high engine performance capability. For path #5 activation at 220kts, the aircraft accelerated out to 270kts and tripped VSS for elevator pressure differential at handback. Only point not accomplished was path 1 at 270kts due to fuel limitations.

NSTR for RTB

6. RECOMMENDATIONS

Press with test. No further RSET config changes needed.

COMPLETED BY	SIGNATURE	DATE
Capt Mark Hammond	e-signed //mah//	12 Sep 18

DAILY/INITIAL FLIGHT TEST REPORT

1. AIRCRAFT TYPE	2. SERIAL NUMBER
LJ-25	N203VS

3. CONDITIONS RELATIVE TO TEST

A. PROJECT / MISSION NO	B. FLIGHT NO / DATA POINT	C. DATE
HAVE MEDUSA	5	13 Sep 18
D. FRONT COCKPIT	**E. FUEL LOAD**	**F. JON**
Hineline/Bakun	5,600	998TMP0004
G. REAR COCKPIT	**H. No Fuel Weight**	**I. WEATHER**
Mak/Carpenter	9916	SKC 190/4 17°C
J. TO TIME / SORTIE TIME	**K. CONFIGURATION / LOADING**	**L. SURFACE CONDITIONS**
0758/1.9	003	2320' PA Alt: 29.93
M. CHASE ACFT / SERIAL NO	**N. CHASE CREW**	**O. CHASE TO TIME / SORTIE TIME**
N/A	N/A	N/A

4. PURPOSE OF FLIGHT / TEST POINTS

Manual Activations – 15K' PA, 270 KIAS, varied entry conditions (15 pts)
Virtual Activations – 15K' PA, 220/270 KIAS, 6.25Hz (6 pts)
Manual Activations – 8K' PA, 270 KIAS, varied entry conditions (15 pts)
Virtual Activations – 8K' PA, 220/270 KIAS, 12.5Hz (3 pts)
Virtual Activations – 8K' PA, 220/270 KIAS, 6.25Hz (6 pts)
Manual Activations – 500' AGL, 270 KIAS, SLUG (1 pt)
Manual Activations – 500' AGL, 270 KIAS, varied entry conditions (10 pts)

5. RESULTS OF TESTS *(Continue on reverse if needed)*

NSTR for ground Ops through climbout. Left seat instruments showed 4kts faster and 100ft higher than right seat instruments. We read winds from straight and level flight in the databand before each test point so the TC could manual enter the values into the laptop. The system activated escape maneuvers in the correct sense the crew was expecting for the most part. A few of the virtual activations resulted in different escape paths than we expected from the sim results.

Manual Activations (15k' PA) – VSS trip (under g) on path 1 activation from left 45° turn entry condition.

Virtual Activations (15k' PA) – VSS trip (under g) on test point 5 during the handback.

Manual Activations (8k' PA) – Immediate VSS trip (elevator pressure delta) on path 3 activation from left 45° turn entry condition. VSS trip (under g) on path 1 activation from left 45° turn entry condition. VSS trip (under g) on path 5 activation from -5° FPA entry condition.

Virtual Activations (8k' PA) – 12.5Hz refresh rate VSS trip (under g) on test points 1, 2, and 3 during the handback. 6.25Hz refresh rate at 220 KIAS VSS trip (under g) on test point 1 during the handback. Did not complete test points 2-6 with 6.25Hz refresh rate due to fuel limitations.

Manual Activations (500' AGL) – Not accomplished due to fuel limitations.

NSTR for RTB

6. RECOMMENDATIONS

Acquire data.

COMPLETED BY	SIGNATURE	DATE
Capt Mike Bakun	e-signed //mab//	13 Sep 18

TPS Form 5314 NOV 86 NOT REALLY AN OFFICIAL FORM, BUT THIS IS WHAT WILL BE USED AT TPS.

DAILY/INITIAL FLIGHT TEST REPORT

1. AIRCRAFT TYPE	2. SERIAL NUMBER
LJ-25	N203VS

3. CONDITIONS RELATIVE TO TEST

A. PROJECT / MISSION NO	B. FLIGHT NO / DATA POINT	C. DATE
HAVE MEDUSA	6	13 Sep 18
D. FRONT COCKPIT	**E. FUEL LOAD**	**F. JON**
Crunch/Solo	5,600	
G. REAR COCKPIT	**H. No Fuel Weight**	**I. WEATHER**
Suplisson/Hex	9916	SKC clm 27 deg
J. TO TIME / SORTIE TIME	**K. CONFIGURATION / LOADING**	**L. SURFACE CONDITIONS**
1202/2.1	001	2283' PA Alt: 29.95
M. CHASE ACFT / SERIAL NO	**N. CHASE CREW**	**O. CHASE TO TIME / SORTIE TIME**
N/A	N/A	N/A

4. PURPOSE OF FLIGHT / TEST POINTS

Manual/Virtual activations at 15k and 8k. Manual activations at 220 KIAS, virtual activations at 1.5625 Hz.

5. RESULTS OF TESTS *(Continue on reverse if needed)*

Taxi/takeoff was uneventful

All points were completed successfully. This sortie included entering in winds before each test point.

5 VSS trips, all during handback on virtual activations at 270 KIAS, for low g as seen previously.

Some turblence seen near the end of the sortie on the 8k points.

A number of very slow handbacks which required the EP to terminate for airspace.

One point still showed some gamma hunting, but it was pretty benign.

6. RECOMMENDATIONS

Continue testing, finish manual/virtual activations and start nuisance testing.

COMPLETED BY	SIGNATURE	DATE
Capt Carl Gotwald	e-signed //cag//	13 Sep 18

TPS Form 5314 NOV 86 NOT REALLY AN OFFICIAL FORM, BUT THIS IS WHAT WILL BE USED AT TPS.

DAILY/INITIAL FLIGHT TEST REPORT

1. AIRCRAFT TYPE	2. SERIAL NUMBER
LJ-25	N203VS

3. CONDITIONS RELATIVE TO TEST

A. PROJECT / MISSION NO	B. FLIGHT NO / DATA POINT	C. DATE
HAVE MEDUSA	7	14 Sep 18
D. FRONT COCKPIT	**E. FUEL LOAD**	**F. JON**
Hineline/Hammond	5,600	
G. REAR COCKPIT	**H. No Fuel Weight**	**I. WEATHER**
Mak	9916	SKC clm 16 deg
J. TO TIME / SORTIE TIME	**K. CONFIGURATION / LOADING**	**L. SURFACE CONDITIONS**
0946/1.7	003	2292' PA Alt: 29.94
M. CHASE ACFT / SERIAL NO	**N. CHASE CREW**	**O. CHASE TO TIME / SORTIE TIME**
N/A	N/A	N/A

4. PURPOSE OF FLIGHT / TEST POINTS

Virtual activations at 8k for 6.25 Hz. Manual/virtual (12.5Hz) activations at 500' AGL, all airspeeds and attitudes. Lateral offset to actual terrain 500'AGL.

5. RESULTS OF TESTS *(Continue on reverse if needed)*

Taxi/takeoff was uneventful

All points were completed successfully. This sortie included entering in winds before each test point. Wind interface inputs were changed after the previous sortie and went unnoticed for the first 3 virtual activations. This led to unexpected path activation for each IC. After the change was found, all points were reflown successfully.

5 VSS trips, all during handback on virtual activations at 270 KIAS, for low g as seen previously.

A number of very slow handbacks which required the EP to terminate for airspace.

The terrain chosen for the lateral offset was the southern ridgeline between Koen and Cuddeback lakes. This terrain was moderately sloping which limited the ability to "walk in" lateral distance for evaluation. Recommend flying the northern portion of the ridge which is steeper and should give more opportunity to decrease offset proportionally. For all points flown near the ridgeline, EP would not have felt comfortable executing a level 60° banked turn. In all cases the RSET never determined path closure which shows promise regarding lack of nuisance alerts.

6. RECOMMENDATIONS

Refly lateral offset on north side of ridgeline.

COMPLETED BY	SIGNATURE	DATE
Capt Mark Hammond	e-signed //mah//	17 Sep 18

TPS Form 5314 NOV 86 NOT REALLY AN OFFICIAL FORM, BUT THIS IS WHAT WILL BE USED AT TPS.

DAILY/INITIAL FLIGHT TEST REPORT

1. AIRCRAFT TYPE	2. SERIAL NUMBER
LJ-25	N203VS

3. CONDITIONS RELATIVE TO TEST

A. PROJECT / MISSION NO	B. FLIGHT NO / DATA POINT	C. DATE
HAVE MEDUSA	8	14 Sep 18
D. FRONT COCKPIT	**E. FUEL LOAD**	**F. JON**
Hineline/Gotwald	5,600	998TMP00
G. REAR COCKPIT	**H. No Fuel Weight**	**I. WEATHER**
Kolesar/Gahan	9916	>5500 Winds 070/04 Temp 28
J. TO TIME / SORTIE TIME	**K. CONFIGURATION / LOADING**	**L. SURFACE CONDITIONS**
1231/1.8	001	2320' PA Alt: 29.91
M. CHASE ACFT / SERIAL NO	**N. CHASE CREW**	**O. CHASE TO TIME / SORTIE TIME**
N/A	N/A	N/A

4. PURPOSE OF FLIGHT / TEST POINTS

Flew manual activations and virtual activations at 500' AGL. Also flew lateral offset to actual terrain at 500' AGL north of Koehn Lake.

5. RESULTS OF TESTS *(Continue on reverse if needed)*

Taxi/takeoff was uneventful.

Manual activation were flown at 500' AGL and 200 KIAS. One g trip was seen during a path 1 handback.

Virtual activations were flown at 500' AGL and both 6.25 Hz and 1.5625 Hz. G trips were seen during every handback at 6.25 Hz. One g trip was seen at 270 KIAS.

Lateral offsets were flown, and no nuisance was noted. A path 1 closure was seen by flying very close to terrain, well inside both pilots comfort level. Pilots also commented that there were times that they did not think a path 1/5 could be executed but the system did.

6. RECOMMENDATIONS

Finish low level nuisance testing.

COMPLETED BY	SIGNATURE	DATE
Capt Carl Gotwald	e-signed //cag//	14 Sep 18

TPS Form 5314 NOV 86 NOT REALLY AN OFFICIAL FORM, BUT THIS IS WHAT WILL BE USED AT TPS.

DAILY/INITIAL FLIGHT TEST REPORT

1. AIRCRAFT TYPE	2. SERIAL NUMBER
LJ-25	N203VS

3. CONDITIONS RELATIVE TO TEST

A. PROJECT / MISSION NO	B. FLIGHT NO / DATA POINT	C. DATE
HAVE MEDUSA	9	17 Sep 18
D. FRONT COCKPIT	**E. FUEL LOAD**	**F. JON**
Hineline/Bakun	5,600	998TMP00
G. REAR COCKPIT	**H. No Fuel Weight**	**I. WEATHER**
Mak/Gotwald	9916	>5500 Winds 210/8 Temp 17C
J. TO TIME / SORTIE TIME	**K. CONFIGURATION / LOADING**	**L. SURFACE CONDITIONS**
0946/1.7	003	2283' PA Alt: 29.95
M. CHASE ACFT / SERIAL NO	**N. CHASE CREW**	**O. CHASE TO TIME / SORTIE TIME**
N/A	N/A	N/A

4. PURPOSE OF FLIGHT / TEST POINTS

Lateral offset to actual terrain 500'AGL south of Koehn to Cudde airspace. Operational low-level nuisance eval on Sidewinder from points C-E for both pilots. Manual activations at 220/270 KIAS and 500' AGL.

5. RESULTS OF TESTS *(Continue on reverse if needed)*

Taxi/takeoff was uneventful.

Lateral offset to terrain 500'AGL: The terrain chosen for the lateral offset was the southern ridgeline between Koehn and Cuddeback lakes. We completed several 360 degree turns at 60 degrees AOB well above the terrain using ground references for lateral offset estimation. Once comfortable with the turn radius, we stepped down to 500' AGL at the offset where I felt comfortable performing a level 60 degree turn. Path 1 remained open in agreement with our expectations. I decreased lateral spacing to the terrain until I felt I could no longer perform a 60 degree turn without striking terrain. Path 1 again remained open. I was able to get close enough to terrain to see Path 1 close for an extended period of time and Path 2 close intermittently.

Operational low-level nuisance eval: Both pilots flew the Sidewinder from points C-E at 500' AGL. Winds were light and no turbulence was noted. There were a few test points between points D-E where the system indicated we could perform a level right turn and avoid terrain; however, the entire crew unanimously disagreed. Recommend thorough analysis of these test points to determine the truth.

Manual activations at 220/270 KIAS and 500' AGL: I hopped back in the seat for these test points. We accomplished all five manual activations from straight and level at 220 KIAS and a path 3 activation from 270 KIAS. The paths activated in the sense that we expected. Engine performance was strong down low with slightly cooler temps. Path 5 activation accelerated to 292 KIAS and achieved 2.4g in the pull. NSTR for the remaining test points and RTB.

6. RECOMMENDATIONS

Press

COMPLETED BY	SIGNATURE	DATE
Capt Mike Bakun	e-signed //mab//	17 Sep 18

DAILY/INITIAL FLIGHT TEST REPORT

1. AIRCRAFT TYPE	2. SERIAL NUMBER
LJ-25	N203VS

3. CONDITIONS RELATIVE TO TEST

A. PROJECT / MISSION NO	B. FLIGHT NO / DATA POINT	C. DATE
HAVE MEDUSA	10	18 Sep 18
D. FRONT COCKPIT	**E. FUEL LOAD**	**F. JON**
Hineline/Hammond/Abel	5,600	998TMP00
G. REAR COCKPIT	**H. No Fuel Weight**	**I. WEATHER**
Kolesar	9916	>5500 clm Temp 12C
J. TO TIME / SORTIE TIME	**K. CONFIGURATION / LOADING**	**L. SURFACE CONDITIONS**
0804/1.9	003	2329' PA Alt: 29.90
M. CHASE ACFT / SERIAL NO	**N. CHASE CREW**	**O. CHASE TO TIME / SORTIE TIME**
N/A	N/A	N/A

4. PURPOSE OF FLIGHT / TEST POINTS

Lateral offset to actual terrain 500'AGL south of Koehn to Cudde airspace. Operational low-level nuisance eval on Sidewinder from points C-E for both pilots. Manual activations at 270 KIAS and 500' AGL and virtual at 270KIAS.

5. RESULTS OF TESTS *(Continue on reverse if needed)*

Taxi/takeoff was uneventful.

Lateral offset to terrain 500'AGL: The terrain chosen for the lateral offset was the southern ridgeline between Koehn and Cuddeback lakes to mimic previous sorties with other project pilots. We completed several 360 degree turns at 60 degrees AOB well above the terrain using ground references for lateral offset estimation. Once comfortable with the turn radius, we stepped down to 500' AGL at the offset where I felt comfortable performing a level 60 degree turn. Path 1 remained open in agreement with our expectations. I decreased lateral spacing to the terrain until I felt I could no longer perform a 60 degree turn without striking terrain. At my comfort level, the RSET never indicated path closure for an extended period of time

Operational low-level nuisance eval: Both pilots flew the Sidewinder from points C-E at 500' AGL. Winds were light and no turbulence was noted. There were a few test points between points D-E where the system indicated we could perform a level right turn and avoid terrain; however, the entire crew unanimously disagreed.

During manual/virtual activations at 500'AGL, SPORT called traffic in our vicinity that did not have approval to be there. We took some time getting eyes on them which resulted in some repeat test points lost. LtCol Abel flew all these points with no significant differences noted from previous flights. VSS tripped on both path 1 and 5 handbacks per usual.

RTB NSTR

6. RECOMMENDATIONS

Press

COMPLETED BY	SIGNATURE	DATE
Capt Mark Hammond	e-signed //mah//	18 Sep 18

TPS Form 5314 NOV 86 NOT REALLY AN OFFICIAL FORM, BUT THIS IS WHAT WILL BE USED AT TPS.

DAILY/INITIAL FLIGHT TEST REPORT

1. AIRCRAFT TYPE	2. SERIAL NUMBER
LJ-25	N203VS

3. CONDITIONS RELATIVE TO TEST

A. PROJECT / MISSION NO	B. FLIGHT NO / DATA POINT	C. DATE
HAVE MEDUSA	11	18 Sep 18
D. FRONT COCKPIT	**E. FUEL LOAD**	**F. JON**
Hineline/Bakun	5,600	998TMP0004
G. REAR COCKPIT	**H. No Fuel Weight**	**I. WEATHER**
Gahan/Suplisson	9916	SKC 200/6 17°C
J. TO TIME / SORTIE TIME	**K. CONFIGURATION / LOADING**	**L. SURFACE CONDITIONS**
1207/1.9		2320' PA Alt: 29.95
M. CHASE ACFT / SERIAL NO	**N. CHASE CREW**	**O. CHASE TO TIME / SORTIE TIME**
N/A	N/A	N/A

4. PURPOSE OF FLIGHT / TEST POINTS

Operational low-level nuisance eval on Sidewinder from points C-E for both pilots. Manual activations at both airspeeds, 5°FPA, 45° bank at 500' AGL and virtual activations at 12.5 Hz for both airspeeds.

5. RESULTS OF TESTS *(Continue on reverse if needed)*

Taxi/takeoff was uneventful.

Operational low-level nuisance eval: I flew the Sidewinder from points C-E at 500' AGL. Winds were light and no turbulence was noted. There were a few test points between points D-E where the system indicated we could perform a level right turn and avoid terrain; however, the entire crew unanimously disagreed. Only during one point along the route did path 2 momentarily close when in proximity to a small mound rising ahead of the mountain terrain. Crew agreed that this closure was appropriate.

VSS tripped on both path 1 and 5 handbacks per usual during slow speed activations.

RTB NSTR

6. RECOMMENDATIONS

Complete Report

COMPLETED BY	SIGNATURE	DATE
Capt Mike Bakun	e-signed //mab//	18 Sep 18

TPS Form 5314 NOV 86 NOT REALLY AN OFFICIAL FORM, BUT THIS IS WHAT WILL BE USED AT TPS.

Appendix C. Data Analysis Procedures

The following pages describe the data analysis procedures used in the Have MEDUSA test project in order to produce the required final data products. The primary data source for analysis was the Learjet VSS Data Acquisition System. This system sampled parameters at 200 Hz, and saved these parameters to a Microsoft Excel compatible file, which was imported into MATLAB.

The remainder of this page is intentionally blank

Objective	1 – Demonstrate the Prediction Accuracy of the RSET System
MOP	1.1 – Path Prediction Error

Required Data Parameters

Description	Name	Units	Source
Time	gps_time	Seconds	DAS
True Latitude	gps_lat	Degrees North	DAS
True Longitude	gps_lon	Degrees East	DAS
True Altitude	gps_alt	Feet	DAS
Indicated Airspeed	Vc	Knots	DAS
Flight Path Angle	gamma_cf	Degrees	DAS
Bank Angle	phi	Degrees	DAS
Heading		Degrees	DAS
Wind Speed		Knots	DAS
Wind Direction		Degrees	DAS
Predicted Latitude		Degrees North	RSET Algorithm
Predicted Longitude		Degrees East	RSET Algorithm
Predicted Altitude		Feet	RSET Algorithm

Qualitative Data Required

Description		Source
Pilot Comments		Handheld Data, noted by FTE on flight cards
Data Quality	Maneuver Quality Determination	Pilot & FTE (real time) FTE (post-flight)
	Data gathering effectiveness and procedure if data are unusable	Determine if effective real-time. If unusable or unsure, repeat test point.

	Repeats	None planned, but approved, fuel allowing.
Analysis Procedure	1. For the entire duration of the RSET commanded autopilot maneuver, latitude (φ), longitude (λ), and altitude (h) was obtained from the aircraft TSPI data (considered the truth source). Also, at the time of RSET activation, the lat, long, and altitude for each time step along the 30 second RSET predicted path was obtained. 2. Both sets of coordinates were converted into Cartesian earth-centered, earth-fixed (ECEF) coordinates (u, v, w) using the equations below. $u = (N+h)\cos\varphi\cos\lambda$ $v = (N+h)\cos\varphi\sin\lambda$ $w = (N(1-e^2)+h)\sin\varphi$ where $a = 20925646.32546\,ft$ $e^2 = 0.0066943799\ \ 9$ $N = \frac{a}{\sqrt{1-e^2\sin^2\varphi}}$ } Ellipsoid Earth model parameters 3. The distance vector (Δu, Δv, Δw) between the two paths was then calculated at each sampled time throughout the maneuver. The aircraft's data acquisition had a different sampling rate (200 Hz) than the RSET path prediction (100 Hz), so the two data sets needed to be matched up in time. $\Delta u = u_2 - u_1$ $\Delta v = v_2 - v_1$ $\Delta w = w_2 - w_1$ 4. The Path Prediction Error (PPE) was calculated at each sampled time $PPE = \sqrt{\Delta u^2 + \Delta v^2 + \Delta w^2}$ 5. The maximum PPE during the RSET commanded maneuver was identified. 6. The actual aircraft path and the RSET predicted path were plotted on the same axes in order to determine whether the direction of the error was towards terrain or away from terrain in both the vertical (climb) and horizontal (turn) directions.	

Data Products	The maximum PPE data was summarized in a table as shown below in Table A1. **Table A1 – Summary Table of Max PPE Results** For each manually activated RSET maneuver, the PPE was plotted as a function of time. Also, the aircraft's actual position and the RSET predicted path was plotted in three dimensions on the same axes in order to show a visualization of the paths. Later, wind vectors were also plotted on the same chart in order to show the effect of wind.

Flight #	Record #	Alt	A/S	Entry	Path	Wind Speed (kts)	Wind in Direction of Error?	Prediction Error (ft)	Out-climb prediction?	Tighter turn radius than prediction?	Error Away from Terrain?
#	#	ft	KIAS	#	#	kts	Yes/No	ft	Yes/No	Yes/No	Yes/No/ Inconclusive

Objective	2 – Demonstrate the impact of changing refresh rate on the RSET system's ability to calculate an achievable escape path.
MOP	2.1 – Terrain Miss Distance

Required Data Parameters

Description	Name	Units	Source
Time	gps_time	Seconds	DAS
True Latitude	gps_lat	Degrees North	DAS
True Longitude	gps_lon	Degrees East	DAS
True Altitude	gps_alt	Feet	DAS
Indicated Airspeed	Vc	Knots	DAS
DTED Point Latitude		Degrees North	DTED Matrix
DTED Point Longitude		Degrees East	DTED Matrix
DTED Point Altitude		Feet	DTED Matrix
Refresh Rate		Hertz	RSET Algorithm

Qualitative Data Required

Description		Source
Pilot Comments		Handheld Data, noted by FTE on flight cards
Data Quality	Maneuver Quality Determination	Pilot & FTE (real time) FTE (post-flight)
	Data gathering effectiveness and procedure if data are unusable	Determine if effective real-time. If unusable or unsure, repeat test point.
	Repeats	None planned, but approved, fuel allowing.
Analysis Procedure	1. For the entire run against virtual terrain, the aircraft's TSPI data (latitude, longitude, and altitude) were obtained. 2. At each time sample, the distance from the aircraft's position to the interpolated DTED elevation at the point directly below the aircraft (same latitude and longitude)	

	was calculated. This value was used to determine if the aircraft impacted the virtual terrain or not (negative or positive value). The RSS distance to the terrain was calculated by defining a plane with the three DTED posts that were closest to the aircraft. These DTED posts formed the base of a tetrahedron with the aircraft position at the apex of the tetrahedron. The smallest difference from the aircraft to terrain was calculated by calculating the height of the tetrahedron (see equations below). This was repeated for every time step during the system activation. The distances from the aircraft to each of the three closest DTED posts were defined as (a, b, c) using the same Cartesian earth-centered, earth-fixed (ECEF) coordinates (u, v, w) from MOP 1.1. The distances between each of the DTED posts were defined as (x, y, z). Then, the closest distance, h, was calculated using the following equations and defined the magnitude of the terrain miss distance. $$X = b^2 + c^2 - z^2$$ $$Y = a^2 + c^2 - y^2$$ $$Z = a^2 + b^2 - x^2$$ $$V = \frac{\sqrt{4abc - a^2X^2 - b^2Y^2 - c^2Z^2 + XYZ}}{12}$$ $$h = \frac{3V}{\frac{1}{2}(xy)}$$ 3. The minimum terrain miss distance for each run was identified.
Data Products	Summary charts of the minimum terrain miss distance for each test condition were generated. In addition, for each run against virtual terrain, the following plots were generated: 1. The aircraft's actual path and the DTED matrix plotted together in a three-dimensional chart. 2. Terrain miss distance as a function of time throughout the entire run. 3. Active RSET path, aircraft virtual altitude and virtual terrain elevation as a function of time throughout the entire run.

Objective	2 – Demonstrate the impact of changing refresh rate on RSET system ability to calculate an achievable escape path
MOP	2.2 – Forward look ahead time

Required Data Parameters

Description	Name	Units	Source
Time	gps_time	Seconds	DAS
True Latitude	gps_lat	Degrees North	DAS
True Longitude	gps_lon	Degrees East	DAS
True Altitude	gps_alt	Feet	DAS
Ground Speed	gps_Vg	Feet per Second	DAS
Indicated Airspeed	Vc	Knots	DAS
Pitch Attitude	theta	Degrees	DAS
Bank Angle	phi	Degrees	DAS
Heading		Degrees	DAS
Wind Speed		Knots	DAS
Wind Direction		Degrees	DAS
Predicted Latitude		Degrees North	RSET Algorithm
Predicted Longitude		Degrees East	RSET Algorithm
Predicted Altitude		Feet	RSET Algorithm
DTED Point Latitude		Degrees North	DTED Matrix
DTED Point Longitude		Degrees East	DTED Matrix
DTED Point Altitude		Feet	DTED Matrix
Terrain Safety Buffer		Feet	RSET Algorithm

Qualitative Data Required

Description		Source
Pilot Comments		Handheld Data, noted by FTE on flight cards
Data Quality	Maneuver Quality Determination	Pilot & FTE (real time) FTE (post-flight)
	Data gathering effectiveness and procedure if data are unusable	Determine if effective real-time. If unusable or unsure, repeat test point.
	Repeats	None planned, but approved, fuel allowing.
Analysis Procedure	1. For the entire run against virtual terrain, the aircraft's TSPI data (latitude, longitude, and altitude) was obtained. 2. The moments at which RSET triggered an escape maneuver were identified. 3. At each of these moments, the forward look-ahead time was determined by finding the time along each of the 5 path predictions at which the algorithm predicted a collision and taking the highest of the five times.	
Data Products	The forward look-ahead times were plotted in a summary chart to compare the impact of refresh rate on forward look-ahead time. The plots also included indications of whether each activation impacted terrain or not.	

Objective	3 – Observe RSET system tendency to nuisance activation.
MOP	3.1 – Path Performance

Required Data Parameters

Description	Name	Units	Source
Time	gps_time	Seconds	DAS
Indicated Airspeed	Vc	Knots	DAS
Flight Path Angle	gamma	Degrees	DAS
Bank Angle	phi	Degrees	DAS
Normal Load Factor	nz	g	DAS

Qualitative Data Required

Description		Source
Pilot Comments		Handheld Data, noted by FTE on flight cards
Data Quality	Maneuver Quality Determination	Pilot & FTE (real time) FTE (post-flight)
	Data gathering effectiveness and procedure if data are unusable	Determine if effective real-time. If unusable or unsure, repeat test point.
	Repeats	None planned, but approved, fuel allowing.
Analysis Procedure	1. For each manually activated RSET maneuver, the normal acceleration, airspeed, flight path angle, and bank angle from the aircraft VSS data were collected for the entire 30 second maneuver. 2. For each time step along the RSET maneuver, the algorithm's g limit was calculated using the equation below. $$n_{z_{limit}} = -\frac{1}{2}\left(-3\frac{V_c - 200}{270 - 200} - 1\right)$$ 3. For each time step along the RSET maneuver, the algorithm's target flight path angle was calculated using the equation below.	

	$\gamma_{command} = 12\left(\frac{V_C - 200}{270 - 200}\right)$
Data Products	Three plots were generated for each manually activated RSET maneuver: 1. Aircraft normal acceleration (n_Z), RSET g limit (n_{Zlimit}), and the VSS g limit (2.8) as a function of time. 2. Aircraft bank angle (φ) and RSET target bank angle (φ_{target}) as a function of time. 3. Aircraft flight path angle (γ) and RSET target flight path angle (γ_{target}) as a function of time.

Objective	3 – Observe RSET system tendency to nuisance activation
MOP	3.2 – Nuisance Activations

Required Data Parameters

Description	Name	Units	Source
Time	gps_time	Seconds	DAS
True Latitude	gps_lat	Degrees North	DAS
True Longitude	gps_lon	Degrees East	DAS
True Altitude	gps_alt	Feet	DAS
Indicated Airspeed	Vc	Knots	DAS
Flight Path Angle	gamma_cf	Degrees	DAS
Bank Angle	phi	Degrees	DAS
Heading		Degrees	
Wind Speed		Knots	
Wind Direction		Degrees	
Predicted Latitude		Degrees North	RSET Algorithm
Predicted Longitude		Degrees East	RSET Algorithm
Predicted Altitude		Feet	RSET Algorithm
DTED Point Latitude		Degrees North	DTED Matrix
DTED Point Longitude		Degrees East	DTED Matrix
DTED Point Altitude		Feet	DTED Matrix
Terrain Safety Buffer		Feet	RSET Algorithm

Qualitative Data Required

Description	Source

Pilot Comments		Handheld Data, noted by FTE on flight cards
Data Quality	Maneuver Quality Determination	Pilot & FTE (real time) FTE (post-flight)
	Data gathering effectiveness and procedure if data are unusable	Determine if effective real-time. If unusable or unsure, repeat test point.
	Repeats	None planned, but approved, fuel allowing.
Analysis Procedure	1. The aircraft's states and TSPI data (latitude, longitude, and altitude) and the surrounding DTED data were obtained for each run against terrain. 2. The RSET data was examined to see if the 60° banked turn TPA towards terrain was closed off (collision detected) at any point along the run. 3. The RSET data was combined with pilot comments to determine nuisance.	
Data Products	Each test run was re-constructed by plotting the position of the aircraft in three dimensions relative to the DTED matrix. The RSET predicted path of the 60° turn towards the terrain was overlaid on the plot at regular intervals along the aircraft path to show whether or not RSET predicted a path closure. Also, the pilot's comments for each run were presented to show whether or not the pilot felt that such a turn into terrain was possible.	

Objective	3 – Observe RSET system tendency to nuisance activation		
MOP	3.3 – Aircrew Comments		
Required Data Parameters			
Time	gps_time	Seconds	DAS
True Latitude	gps_lat	Degrees North	DAS
True Longitude	gps_lon	Degrees East	DAS
True Altitude	gps_alt	Feet	DAS
Indicated Airspeed	Vc	Knots	DAS
Flight Path Angle	gamma_cf	Degrees	DAS
Bank Angle	phi	Degrees	DAS
Heading		Degrees	
Wind Speed		Knots	
Wind Direction		Degrees	
Predicted Latitude		Degrees North	RSET Algorithm
Predicted Longitude		Degrees East	RSET Algorithm
Predicted Altitude		Feet	RSET Algorithm
DTED Point Latitude		Degrees North	DTED Matrix
DTED Point Longitude		Degrees East	DTED Matrix
DTED Point Altitude		Feet	DTED Matrix
Terrain Safety Buffer		Feet	RSET Algorithm
Qualitative Data Required			
Description		Source	
Pilot Comments		Handheld Data, noted by FTE on flight cards	

Data Quality	Maneuver Quality Determination	Pilot & FTE (real time) FTE (post-flight)
	Data gathering effectiveness and procedure if data are unusable	Determine if effective real-time. If unusable or unsure, repeat test point.
	Repeats	None planned, but approved, fuel allowing.
Analysis Procedure	1. The aircraft's states and TSPI data (latitude, longitude, and altitude) and the surrounding DTED data were obtained for each operationally representative low-level profile. 2. At any point during the profile when RSET predicted that an escape path activation was necessary, pilot comments were gathered along with the TSPI data to determine whether nuisance occurred.	
Data Products	Aircrew comments were summarized and presented.	

Appendix D. Test Points

The following pages present a record of the test points gathered during the 11 Have MEDUSA test sorties from 05 September 2018 to 18 September 2018.

The remainder of this page is intentionally blank

Learjet Flight #	Flight #	Record #	Point Description
2111	1	1	Manual, 15k ft, 220 KIAS, SLUF entry, Path #3
2111	1	2	Manual, 15k ft, 220 KIAS, SLUF entry, Path #2
2111	1	3	Manual, 15k ft, 220 KIAS, SLUF entry, Path #1
2111	1	4	Manual, 15k ft, 220 KIAS, SLUF entry, Path #4
2111	1	5	Manual, 15k ft, 220 KIAS, SLUF entry, Path #5
2111	1	6	Manual, 15k ft, 270 KIAS, SLUF entry, Path #3
2111	1	7	Manual, 15k ft, 270 KIAS, SLUF entry, Path #2
2111	1	8	Manual, 15k ft, 270 KIAS, SLUF entry, Path #5
2111	1	9	Manual, 15k ft, 270 KIAS, SLUF entry, Path #1
2111	1	10	Manual, 15k ft, 220 KIAS, SLUF entry, Path #3
2111	1	11	Manual, 15k ft, 220 KIAS, SLUF entry, Path #1
2111	1	12	Manual, 15k ft, 270 KIAS, SLUF entry, Path #4
2111	1	13	Virtual, 15k ft, 220 KIAS, 12.5 Hz, IC #1
2111	1	14	Virtual, 15k ft, 270 KIAS, 1.5625 Hz, IC #1
2111	1	15	Virtual, 15k ft, 270 KIAS, 1.5625 Hz, IC #1
2111	1	16	Manual, 8k ft, 270 KIAS, SLUF entry, Path #3
2111	1	17	Manual, 8k ft, 270 KIAS, SLUF entry, Path #1
2111	1	18	Manual, 8k ft, 220 KIAS, SLUF entry, Path #5
2111	1	19	Manual, 8k ft, 220 KIAS, SLUF entry, Path #4
2111	1	20	Manual, 8k ft, 220 KIAS, SLUF entry, Path #2
2111	1	21	Virtual, 8k ft, 270 KIAS, 12.5 Hz, IC #1
2111	1	22	Virtual, 8k ft, 270 KIAS, 12.5 Hz, IC #1
2111	1	23	Virtual, 8k ft, 270 KIAS, 12.5 Hz, IC #1
2111	1	24	Virtual, 8k ft, 270 KIAS, 12.5 Hz, IC #1
2111	1	25	Virtual, 8k ft, 270 KIAS, 12.5 Hz, IC #1
2113	2	1	Manual, 15k ft, 220 KIAS, SLUF entry, Path #3
2113	2	2	Manual, 15k ft, 220 KIAS, SLUF entry, Path #2
2113	2	3	Manual, 15k ft, 220 KIAS, SLUF entry, Path #1
2113	2	4	Manual, 15k ft, 270 KIAS, SLUF entry, Path #3
2113	2	5	Manual, 15k ft, 270 KIAS, SLUF entry, Path #2
2113	2	6	Manual, 15k ft, 270 KIAS, SLUF entry, Path #5
2113	2	7	Virtual, 15k ft, 220 KIAS, 12.5 Hz, IC #1
2113	2	8	Virtual, 15k ft, 220 KIAS, 12.5 Hz, IC #2
2113	2	9	Virtual, 15k ft, 220 KIAS, 12.5 Hz, IC #3
2113	2	10	Virtual, 15k ft, 220 KIAS, 12.5 Hz, IC #3
2113	2	11	Virtual, 15k ft, 220 KIAS, 12.5 Hz, IC #3
2113	2	12	Virtual, 15k ft, 220 KIAS, 12.5 Hz, IC #3
2113	2	13	Virtual, 15k ft, 220 KIAS, 12.5 Hz, IC #3
2113	2	14	Virtual, 15k ft, 220 KIAS, 12.5 Hz, IC #3
2113	2	15	Virtual, 15k ft, 220 KIAS, 12.5 Hz, IC #3
2113	2	16	Virtual, 15k ft, 220 KIAS, 12.5 Hz, IC #3

Learjet Flight #	Flight #	Record #	Point Description
2113	2	17	Virtual, 15k ft, 220 KIAS, 12.5 Hz, IC #3
2113	2	18	Virtual, 15k ft, 270 KIAS, 12.5 Hz, IC #1
2113	2	19	N/A
2113	2	20	Virtual, 15k ft, 270 KIAS, 12.5 Hz, IC #1
2113	2	21	Virtual, 15k ft, 270 KIAS, 12.5 Hz, IC #2
2113	2	22	Virtual, 15k ft, 270 KIAS, 12.5 Hz, IC #3
2113	2	23	Manual, 8k ft, 220 KIAS, SLUF entry, Path #3
2113	2	24	Manual, 8k ft, 220 KIAS, SLUF entry, Path #5
2113	2	25	Manual, 8k ft, 220 KIAS, SLUF entry, Path #4
2113	2	26	Manual, 8k ft, 270 KIAS, SLUF entry, Path #3
2113	2	27	Manual, 8k ft, 270 KIAS, SLUF entry, Path #3
2113	2	28	Manual, 8k ft, 270 KIAS, SLUF entry, Path #4
2113	2	29	Low Level Fam
2113	2	30	Low Level Fam
2113	2	31	Low Level Fam
2114	3	1	Manual, 15k ft, 270 KIAS, φ = 45° entry, Path #3
2114	3	2	Manual, 15k ft, 270 KIAS, φ = 45° entry, Path #2
2114	3	3,4,6,7	Manual, 15k ft, 270 KIAS, φ = 45° entry, Path #4
2114	3	8	Manual, 15k ft, 270 KIAS, φ = 45° entry, Path #1
2114	3	9	Manual, 15k ft, 270 KIAS, φ = 45° entry, Path #5
2114	3	10	Manual, 15k ft, 270 KIAS, γ = 5° entry, Path #3
2115	4	1	N/A
2115	4	2	Manual, 15k ft, 220 KIAS, SLUF entry, Path #3
2115	4	3	Manual, 15k ft, 220 KIAS, SLUF entry, Path #2
2115	4	4	Manual, 15k ft, 220 KIAS, SLUF entry, Path #4
2115	4	5	Manual, 15k ft, 220 KIAS, SLUF entry, Path #1
2115	4	6	Manual, 15k ft, 220 KIAS, SLUF entry, Path #5
2115	4	7	Manual, 15k ft, 270 KIAS, SLUF entry, Path #3
2115	4	8	Manual, 15k ft, 270 KIAS, SLUF entry, Path #3
2115	4	9	Manual, 15k ft, 270 KIAS, SLUF entry, Path #3
2115	4	10	Manual, 15k ft, 270 KIAS, SLUF entry, Path #4
2115	4	11	Manual, 15k ft, 270 KIAS, SLUF entry, Path #2
2115	4	12	Manual, 15k ft, 270 KIAS, SLUF entry, Path #5
2115	4	13	Manual, 15k ft, 270 KIAS, SLUF entry, Path #1
2115	4	14	Virtual, 15k ft, 220 KIAS, 12.5 Hz, IC #1
2115	4	15	Virtual, 15k ft, 220 KIAS, 12.5 Hz, IC #2
2115	4	16	Virtual, 15k ft, 220 KIAS, 12.5 Hz, IC #3
2115	4	17	Virtual, 15k ft, 270 KIAS, 12.5 Hz, IC #1
2115	4	18	Virtual, 15k ft, 270 KIAS, 12.5 Hz, IC #2
2115	4	19	Virtual, 15k ft, 270 KIAS, 12.5 Hz, IC #3
2115	4	20	Manual, 8k ft, 220 KIAS, SLUF entry, Path #3

Learjet Flight #	Flight #	Record #	Point Description
2115	4	21	Manual, 8k ft, 220 KIAS, SLUF entry, Path #4
2115	4	22	Manual, 8k ft, 220 KIAS, SLUF entry, Path #2
2115	4	23	Manual, 8k ft, 220 KIAS, SLUF entry, Path #5
2115	4	24	Manual, 8k ft, 220 KIAS, SLUF entry, Path #1
2115	4	25	Manual, 8k ft, 270 KIAS, SLUF entry, Path #3
2115	4	26	N/A
2115	4	27	Manual, 8k ft, 270 KIAS, SLUF entry, Path #2
2115	4	28	Manual, 8k ft, 270 KIAS, SLUF entry, Path #4
2115	4	29	Manual, 8k ft, 270 KIAS, SLUF entry, Path #1
2115	4	30	Manual, 8k ft, 270 KIAS, SLUF entry, Path #5
2115	4	31	Virtual, 8k ft, 220 KIAS, 12.5 Hz, IC #1
2115	4	32	Virtual, 8k ft, 220 KIAS, 12.5 Hz, IC #2
2115	4	33	Virtual, 8k ft, 220 KIAS, 12.5 Hz, IC #3
2115	4	34	Manual, 500 ft, 220 KIAS, SLUF entry, Path #3
2115	4	35	Manual, 500 ft, 220 KIAS, SLUF entry, Path #2
2115	4	36	Manual, 500 ft, 220 KIAS, SLUF entry, Path #4
2115	4	37	Manual, 500 ft, 220 KIAS, SLUF entry, Path #1
2115	4	38	Manual, 500 ft, 220 KIAS, SLUF entry, Path #5
2115	4	39	Manual, 500 ft, 270 KIAS, SLUF entry, Path #3
2115	4	40	Manual, 500 ft, 270 KIAS, SLUF entry, Path #2
2115	4	41	Manual, 500 ft, 270 KIAS, SLUF entry, Path #4
2115	4	42	Manual, 500 ft, 270 KIAS, SLUF entry, Path #5
2116	5	1	Manual, 15K ft, 270 KIAS, 45^{o} entry, Path #3
2116	5	2	Manual, 15K ft, 270 KIAS, 45^{o} entry, Path #2
2116	5	3	Manual, 15K ft, 270 KIAS, 45^{o} entry, Path #4
2116	5	4	Manual, 15K ft, 270 KIAS, 45^{o} entry, Path #1
2116	5	5	Manual, 15K ft, 270 KIAS, 45^{o} entry, Path #5
2116	5	6	Manual, 15K ft, 270 KIAS, 5^{o} entry, Path #3
2116	5	7	Manual, 15K ft, 270 KIAS, 5^{o} entry, Path #2
2116	5	8	Manual, 15K ft, 270 KIAS, 5^{o} entry, Path #4
2116	5	9	Manual, 15K ft, 270 KIAS, 5^{o} entry, Path #1
2116	5	10	Manual, 15K ft, 270 KIAS, 5^{o} entry, Path #5
2116	5	11	Manual, 15K ft, 270 KIAS, -5^{o} entry, Path #3
2116	5	12	Manual, 15K ft, 270 KIAS, -5^{o} entry, Path #2
2116	5	13	Manual, 15K ft, 270 KIAS, -5^{o} entry, Path #4
2116	5	14	Manual, 15K ft, 270 KIAS, -5^{o} entry, Path #1
2116	5	15	Manual, 15K ft, 270 KIAS, -5^{o} entry, Path #5
2116	5	16	Virtual, 15k ft, 270 KIAS, 6.25 Hz, IC #1
2116	5	17	Virtual, 15k ft, 270 KIAS, 6.25 Hz, IC #2
2116	5	18	Virtual, 15k ft, 270 KIAS, 6.25 Hz, IC #3
2116	5	19	Virtual, 15k ft, 220 KIAS, 6.25 Hz, IC #1

Learjet Flight #	Flight #	Record #	Point Description
2116	5	20	Virtual, 15k ft, 220 KIAS, 6.25 Hz, IC #2
2116	5	21	Virtual, 15k ft, 220 KIAS, 6.25 Hz, IC #3
2116	5	22&23	Manual, 8K ft, 270 KIAS, 45^{o} entry, Path #3
2116	5	24	Manual, 8K ft, 270 KIAS, 45^{o} entry, Path #2
2116	5	25	Manual, 8K ft, 270 KIAS, 45^{o} entry, Path #4
2116	5	26	Manual, 8K ft, 270 KIAS, 45^{o} entry, Path #1
2116	5	27	Manual, 8K ft, 270 KIAS, 45^{o} entry, Path #5
2116	5	28	Manual, 8K ft, 270 KIAS, 5^{o} entry, Path #3
2116	5	29	Manual, 8K ft, 270 KIAS, 5^{o} entry, Path #2
2116	5	30	Manual, 8K ft, 270 KIAS, 5^{o} entry, Path #4
2116	5	31	Manual, 8K ft, 270 KIAS, 5^{o} entry, Path #1
2116	5	32	Manual, 8K ft, 270 KIAS, 5^{o} entry, Path #5
2116	5	33	Manual, 8K ft, 270 KIAS, -5^{o} entry, Path #3
2116	5	34	Manual, 8K ft, 270 KIAS, -5^{o} entry, Path #2
2116	5	35	Manual, 8K ft, 270 KIAS, -5^{o} entry, Path #4
2116	5	36	Manual, 8K ft, 270 KIAS, -5^{o} entry, Path #1
2116	5	37	Manual, 8K ft, 270 KIAS, -5^{o} entry, Path #5
2116	5	38	Virtual, 8k ft, 270 KIAS, 12.5 Hz, IC #1
2116	5	39	Virtual, 8k ft, 270 KIAS, 12.5 Hz, IC #2
2116	5	40	Virtual, 8k ft, 270 KIAS, 12.5 Hz, IC #3
2116	5	41	Virtual, 8k ft, 270 KIAS, 6.25 Hz, IC #1
2117	6	1	Manual, 15k ft, 220 KIAS, 45° entry, Path #3
2117	6	2	Manual, 15k ft, 220 KIAS, 45° entry, Path #2
2117	6	3	Manual, 15k ft, 220 KIAS, 45° entry, Path #4
2117	6	4	Manual, 15k ft, 220 KIAS, 45° entry, Path #1
2117	6	5	Manual, 15k ft, 220 KIAS, 45° entry, Path #5
2117	6	6	Manual, 15K ft, 220 KIAS, 5^{o} entry, Path #3
2117	6	7	Manual, 15K ft, 220 KIAS, 5^{o} entry, Path #2
2117	6	8	Manual, 15K ft, 220 KIAS, 5^{o} entry, Path #4
2117	6	9	Manual, 15K ft, 220 KIAS, 5^{o} entry, Path #1
2117	6	10	Manual, 15K ft, 220 KIAS, 5^{o} entry, Path #5
2117	6	11	Manual, 15K ft, 220 KIAS, -5^{o} entry, Path #3
2117	6	12	Manual, 15K ft, 220 KIAS, -5^{o} entry, Path #2
2117	6	13	Manual, 15K ft, 220 KIAS, -5^{o} entry, Path #4
2117	6	14	Manual, 15K ft, 220 KIAS, -5^{o} entry, Path #1
2117	6	15	Manual, 15K ft, 220 KIAS, -5^{o} entry, Path #5
2117	6	16	Virtual, 15k ft, 220 KIAS, 1.5625 Hz, IC #1
2117	6	17	Virtual, 15k ft, 220 KIAS, 1.5625 Hz, IC #2
2117	6	18	Virtual, 15k ft, 220 KIAS, 1.5625 Hz, IC #3
2117	6	19	Virtual, 15k ft, 270 KIAS, 1.5625 Hz, IC #1
2117	6	20	Virtual, 15k ft, 270 KIAS, 1.5625 Hz, IC #2

Learjet Flight #	Flight #	Record #	Point Description
2117	6	21	Virtual, 15k ft, 270 KIAS, 1.5625 Hz, IC #3
2117	6	22	Manual, 8k ft, 220 KIAS, 45° entry, Path #3
2117	6	23	Manual, 8k ft, 220 KIAS, 45° entry, Path #2
2117	6	24	Manual, 8k ft, 220 KIAS, 45° entry, Path #4
2117	6	25	Manual, 8k ft, 220 KIAS, 45° entry, Path #1
2117	6	26	Manual, 8k ft, 220 KIAS, 45° entry, Path #5
2117	6	27	Manual, 8k ft, 220 KIAS, 5° entry, Path #3
2117	6	28	Manual, 8k ft, 220 KIAS, 5° entry, Path #2
2117	6	29	N/A
2117	6	30	Manual, 8k ft, 220 KIAS, 5° entry, Path #4
2117	6	31	Manual, 8k ft, 220 KIAS, -5° entry, Path #3
2117	6	32	Manual, 8k ft, 220 KIAS, -5° entry, Path #2
2117	6	33	Manual, 8k ft, 220 KIAS, -5° entry, Path #4
2117	6	34	Manual, 8k ft, 220 KIAS, -5° entry, Path #1
2117	6	35	Manual, 8k ft, 220 KIAS, 5° entry, Path #1
2117	6	36	Manual, 8k ft, 220 KIAS, 5° entry, Path #5
2117	6	37	Manual, 8k ft, 220 KIAS, -5° entry, Path #5
2117	6	38	Virtual, 8k ft, 220 KIAS, 1.5625 Hz, IC #1
2117	6	39	Virtual, 8k ft, 220 KIAS, 1.5625 Hz, IC #2
2117	6	40	Virtual, 8k ft, 220 KIAS, 1.5625 Hz, IC #3
2117	6	41	Virtual, 8k ft, 270 KIAS, 1.5625 Hz, IC #1
2117	6	42	Virtual, 8k ft, 270 KIAS, 1.5625 Hz, IC #2
2117	6	43	Virtual, 8k ft, 270 KIAS, 1.5625 Hz, IC #3
2118	7	5	Virtual, 8k ft, 270 KIAS, 6.25 Hz, IC #3
2118	7	6	Virtual, 8k ft, 270 KIAS, 6.25 Hz, IC #2
2118	7	7	Virtual, 8k ft, 220 KIAS, 6.25 Hz, IC #1
2118	7	8	Virtual, 8k ft, 220 KIAS, 6.25 Hz, IC #2
2118	7	9	Virtual, 8k ft, 220 KIAS, 6.25 Hz, IC #2
2118	7	10	Manual, 500 ft AGL, 270 KIAS, SLUF entry, Path #1
2118	7	11	Manual, 500 ft AGL, 270 KIAS, 45^{o} entry, Path #3
2118	7	12	Manual, 500 ft AGL, 270 KIAS, 45^{o} entry, Path #2
2118	7	13	Manual, 500 ft AGL, 270 KIAS, 45^{o} entry, Path #4
2118	7	14	Manual, 500 ft AGL, 270 KIAS, 45^{o} entry, Path #1
2118	7	15	Manual, 500 ft AGL, 270 KIAS, 45^{o} entry, Path #5
2118	7	16	Manual, 500 ft AGL, 270 KIAS, 5^{o} entry, Path #3
2118	7	17	Manual, 500 ft AGL, 270 KIAS, 5^{o} entry, Path #2
2118	7	18	Manual, 500 ft AGL, 270 KIAS, 5^{o} entry, Path #4
2118	7	19	Manual, 500 ft AGL, 270 KIAS, 5^{o} entry, Path #1
2118	7	20	Manual, 500 ft AGL, 270 KIAS, 5^{o} entry, Path #5
2118	7	21	Virtual, 500 ft AGL, 270 KIAS, 12.5 Hz, IC #1
2118	7	22	Virtual, 500 ft AGL, 270 KIAS, 12.5 Hz, IC #2

Learjet Flight #	Flight #	Record #	Point Description
2118	7	23	Virtual, 500 ft AGL, 270 KIAS, 12.5 Hz, IC #3
2118	7	24	Virtual, 500 ft AGL, 220 KIAS, 12.5 Hz, IC #1
2118	7	25	Virtual, 500 ft AGL, 220 KIAS, 12.5 Hz, IC #2
2118	7	26	Virtual, 500 ft AGL, 220 KIAS, 12.5 Hz, IC #3
2118	7	27	Lateral Offset to Actual Terrain
2118	7	28	Lateral Offset to Actual Terrain
2118	7	29	Lateral Offset to Actual Terrain
2119	8	1	N/A
2119	8	2	Manual, 500 ft, 220 KIAS, 45° entry, Path #3
2119	8	3	Manual, 500 ft, 220 KIAS, 45° entry, Path #2
2119	8	4	Manual, 500 ft, 220 KIAS, 45° entry, Path #1
2119	8	5	Manual, 500 ft, 220 KIAS, 45° entry, Path #5
2119	8	6	Manual, 500 ft, 220 KIAS, 45° entry, Path #4
2119	8	7	Manual, 500 ft, 220 KIAS, 5° entry, Path #3
2119	8	8	Manual, 500 ft, 220 KIAS, 5° entry, Path #2
2119	8	9	Manual, 500 ft, 220 KIAS, 5° entry, Path #1
2119	8	10	Manual, 500 ft, 220 KIAS, 5° entry, Path #5
2119	8	11	Manual, 500 ft, 220 KIAS, 5° entry, Path #4
2119	8	12	Virtual, 500 ft, 220 KIAS, 6.25 Hz, IC #1
2119	8	13	Virtual, 500 ft, 220 KIAS, 6.25 Hz, IC #2
2119	8	14	Virtual, 500 ft, 220 KIAS, 6.25 Hz, IC #3
2119	8	15	Virtual, 500 ft, 270 KIAS, 6.25 Hz, IC #1
2119	8	16	Virtual, 500 ft, 270 KIAS, 6.25 Hz, IC #2
2119	8	17	Virtual, 500 ft, 270 KIAS, 6.25 Hz, IC #3
2119	8	18	Virtual, 500 ft, 220 KIAS, 1.5625 Hz, IC #1
2119	8	19	N/A
2119	8	20	Virtual, 500 ft, 220 KIAS, 1.5625 Hz, IC #2
2119	8	21	Virtual, 500 ft, 220 KIAS, 1.5625 Hz, IC #3
2119	8	22	Virtual, 500 ft, 270 KIAS, 1.5625 Hz, IC #1
2119	8	23	Virtual, 500 ft, 270 KIAS, 1.5625 Hz, IC #1
2119	8	24	Virtual, 500 ft, 270 KIAS, 1.5625 Hz, IC #2
2119	8	25	Virtual, 500 ft, 270 KIAS, 1.5625 Hz, IC #3
2119	8	26	Virtual, 500 ft, 270 KIAS, 1.5625 Hz, IC #3
2119	8	27	N/A
2119	8	28	RSET disconnect check
2119	8	29	Practicing level turn above 2,000 ft AGL
2119	8	30	Descending to 500 ft AGL
2119	8	31	Lateral Offset to Actual Terrain
2119	8	32	Lateral Offset to Actual Terrain
2119	8	33	Lateral Offset to Actual Terrain
2120	9	1	Lateral Offset to Actual Terrain

Learjet Flight #	Flight #	Record #	Point Description
2120	9	2	Lateral Offset to Actual Terrain
2120	9	3	Low Level Flight
2120	9	4	Low Level Flight
2120	9	5	Low Level Flight
2120	9	6	Low Level Flight
2120	9	7	Manual, 500 ft, 220 KIAS, SLUF entry, Path #3
2120	9	7 to 8	Manual, 500 ft, 220 KIAS, SLUF entry, Path #2
2120	9	9	Manual, 500 ft, 220 KIAS, SLUF entry, Path #4
2120	9	10	Manual, 500 ft, 220 KIAS, SLUF entry, Path #1
2120	9	11	Manual, 500 ft, 220 KIAS, SLUF entry, Path #5
2120	9	12	Manual, 500 ft, 270 KIAS, SLUF entry, Path #3
2121	10	1	Lateral Offset to Actual Terrain
2121	10	2	Lateral Offset to Actual Terrain
2121	10	3	Low Level Flight
2121	10	4	Low Level Flight
2121	10	5	Low Level Flight
2121	10	6	Low Level Flight
2121	10	7	Manual, 500 ft, 270 KIAS, SLUF entry, Path #2
2121	10	8	Manual, 500 ft, 270 KIAS, SLUF entry, Path #4
2121	10	9	Manual, 500 ft, 270 KIAS, SLUF entry, Path #1
2121	10	10	Manual, 500 ft, 270 KIAS, SLUF entry, Path #5
2121	10	11	Virtual, 500 ft, 220 KIAS, 12.5 Hz, IC #1
2121	10	12	Virtual, 500 ft, 220 KIAS, 12.5 Hz, IC #2
2122	11	1	Low Level Flight
2122	11	2	Low Level Flight
2122	11	3	Low Level Flight
2122	11	4	Low Level Flight
2122	11	5	Low Level Flight
2122	11	6	Low Level Flight
2122	11	7	Low Level Flight
2122	11	8	Virtual, 500 ft AGL, 220 KIAS, 12.5 Hz, IC #1
2122	11	9	Virtual, 500 ft AGL, 220 KIAS, 12.5 Hz, IC #2
2122	11	10	Virtual, 500 ft AGL, 220 KIAS, 12.5 Hz, IC #3
2122	11	11	Virtual, 500 ft AGL, 270 KIAS, 12.5 Hz, IC #1
2122	11	12	Virtual, 500 ft AGL, 270 KIAS, 12.5 Hz, IC #2
2122	11	13	Virtual, 500 ft AGL, 270 KIAS, 12.5 Hz, IC #3
2122	11	14	Manual, 500 ft, 270 KIAS, 45° entry, Path #3
2122	11	15	Manual, 500 ft, 270 KIAS, 45° entry, Path #4
2122	11	16	Manual, 500 ft, 270 KIAS, 45° entry, Path #2
2122	11	17	Manual, 500 ft, 270 KIAS, 45° entry, Path #1
2122	11	18	Manual, 500 ft, 270 KIAS, 45° entry, Path #1

Learjet Flight #	Flight #	Record #	Point Description
2122	11	19	Manual, 500 ft, 270 KIAS, 45° entry, Path #5
2122	11	20	Manual, 500 ft, 220 KIAS, 45° entry, Path #3
2122	11	21	Manual, 500 ft, 220 KIAS, 45° entry, Path #2
2122	11	22	Manual, 500 ft, 220 KIAS, 45° entry, Path #4

Appendix E. Path Prediction Error Results

The following pages present the results of the Path Prediction Error (PPE) analysis.

The remainder of this page is intentionally blank

Flt #	Rec #	Alt	A/S	Entry	Path	Wind (kts)	Wind (deg)	Prediction Error (ft)	Out-climb prediction?	Tighter than prediction?	Error Away from Terrain?
4	2	15000	220	1	3	31	Yes	1672	No	N/A	No
4	3	15000	220	1	2	34	Yes	1719	No	No	No
4	4	15000	220	1	4	33	Yes	1654	Yes	Yes	Yes
4	5	15000	220	1	1	32	Yes	1651	Yes	Yes	Yes
4	6	15000	220	1	5	37	Yes	1636	Yes	No	Inconclusive
4	9	15000	270	1	3	33	No	1399	Yes	N/A	Yes
4	10	15000	270	1	4	37	Yes	1024	Yes	No	Inconclusive
4	11	15000	270	1	2	30	Yes	1671	Yes	Yes	Yes
4	12	15000	270	1	5	31	Yes	1816	Yes	Yes	Yes
4	13	15000	270	1	1	37	Yes	1524	No	No	No
4	20	8000	220	1	3	24	Yes	1191	Yes	N/A	Yes
4	21	8000	220	1	4	28	No	1256	No	Yes	Inconclusive
4	22	8000	220	1	2	28	Yes	1272	Yes	No	Inconclusive
4	23	8000	220	1	5	25	Yes	962	Yes	No	Inconclusive
4	24	8000	220	1	1	27	Yes	773	Yes	No	Inconclusive
4	25	8000	270	1	3	25	Yes	2505	Yes	N/A	Yes
4	27	8000	270	1	2	26	Yes	1602	No	No	No
4	28	8000	270	1	4	28	Yes	1365	No	No	No
4	29	8000	270	1	1	26	Yes	1445	No	No	No
4	30	8000	270	1	5	28	Yes	514	Yes	Yes	Yes
4	34	500	220	1	3	17	No	172	No	N/A	No
4	35	500	220	1	2	12	Yes	659	Yes	Yes	Yes
4	36	500	220	1	4	14	Yes	918	No	No	No
4	37	500	220	1	1	13	No	1408	Yes	No	Inconclusive
4	38	500	220	1	5	13	No	2332	Yes	No	Inconclusive
4	39	500	270	1	3	13	Yes	481	Yes	N/A	Yes
4	40	500	270	1	2	16	Yes	728	No	No	No
4	41	500	270	1	4	17	Yes	350	Yes	Yes	Yes
4	42	500	270	1	5	18	Yes	864	No	Yes	Inconclusive
5	1	15000	270	2	3	34	Yes	1922	No	N/A	No
5	2	15000	270	2	2	37	Yes	2862	No	No	No
5	3	15000	270	2	4	31	Yes	947	Yes	No	Inconclusive
5	4	15000	270	2	1	32	Yes	1821	Yes	Yes	Yes
5	5	15000	270	2	5	35	Yes	1843	No	No	No
5	6	15000	270	3	3	28	Yes	754	Yes	N/A	Yes
5	7	15000	270	3	2	30	Yes	1687	Yes	Yes	Yes
5	8	15000	270	3	4	32	Yes	1524	Yes	Yes	Yes
5	9	15000	270	3	1	43	Yes	4447	No	No	No
5	10	15000	270	3	5	43	Yes	1201	No	Yes	Inconclusive
5	11	15000	270	4	3	34	No	1404	No	N/A	No
5	12	15000	270	4	2	37	Yes	1290	Yes	No	Inconclusive
5	13	15000	270	4	4	36	Yes	1571	No	No	No
5	14	15000	270	4	1	42	Yes	6568	No	No	No
5	15	15000	270	4	5	41	Yes	4914	No	No	No
5	24	8000	270	2	2	45	Yes	2061	No	No	No
5	25	8000	270	2	4	45	No	2392	No	Yes	No
5	26	8000	270	2	1	30	Yes	748	No	No	No
5	27	8000	270	2	5	25	Yes	1733	No	Yes	No
5	28	8000	270	3	3	33	Yes	1553	Yes	N/A	Yes
5	29	8000	270	3	2	28	Yes	1936	Yes	Yes	Yes
5	30	8000	270	3	4	21	Yes	1337	Yes	Yes	Yes
5	31	8000	270	3	1	29	Yes	2588	No	No	No
5	32	8000	270	3	5	26	Yes	2430	Yes	Yes	Yes
5	33	8000	270	4	3	27	Yes	1140	No	N/A	No
5	34	8000	270	4	2	33	No	1935	No	No	No
5	35	8000	270	4	4	35	Yes	1632	No	No	No
5	36	8000	270	4	1	38	Yes	2864	No	No	No
5	37	8000	270	4	5	30	Yes	2411	Yes	Yes	Yes
5	23	8000	270	2	3	28	Yes	2007	No	N/A	No
6	1	15000	220	2	3	36	Yes	1914	No	N/A	No
6	2	15000	220	2	2	33	Yes	1702	No	No	No

Flt #	Rec #	Alt	A/S	Entry	Path	Wind (kts)	Wind (deg)	Prediction Error (ft)	Out-climb prediction?	Tighter than prediction?	Error Away from Terrain?
6	3	15000	220	2	4	34	Yes	2285	No	No	No
6	4	15000	220	2	1	32	Yes	1786	No	No	No
6	5	15000	220	2	5	23	Yes	1353	Yes	No	No
6	6	15000	220	3	3	30	Yes	1601	Yes	N/A	Yes
6	7	15000	220	3	2	27	Yes	2057	Yes	Yes	Yes
6	8	15000	220	3	4	25	Yes	1176	Yes	Yes	Yes
6	9	15000	220	3	1	31	Yes	3422	Yes	Yes	Yes
6	10	15000	220	3	5	34	Yes	2612	Yes	No	Inconclusive
6	11	15000	220	4	3	31	Yes	1256	Yes	N/A	Yes
6	12	15000	220	4	2	35	Yes	1964	Yes	Yes	Yes
6	13	15000	220	4	4	29	Yes	660	Yes	Yes	Yes
6	14	15000	220	4	1	36	Yes	3685	No	No	No
6	15	15000	220	4	5	38	Yes	2803	No	No	No
6	22	8000	220	2	3	30	No	1768	No	N/A	No
6	23	8000	220	2	2	24	Yes	2019	Yes	Yes	Yes
6	24	8000	220	2	4	27	Yes	1258	Yes	No	Inconclusive
6	25	8000	220	2	1	25	Yes	2632	Yes	Yes	Yes
6	26	8000	220	2	5	32	Yes	2369	No	No	No
6	27	8000	220	3	3	27	Yes	771	Yes	N/A	Yes
6	28	8000	220	3	2	19	Yes	1383	Yes	Yes	Yes
6	30	8000	220	3	4	11	Yes	721	Yes	Yes	Yes
6	31	8000	220	4	3	28	Yes	732	No	N/A	No
6	32	8000	220	4	2	33	Yes	3184	No	No	No
6	33	8000	220	4	4	32	Yes	1641	No	No	No
6	34	8000	220	4	1	34	Yes	5192	No	No	No
6	35	8000	220	3	1	28	Yes	2727	Yes	Yes	Yes
6	36	8000	220	3	5	28	Yes	2482	Yes	No	Inconclusive
6	37	8000	220	4	5	30	Yes	1294	Yes	Yes	Yes
7	10	500	270	1	1	5	Yes	383	Yes	Yes	Yes
7	11	500	270	2	3	16	Yes	913	No	N/A	No
7	12	500	270	2	2	6	Yes	915	Yes	Yes	Yes
7	13	500	270	2	4	7	Yes	291	Yes	No	Inconclusive
7	14	500	270	2	1	12	Yes	2036	No	No	No
7	15	500	270	2	5	10	Yes	751	No	No	No
7	16	500	270	3	3	6	Yes	346	Yes	N/A	Yes
7	17	500	270	3	2	8	Yes	739	No	No	No
7	18	500	270	3	4	8	Yes	652	Yes	Yes	Yes
7	19	500	270	3	1	10	Yes	687	No	No	No
7	20	500	270	3	5	14	Yes	516	No	Yes	Inconclusive
8	2	500	220	2	3	2	No	806	No	N/A	No
8	3	500	220	2	2	9	Yes	853	Yes	Yes	Yes
8	4	500	220	2	1	8	No	967	Yes	Yes	Yes
8	5	500	220	2	5	8	Yes	3640	Yes	No	Inconclusive
8	6	500	220	2	4	11	Yes	592	No	Yes	Inconclusive
8	7	500	220	3	3	5	Yes	409	No	N/A	No
8	8	500	220	3	2	10	No	880	No	No	No
8	9	500	220	3	1	12	Yes	4464	No	No	No
8	10	500	220	3	5	10	No	1742	Yes	No	Inconclusive
8	11	500	220	3	4	11	No	232	No	Yes	Inconclusive
9	7	500	220	1	3	19	No	565	No	N/A	No
9	8	500	220	1	2	9	Yes	301	No	No	No
9	9	500	220	1	4	1	Yes	1191	Yes	Yes	Yes
9	10	500	220	1	1	14	Yes	4114	Yes	Yes	Yes
9	11	500	220	1	5	12	Yes	1064	Yes	No	Inconclusive
9	12	500	270	1	3	16	Yes	603	Yes	N/A	Yes
10	7	500	270	1	2	13	Yes	1471	No	No	No
10	8	500	270	1	4	14	Yes	1090	Yes	Yes	Yes
10	9	500	270	1	1	20	Yes	2486	No	No	No
10	10	500	270	1	5	17	Yes	973	No	No	No

Appendix F. Virtual Terrain Activation Results

The following page presents the results of the virtual terrain activation analysis.

The remainder of this page is intentionally blank

Test Flight	Rec #	Alt (ft)	MSL AGL	Airspeed (KIAS)	IC	Refresh Rate (Hz)	Set Buffer	Forward Look-Ahead Time (sec)	RSS Dist. (ft)	HaT (ft)
5	16	15000	MSL	270	1	6.25	100	3	-13	-220
5	17	15000	MSL	270	2	6.25	100	5	16	23
5	18	15000	MSL	270	3	6.25	100	21	-9	-422
5	19	15000	MSL	220	1	6.25	100	8	191	226
5	20	15000	MSL	220	2	6.25	100	11	337	342
5	21	15000	MSL	220	3	6.25	100	20	547	576
5	38	8000	MSL	270	1	12.5	100	3	37	109
5	39	8000	MSL	270	2	12.5	100	1	211	212
5	40	8000	MSL	270	3	12.5	100	5	110	133
5	41	8000	MSL	270	1	6.25	100	15	135	151
6	16	15000	MSL	220	1	1.5625	100	15	121	154
6	17	15000	MSL	220	2	1.5625	100	6	-11	-45
6	18	15000	MSL	220	3	1.5625	100	28	-9	-294
6	19	15000	MSL	270	1	1.5625	100	15	145	153
6	20	15000	MSL	270	2	1.5625	100	5	15	44
6	21	15000	MSL	270	3	1.5625	100	30	105	106
6	38	8000	MSL	220	1	1.5625	100	10	-20	-33
6	39	8000	MSL	220	2	1.5625	100	7	173	184
6	40	8000	MSL	220	3	1.5625	100	8	50	75
6	41	8000	MSL	270	1	1.5625	100	3	95	101
6	42	8000	MSL	270	2	1.5625	100	3	105	137
6	43	8000	MSL	270	3	1.5625	100	6	-32	-24
7	5	8000	MSL	270	3	6.25	100	17	47	74
7	6	8000	MSL	270	2	6.25	100	4	15	71
7	7	8000	MSL	220	1	6.25	100	10	100	132
7	8	8000	MSL	220	2	6.25	100	11	239	242
7	9	8000	MSL	220	3	6.25	100	10	94	102
7	21	8000	MSL	270	1	6.25	100	15	90	190
7	22	500	AGL	270	2	12.5	100	4	119	123
7	23	500	AGL	270	3	12.5	100	5	108	125
7	24	500	AGL	220	1	12.5	100	11	136	169
7	25	500	AGL	220	2	12.5	100	7	157	179
8	12	500	AGL	220	1	6.25	100	14	46	48
8	13	500	AGL	220	2	6.25	100	8	87	141
8	14	500	AGL	220	3	6.25	100	7	149	157
8	15	500	AGL	270	1	6.25	100	19	45	137
8	16	500	AGL	270	2	6.25	100	3	79	82
8	17	500	AGL	270	3	6.25	100	6	4	141
8	18	500	AGL	220	1	1.5625	100	8	70	86
8	20	500	AGL	220	2	1.5625	100	5	139	172
8	21	500	AGL	220	3	1.5625	100	17	-11	-124
8	24	500	AGL	270	2	1.5625	100	2	138	143
8	26	500	AGL	270	3	1.5625	100	2	715	720
10	11	500	AGL	220	1	12.5	200	3	102	174
10	12	500	AGL	220	2	12.5	200	6	34	99
11	8	500	AGL	220	1	12.5	200	16	184	221
11	9	500	AGL	220	2	12.5	200	1	175	203
11	10	500	AGL	220	3	12.5	200	11	251	270
11	11	500	AGL	270	1	12.5	200	5	128	151
11	12	500	AGL	270	2	12.5	200	4	187	214
11	13	500	AGL	270	3	12.5	200	4	95	151

Appendix G. RSET Configuration Tracker

The following pages present a record of the configuration changes made during the Have MEDUSA test program.

The remainder of this page is intentionally blank

Flight #	EP(s)	TC(s)	Changes Made Before Flight	Issues Discovered During or After Flight
1	Gotwald	Gahan Mak Jian Ming	*Baseline configuration resulting from simulator and ground tests.	*Actual control surface rate limits significantly different than the requested rate limits (persistent variables issue), causing numerous VSS trips. *Wind data from Learjet was not being passed to RSET - variable names too long (discovered post flight 2). *Initial horizontal stab position was incorrectly being passed to RSET as the aileron position (discovered flight 3). *Learjet sending unreliable heading value (Psi) to RSET instead of INS ground track value (discovered post flight 3). *C.G. offset set to a fixed value instead of changing based on current fuel balance (discovered post flight 3).
2	Hammond	Kolesar Gahan	*Issue with rate limit variables resolved.	*Wind data from Learjet was not being passed to RSET - variable names too long. *Initial horizontal stab position was incorrectly being passed to RSET as the aileron position (discovered flight 3). *Learjet sending unreliable heading value (Psi) to RSET instead of INS ground track value (discovered post flight 3). *C.G. offset set to a fixed value instead of changing based on current fuel balance (discovered post flight 3). *MATLAB froze mid-flight and required a lot of troubleshooting to get all settings set up.
3	Bakun	Mak Jian Ming Gahan	*Wind variable names changed so they are properly passed to RSET *Extensive list of VSS parameters added to recording list	*Initial horizontal stab position was incorrectly being passed to RSET as the aileron position. *Learjet sending unreliable heading value (Psi) to RSET instead of INS ground track value. *C.G. offset set to a fixed value instead of changing based on current fuel balance. *Learjet sending unreliable wind speed data to RSET (~80 kts) *Learjet reported incorrect causes for valid VSS trips

Flight #	EP(s)	TC(s)	Changes Made Before Flight	Issues Discovered During or After Flight
4	Hammond	Gahan	*Initial aileron position issue fixed. *Aircraft heading parameter changed from "psi" to "ins_track_true" *Updated Lear 3 mass property calculation in order to pass correct c.g. offset to RSET *Wind set to zero *Autopilot updated to improve smoothness (removed Nz feedback; added lower Nz bound)	*Max gamma changed to 12 deg during flight to prevent excessive airspeed loss. *Under-g VSS trips during hand-back after multiple automatic activations.
5	Bakun	Mak Jian Ming	*Drop-down menu for number of back seat passengers added to GUI in order to increase accuracy of weight & balance measurement *Fields added to GUI for entering wind speed and direction before each test point. Wind speed/direction will be considered constant throughout each test point.	
6	Gotwald	Kolesar	None	
7	Hammond	Mak Jian Ming	*Drop-down field for DTED region added to GUI	
8	Gotwald	Gahan	None	
9	Bakun Gotwald	Mak Jian Ming	None	
10	Hammond Lt Col Abel	Kolesar	None	
11	Bakun	Gahan	None	

Appendix H. 412th Test Wing Rating Criteria

Figure H.1 presents the test objective rating criteria used by the 412th Test Wing as of the September 2018 Have MEDUSA TMP.

How Well Does the System Meet Mission and/or Task Requirements?	Changes Recommended for Improvement	Mission/Task Impact	Descriptor	Rating
Exceeds requirements.	None	None	Excellent	Satisfactory
Meets all or a majority of the requirements.	Negligible changes needed to enhance or improve operational test or field use	Negligible	Good	Satisfactory
Some requirements met; can do the job, but not as well as it could or should.	Minor changes needed to improve operational test or field use	Minor	Adequate	Satisfactory
Minimum level of acceptable capability and/or some noncritical requirements not met.	Moderate changes needed to reduce risk in operational test or field use	Moderate	Borderline	Marginal
One or some of the critical functional requirements were not met.	Substantial changes needed to achieve satisfactory functionality	Substantial	Deficient	Unsatisfactory
A majority or all of the functional requirements were not met.	Major changes required to achieve system functionality	Major	Unacceptable	Unsatisfactory
Mission not safe.	Critical changes mandatory	Critical	Unsafe	Failed

Figure H.1. 412th Test Wing Rating Criteria

Appendix I. Digital Appendix

Raw flight test data, additional figures, and MATLAB code used to reduce the flight test data are available by contacting the Air Force Institute of Technology Point of Contact:

Dr. Richard Cobb
AFIT/ENY
2950 Hobson Way, Bldg 640
Room 345
Wright-Patterson AFB, OH 45433
937-255-3636

Please see Section 3.8.3 for recommended minimum system specifications for running the RSET system. The files are held in four folders. Their structure is listed below.

0. RSET System MATLAB Code
    a. All files needed to run the RSET System
    b. Primary file is "HaveMEDUSA.slx"
1. Raw Data
    a. All flight test data gathered from flights 4 - 11
    b. Data is separated as data gathered from the RSET algorithm and that gathered from the Learjet sensors.
    c. RSET data: "Flight XX MEDUSA data"
    d. Learjet data: "Flight XXX VSS data"
2. Data Reduction Scripts
    a. For calculating PPE: "Manual_path_prediction_error_v6.m"
    b. For calculating RSS distance from terrain: "closest_point_approach_v9.m"
3. Figures and Plots
    a. Contains manual and virtual terrain activation figures
    b. Manual figures: "Flight XX_Man_Act"
    c. Virtual figures: "Flight XX Virtual Figures"

Appendix J. Hand-Back Survey

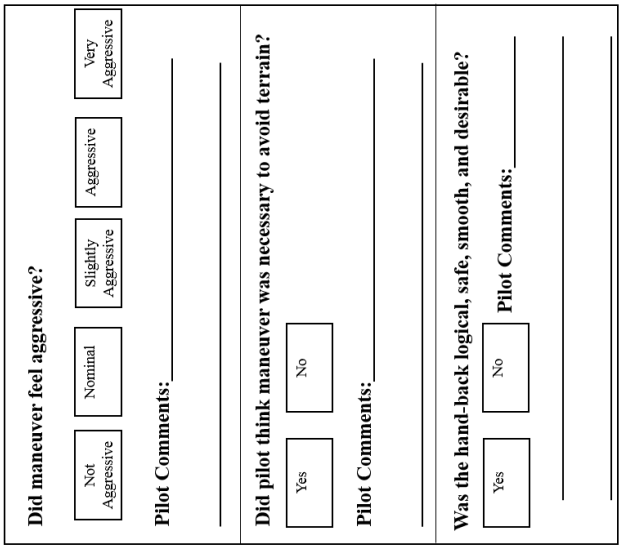

Did maneuver feel aggressive?

Not Aggressive | Nominal | Slightly Aggressive | Aggressive | Very Aggressive

Pilot Comments:_____

Did pilot think maneuver was necessary to avoid terrain?

Yes | No

Pilot Comments:_____

Was the hand-back logical, safe, smooth, and desirable?

Yes | No | Pilot Comments:_____

Pt # | Date | Pilot | Alt/Airspeed

Initial Aircraft Control Input:

Smooth | Abrupt VSS trip?__ | Pulsing | Comments:

Pilot Comments:_____

Aircraft Control Through Maneuver :

Smooth | Abrupt VSS trip?__ | Pulsing | Comments:

Pilot Comments:_____

Appendix K. Aircrew Comments

"Felt smooth and safe. Adequate for system maturity."

"Hand-back took a little too long in order to stay smooth. I would probably pickle off and take command earlier to recover faster."

"Higher airspeed hand-back was more aggressive vs lower energy state hand-backs, but not undesirable."

"During low speed points, its hard to tell if the aircraft is in a hand-back state or attempting a different path. Visual indication of system state would be useful."

"In a non-combat environment this would be totally fine. It gets the aircraft back to a place I feel comfortable taking control."

"The hand-back may be problematic for spec ops terrain masking missions as the RSET doesnt account for these mission-specific requirements."

"Mission must be accounted for in the hand-back design"

"The stick shaker was a nice way to identify the RSET was controlling the aircraft. Termination of stick shaker made it unambiguous that the hand-back was complete."

"While slightly too aggressive at times, a hand-back sequence needs to be incorporated."

"Low speed was very smooth."

Bibliography

1. International Civil Aviation Organization. Controlled Flight into Terrain: Education and Training Aid. Technical Report January, International Civil Aviation Organization, 2005.

2. Department of Defense. Flying Qualities of Piloted Aircraft. *MIL-STD-1797B*, 2006.

3. Federal Aviation Administration. Airworthiness Criteria for the Installation Approval of a Terrain Awareness and Warning System (TAWS) for Part 25 Airplanes. *Advisory Circular*, 2000.

4. IATA. Controlled Flight Into Terrain Accident Analysis Report: 2008-2017. Technical report, International Air Transport Association, 2018.

5. Federal Aviation Administration. Advisory Circular: General Aviation Controlled Flight into Terrain Awareness. 2003.

6. Major Michael L Moroze and Michael P Snow. Causes and Remedies of Controlled Flight Into Terrain in Military and Civil Aviation. 1997.

7. E.M. Griffin, R.M. Turner, S.C. Whitcomb, D.E. Swihart, J.M. Bier, K.L. Hobbs, and A.C. Burns. Automatic ground collision avoidance system design for preblock 40 F-16 configurations. *2012 Asia-Pacific International Symposium on Aerospace Technology*, pages 1–7, 2012.

8. Donald A. Rumsfeld. Reducing Preventable Accidents, 2003.

9. Defense Safety Oversight Council. Defense Safety Oversight Council Safety Technology Working Group Fighter / Attack Automatic Collision Avoidance Systems Business Case. 2006.

10. Robert M. Gates. Memorandum for Secretaries of the Military Departments: Zero Preventable Accidents, 2007.

11. Michael T. Lippert. Life or Death in 250 Milliseconds, 2017. URL `https://www.usni.org`.

12. Matt Kamlet. Collision Avoidance System Saves Unconscious F-16 Pilot In Fourth Confirmed Rescue, 2017. URL `https://www.nasa.gov/centers/armstrong/features/auto-gcas{\_}performs{\_}fourth{\_}confirmed{\_}save.html`.

13. Lockheed Martin. Saving the Good Guys: Seventh Save Illustrates Life-Saving Auto GCAS Technology, 2019. URL `https://www.lockheedmartin.com/en-us/news/features/2016/`

saving-the-good-guys--seventh-save-illustrates-life-saving-auto-.html.

14. Angela W. Suplisson. *Optimal Recovery Trajectories for Automatic Ground Collision Avoidance Systems (Auto GCAS)*. PhD dissertation, Air Force Institute of Technology, 2015.

15. John V. Trombetta. *Multi-Trajectory Automatic Ground Collision Avoidance System with Flight Tests (Project Have ESCAPE)*. Master's thesis, Air Force Institute of Technology, 2016.

16. Brandon Shapiro. Point of Recovery : Ground Collision Avoidance System saving pilots lives. *Airman Magazine*, pages 1–3, 2016. URL http://www.acc.af.mil/News/Article-Display/Article/1026196/point-of-recovery-ground-collision-avoidance-system-saving-pilots-lives/.

17. Richard Cree. C-130 Retrofit Kit Offerings, 2011.

18. Angela W. Suplisson, Andrew S. LeValley, David A. Wagner, and Mary K. Weidman. Saving Lives Automatically: One Aircrew at a Time, 2017.

19. Flight Safety Foundation. Noncompliance With Departure Procedures Sets Course for Impact With Mountain. *Accident Prevention*, 57(8):8, 2000.

20. Robert A. Skolasky. *AFI 51-503, 17 August 1996, C-130 Aircraft, USAF, S/N 74-1662 Accident Investigation Board Findings*. United States Air Force, 1996.

21. Mikael Karanikas and Agne Widholm. Accident involving a Royal Norwegian Air Force aircraft of type C-130 with call sign HAZE 01, on 15 March 2012 at Kebnekaise, Norrbotten County, Sweden. Technical Report RM 2013:02e, Swedish Accident Investigation Authority, 2013.

22. Donald E. Swihart, Arthur F. Barfield, Edward M. Griffin, Richard C. Lehmann, Shawn C. Whitcomb, Billie Flynn, Mark A. Skoog, and Kevin E. Processor. Automatic ground collision avoidance system design, integration, & flight test. *IEEE Aerospace and Electronic Systems Magazine*, 26(5):4–11, 2011. ISSN 08858985. doi: 10.1109/MAES.2011.5871385.

23. Paul Sorokowski, Mark Skoog, Capt Scott Burrows, and Sarahkatie Thomas. Small UAV Automatic Ground Collision Avoidance System Design Considerations and Flight Test Results. (June), 2015.

24. J K Kuchar and L C Yang. A review of conflict detection and resolution modeling methods. *IEEE Transactions on Intelligent Transportation Systems*, 1(4):179–189, 2000. ISSN 15249050. doi: 10.1109/6979.898217. URL http://ieeexplore.ieee.org/lpdocs/epic03/wrapper.htm?arnumber=898217.

25. Casey E. Richardson, Charles A. Eger, and Tucker R. Hamilton. Automatic air collision avoidance system. In *AIAA Modeling and Simulation Technologies Conference*, Kissimmee, FL, 2015. ISBN 0-7803-7631-5. doi: 10.1109/SICE.2002.1195482. URL `https://arc.aiaa.org/doi/abs/10.2514/6.2015-0657`.

26. Amy Burns, Daniel Harper, Arthur F. Barfield, Shawn Whitcomb, and Brian Jurusik. Auto GCAS for analog flight control system. *AIAA/IEEE Digital Avionics Systems Conference - Proceedings*, pages 1–11, 2011. doi: 10.1109/DASC.2011.6096148.

27. James K Kuchar and Lee C Yang. Survey of Conflict Detection and Resolution Modeling Methods. *Proceedings AIAA Guidance Navigation Control Conference*, pages 1388–1397, 1997. doi: 10.1109/6979.898217. URL `http://ieeexplore.ieee.org/document/898217/`.

28. Honeywell. MK VI and MK VII Enhanced Ground Proximity Warning System (EGPWS) Pilot's Guide, 2004.

29. Honeywell. MKV-A EGPWS Pilot's Guide, sep 2013.

30. Otto Huisman and A. Rolf. *Principles of Geographic Information Systems*. The International Institute for Geo-Information Science and Earth Observation, 4th edition, 2009. ISBN 9789061642695. doi: 10.1016/j.jmva.2014.02.006.

31. E Rodriguez, Cs Morris, and Je Belz. An assessment of the SRTM topographic products. *Photogrammetric Engineering and Remote Sensing*, 72(3):249–260, 2006. doi: 0099-1112/06/72030249/$3.00/0.

32. Seongheon Lee, Hyochoong Bang, and Dongjin Lee. Predictive ground collision avoidance system for UAV applications: PGCAS design for fixed-wing UAVs and processor in the loop simulation. *2016 International Conference on Unmanned Aircraft Systems, ICUAS 2016*, pages 1287–1292, 2016. doi: 10.1109/ICUAS.2016.7502561.

33. David Kidner, Mark Dorey, and Derek Smith. What's the point? Interpolation and extrapolation with a regular grid DEM. *GeoComputation.org*, pages 1–16, 1999. URL `http://www.geocomputation.org/1999/082/gc{\_}082.htm`.

34. Alan H. Barr. Superquadrics and Angle-Preserving Transformations. *IEEE Computer Graphics and Applications*, 1(1):11–23, 1981. ISSN 02721716. doi: 10.1109/MCG.1981.1673799.

35. Mark A Skoog and James L Less. Development and Flight Demonstration of a Variable Autonomy Ground Collision Avoidance System. *American Institute of Aeronautics and Astronautics*, pages 1–22, 2014.

36. Thomas Anderson, Warren Jones, and Kathleen Beamon. Design and implementation of TAWS for rotary wing aircraft. *... Conference, 2011 IEEE*, 2011. URL http://ieeexplore.ieee.org/xpls/abs{_}all.jsp?arnumber=5747519.

37. US Navy. NATOPS Flight Manual Navy Model F/A-18 E/F 165533 and Up Aircraft, A1-F18EA-NFM-000. Technical Report September, 2008.

38. Roland Goerke and Werner Berger. A400M TACTICAL GROUND COLLISION AVOIDANCE SYSTEM T-GCAS ®. *IEEE Transactions on Aerospace and Electronic Systems*, pages 1–7, 2012.

39. Roland Goerke and Werner Berger. Tactical ground collision avoidance system T-GCAS. *AIAA/IEEE Digital Avionics Systems Conference - Proceedings*, 2012. ISSN 21557195. doi: 10.1109/DASC.2012.6382953.

40. Unknown. Comparative image of C-17, A400M, and C-130J. URL https://aviation.stackexchange.com/questions/14944/why-does-an-aircraft-as-big-as-the-airbus-a400m-use-turboprops.

41. Donald Swihart and Finley Barfield. Results of a Joint US/Swedish Auto Ground Collision Avoidance System Program. Technical report, Air Force Research Laboratory, 1998.

42. Anders Erlandsson and Bjorn Rubensson. HANDLING OF FLIGHT SAFETY AT SAAB FLIGHT TEST DEPARTMENT IN GENERAL AND EXAMPLES FROM GCAS FLIGHT TEST, 2014.

43. Dean Gesch, Michael Oimoen, Susan Greenlee, Charles Nelson, Michael Steuck, and Dean Tyler. The National Elevation Dataset. 68(1):1–9, 2002.

44. Arvind U. Raghunathan, Vipin Gopal, Dharmashankar Subramanian, Lorenz T. Biegler, and Tariq Samad. Dynamic optimization strategies for three-dimensional conflict resolution of multiple aircraft. *Journal of Guidance, Control, and Dynamics*, 27(4):586–594, 2004. ISSN 0731-5090. doi: 10.2514/1.11168. URL http://cat.inist.fr/?aModele=afficheN{\&}cpsidt=15974157.

45. Seongheon Lee, Dongjin Lee, and Hyochoong Bang. Modified Algorithm of Predictive Ground Collision Avoidance System for the Low Level Terrain Flight. (Iccas):197–200, 2015.

46. Donald E Swihart and Program Manager. Automatic Collision Avoidance Technology. pages 1–35, 2004.

47. Tom Berger, Mark Tischler, Steven G. Hagerott, M Christopher Cotting, William R. Gray, James Gresham, Justin George, Kyle Krogh, Alessandro D'Argenio, and Justin Howland. Development and Validation of a Flight-Identified Full-Envelope Business Jet Simulation Model Using a Stitching Architecture. *AIAA Modeling and Simulation Technologies Conference*, (January):

1–35, 2017. doi: 10.2514/6.2017-1550. URL http://arc.aiaa.org/doi/10.2514/6.2017-1550.

48. Eric L. Tobias and Mark B. Tischler. A Model Stitching Architecture for Continuous Full Flight-Envelope Simulation of Fixed-Wing Aircraft and Rotorcraft from Discrete-Point Linear Models. Technical Report April, 2016.

49. Andrés Marcos and Gary J. Balas. Development of Linear-Parameter-Varying Models for Aircraft. *Journal of Guidance, Control, and Dynamics*, 27(2):218–228, 2004. ISSN 0731-5090. doi: 10.2514/1.9165.

50. Mark B. Tischler and Robert K. Remple. *Aircraft and Rotorcraft System Identification: Engineering Methods with Flight Test Examples*. 2006.

51. D.J. Murray-Smiith. Methods for the External Validation of Continous System Simulation Models: A Review. pages 5–31, 1998.

52. R Jategaonkar, D Fischenberg, and W Gruenhagen. Aerodynamic Modeling and System Identification from Flight DataRecent Applications at DLR. *Journal of Aircraft*, 41(May):681–691, 2004. ISSN 0021-8669. doi: 10.2514/1.3165. URL http://arc.aiaa.org/doi/pdf/10.2514/1.3165.

53. US Air Force. Flying Operations, General Flight Rules. (October), 2017.

54. Lucian Dragut and Thomas Blaschke. Automated classification of landform elements using object-based image analysis. *Geomorphology*, 81(3-4):330–344, 2006. ISSN 0169555X. doi: 10.1016/j.geomorph.2006.04.013.

55. Norman C Weingarten. History of in-flight simulation & flying qualities research at calspan. *AIAA Journal of Aircraft*, 42(2):290–298, 2005. doi: doi:10.2514/6.2003-5464.

56. Jay Kemper and M Christopher Cotting. Simulator Design for Flying and Handling Qualities Instruction. *AIAA Modeling and Simulation Technologies Conference*, (412):1–15, 2016. doi: doi:10.2514/6.2016-1664. URL http://dx.doi.org/10.2514/6.2016-1664.

57. Airborne Testbeds. URL https://www.calspan.com/services/aircraft-operation/flight-testing/sensors-airborne-services-test-beds/.

58. Paul Schifferle. Variable Stability Learjet In-Flight Simulator Capabilities. 2014. URL http://www.calspan.com/wp-content/uploads/2015/08/calspan-aerospace-learjet-ifs-12-jan-2015.pdf.

59. Mark W. Vahle. *Application and Validation of Off-Nominal Aircraft Performance Models*. Master's thesis, Air Force Institute of Technology, 2017.

60. Malcom Cotting. USAF Test Pilot School, Personal Communication, aug 2017.

61. Stephanie Simon. Air Force Research Laboratory, Personal Communication, aug 2017.

62. Jay Kemper. Calspan Corporation, Personal Communication, sep 2017.

63. William H. Press, Brian P. Flannery, Saul A. Teukolsky, and William T. Vetterling. *Numerical Recipes: The Art of Scientific Computing*. Cambridge University Press, 1st edition, 1986.

64. Brian L. Stevens and Frank K. Lewis. *Aircraft Control and Simulation*. Wiley-Interscience, 2nd edition, 2003.

65. Robert C. Nelson. *Flight Stability and Automatic Control*. McGraw Hill Education, 2nd edition, 2007.

66. Katsuhiko Ogata. *Modern Control Engineering*. Pearson, 5th edition, 2009.

67. Department of Defense. Performance Specifications: Digital Terrain Elevation Data (DTED) (MIL-PRF-89020B). Technical report, 1996.

68. Donald E. Kirk. *Optimal Control Theory: An Introduction*. Dover Publications, 1st edition, 2004.

69. R. Bellman and S. Dreyfus. Applied Dynamic Programming, 1962. ISSN 0022247X.

70. James V. Carpenter. *Automatic Ground Collision Avoidance System for Performance Limited Aircraft*. Master's thesis, Air Force Institute of Technology, 2018.

71. John V Trombetta, Sebastien Allard, Russell Neice, Yoichiro Kita, and Justin Wilson. Limited Evaluation of Automatic Ground Collision Avoidance Algorithm for Climb Limited Aircraft (Project Have ESCAPE). Technical report, USAF TPS, Edwards AFB, 2015.

72. John Easter. Learjet Flight Syllabus and Background Material for the US Air Force/US Naval Test Pilot School Variable Stability Programs. TM-FRG-LJ1-0061-R05. Technical report, Calspan Corporation, Niagara Falls, New York, 2011.

Vita

Captain Kenneth C. Gahan was born on January 20th, 1986, in Huntsville, Alabama. He graduated from Tennessee Technological University in 2009 with a Bachelor of Science in Mechanical Engineering. He worked for 2 years as a Propulsion Test Engineer before commissioning into the United States Air Force through Officer Training School (OTS). Following OTS he attended Undergraduate Combat Systems Officer Training at Naval Air Station Pensacola, Florida, where he was recognized as a Distinguished Graduate and assigned to fly the EC-130H Compass Call. He completed Compass Call training at Davis-Monthan AFB, Arizona, again as a Distinguished Graduate. He served as an Electronic Warfare Officer from 2013 to 2016 and deployed to Afghanistan in support of Operation Enduring Freedom (OEF) and Kuwait in support of Operation Inherent Resolve (OIR). In 2015 Captain Gahan was selected for the joint AFIT/USAF Test Pilot School (TPS) Program. Prior to attending the Air Force Institute of Technology (AFIT) at Wright-Patterson AFB, Ohio, he completed Squadron Officer School at Maxwell AFB, Alabama, where he was a Distinguished Graduate and Top Squadron Graduate. In August 2016 he began his AFIT studies toward a Master of Science in Aeronautical Engineering. In November 2017 he departed AFIT for TPS to begin training and complete his AFIT research. As a member of USAF TPS Class 18A at Edwards AFB, California, Capt Gahan was once again recognized as a Distinguished Graduate. Following TPS he was assigned to the 645th Aeronautical Systems Squadron in Greenville, Texas to test the EC-130H, EC-37, and RC-135 for the Big Safari program.

REPORT DOCUMENTATION PAGE

Form Approved
OMB No. 0704–0188

1. REPORT DATE *(DD–MM–YYYY)*	2. REPORT TYPE	3. DATES COVERED *(From — To)*
01–03–2019	Master's Thesis	Oct 2016 — Mar 2019

4. TITLE AND SUBTITLE

MULTI-PATH AUTOMATIC GROUND COLLISION AVOIDANCE SYSTEM FOR PERFORMANCE LIMITED AIRCRAFT WITH FLIGHT TESTS: PROJECT HAVE MEDUSA

5a. CONTRACT NUMBER

5b. GRANT NUMBER

5c. PROGRAM ELEMENT NUMBER

6. AUTHOR(S)

Captain Kenneth C. Gahan, USAF

5d. PROJECT NUMBER

5e. TASK NUMBER

5f. WORK UNIT NUMBER

7. PERFORMING ORGANIZATION NAME(S) AND ADDRESS(ES)

Air Force Institute of Technology
Graduate School of Engineering and Management (AFIT/EN)
2950 Hobson Way
WPAFB OH 45433-7765

8. PERFORMING ORGANIZATION REPORT NUMBER

AFIT-ENY-MS-19-M-213

9. SPONSORING / MONITORING AGENCY NAME(S) AND ADDRESS(ES)

Department of Aeronautics and Astronautics
2950 Hobson Way
WPAFB OH 45433-7765
DSN -, COMM 937-255-3636
Email: kenneth.gahan@afit.edu

10. SPONSOR/MONITOR'S ACRONYM(S)

AFOSR / AFRL/RQ

11. SPONSOR/MONITOR'S REPORT NUMBER(S)

12. DISTRIBUTION / AVAILABILITY STATEMENT

DISTRIBUTION STATEMENT A:
APPROVED FOR PUBLIC RELEASE; DISTRIBUTION UNLIMITED.

13. SUPPLEMENTARY NOTES

14. ABSTRACT

A multi-path Auto-GCAS for performance limited aircraft was developed and improved to prevent controlled flight into terrain. Research includes flight test results from the USAF TPS Project Have Multi-Path Escape Decisions Using Sophisticated Algorithms (MEDUSA). The tested Rapidly Selectable Escape Trajectory (RSET) system included 5-paths which continuously updated at a rate of up to 12.5 Hz. The research employed Level 1 DTED as the offending terrain and an 18 DoF Stitched aerodynamic model to create terrain avoidance paths based on the aircraft's state and location. The system then triggered when all paths predicted collision with the DTED and automatically activated the path which had the longest time until impact. A buffer of 200 ft added to the DTED to allowed for processing and execution of the maneuver. Path prediction error (PPE) was larger than expected for the 30-second path predictions. At 12.5 Hz the RSET system avoided terrain in all cases tested and was able to achieve and maintain target load factor and flight path angle with momentary overshoots, and showed no tendency for nuisance activations. Hand-back was favorable.

15. SUBJECT TERMS

multi-path, Auto-GCAS, controlled flight into terrain, safety, Test Pilot School, Calspan Learjet VSS, MATLAB, Simulink, rapidly selectable escape trajector, RSET, Have MEDUSA, stitched model, DTED, Thesis

16. SECURITY CLASSIFICATION OF:			17. LIMITATION OF ABSTRACT	18. NUMBER OF PAGES	19a. NAME OF RESPONSIBLE PERSON
a. REPORT	b. ABSTRACT	c. THIS PAGE			Dr. Richard G. Cobb, AFIT/ENY
U	U	U	U	235	19b. TELEPHONE NUMBER *(include area code)* (937) 255-3636, x4559; richard.cobb@afit.edu